

The Molecular Biomarkers of Sperm Fitness

Jayme Cohen



Thesis submitted for the degree of Doctor of Philosophy

School of Biological Sciences
University of East Anglia

October 2025

© This copy of the thesis has been supplied on condition that anyone who consults it is understood to recognise that its copyright rests with the author and that use of any information derived there from must be in accordance with current UK Copyright Law. In addition, any quotation or extract must include full attribution.

Declaration

I, Jayme Leah Cohen, confirm that the work presented in this thesis is my own. Where information has been derived from other sources, I confirm that this has been indicated in the thesis.

Abstract

Sperm are among the most specialised and variable cell types in the animal body, differing not only across species but also between and within individuals. This molecular and phenotypic diversity has important implications for fertility, yet the mechanisms generating variation among sperm and their evolutionary and clinical consequences remain poorly understood. This thesis combines quantitative proteomics, bioinformatics, and single-cell analysis to investigate how environmental and physiological stress shape sperm phenotype and to test whether molecular heterogeneity within ejaculates provides a substrate for haploid selection. In Chapter 1, tandem mass tag proteomics revealed that acute heat stress in zebrafish (*Danio rerio*) testes induces a coordinated shift in the proteome, with depletion of proteins linked to spermatogenesis and motility and enrichment of chaperones and stress-response factors, demonstrating dynamic germline remodelling under environmental challenge. Chapter 2 presents a comprehensive zebrafish sperm proteome that establishes a baseline for functional and comparative work and shows that stress-induced testicular changes translate into altered sperm protein composition. In Chapter 3, fractionation of human ejaculates by swim-up and methyl-cellulose migration revealed consistent proteomic differences between higher- and lower-fitness sperm subpopulations, identifying candidate surface biomarkers of sperm quality. Chapter 4 validated two of these candidates, OLFM4 and CTNG, as accessible on the sperm surface and inversely associated with sperm longevity using spectral imaging flow cytometry. Together, these studies demonstrate that sperm phenotypes reflect underlying molecular differences that can be detected, quantified, and linked to fitness-related traits. They provide molecular evidence for haploid selection acting within ejaculates and establish a translational foundation for biomarker-based sperm assessment in assisted reproduction.

Access Condition and Agreement

Each deposit in UEA Digital Repository is protected by copyright and other intellectual property rights, and duplication or sale of all or part of any of the Data Collections is not permitted, except that material may be duplicated by you for your research use or for educational purposes in electronic or print form. You must obtain permission from the copyright holder, usually the author, for any other use. Exceptions only apply where a deposit may be explicitly provided under a stated licence, such as a Creative Commons licence or Open Government licence.

Electronic or print copies may not be offered, whether for sale or otherwise to anyone, unless explicitly stated under a Creative Commons or Open Government license. Unauthorised reproduction, editing or reformatting for resale purposes is explicitly prohibited (except where approved by the copyright holder themselves) and UEA reserves the right to take immediate 'take down' action on behalf of the copyright and/or rights holder if this Access condition of the UEA Digital Repository is breached. Any material in this database has been supplied on the understanding that it is copyright material and that no quotation from the material may be published without proper acknowledgement.

Acknowledgements

Completing this PhD has been a trial of attrition, an experience that has tested me both personally and academically, pushed me far beyond my comfort zone, and ultimately allowed me to grow into the person I am today. I am deeply grateful to all those who have supported, challenged, and inspired me along the way.

First and foremost, I would like to thank Professor Simone Immler, who has been my mentor, role model, and constant source of inspiration for all these years. Her guidance, trust, and encouragement have shaped not only my scientific career but also my personal growth, and I could not have asked for a better person to learn from.

I owe immense gratitude to my parents and grandparents, whose love, patience, and unwavering support have sustained me even when I have been difficult to deal with. Their belief in me, even in the moments when I doubted myself, has been the foundation that allowed me to keep going.

To Ruth, thank you for your endless help and support in keeping everything running smoothly; to Justin, for bringing positivity and good vibes to the lab; to Daniel, for the sharp scientific debates that kept me thinking; and to the rest of the Immler Lab, for creating such a stimulating, kind, and collaborative environment.

I would also like to thank Andy and the team at the Earlham Institute for all their support, guidance, and for teaching me so many new skills throughout this project. Working with you has been an invaluable part of my scientific development.

I am also grateful to the Fireflies, my office family, for their humour, encouragement, and friendship throughout this journey. You made even the longest days brighter.

Finally, a heartfelt thank you to the true emotional support team, Coco, Ben, Enzo, Chip, Milo, Monty, and all the other wonderful dogs I have met along the way, for the comfort, joy, and unconditional love that only a wagging tail can bring.

Abbreviations

ABWT – AB Wild-Type (zebrafish strain)

ACN – Acetonitrile

AIC – Akaike Information Criterion

ALH – Amplitude of Lateral Head Displacement

AOC3 – Amine Oxidase, Copper Containing 3 (Vascular Adhesion Protein-1)

ART – Assisted Reproductive Technology / Technologies

ATP – Adenosine Triphosphate

BD – Becton Dickinson (BD Biosciences)

BH – Benjamini–Hochberg (method for multiple-testing correction)

BH-FDR – Benjamini–Hochberg False Discovery Rate

BCF – Beat Cross Frequency

BPA – Bisphenol A

CASA – Computer-Assisted Sperm Analysis

CE – Collision Energy

CHIMERS – CHIMERS Search Engine (MSAID, Munich)

CID – Collision-Induced Dissociation

CO₂ – Carbon Dioxide

CRISPR – Clustered Regularly Interspaced Short Palindromic Repeats

CTNG – Gamma Catenin (Junction Plakoglobin / JUP)

CV – Compensation Voltage (FAIMS)

CytoNorm – Cytometry Normalization Algorithm (R package)

DAPI – 4',6-Diamidino-2-Phenylindole

DDSi – DNA Degradation Index

DEFB126 – Beta-Defensin 126

DESeq2 – Differential Expression Sequencing 2 (R package)

DHARMa – Residual Diagnostics for Hierarchical Regression Models (R package)

DNA – Deoxyribonucleic Acid

DTT – Dithiothreitol

EPPS – N-(2-Hydroxyethyl)piperazine-N'-(3-propanesulfonic acid)

FACS – Fluorescence-Activated Cell Sorting

FAIMS – Field Asymmetric Ion Mobility Spectrometry

FDR – False Discovery Rate

FISH – Fluorescence In Situ Hybridisation

FMO – Fluorescence Minus One (control)

f/s – Frames per Second

GIM – Genoinformative Marker

GLM – Generalised Linear Model

GO – Gene Ontology

HCD – Higher-energy Collisional Dissociation

HFEA – Human Fertilisation and Embryology Authority

HPA – Hypothalamic–Pituitary–Adrenal (axis)

HPG – Hypothalamic–Pituitary–Gonadal (axis)

HPLC – High-Performance Liquid Chromatography

HSF1 – Heat Shock Factor 1

HSP – Heat Shock Protein

HSP47 – Heat Shock Protein 47 (Serpin H1)

HSP70 – Heat Shock Protein 70

Hsp90 – Heat Shock Protein 90

HTF – Human Tubal Fluid (medium)

ICSI – Intracytoplasmic Sperm Injection

IHC – Immunohistochemistry

IQR – Interquartile Range

ISAS – Integrated Semen Analysis System

IZUMO1 – Izumo Sperm–Egg Fusion Protein 1

IVF – In Vitro Fertilisation

JUP – Junction Plakoglobin (γ -Catenin / CTNG)

JUNO – Oocyte Receptor for IZUMO1 (Folate Receptor 4)

KEGG – Kyoto Encyclopedia of Genes and Genomes

Kif – Kinesin-like Protein Family

LC–MS/MS – Liquid Chromatography–Tandem Mass Spectrometry

LFC – \log_2 Fold Change

LIN – Linearity (VSL/VCL \times 100)

MC – Methyl Cellulose (assay)

MS – Mass Spectrometry

MS1 / MS2 / MS3 – Mass Spectrometry stages 1–3

NaCl – Sodium Chloride

NCBI – National Center for Biotechnology Information
NH₄HCO₃ – Ammonium Bicarbonate
OLFM4 – Olfactomedin 4
OT – Orbitrap Mass Spectrometer
P1 – Primary Gated Sperm Population (in Flow Cytometry)
PBS – Phosphate Buffered Saline
PDB – Protein Data Bank
PE – R-Phycoerythrin
pH – Potential of Hydrogen
PFA – Paraformaldehyde
PLC ζ – Phospholipase C zeta
PyMOL – Python Molecular Graphics Viewer
R – R Statistical Programming Language
RNA – Ribonucleic Acid
rpm – Revolutions Per Minute
RTS – Real Time Search
SDS – Sodium Dodecyl Sulfate
SDC – Sodium Deoxycholate
SPE – Solid Phase Extraction
SPS – Synchronous Precursor Selection
SPAM1 – Sperm Adhesion Molecule 1
STR – Straightness (VSL/VAP \times 100)
STRING – Search Tool for the Retrieval of Interacting Genes / Proteins
SW – Swim-Up (assay)
TFA – Trifluoroacetic Acid
TMT – Tandem Mass Tag
TMT10 – Tandem Mass Tag 10-plex kit
TMTpro – Tandem Mass Tag Pro (high-plex version)
UHPLC – Ultra-High-Performance Liquid Chromatography
UniProt – Universal Protein Knowledgebase
VAP – Average Path Velocity
VCL – Curvilinear Velocity
VSL – Straight-Line Velocity
WOB – Wobble (VAP/VCL \times 100)

ZIRC – Zebrafish International Resource Center

ZMYND15 – Zinc Finger MYND-type Containing Protein 15

ZP – Zona Pellucida

Table of Contents

DECLARATION.....	2
ABSTRACT	3
ACKNOWLEDGEMENTS.....	4
ABBREVIATIONS.....	5
TABLE OF FIGURES.....	12
1 INTRODUCTION	16
1.1 IMPORTANCE OF SEXUAL REPRODUCTION	16
1.2 THE BIPHASIC LIFECYCLE	17
1.3 SEXUAL DIMORPHISM IN GAMETES	19
1.4 HAPLOID SELECTION IN GAMETES	20
1.5 POTENTIAL FOR HAPLOID SELECTION WITHIN EJACULATES	21
1.5.1 COMPETITION AMONG SPERM WITHIN AN EJACULATE	21
1.5.2 INTERACTION WITH THE FEMALE REPRODUCTIVE ENVIRONMENT	22
1.5.3 SELECTIVE BINDING AND FUSION WITH THE OOCYTE	22
1.6 EVIDENCE THAT SPERM FITNESS INFLUENCES OFFSPRING QUALITY	23
1.7 THE MALE FERTILITY CRISIS	24
1.8 CURRENT CLINICAL METHODS FOR SPERM SELECTION	26
1.9 THE GENOMIC AND TRANSCRIPTOMIC DIFFERENCES IN SPERM FITNESS	27
1.10 SPERM PROTEOMICS	28
1.11 WHAT IS A BIOMARKER?.....	30
1.12 BEYOND SPERM: THE TESTICULAR ORIGINS OF SPERM QUALITY.....	30
1.13 THE IMPORTANCE OF ANIMAL MODELS	31
1.14 THIS THESIS: THE MOLECULAR BIOMARKERS OF SPERM FITNESS.....	32
2 THE EFFECTS OF HEAT STRESS ON THE ZEBRAFISH TESTES PROTEOME	34
2.1 ABSTRACT.....	34
2.2 INTRODUCTION	35
2.3 METHODS	40
2.3.1 ZEBRAFISH HUSBANDRY	40
2.3.2 EXPERIMENTAL SET UP.....	40
2.3.3 PROTEIN EXTRACTION AND LC-MS/MS	41
2.3.4 WEIGHT DATA ANALYSIS	43
2.3.5 PROTEOME DATA ANALYSIS.....	44
2.4 RESULTS.....	46
2.4.1 RELATIVE TESTES WEIGHT	46
2.4.2 TESTES PROTEOME.....	51
2.4.3 THE GO TERMS AND STRING ANALYSIS	54
2.5 DISCUSSION	59
2.5.1 THE GLOBAL ZEBRAFISH TESTES PROTEOME	59
2.5.2 THE EFFECTS OF HEAT STRESS ON THE TESTES PROTEOME	59
2.5.3 THE EFFECTS OF HEAT STRESS ON TESTES SIZE	61
2.5.4 THE GO TERMS AND STRING ANALYSES OF HEAT-STRESSED TESTES.....	62

2.5.5 CONCLUSION	65
3 THE ZEBRAFISH SPERM PROTEOME	67
3.1 ABSTRACT.....	67
3.2 INTRODUCTION	68
3.3 METHODS.....	70
3.3.1 ZEBRAFISH HUSBANDRY AND EXPERIMENTAL SET UP	70
3.3.2 PROTEOMICS.....	71
3.3.3 DATA ANALYSIS	73
3.4 RESULTS.....	74
3.5 DISCUSSION	78
4 THE PROTEOMIC BIOMARKERS OF HUMAN SPERM QUALITY	83
4.1 ABSTRACT.....	83
4.2 INTRODUCTION	84
4.3 METHODS.....	88
4.3.1 SPERM PARAMETER ANALYSIS.....	88
4.3.2 SPERM SELECTION ASSAYS	88
4.3.3 SAMPLE PREPARATION FOR PROTEOMICS	89
4.3.4 PROTEIN EXTRACTION AND PEPTIDE PREPARATION	90
4.3.5 TMT LABELLING AND FRACTIONATION	90
4.3.6 MASS SPECTROMETRY ACQUISITION	90
4.3.7 DATA PROCESSING AND PROTEIN IDENTIFICATION.....	91
4.3.8 FILTERING AND STRUCTURAL ANALYSIS	91
4.4 RESULTS.....	91
4.5 DISCUSSION	102
4.5.1 OVERVIEW OF FINDINGS AND PROTEOMIC DEPTH.....	102
4.5.2 COMPARISON OF SELECTION METHODS	103
4.5.3 CANDIDATE BIOMARKERS.....	104
4.5.4 FUNCTIONAL ENRICHMENT ANALYSIS	106
4.5.5 INTEGRATION WITH GENOMIC DATA.....	107
4.5.6 EXPERIMENTAL DESIGN LIMITATIONS	108
4.5.7 CONCLUSION	109
5 VALIDATION OF CELL SURFACE BIOMARKERS FOR SPERM LONGEVITY AND FITNESS	110
5.1 ABSTRACT.....	110
5.2 INTRODUCTION	111
5.3 METHODS.....	118
5.3.1 BIOMARKER CANDIDATE SELECTION	118
5.3.2 BIOMARKER TITRATION AND EXPERIMENTAL DESIGN.....	118
5.3.3 SAMPLE COLLECTION AND PREPARATION.....	119
5.3.4 FLOW CYTOMETRY	120
5.3.5 DATA ANALYSIS AND STATISTICAL MODELLING	121
5.4 RESULTS.....	122
5.4.1 OLFM4	122

5.4.2	CTNG.....	125
5.4.3	AOC3.....	128
5.5	DISCUSSION	131
6	GENERAL DISCUSSION.....	135
6.1	EVIDENCE OF THE EFFECT OF ENVIRONMENTAL STRESS ON SPERM PRODUCTION.....	137
6.2	EVIDENCE OF PHENOTYPIC VARIATION BETWEEN EJACULATES.....	139
6.3	EVIDENCE OF WITHIN-EJACULATE SPERM VARIATION	141
6.4	VALIDATION OF BIOMARKERS OF SPERM FITNESS.....	145
6.5	MOLECULAR EVIDENCE SUPPORTING HAPLOID SELECTION	147
6.6	CROSS-SPECIES TRANSLATION AND MODEL CHOICE	148
6.7	BROADER IMPLICATIONS	149
6.7.1	EVOLUTIONARY SIGNIFICANCE	149
6.7.2	RELEVANCE TO HUMAN FERTILITY AND ART.....	150
6.8	CRITICAL REFLECTIONS AND LIMITATIONS.....	151
6.9	FUTURE DIRECTIONS	152
6.10	CONCLUSIONS.....	155
APPENDIX.....		156
REFERENCES		157

1 Table of Figures

2 FIGURE 2-1: SCATTERPLOT SHOWING THE RELATIONSHIP BETWEEN SOMATIC BODY WEIGHT (TOTAL BODY	46
3 MASS MINUS TESTES; X-AXIS) AND CORRECTED TESTIS MASS (Y-AXIS) FOR INDIVIDUAL MALES IN THE	
4 CONTROL (28°C, BLUE) AND HEAT-TREATED (34°C, RED) GROUPS. POINTS REPRESENT INDIVIDUAL	
5 FISH, AND COLOURED LINES SHOW GROUP-SPECIFIC LINEAR REGRESSION FITS WITH 95%	
6 CONFIDENCE INTERVALS.	
7 FIGURE 2-2: EFFECT OF HEAT TREATMENT ON ZEBRAFISH BODY WEIGHT AND TESTES WEIGHT- SCATTER PLOTS SHOW	51
8 INDIVIDUAL VALUES FOR CONTROL (N = 21) AND HEAT-TREATED FISH (N =21), WITH RED DOTS INDICATING THE	
9 MEAN AND ERROR BARS REPRESENTING STANDARD ERROR OF THE MEAN. A) TOTAL FISH WEIGHT BEFORE	
10 TREATMENT (T0) , B) TOTAL SOMATIC WEIGHT AFTER TREATMENT (T2W) , CALCULATED AS TOTAL BODY WEIGHT	
11 MINUS TESTES , C) TESTES WEIGHT AFTER TREATMENT AND D) PROPORTION OF TOTAL BODY WEIGHT ACCOUNTED	
12 FOR BY TESTES MASS	
13 FIGURE 2-3- HEATMAP AND VOLCANO PLOT OF DIFFERENCES IN TESTES PROTEOME AS A RESULT OF HEAT STRESS. (A)	53
14 VOLCANO PLOT SHOWING THE 5415 IDENTIFIED PROTEINS, WITH SIGNIFICANTLY MORE ABUNDANT PROTEINS IN	
15 HEAT TREATED TESTES ($P_{ADJ} < 0.05$, LFC > 0.5) SHOWN IN ORANGE, WHILST SIGNIFICANTLY LESS ABUNDANT	
16 PROTEINS IN HEAT TREATED TESTES ($P_{ADJ} < 0.05$, LFC < -0.5) SHOWN IN VIOLET. (B) A HEATMAP WITH ALL 5415	
17 IDENTIFIED PROTEINS LFC > 0.5 AND $P_{ADJ} < 0.05$	
18 FIGURE 2-4: GO TERMS OF GENES LINKED TO PROTEINS THAT ARE DOWNREGULATED IN HEAT-STRESSED ZEBRAFISH	55
19 TESTES. DOT PLOTS SHOWING THE TOP 10 TERMS FOR EACH GO ANALYSIS (BIOLOGICAL PROCESSES, CELLULAR	
20 COMPONENTS AND MOLECULAR FUNCTION) AND KEGG PATHWAYS ENRICHED FOR PROTEINS THAT WERE LESS	
21 ABUNDANT IN HEAT TREATED TESTES COMPARED TO CONTROL TESTES. THE GO TERMS WERE CALCULATED AGAINST	
22 A BACKGROUND OF THE ENTIRE ZEBRAFISH GENOME.	
23 FIGURE 2-5: GO TERMS OF GENES LINKED TO PROTEINS THAT ARE UPREGULATED IN HEAT-STRESSED ZEBRAFISH TESTES.	56
24 DOT PLOTS SHOWING THE TOP 10 TERMS FOR EACH GO TERM (BIOLOGICAL PROCESSES, CELLULAR COMPONENTS	
25 AND MOLECULAR FUNCTION) AND KEGG PATHWAYS ENRICHED FOR PROTEINS THAT WERE MORE ABUNDANT IN	
26 HEAT TREATED TESTES COMPARED TO CONTROL TESTES. THESE GO TERMS WERE CALCULATED AGAINST A	
27 BACKGROUND OF THE ENTIRE ZEBRAFISH GENOME.	
28 FIGURE 2-6- STRING NETWORK OF PROTEIN–PROTEIN INTERACTIONS FOR PROTEINS SIGNIFICANTLY LESS	57
29 ABUNDANT IN TESTES OF HEAT-TREATED MALES ($P_{ADJ} F < 0.05$, LFC ≤ -0.5). NODES REPRESENT	
30 PROTEINS AND ARE COLOUR-CODED ACCORDING TO STRING FUNCTIONAL ENRICHMENT CLUSTERS.	
31 EACH NODE CONTAINS THE PREDICTED TERTIARY STRUCTURE GENERATED BY THE STRING/PDB	
32 MODEL. EDGES REPRESENT PROTEIN–PROTEIN ASSOCIATIONS, WITH EDGE COLOURS INDICATING THE	
33 EVIDENCE SOURCE; KNOWN INTERACTIONS: CURATED DATABASES (LIGHT BLUE), EXPERIMENTALLY	
34 DETERMINED (PINK), PREDICTED INTERACTIONS: GENE NEIGHBOURHOOD (GREEN), GENE FUSIONS	
35 (RED), GENE CO-OCCURRENCE (BLUE), OTHER EVIDENCE: TEXT MINING (YELLOW), CO-EXPRESSION	
36 (BLACK), PROTEIN HOMOLOGY (PURPLE). A MINIMUM INTERACTION CONFIDENCE SCORE OF 0.7 (HIGH	
37 CONFIDENCE) WAS APPLIED, AND ALL DISCONNECTED PROTEINS WERE HIDDEN.	
38 FIGURE 2-7- STRING NETWORK OF PROTEIN–PROTEIN INTERACTIONS FOR PROTEINS SIGNIFICANTLY	58
39 MORE ABUNDANT IN TESTES OF HEAT-TREATED MALES ($P_{ADJ} < 0.05$, LFC ≥ 0.5). NODES REPRESENT	
40 PROTEINS AND ARE COLOUR-CODED ACCORDING TO STRING FUNCTIONAL ENRICHMENT CLUSTERS.	
41 EACH NODE CONTAINS THE PREDICTED TERTIARY STRUCTURE OF THE PROTEIN, AS GENERATED BY	
42 THE STRING/PDB MODELLING PIPELINE. EDGES REPRESENT PREDICTED OR KNOWN PROTEIN–	
43 PROTEIN ASSOCIATIONS, AND EDGE COLOURS CORRESPOND TO THE SPECIFIC UNDERLYING EVIDENCE	
44 SOURCE: KNOWN INTERACTIONS: CURATED DATABASES (LIGHT BLUE), EXPERIMENTALLY DETERMINED	
45 (PINK), PREDICTED INTERACTIONS: GENE NEIGHBOURHOOD (GREEN), GENE FUSIONS (RED), GENE CO-	
46 OCCURRENCE (BLUE), OTHER EVIDENCE SOURCES: TEXT MINING (YELLOW), CO-EXPRESSION (BLACK),	
47 PROTEIN HOMOLOGY (PURPLE). A MINIMUM INTERACTION CONFIDENCE SCORE OF 0.7 (HIGH	
48 CONFIDENCE) WAS APPLIED. DISCONNECTED PROTEINS WERE HIDDEN TO IMPROVE CLARITY OF THE	
49 INTERACTION NETWORK.	
50 FIGURE 2-8: VENN DIAGRAMS COMPARING THE ZEBRAFISH TESTES PROTEOME AND ZEBRAFISH SPERM PROTEOME	
51 (CHAPTER 3). (A) VENN DIAGRAM REPRESENTING THE OVERALL OVERLAP BETWEEN THE ZEBRAFISH SPERM	
52 PROTEOME (CHAPTER 3) WITH THE COMBINED ZEBRAFISH TESTES PROTEOME. (B) VENN DIAGRAM SHOWING THE	
53 OVERLAP OF THE SPERM PROTEOME (CHAPTER 3) WITH THE SIGNIFICANT PROTEINS OF HIGHER ABUNDANCE IN THE	

54	HEAT-TREATED TESTES. (C) VENN DIAGRAM SHOWING THE OVERLAP OF THE SPERM PROTEOME (CHAPTER 3) WITH	
55	THE SIGNIFICANT PROTEINS OF LOWER ABUNDANCE IN THE HEAT-TREATED TESTES.....	64
56	FIGURE 3-1: HEATMAP COMPARING HEAT-TREATED AND CONTROL SPERM PROTEOMES, SHOWING THE 4168	
57	QUANTIFIABLE PROTEINS IDENTIFIED. LOG SCALE.	75
58	FIGURE 3-2: THE STRING DATABASE MAP GENERATED THROUGH THE INPUT OF THE PROTEIN ACCESSION ID OF THE 25	
59	MOST ABUNDANT PROTEINS DETECTED IN THIS DATA.....	76
60	FIGURE 3-3: TOP 20 GO TERMS RANKED BY FOLD-ENRICHMENT FOR THE ZEBRAFISH SPERM PROTEOME, BASED ON THE	
61	4844 ASSIGNED GENEIDs FOR (A) CELLULAR COMPONENT GO TERMS, (B) BIOLOGICAL PROCESS GO TERMS AND	
62	(C) MOLECULAR FUNCTION GO TERMS FOR THE SPERM PROTEOME.....	77
63	FIGURE 4-1: OVERLAP OF CONFIDENTLY IDENTIFIED PROTEINS ACROSS ALL DONORS. VENN DIAGRAM SHOWING THE	
64	INTERSECTION OF PROTEINS IDENTIFIED IN EACH OF THE FIVE HUMAN DONORS FOLLOWING TMT-LABELLED LC-	
65	MS/MS. PROTEINS WERE RETAINED IN THE FINAL DATASET IF THEY WERE SUPPORTED BY AT LEAST TWO UNIQUE	
66	PEPTIDES AND DETECTED IN A MINIMUM OF THREE DONORS, RESULTING IN A HIGH-CONFIDENCE PROTEOME OF	
67	4,616 PROTEINS USED FOR DOWNSTREAM COMPARATIVE AND ENRICHMENT ANALYSES.....	92
68	FIGURE 4-2: VOLCANO PLOTS SHOWING DIFFERENTIAL PROTEIN ABUNDANCE BETWEEN SELECTED AND UNSELECTED	
69	SPERM POOLS. THE PLOTS DISPLAY THE $-\log_2$ FOLD-CHANGE IN PROTEIN ABUNDANCE (X-AXIS) AGAINST THE $-\log_{10} P_{adj}$ (Y-AXIS) FOR EACH DONOR, COMPARING SELECTED (T4/EDGE) AND UNSELECTED (T0/CENTRE) SPERM	
70	SUBPOPULATIONS. PROTEINS WITH SIGNIFICANTLY HIGHER (RIGHT, PURPLE) OR LOWER (LEFT, ORANGE)	
71	ABUNDANCE IN SELECTED SPERM ARE HIGHLIGHTED. THE TOP CANDIDATE PROTEINS, SHORTLISTED BASED ON	
72	CONSISTENCY ACROSS DONORS AND MAGNITUDE OF CHANGE, ARE LABELLED ON EACH PLOT. CUT-OFF	
73	THRESHOLDS FOR DIFFERENTIAL ABUNDANCE INCLUDED A MINIMUM TWOFOLD CHANGE ACROSS AT LEAST THREE	
74	DONORS AND A $P_{adj} < 0.05$ IN AT LEAST ONE DONOR.	93
75	FIGURE 4-3: A) BUBBLE PLOT SHOWING THE TOP 10 SIGNIFICANTLY ENRICHED GO BIOLOGICAL PROCESS TERMS	
76	AMONG PROTEINS WITH LOWER ABUNDANCE IN SELECTED SPERM COMPARED TO UNSELECTED SPERM. B) BUBBLE	
77	PLOT SHOWING THE TOP 10 SIGNIFICANTLY ENRICHED GO BIOLOGICAL PROCESS TERMS AMONG PROTEINS WITH	
78	HIGHER ABUNDANCE IN SELECTED SPERM COMPARED TO UNSELECTED SPERM. GENE ONTOLOGY (GO) TERM	
79	ANALYSIS WAS PERFORMED USING BIOMART (HAW ET AL., 2011; SMEDLEY ET AL., 2015) AND BIOCONDUCTOR	
80	(GENTLEMAN ET AL., 2004) PACKAGES THROUGH R.	96
81	FIGURE 4-4: A) BUBBLE PLOT DISPLAYING THE TOP 10 GO CELLULAR COMPONENT ENRICHMENT FOR PROTEINS WITH	
82	LOWER ABUNDANCE IN SELECTED SPERM. B) BUBBLE PLOT DISPLAYING THE TOP 10 GO CELLULAR COMPONENT	
83	ENRICHMENT FOR PROTEINS WITH HIGHER ABUNDANCE IN SELECTED SPERM. GENE ONTOLOGY (GO) TERM	
84	ANALYSIS WAS PERFORMED USING BIOMART (HAW ET AL., 2011; SMEDLEY ET AL., 2015) AND BIOCONDUCTOR	
85	(GENTLEMAN ET AL., 2004) PACKAGES THROUGH R.	97
86	FIGURE 4-5: A) BUBBLE PLOT DISPLAYING THE TOP 10 GO MOLECULAR FUNCTION ENRICHMENT FOR PROTEINS WITH	
87	LOWER ABUNDANCE IN SELECTED SPERM. B) BUBBLE PLOT DISPLAYING THE TOP 10 GO MOLECULAR FUNCTION	
88	ENRICHMENT FOR PROTEINS WITH HIGHER ABUNDANCE IN SELECTED SPERM. GENE ONTOLOGY (GO) TERM	
89	ANALYSIS WAS PERFORMED USING BIOMART (HAW ET AL., 2011; SMEDLEY ET AL., 2015) AND BIOCONDUCTOR	
90	(GENTLEMAN ET AL., 2004) PACKAGES THROUGH R.	98
91	FIGURE 4-6: A) BUBBLE PLOT DISPLAYING THE TOP 10 KEGG PATHWAY ENRICHMENT FOR PROTEINS WITH LOWER	
92	ABUNDANCE IN SELECTED SPERM. B) BUBBLE PLOT DISPLAYING THE TOP 10 KEGG PATHWAY ENRICHMENT FOR	
93	PROTEINS WITH HIGHER ABUNDANCE IN SELECTED SPERM. GENE ONTOLOGY (GO) TERM ANALYSIS WAS	
94	PERFORMED USING BIOMART (HAW ET AL., 2011; SMEDLEY ET AL., 2015) AND BIOCONDUCTOR (GENTLEMAN ET	
95	AL., 2004) PACKAGES THROUGH R.	99
96	FIGURE 4-7: BUBBLE PLOTS DISPLAYING THE TOP 10 GO TERMS ENRICHED FOR BIOLOGICAL PROCESSES, CELLULAR	
97	COMPONENTS, MOLECULAR FUNCTIONS AND KEGG PATHWAYS FOR SHORTLISTED PROTEINS HIGHER IN	
98	ABUNDANCE IN SELECTED SPERM. GENE ONTOLOGY (GO) TERM ANALYSIS WAS PERFORMED USING BIOMART	
99	(HAW ET AL., 2011; SMEDLEY ET AL., 2015) AND BIOCONDUCTOR (GENTLEMAN ET AL., 2004) PACKAGES	
100	THROUGH R.	100
101	FIGURE 4-8: BUBBLE PLOTS DISPLAYING THE TOP 10 GO TERMS ENRICHED FOR BIOLOGICAL PROCESSES, CELLULAR	
102	COMPONENTS, MOLECULAR FUNCTIONS AND KEGG PATHWAYS FOR SHORTLISTED PROTEINS LOWER IN	
103	ABUNDANCE IN SELECTED SPERM. GENE ONTOLOGY (GO) TERM ANALYSIS WAS PERFORMED USING BIOMART	
104	(HAW ET AL., 2011; SMEDLEY ET AL., 2015) AND BIOCONDUCTOR (GENTLEMAN ET AL., 2004) PACKAGES	
105	THROUGH R.	101
106	FIGURE 4-9: OVERLAP OF CONFIDENTLY IDENTIFIED PROTEINS ACROSS THE THREE TMT EXPERIMENTS AND TWO	
107	GENOMICS DATASETS (MARCU, 2024). VENN DIAGRAM SHOWING THE INTERSECTION OF PROTEINS IDENTIFIED IN	
108	EACH OF THE THREE TMT-LABELLED LC-MS/MS. PROTEIN IDs WERE CONVERTED TO ENTREZ IDs WHICH WERE	
109	COMPARED WITH THE ENTREZ IDs DETERMINED BY MARCU ET AL. 2024.	102
110		

111	FIGURE 5-1: GATING STRATEGY USED FOR IMAGING FLOW CYTOMETRY ACQUISITION. GRAPHS GENERATED USING BD	121
112	FACSCORUS SOFTWARE ILLUSTRATING THE GATING STRATEGY USED DURING SAMPLE ACQUISITION ON THE BD	
113	FACSDISCOVERY S8 IMAGING FLOW CYTOMETER. GATING WAS PERFORMED TO IDENTIFY A P1 POPULATION OF	
114	SINGLE SPERM CELLS BASED ON FORWARD AND SIDE SCATTER PROPERTIES, AND TO EXCLUDE DEBRIS AND	
115	AGGREGATES. GATES WERE VALIDATED USING THE IMAGES GENERATED ON THE S8.	121
116	FIGURE 5-2: OLFM4 STAINING RESULTS ACROSS DONORS. BIEXPONENTIAL FLOW CYTOMETRY PLOTS DISPLAYING	
117	OLFM4 STAINING ON SPERMATOZOA FROM EACH DONOR, WITH EFLUOR 520 VIABILITY STAINING ON THE Y-AXIS	
118	AND OLFM4-PE FLUORESCENCE ON THE X-AXIS. EACH PLOT REPRESENTS A SINGLE DONOR SAMPLE. THE FIRST	
119	TEN CELL IMAGES FROM EACH SAMPLE, CAPTURED USING THE BD FACSDISCOVERY S8 IMAGING SYSTEM, ARE	
120	SHOWN BELOW THE CORRESPONDING PLOT TO ILLUSTRATE REPRESENTATIVE STAINING PATTERNS AND CELL	
121	MORPHOLOGY. GATING WAS APPLIED TO DISTINGUISH LIVE AND DEAD SPERM CELLS, AND TO ASSESS OLFM4	
122	SURFACE EXPRESSION UNDER NON-PERMEABILISED CONDITIONS. THREE GATING POPULATIONS, LIVE CELLS,	
123	DEAD CELLS, AND OLFM4-POSITIVE CELLS, WERE APPLIED FOR ALL SAMPLES TO SUPPORT STANDARDISED	
124	COMPARISON ACROSS DONORS.....	123
125	FIGURE 5-3: CTNG STAINING RESULTS ACROSS DONORS. BIEXPONENTIAL FLOW CYTOMETRY PLOTS DISPLAYING CTNG	
126	STAINING ON SPERMATOZOA FROM EACH DONOR, WITH EFLUOR 520 VIABILITY STAINING ON THE Y-AXIS AND	
127	CTNG-V450 FLUORESCENCE ON THE X-AXIS. EACH PLOT REPRESENTS A SINGLE DONOR SAMPLE. THE FIRST TEN	
128	CELL IMAGES FROM EACH SAMPLE, CAPTURED USING THE BD FACSDISCOVERY S8 IMAGING SYSTEM, ARE SHOWN	
129	BELOW THE CORRESPONDING PLOT TO ILLUSTRATE REPRESENTATIVE STAINING PATTERNS AND CELL MORPHOLOGY.	
130	GATING WAS APPLIED TO DISTINGUISH LIVE AND DEAD SPERM CELLS, AND TO ASSESS CTNG SURFACE	
131	EXPRESSION UNDER NON-PERMEABILISED CONDITIONS. THREE GATING POPULATIONS, LIVE CELLS, DEAD CELLS,	
132	AND CTNG-POSITIVE CELLS, WERE APPLIED FOR ALL SAMPLES TO SUPPORT STANDARDISED COMPARISON ACROSS	
133	DONORS.....	126
134	FIGURE 5-4: AOC3 STAINING RESULTS ACROSS DONORS. BIEXPONENTIAL FLOW CYTOMETRY PLOTS DISPLAYING AOC3	
135	STAINING ON SPERMATOZOA FROM EACH DONOR, WITH EFLUOR 520 VIABILITY STAINING ON THE Y-AXIS AND	
136	AOC3-AF594 FLUORESCENCE ON THE X-AXIS. EACH PLOT REPRESENTS A SINGLE DONOR SAMPLE. THE FIRST TEN	
137	CELL IMAGES FROM EACH SAMPLE, CAPTURED USING THE BD FACSDISCOVERY S8 IMAGING SYSTEM, ARE SHOWN	
138	BELOW THE CORRESPONDING PLOT TO ILLUSTRATE REPRESENTATIVE STAINING PATTERNS AND CELL MORPHOLOGY.	
139	GATING WAS APPLIED TO DISTINGUISH LIVE AND DEAD SPERM CELLS, AND TO ASSESS AOC3 SURFACE EXPRESSION	
140	UNDER NON-PERMEABILISED CONDITIONS.....	129
141	TABLE 2-1- RESULTS FOR GAMMA GLM 1- CORRECTED TESTES WEIGHTS AGAINST FINAL BODY WEIGHT. .47	
142	TABLE 2-2- RESULTS FOR GAMMA GLM 2- CORRECTED TESTES WEIGHTS AGAINST ADJUSTED FINAL BODY	
143	WEIGHT.	48
144	TABLE 2-3- RESULTS FOR GAMMA GLM 3- PROPORTION AGAINST ADJUSTED FINAL BODY WEIGHT.....49	
145	TABLE 2-4- RESULTS FOR GAMMA GLM 4- TESTES CORRECTED AGAINST CHANGE IN BODY WEIGHT.50	
146	TABLE 4-1: NUMBER OF PROTEINS OF SIGNIFICANTLY HIGHER AND LOWER ABUNDANCE IN SELECTED	
147	SPERM BY DONOR.....	95
148	TABLE 5-1: PROPORTION OF CELLS WITHIN LIVE/DEAD GATES AND ABOVE THE THRESHOLD OF 10^5 (OLFM4-	
149	POSITIVE). FLOW-CYTOMETRY-DERIVED CELL COUNTS AND PERCENTAGES FOR EACH OLFM4-	
150	STAINED SAMPLE. “TOTAL DEAD” AND “TOTAL LIVE” CORRESPOND TO EVENTS FALLING WITHIN THE	
151	VIABILITY GATES; CELLS THAT FELL BETWEEN GATES AND COULD NOT BE CLASSIFIED WERE THEREFORE	
152	EXCLUDED FROM THE DATASET. “DEAD + POSITIVE” AND “LIVE + POSITIVE” REPRESENT THE SUBSETS	
153	WITHIN EACH VIABILITY GATE THAT WERE OLFM4-POSITIVE. PERCENTAGES ARE SHOWN RELATIVE TO	
154	P1 (ALL CONFIRMED SINGLET SPERM CELLS). “TOTAL CELL COUNT” REFLECTS ALL RECORDED EVENTS	
155	WITHIN P1.....	124
156	TABLE 5-2: GENERALISED LINEAR MIXED-EFFECTS MODEL (GLMM) RESULTS COMPARING OLFM4	
157	EXPRESSION ON LIVE VERSUS DEAD SPERM CELLS.	125
158	TABLE 5-3: PROPORTION OF CELLS WITHIN LIVE/DEAD GATES AND ABOVE THE THRESHOLD OF 10^5 (CTNG	
159	POSITIVE). FLOW-CYTOMETRY-DERIVED CELL COUNTS AND PERCENTAGES FOR EACH CTNG-STAINED	
160	SAMPLE. “TOTAL DEAD” AND “TOTAL LIVE” CORRESPOND TO EVENTS FALLING WITHIN THE VIABILITY	
161	GATES; CELLS THAT FELL BETWEEN GATES AND COULD NOT BE CLASSIFIED WERE THEREFORE	
162	EXCLUDED FROM THE DATASET. “DEAD + POSITIVE” AND “LIVE + POSITIVE” REPRESENT THE SUBSETS	
163	WITHIN EACH VIABILITY GATE THAT WERE CTNG- POSITIVE. PERCENTAGES ARE SHOWN RELATIVE TO	

164	P1 (ALL CONFIRMED SINGLET SPERM CELLS). “TOTAL CELL COUNT” REFLECTS ALL RECORDED EVENTS	
165	WITHIN P1.....	127
166	TABLE 5-4: GENERALISED LINEAR MODEL (GLMM) RESULTS COMPARING CTNG EXPRESSION ON LIVE	
167	VERSUS DEAD SPERM CELLS.	128
168	TABLE 5-5: PROPORTION OF CELLS WITHIN LIVE/DEAD GATES AND ABOVE THE THRESHOLD OF 10^5 (AOC3	
169	POSITIVE). FLOW-CYTOMETRY-DERIVED CELL COUNTS AND PERCENTAGES FOR EACH AOC3-STAINED	
170	SAMPLE. “TOTAL DEAD” AND “TOTAL LIVE” CORRESPOND TO EVENTS FALLING WITHIN THE VIABILITY	
171	GATES; CELLS THAT FELL BETWEEN GATES AND COULD NOT BE CLASSIFIED WERE THEREFORE	
172	EXCLUDED FROM THE DATASET. “DEAD + POSITIVE” AND “LIVE + POSITIVE” REPRESENT THE SUBSETS	
173	WITHIN EACH VIABILITY GATE THAT WERE AOC3-POSITIVE. PERCENTAGES ARE SHOWN RELATIVE TO	
174	P1 (ALL CONFIRMED SINGLET SPERM CELLS). “TOTAL CELL COUNT” REFLECTS ALL RECORDED EVENTS	
175	WITHIN P1.....	130
176	TABLE 5-6: GENERALISED LINEAR MIXED EFFECTS MODEL (GLMM) RESULTS COMPARING AOC3	
177	EXPRESSION ON LIVE VERSUS DEAD SPERM CELLS.	131
178		
179		

180 **1 Introduction**

181 **1.1 Importance of Sexual Reproduction**

182 Reproduction is the fundamental biological process by which life persists. Without
183 this ability, no population can survive more than a single generation. Reproduction
184 can broadly be categorised into sexual and asexual processes. Asexual
185 reproduction involves the production of genetically identical offspring from a single
186 parent, without the fusion of gametes, while sexual reproduction involves the
187 combination of genetic material from two parents through the fusion of gametes,
188 generating genetically diverse offspring. However, this is complicated as most
189 eukaryotic life can be considered partially clonal and therefore undergo both
190 asexual and sexual reproduction throughout their lifetime (Beukeboom & Perrin,
191 2014; Krueger-Hadfield, 2024).

192
193 Sexual reproduction is achieved in a variety of ways across taxa. Dioecious
194 species have distinct male and female individuals with distinct gamete cells which
195 undergo fusion to form an offspring, while hermaphroditic species possess both
196 sets of reproductive organs and produce male and female gametes, either
197 simultaneously or sequentially. Current scientific theory suggests that dioecious
198 species evolved via an intermediate state of gynodioecy from hermaphroditic
199 ancestors. The evolutionary trade-offs between these systems have previously
200 been predicted to depend on mate availability, ecological stability, and the
201 importance of outcrossing for maintaining genetic health (Otto & Lenormand,
202 2002).

203
204 Sexual reproduction is energetically expensive and inefficient because it requires
205 the production of specialised gametes, the maintenance of complex reproductive
206 systems, and the coordination of mating behaviours that often involve significant
207 energy expenditure and risk (Wootton, 1985). Sexual reproduction results in only
208 half of an individual's genes being passed on to offspring, the so-called "two-fold
209 cost of sex" (Gibson et al., 2017). Despite these costs, sexual reproduction
210 remains nearly universal among eukaryotes, suggesting that that there are long-

211 term evolutionary advantages that outweigh its short-term inefficiencies. These
212 advantages, including the generation of genetic diversity and the removal of
213 deleterious mutations, underpin the evolution of the biphasic lifecycle.

214

215 **1.2 The Biphasic Lifecycle**

216 Amongst sexually reproducing eukaryotic organisms, the alternation between
217 haploid and diploid genomes, known as the biphasic lifecycle, is ubiquitous
218 (Strasburger, 1905), where the haploid phase has one set of chromosomes, and
219 the diploid phase has two copies of each chromosome (Immler, 2019; Otto &
220 Goldstein, 1992). These phases are separated by several processes, including
221 meiosis, fertilisation, syngamy, and zygote formation (Purchase et al., 2021).
222 There are three main categories of biphasic life cycles: diplontic, haplontic, and
223 haplo-diplontic (Mable & Otto, 1998).

224

225 In diplontic organisms, such as higher animals and some land plants, the diploid
226 phase is dominant, and only a short part of the lifecycle occurs in the haploid
227 phase. Conversely, in haplontic organisms, such as green algae, it is the haploid
228 phase in which the majority of development occurs. Many types of moss, ferns,
229 and fungi are considered to have a haploid-diplontic lifecycle, as development
230 occurs substantially within both diploid and haploid phases (Hughes & Otto, 1999).
231 Each lifecycle has advantages and disadvantages, primarily due to the differences
232 in how natural selection can act to induce genetic variation depending on the
233 ploidy of the genome.

234

235 Selection operates differently on haploid and diploid genomes because alleles in
236 diploids can be masked by their homologous partners. Many deleterious mutations
237 are known to be at least partly recessive (Caballero & García-Dorado, 2013; C. D.
238 Jenkins & Kirkpatrick, 1995), meaning that their negative effects are expressed
239 only when both alleles at a locus have the mutation. In diploid organisms, the
240 presence of a non-mutated allele can therefore conceal (“mask”) the effect of a
241 harmful mutation, reducing its exposure to purifying selection (Mable & Otto, 1998;
242 Michod & Gayley, 1992). This masking effect allows deleterious alleles to persist

243 at low frequencies in populations, increasing the overall genetic load (Mable &
244 Otto, 1998; Michod & Gayley, 1992).

245

246 In phenotypes expressed by haploid genomes, each locus carries a single allele,
247 so every mutation, beneficial or deleterious, is directly exposed to selection if
248 expressed (Mable & Otto, 1998, 2001) . Consequently, population genetic models
249 have shown that purifying selection acts more efficiently on phenotypes expressed
250 by haploid rather than by diploid genomes, resulting in faster removal of recessive
251 deleterious mutations (Immler & Otto, 2018; Mable & Otto, 1998; Michod &
252 Gayley, 1992). While this direct exposure increases the risk that an individual
253 haploid will suffer the immediate effects of harmful mutations, it also accelerates
254 the elimination of such alleles from the population as a whole.

255

256 Because of masking, when directly compared, individuals with diploid genomes
257 are often shown to have a higher fitness (Perrot et al., 1991). However, due to the
258 increased effects of purifying selection, overall populations with haploid genomes
259 may be considered to have a higher fitness than diploitic populations (Mable &
260 Otto, 1998). Higher fitness effects of masking were observed when the initial
261 responses of both haploid and diploid *Saccharomyces cerevisiae* yeast to a
262 mutagenic environment were compared, although both ploidy samples recovered
263 fitness at similar rates (Mable & Otto, 2001). This suggests that, while masking is
264 effective in preventing a rapid loss of fitness in response to mutation, the
265 increased selective pressure experienced by haploid genomes enables faster
266 recovery of fitness in response to a mutagenic event.

267

268 Overall, a predominantly diploid phase may be evolutionarily favoured in
269 environments with weak selection against deleterious mutations and strong
270 dominance of wild-type alleles, while haploid phases are favoured when selection
271 is strong and mutation rates are high (C. D. Jenkins & Kirkpatrick, 1995; Mable &
272 Otto, 2001; Otto & Goldstein, 1992; Otto & Marks, 1996; Perrot et al., 1991).
273 These contrasting outcomes underscore how the balance between exposure and
274 masking of genetic variation shapes the evolution of the biphasic lifecycle.

275 In diploontic species, the haploid phase is restricted to the gametes and, in some
276 lineages, to mitochondrial genomes. Consequently, gametes represent a key
277 stage where selection acts directly on haploid phenotypes before fertilisation, with
278 direct effect on the evolution of the offspring produced (Immler, 2019).

279

280 **1.3 Sexual Dimorphism in Gametes**

281 Most species that undergo sexual reproduction exhibit anisogamy, where males
282 and females produce gametes of different sizes. Male gametes are by definition
283 smaller and produced in larger quantities, whereas female gametes are larger but
284 typically produced in smaller quantities. These differences arise from a fixed
285 energy budget for gamete production, where the total reproductive investment per
286 individual is constrained. Under such constraints, the number of gametes that can
287 be produced is inversely related to their size. Because zygote size is positively
288 correlated with zygote fitness, selection favours the evolution of one large,
289 resource-rich gamete and one of many small, mobile gamete when fusion occurs
290 between dissimilar gametes (Parker et al., 1972).

291

292 This pattern is explained by disruptive selection theory, which proposes that
293 gamete size variation was driven by selection favouring two extremes under
294 conditions of random gamete fusion, as originally modelled for external fertilisers
295 (Parker et al., 1972) Large gametes have a higher probability of successful zygote
296 development due to greater energetic reserves, while smaller gametes gain an
297 advantage through increased numbers and encounter rates. Over evolutionary
298 time, these contrasting selective pressures produced the differentiation between
299 oocytes and sperm, an outcome that persists even in species with internal
300 fertilisation and reduced sperm competition (Parker, 1982).

301

302 Because oocytes are relatively few, energetically costly to produce, and have a
303 high probability of being fertilised, they experience limited opportunity for haploid
304 selection (Parker et al., 1972). Sperm, by contrast, are numerous, less
305 energetically costly, and subject to intense post-copulatory competition and
306 selection pressures. This suggests that haploid selection will have less opportunity

307 to act on the oocytes than on the smaller, more numerous, less costly, and more
308 varied sperm (Immler & Otto, 2018).

309

310 **1.4 Haploid Selection in Gametes**

311 In predominantly diploid organisms, such as many animals, the haploid phase is
312 restricted to the gametes, providing a brief but potentially important window during
313 which selection can act directly on haploid phenotypes before fertilisation (Mable &
314 Otto, 1998; Perrot et al., 1991). The theoretical possibility of haploid selection has
315 long been recognised, as alleles in haploid genomes are directly exposed to
316 selection without the masking effects of dominance that occur in diploids (Immler,
317 2019; Immler & Otto, 2018).

318

319 For many years, however, it was assumed that selection during this stage was
320 minimal, largely because gametes, particularly sperm, were thought to be
321 transcriptionally inactive (Joseph & Kirkpatrick, 2004). This view stemmed from
322 early observations that sperm lacking nuclei were still capable of fertilisation
323 (Lindsley & Grell, 1969; Lyon et al., 1972; Muller & Settles, 1927) and from
324 evidence of extensive cytoplasmic bridges between developing spermatids, which
325 allow for the sharing of gene products and equalising of gene expression among
326 cells (Greenbaum et al., 2011; Weber & Russell, 1987). These features were
327 interpreted as mechanisms that reduce haploid individuality and therefore
328 minimise the scope for selection to act at the gamete level.

329

330 More recent findings have challenged this assumption. Studies have shown that
331 post-meiotic transcription occurs in spermatids from the fruitfly *Drosophila*
332 *melanogaster* (Barreau et al., 2008), indicating that haploid genomes can exhibit
333 gene expression activity. In addition, unequal sharing of transcripts and proteins
334 among connected spermatids has been observed in mammals, including the
335 mouse gene *Spam1* (Zheng et al., 2001), suggesting that cytoplasmic sharing is
336 incomplete and that individual sperm may retain haploid-specific expression
337 patterns. Such evidence implies that haploid gene expression could contribute to

338 functional variation among sperm produced by the same individual, creating the
339 opportunity for selection to act on the haploid genome.

340

341 Understanding the mechanisms and consequences of haploid selection in
342 gametes is therefore essential to explaining how genetic variation is filtered before
343 fertilisation and how this process might influence both reproductive success and
344 the genetic quality of offspring.

345

346 **1.5 Potential for Haploid Selection Within Ejaculates**

347 Although variation in sperm phenotype alone is not direct evidence of haploid
348 selection, it defines the phenotypic substrate upon which such selection could
349 occur prior to fertilisation. Within-ejaculate variation in sperm morphology,
350 physiology, and motility has been observed across a wide range of taxa, including
351 mammals, birds, and fish (Firman & Simmons, 2015; Lüpold & Pitnick, 2018). This
352 variation forms the foundation for potential haploid selection within the ejaculate.

353

354 **1.5.1 Competition among sperm within an ejaculate**

355 When multiple sperm from the same male compete to fertilise a single oocyte,
356 even subtle performance differences can influence success. In externally fertilising
357 Atlantic salmon (*Salmo salar*), sperm velocity has been shown to predict
358 fertilisation success under competitive conditions (Gage et al., 2004). Similarly, in
359 domestic fowl (*Gallus gallus domesticus*), a simple sperm mobility assay
360 accurately predicts both competitive and non-competitive fertility outcomes,
361 demonstrating that faster, more motile sperm have higher fertilisation potential
362 (Froman et al., 2002). Comparable results have been reported in mice (*Mus*
363 *musculus*), where sperm motility and morphology contribute significantly to the
364 likelihood of reaching and fertilising the oocyte (Firman & Simmons, 2010). Whilst
365 these results were originally shown between ejaculates from separate males,
366 similar competition between sperm from the same ejaculate occurs (Alavioon et
367 al., 2017). These findings illustrate that phenotypic variation among a male's own
368 sperm can influence which haploid genotypes achieve fertilisation.

369

370 **1.5.2 Interaction with the female reproductive environment**

371 The female reproductive tract imposes powerful selective filters, meaning only a
372 fraction of ejaculated sperm reach the fertilisation site. In mammals, sperm must
373 traverse the cervix, uterotubal junction, and oviductal reservoir, each stage
374 selecting for sperm with specific traits such as progressive motility, intact
375 acrosomes, and appropriate membrane properties (Suarez & Pacey, 2006). For
376 example, studies in mice have shown that thermotactic and chemotactic
377 responses within the oviduct enrich for sperm with higher DNA integrity and
378 improved embryo development rates (Bahat & Eisenbach, 2006; Pérez-Cerezales
379 et al., 2018). Similarly, in cattle (*Bos taurus*), oviductal epithelial binding selects for
380 sperm with more stable plasma membranes and higher fertilisation potential
381 (Lefebvre & Suarez, 1996). These findings demonstrate that the female
382 environment can act as a selective landscape for sperm phenotypes, indirectly
383 filtering haploid genomes.

384

385 **1.5.3 Selective binding and fusion with the oocyte**

386 A third form of selection occurs at the level of sperm–oocyte interaction. The
387 binding of sperm to zona pellucida (ZP) glycoproteins acts as a critical checkpoint
388 that discriminates between competent and incompetent sperm. Studies in humans
389 have shown that binding to solubilised ZP or recombinant ZP proteins enriches for
390 sperm with lower DNA fragmentation and improved fertilisation rates (Huszar et
391 al., 2007; F. Liu et al., 2011). At the plasma membrane, molecular recognition
392 between IZUMO1 on sperm and JUNO on the oocyte represents an essential
393 ligand–receptor pair required for fusion (Bianchi et al., 2014). Differences in the
394 abundance or accessibility of IZUMO1 may therefore contribute to fertilisation bias
395 within ejaculates (Sebkova et al., 2014). Collectively, these studies define the
396 major points where selection can act on sperm prior to fertilisation, setting the
397 stage for assessing whether these processes reflect true haploid selection.

398

399 While these processes define the points at which selective pressures can act on
400 sperm, the extent to which they translate into differential reproductive success

401 remains a key question. Understanding whether variation in sperm phenotype
402 leads to measurable differences in embryo viability or offspring performance is
403 required to provide crucial evidence for haploid selection in action.

404

405 **1.6 Evidence that Sperm Fitness Influences Offspring**

406 **Quality**

407 Sperm fitness is defined as the capacity of an individual sperm cell to reach,
408 fertilise, and successfully support zygote and embryo development. It integrates
409 multiple factors, including motility, longevity, morphology, metabolism, and the
410 integrity of nuclear and mitochondrial genomes (Marcu et al., 2024). Experimental
411 studies across species demonstrate that variation in sperm fitness within a single
412 ejaculate can have measurable effects on embryo and offspring outcomes.

413

414 In zebrafish (*Danio rerio*), sperm longevity has been directly linked to offspring
415 performance. When sperm were sorted into long-lived and short-lived fractions
416 from the same ejaculate, offspring produced by long-lived sperm exhibited
417 increased embryo viability and reduced developmental abnormalities (Alavioon et
418 al., 2017). A subsequent study demonstrated that these offspring also showed
419 increased gamete production, increased reproductive fitness during adulthood and
420 delayed reproductive ageing, suggesting long-term transgenerational fitness
421 effects of within-ejaculate sperm selection (Alavioon et al., 2019).

422

423 At the molecular level, emerging data indicate that sperm cells from the same
424 male differ not only phenotypically but also in gene and protein expression. Early
425 work in mice showed that the sperm membrane glycoprotein SPAM1 is not evenly
426 shared across spermatids due to incomplete cytoplasmic bridge diffusion, leading
427 to functional heterogeneity among mature sperm (Martin-DeLeon, 2006).

428

429 Epigenetic variation among sperm provides an additional mechanism for
430 differential fitness. Human and mouse sperm exhibit non-random patterns of
431 histone retention and DNA methylation at genes involved in embryonic
432 development and metabolism (Jenkins & Carrell, 2012; Lismore & Kimmins, 2023).

433 In livestock such as boar (*Sus scrofa*) and bull (*Bos taurus*), specific methylation
434 patterns and small RNA profiles have been associated with male fertility and early
435 embryo development (Kropp et al., 2017). These findings suggest that both
436 genetic and epigenetic heterogeneity among sperm can influence fertilisation
437 outcomes and potentially contribute to offspring phenotype.

438

439 Taken together, these studies demonstrate that sperm are not functionally
440 equivalent, and that selection acting among haploid gametes can produce
441 measurable effects on embryo development and offspring fitness. These findings
442 highlight sperm fitness as a powerful determinant of reproductive success and
443 evolutionary potential.

444

445 **1.7 The Male Fertility Crisis**

446 One of the clearest applications for research into selection acting upon male
447 gametes, and the influence of sperm fitness on offspring outcomes, is in the
448 improvement of assisted reproductive technologies (ART). Procedures such as *in*
449 *vitro* fertilisation (IVF) and intracytoplasmic sperm injection (ICSI) are now among
450 the most common clinical interventions for infertility, accounting for an estimated
451 3–6% of all births in high-income countries (European IVF Monitoring Consortium
452 (EIM) et al., 2022).

453

454 Despite the widespread adoption of ART, success rates remain limited. Globally,
455 only 20–30% of IVF cycles and around 25% of ICSI cycles result in a live birth per
456 treatment attempt, with rates falling sharply to below 10% in women over 40
457 (Adamson et al., 2025; Alavioon et al., 2021; European IVF Monitoring Consortium
458 (EIM) et al., 2022; Griesinger & Larsson, 2023; HFEA, 2022). Even when
459 fertilisation occurs, 20–50% of embryos fail to implant, and miscarriage rates
460 remain between 10-13% depending on patient age and clinical protocol (Gardner
461 et al., 2015; Hu et al., 2018; Kalra & Molinaro, 2008).

462

463 A central limitation of these technologies is that they bypass many of the natural
464 selective pressures, such as temperature gradients, pH variation, and biochemical

465 interactions within the female reproductive tract, that normally filter for the most
466 functionally competent sperm under natural conception (Alavioon et al., 2021). In
467 ICSI, for instance, sperm are selected based largely on subjective assessments of
468 motility and morphology, allowing suboptimal sperm to be used in fertilisation
469 (Palermo et al., 2017). The removal of these natural selection mechanisms has
470 been associated with the use of lower-quality sperm and may contribute to poorer
471 developmental outcomes in ART-derived embryos and offspring compared to
472 natural conceptions (Alavioon et al., 2021; Nixon et al., 2023; van Oosterhout et
473 al., 2022).

474
475 The importance of understanding sperm fitness and selection is amplified by the
476 ongoing male fertility crisis, characterised by substantial global declines in sperm
477 count, motility, and morphology (Levine et al., 2017; Sengupta et al., 2017, 2018).
478 Meta-analyses indicate that sperm counts in men from Western countries have
479 fallen by over 50% since the 1970s, with similar downward trends now reported
480 across other continents (Levine et al., 2023). These widespread declines suggest
481 that the reliance on ART will continue to increase, underscoring the need for more
482 refined and biologically informed methods for assessing and selecting sperm in
483 clinical contexts (De Jonge & Barratt, 2019; European IVF Monitoring Consortium
484 (EIM) et al., 2022).

485
486 Environmental and lifestyle factors have also been strongly implicated in declining
487 sperm quality. Exposure to endocrine-disrupting chemicals such as bisphenol A
488 (BPA), phthalates, and pesticides has been shown to impair spermatogenesis and
489 reduce motility (Skakkebæk et al., 2022). Similarly, obesity, heat exposure, chronic
490 stress, and poor diet negatively affect both sperm development and function
491 (Carvalho et al., 2021; Pini et al., 2020; Sharma et al., 2013). These factors alter
492 the testicular environment and may contribute to the molecular and phenotypic
493 heterogeneity observed among sperm within a single ejaculate. Understanding
494 how such stressors influence sperm fitness is therefore critical for improving
495 reproductive outcomes both in natural and assisted settings.

496

497 Much of the existing clinical fertility research treats ejaculate quality as a single
498 metric per individual (Said & Land, 2011) averaging across all sperm cells and
499 ignoring the within-ejaculate variation that might better predict fertilisation success
500 (Alavioon et al., 2021). This population-level approach is useful for identifying
501 general trends, helping in the categorisation and diagnosis of disease and other
502 potential causes of infertility, but fails to identify which specific sperm are
503 functionally superior and therefore fails to provide tailored solutions for individuals
504 facing infertility.

505

506 **1.8 Current Clinical Methods for Sperm Selection**

507 With the increased application of IVF in humans, and the increasing information to
508 suggest that selection for the highest fitness gametes is crucial to the success of
509 these methods, many clinical practices have implemented methods to isolate
510 "better" sperm (Said & Land, 2011). Clinics commonly use swim-up and density
511 gradient centrifugation to isolate motile sperm under the assumption that
512 movement reflects health and fertilising ability (Said & Land, 2011). However,
513 while these methods effectively separate motile cells from immotile cells, they do
514 not guarantee removal of sperm with DNA damage, epigenetic abnormalities, or
515 mitochondrial dysfunction. Some studies have shown that sperm selected through
516 these techniques still yield poor fertilisation outcomes or lead to early embryo
517 arrest (Ribas-Maynou et al., 2021).

518

519 One of the critical issues in sperm selection is the assumption that motility equals
520 functionality, however, whilst motility is necessary for sperm to reach and
521 penetrate the oocyte, it is not sufficient on its own to ensure fertilisation success or
522 embryo viability (Ribas-Maynou et al., 2021). This pattern is not restricted to
523 humans. Similar findings have been reported in livestock species, including cattle
524 (*Bos taurus*) (Samardzija et al., 2006) and boar (*Sus scrofa*) (Noguchi et al.,
525 2015), where sperm selected for motility using density gradients showed mixed
526 results for improved conception or embryo development rates. These results
527 underscore that high motility alone does not guarantee functional competence and
528 that other molecular or structural defects may persist undetected.

529
530 This discrepancy suggests that current selection methods are oversimplified and
531 overlook key molecular aspects of sperm quality. Identifying molecular markers or
532 phenotypic indicators of “functional” rather than just “live and moving” sperm
533 remains a major unmet need in reproductive biology.

534

535 **1.9 The Genomic and Transcriptomic Differences in** 536 **Sperm Fitness**

537 One key approach to linking sperm phenotype and haploid genotype is genomic
538 and transcriptomic sequencing of sperm subpopulations. In mammals, single-cell
539 RNA sequencing across spermatids in multiple species found that many genes
540 exhibit allele-biased expression, i.e. they are not fully shared through cytoplasmic
541 bridges, a pattern termed “genoinformative markers” (GIMs) (Bhutani et al., 2021).
542 This result suggests that individual sperm cells may maintain haploid-specific gene
543 expression potential.

544

545 In addition, in Mexican Tetra (*Astyanax mexicanus*) sperm subpopulations
546 separated by phenotypic dye properties differed in their haploid genotype
547 frequencies, indicating that phenotype classes correspond to distinct haplotypes
548 (Borowsky et al., 2018). More recently, long-read sequencing of individual human
549 sperm detected structural variation and genome-level heterogeneity at the haploid
550 level (H. Xie et al., 2023). These findings reinforce the idea that sperm genomes
551 are not identical within a male and may carry unique allelic compositions.

552

553 Together, these genomic observations imply that genetic heterogeneity within
554 ejaculates is not random noise but a substrate on which selection might act. They
555 support the hypothesis that haploid selection could modulate the transmission of
556 genetic variants by favouring sperm with fitter haplotypes.

557

558 Alongside genomic approaches, transcriptomic analyses complement this view by
559 examining how expression differences among sperm might contribute to fitness. In
560 zebrafish (*Danio rerio*), single-cell genome and transcriptome sequencing of post-

561 meiotic spermatids revealed that a considerable fraction of genes (~6 %) show
562 allele-specific expression, challenging the assumption of complete sharing via
563 cytoplasmic bridges and reaffirming that haploid expression differences may drive
564 phenotypic diversity (Marcu, 2024). These findings point to a potential mechanism
565 by which sperm not only reflect the haploid genotype but also act as vectors of
566 paternal environmental effects via regulatory RNAs. Collectively, these studies
567 suggest that variation in the sperm transcriptome, including both coding and non-
568 coding elements, may play a functional role in fertilisation success and early
569 embryogenesis.

570
571 Together, genomic and transcriptomic studies provide converging evidence that
572 haploid selection within ejaculates can shape sperm function and influence
573 offspring phenotypes. These findings challenge the classical view of sperm as
574 passive carriers of paternal DNA and instead support a model in which both
575 genetic and regulatory variation among sperm contributes to reproductive success.

576

577 **1.10 Sperm Proteomics**

578 Whilst the most common methods to study the potential of selection, and the
579 phenotype of gametes, have often been either genomic or transcriptomic in nature
580 (Immler, 2019), another analytical method used to elucidate phenotypes has been
581 proteomics (Hashemitabar et al., 2015). This method has often been underutilised
582 due to its lack of material amplification methods and high cost; however,
583 proteomics remains the clearest snapshot of the phenotype of a cell at the time of
584 study, including post-translational modifications and total abundance of proteins
585 and co-factors (Cannarella et al., 2020).

586

587 Proteomic studies of sperm have revealed significant variation in protein
588 expression profiles between fertile and sub-fertile men (Amaral, Castillo, et al.,
589 2014; Selvam et al., 2019), or between high- and low-motility sperm samples (57).
590 In addition to humans, sperm proteomes have been investigated across species
591 such as cattle (D'Amours et al., 2019a), boar (Zigo et al., 2023), and mice (Baker,

592 Hetherington, Reeves, & Aitken, 2008), all showing distinct proteomic signatures
593 associated with sperm motility, longevity, or fertilisation success.

594

595 For example, in humans, sperm from asthenozoospermic individuals show altered
596 expression in proteins linked to mitochondrial function, flagellar motility, and stress
597 response (34). In both mice and humans, obesity and metabolic stress alter sperm
598 protein profiles involved in mitochondrial respiration, chromatin condensation, and
599 oxidative balance, reducing fertilisation success (Carvalho et al., 2021; Pini et al.,
600 2020). These findings demonstrate that the sperm proteome is sensitive to both
601 intrinsic genetic variation and external physiological conditions.

602

603 Understanding the sperm proteome could enable the development of non-invasive
604 diagnostic tools for sperm function, especially in the context of ART. For instance,
605 targeted identification of surface or secreted proteins may allow real-time selection
606 of high-quality sperm using minimally invasive assays. Beyond fertility, sperm
607 proteomics may also shed light on male reproductive aging, the effects of
608 environmental exposures, or transgenerational inheritance mechanisms
609 (Cannarella et al., 2020).

610

611 One major challenge in sperm proteomics is the small amount of protein present in
612 each cell, combined with their high DNA content, compact chromatin and
613 specialised morphology (Codina et al., 2015). Isolating enough protein for robust
614 mass spectrometry without pooling across individuals, and therefore losing
615 resolution of subpopulations, is technically difficult. Additionally, single-cell
616 proteomics in sperm remains in its infancy due to these limitations, making non-
617 destructive or high-throughput applications even more crucial for moving the field
618 forward (Ahmad & Budnik, 2023). This is important because resolving protein
619 expression at the level of individual sperm would allow functional heterogeneity to
620 be directly linked to fertilisation potential, rather than being masked by population
621 averages.

622

623 **1.11 What is a Biomarker?**

624 Whilst sperm proteomics remains technically difficult, one of its primary uses has
625 been in the identification of biomarkers. A biomarker is a measurable indicator of a
626 biological state or condition. In the context of sperm, biomarkers could be used to
627 predict fertilisation potential, embryo viability, or even offspring health outcomes
628 (Intasqui et al., 2018). They could also guide treatment decisions in ART, help
629 identify the best sperm in a sample, or provide early indicators of male subfertility.

630

631 In humans, biomarkers such as the DNA degradation index (DDSi) have been
632 correlated with fertility outcomes (Esteves et al., 2015). These markers are
633 increasingly being tested as adjuncts to standard semen analysis in both clinical
634 and research settings.

635

636 Current diagnostics in male fertility are limited in predictive power, especially in
637 normozoospermic men who still experience unexplained infertility (Pandruvada et
638 al., 2021). Molecular biomarkers could fill this gap by revealing functionally
639 relevant differences not visible through morphology or motility analysis. Their
640 development could also improve ART outcomes by enabling personalised
641 selection strategies that go beyond population averages.

642

643 **1.12 Beyond Sperm: The Testicular Origins of Sperm
644 Quality**

645 Whilst the identification of potential biomarkers for sperm fitness remains a large
646 research target in reproductive biology, it must be remembered that the origin of
647 sperm phenotypes and the understanding of the potential role of any biomarker
648 identified relies not only on understanding sperm biology but also the biology of
649 the testes. Sperm quality is not only shaped during ejaculation but also depends
650 heavily on the testicular environment during spermatogenesis. Testis-specific gene
651 expression profiles, protein turnover, and local stress responses (e.g., to heat or
652 toxins) can all impact the molecular composition and function of mature sperm.
653 Transient scrotal heat stress in mice for instance leads to widespread

654 transcriptomic and proteomic changes in developing germ cells, impairing motility
655 and fertilisation capacity in mature sperm (Paul et al., 2008; Y.-F. Zhu et al., 2006).
656 Similarly, in humans, testicular biopsies from infertile men frequently show
657 dysregulation in stress-response and mitochondrial pathways that correspond with
658 altered sperm proteomes (Davalieva et al., 2022; Liang et al., 2021). These
659 examples illustrate that many features of sperm phenotype, and therefore potential
660 biomarkers, originate upstream in the testes.

661
662 By combining testis and sperm datasets, researchers can better identify the origin
663 and functional significance of candidate biomarkers. Integrative approaches linking
664 testicular transcriptomes, sperm proteomes, and fertilisation outcomes are
665 beginning to reveal which proteins persist into mature sperm because they serve
666 continued roles, and which are simply developmental relicts (Amaral, Castillo, et
667 al., 2014; Castillo et al., 2023).

668
669 One of the central questions in sperm biomarker research is whether key proteins
670 or transcripts are relicts from the testis or have active functional roles in mature
671 sperm. Given the compacted nature of sperm chromatin and their limited
672 transcriptional capacity, many molecules may simply be remnants of development
673 (Robles et al., 2017). However, others, particularly surface proteins or those
674 involved in signalling, such as IZUMO1 (Bianchi et al., 2014), retain active roles
675 during fertilisation and early embryo development, suggesting that their detection
676 could carry strong predictive value.

677

678 **1.13 The Importance of Animal Models**

679 Given the ongoing decline in human fertility and the increasing demand for ART,
680 understanding sperm biology in humans is a top research priority. However, direct
681 studies on human gametes are often limited by ethical, legal, and technical
682 constraints.

683

684 Unlike in model organisms, it is illegal and unethical to generate or manipulate
685 human embryos beyond certain developmental stages, nor can we follow resulting

686 offspring. This restricts the ability to link sperm traits to developmental outcomes in
687 humans and highlights the need for model systems (Stouffer & Woodruff, 2017a).
688 Animal models allow for controlled manipulation of environmental conditions,
689 genetic backgrounds, and experimental interventions that are not possible in
690 humans. They provide the means to conduct hypothesis-driven experiments on
691 fertility and reproduction.

692
693 Zebrafish are a powerful vertebrate model for reproductive biology due to their
694 external fertilisation, high fecundity, transparent embryos, and generation times
695 (Hoo et al., 2016). Their sperm can be collected non-lethally and fertilisation
696 outcomes can be monitored in real time. Zebrafish are especially relevant in the
697 context of environmental stress because they are sensitive to water temperature,
698 pollutants, and endocrine-disrupting chemicals, all of which are known to affect
699 fertility (Hajam, Rani, Sharma, Kumar, & Verma, 2021). Their use provides insight
700 into how broader ecological changes may impact reproductive success in both
701 wildlife and aquaculture. Combined with available genetic tools like CRISPR,
702 transgenics, and lineage tracing, zebrafish offer a comprehensive platform for
703 linking sperm phenotype to embryo outcome.

704

705 **1.14 This Thesis: The Molecular Biomarkers of Sperm** 706 **Fitness**

707 This thesis investigates how molecular variation in sperm relates to functional
708 sperm phenotypes and potential biomarkers of fertilisation success. Building on
709 the theoretical framework of haploid selection, and previous genomic and
710 transcriptomic empirical evidence of this, the following chapters use both zebrafish
711 and human models to explore how environmental factors, developmental context,
712 and phenotypic selection shape the sperm proteome, and how this can be
713 leveraged for biomarker discovery.

714

715 Chapter 2 begins with a proteomic analysis of zebrafish testes under thermal
716 stress, aiming to identify how environmental temperature affects protein
717 expression during spermatogenesis. This chapter establishes the testicular context

718 in which sperm phenotypes arise and highlights stress-responsive proteins that
719 may be carried into mature sperm.

720

721 Chapter 3 shifts focus to the mature sperm proteome in zebrafish. By profiling
722 sperm from the same individuals used in Chapter 1, this chapter explores the
723 molecular consequences of altered testicular conditions and identifies candidate
724 proteins associated with sperm longevity, motility, and overall fitness. Together,
725 Chapters 2 and 3 establish zebrafish as a model for understanding how
726 environmental and developmental factors shape sperm molecular phenotypes.

727

728 Chapter 4 extends this approach to humans, comparing the proteomes of sperm
729 populations that differ in phenotypes that can be separated through assays such
730 as swim-up and methyl cellulose. This chapter identifies proteins with differential
731 abundance between selected and un-selected sperm. The findings highlight
732 biomarkers with translational potential for sperm proteomics in clinical fertility
733 research.

734

735 Chapter 5 focuses on validating the candidate sperm proteins as biomarkers
736 identified in chapter 4, using flow cytometry. This chapter tests whether protein
737 expression levels can distinguish high- from low-fitness sperm within an ejaculate.
738 It represents a step toward functional application, evaluating whether proteomic
739 signals identified in earlier chapters can be used to develop improved sperm
740 selection tools for assisted reproduction.

741

742 Overall, this thesis integrates proteomic profiling with functional assays to explore
743 the molecular basis of sperm fitness and within-ejaculate variation. It aims to
744 contribute both to fundamental understanding of haploid selection and to the
745 development of practical tools for fertility diagnostics and treatment.

746

747

748

749 **2 The Effects of Heat Stress on the**

750 **Zebrafish Testes Proteome**

751 **2.1 Abstract**

752 With global temperatures rising, a clear threat has emerged to reproductive fitness
753 across species, with thermal stress emerging as a particularly important factor.
754 However, the molecular consequences of these changes are still poorly
755 understood. In ectotherm aquatic species, rising water temperatures can directly
756 influence physiological processes as internal body conditions directly correlate
757 with external environmental temperature. Male fertility appears to be particularly
758 vulnerable as thermal fluctuations can impair spermatogenesis, alter sperm
759 quality, and ultimately reduce reproductive fitness. While genomic and
760 transcriptomic analyses have provided important insights into how organisms
761 respond to heat stress, these approaches are limited in their ability to capture
762 changes at the protein level, where much of the functional impact of temperature
763 changes is realised.

764

765 Here, quantitative proteomic profiling via liquid chromatography tandem mass
766 spectrometry (LC-MS/MS) was used to assess the effect of a two-week period of
767 elevated temperature on the testes proteome of adult male zebrafish *Danio rerio*.
768 A global proteome of 5415 proteins was generated, and a total of 377 proteins
769 were found to have significantly different abundance between the heat treated
770 (34°C) and control groups (28°C). Notably, these molecular changes were
771 accompanied by a consistent reduction in gonad size in heat-stressed individuals,
772 independent of somatic growth. The abundance of peptides involved in processes
773 of spermatogenesis was significantly reduced in the heat-treated testes whilst the
774 abundance of molecular repair peptides was significantly increased. These
775 findings suggest that heat stress alters the molecular composition of the testes in a
776 way that is likely to impact sperm performance, alongside of morphological
777 changes to the organ itself. Our results demonstrate that even a moderate
778 increase in temperature over a short period of time has fundamental effects on the

779 molecular composition and function of testes, supporting the idea that male
780 reproductive fitness is particularly vulnerable to increasing temperatures.

781 **2.2 Introduction**

782 Sexual reproduction is the result of an intricate and delicate balance of
783 molecular and physiological pathways and is known to be highly sensitive to
784 environmental fluctuations, with a “reproductive stress axis” forming the interface
785 of physiological stress response and reproductive output. This reproductive
786 stress axis involves many different endocrine pathways depending on the taxa
787 experiencing stress, however, these are primarily the hypothalamic-pituitary-
788 adrenal (HPA) and the hypothalamic-pituitary-gonadal (HPG) axes, the effects of
789 which have been noted in the reproductive and growth outcomes of various fish
790 (Boni, 2019; Canosa & Bertucci, 2023; Chand & Lovejoy, 2011; Schreck, 2010),
791 and mammals such as sheep (*Ovis aries*) (Naqvi et al., 2012), mice (*Mus*
792 *musculus*), rhesus macaques (*Macaca mulatta*) and humans (Chand & Lovejoy,
793 2011; Toufexis et al., 2014).

794

795 One of the fundamental aspects of sexual reproduction in animals is
796 gametogenesis, the generation and storage of gametes, which depends on the
797 coordinated interaction between somatic and germ cells, typically occurring in the
798 gonads (Oatley & Brinster, 2012), and is therefore directly influenced by the HPG
799 stress axis. In males, spermatogenesis occurs in the testes (de Kretser et al.,
800 1998), which serve as a physiological interface between the external environment,
801 the organismal physiology and the germ cells (Godmann et al., 2009). Therefore,
802 the testes are a critical focal point for understanding how environmental factors,
803 including temperature, toxins, and nutrition, can affect both an individual organism
804 and potentially a population as a whole (Boni, 2019; Rahman et al., 2018).

805

806 One environmental stressor that is of major current importance is thermal stress -
807 particularly in aquatic species due to globally rising water temperatures (Alfonso et
808 al., 2021; Barbarossa et al., 2021; Cheng et al., 2022). In aquatic animals, gonads
809 are commonly internally located due to the nature of ectothermic physiology where

810 the body condition of the animal is directly influenced by environmental
811 temperatures. This means that for most aquatic species, heat stress can have
812 immediate and potentially dire effects on reproduction (Alix et al., 2020). In species
813 such as the brown trout (*Salmo trutta*), water temperature of 13°C – just 3°C
814 above the optimal 0-10°C spawning temperature - can have both an indirect
815 negative effect on fertility as the adult fish experiences a change in temperature
816 causing physiological effects on the gonads, as well as direct effects on the
817 gametes themselves as they are directly exposed to the higher temperature
818 (Fenkes et al., 2017). Similar negative effects of increased water temperature
819 have been noted across other aquatic species, with partial to complete regression
820 in the testes of fish including yellowtail tetra (*Astyanax altiparanae*) (de Siqueira-
821 Silva et al., 2015), European bullheads (*Cottus gobio*) (Dorts et al., 2012), and
822 Pejerry (*Odontesthes bonariensis*) (Elisio et al., 2012).

823

824 In other ectothermic species such as insects including the red flour beetle
825 (*Tribolium castaneum*) fertility output was found to reduce significantly before
826 lethal thermal limits were achieved, with significant reductions of up to 40% in
827 testes volume (Cole et al., 2025). Similar male sub-fertility was achieved in high
828 temperatures before lethality in the parasitoid wasp (*Anisopteromalus calandrae*)
829 with observation of up to 100 times less sperm produced by stressed males
830 compared to the control (Nguyen et al., 2013). These findings illustrate that even
831 moderate thermal stress can severely impair male fertility in ectothermic species,
832 emphasising that reproductive function is often compromised well before survival
833 thresholds are reached.

834

835 Notably, in zebrafish *Danio rerio*, prolonged increased heat exposure of 6° above
836 the optimal 28°C over a period of two weeks caused reductions in overall male
837 fertility rates, although the offspring were found to have no significant differences
838 in survival or abnormality rates compared to the offspring of control males (Irish et
839 al., 2024). Similarly, assays including heat stress in combination with other
840 stressors such as predatory cues, overcrowding and starvation for a period of 21
841 days revealed negative consequences for sperm production, number and quality in

842 zebrafish (Valcarce et al., 2023). Zebrafish are not only a prime example of the
843 effects of stress on reproduction in aquatic and ectothermic species, they are also
844 a commonly used model organism for mammalian and human reproduction,
845 despite the differences in modality of reproduction as over 70% of genes are
846 homologous (Hoo et al., 2016).

847
848 Inbreeding is an important consideration when interpreting reproductive
849 phenotypes in fish, as laboratory-maintained strains typically experience far higher
850 levels of inbreeding than wild populations. Captive lines bred over many
851 generations often accumulate elevated homozygosity and reduced genetic
852 diversity, which can lead to inbreeding depression affecting reproductive traits
853 such as sperm count, morphology, and motility (Kincaid, 1983; Wright et al., 2008).
854 As a result, laboratory fish may be more susceptible to environmental or
855 physiological stressors, including those that affect spermatogenesis or sperm
856 function.

857
858 Conversely, the reduced genetic variability within inbred laboratory strains may
859 lead to lower inter-individual variation, making phenotypic trends easier to detect
860 and less obscured by background noise. Wild populations typically show broader
861 individual variability because of their heterogeneous genetic backgrounds
862 (Gjedrem & Baranski, 2009). Taken together, these differences underline the
863 importance of considering both genetic background and domestication history
864 when interpreting results from laboratory zebrafish and comparing them to studies
865 using wild strains.

866
867 However, despite their utility as a model organism, another key point of note is that
868 zebrafish and other ectotherms lack the protective adaptations seen in internally
869 fertilising endotherms, where external testes help buffer gametogenesis against
870 heat stress. In many terrestrial mammals for example, testes are located externally
871 for better temperature regulation (Kastelic & Rizzoto, 2021). Nevertheless, high
872 temperatures can still have negative consequences for the fertility of these
873 species. For example, in humans, heat stress has been found to result in a
874 decrease in both sperm motility and quality in men exposed to high temperatures

875 as a result of their professional occupation, leading to potential fertility issues
876 (Hoang-Thi et al., 2022). Similarly, in house mice (*Mus musculus*), exposure to
877 higher temperatures was found to cause a reduction in sperm quality as well as
878 morphological changes to both testes structure and size (Rizzoto et al., 2020).

879

880 Besides direct assays on reproductive output, molecular analyses of heat stress to
881 date have largely focused on genetic effects, or effects at the transcriptomic level
882 (Guan et al., 2025; Jayakodi et al., 2019). Genetic analysis of dairy cattle *Bos*
883 *taurus* for example revealed six specific genomic regions which were found to
884 correlate with the likelihood of conception under heat stress conditions, including
885 candidate genes *BRWD1*, *EXD2*, *ADAM20*, *EPAS1*, *TAOK3*, and *NOS1* implicated
886 in both fertilisation and heat stress response, providing a useful guide for future
887 breeding (Sigdel et al., 2020). In the Mexican four-eyed octopus, *Octopus maya*,
888 transcriptome analysis revealed several genes including *ZMYND15* involved in
889 histone interactions and haploid gene regulation, and *KLHL10* involved in sperm
890 maturation through protein ubiquitination, that were downregulated when exposed
891 to thermal stress leading to infertility (López-Galindo et al., 2019).

892

893 While gene expression data provides information of the possible effects of
894 temperature on molecular processes, the translation to effects at the protein level
895 are often not as direct and require more in depth analyses at the proteome level.
896 Proteomics, the identification, classification and quantification of proteins in a
897 tissue, can help elucidate these details. However, the general high cost and high
898 input material requirements have typically precluded the possibility of proteomic
899 experiments on low abundance tissue, especially as proteins cannot currently be
900 amplified in volume like RNA and DNA (Chalmel & Rolland, 2015). Despite these
901 limitations, the number of proteomic studies of reproductive responses to stress is
902 growing (Panner Selvam et al., 2019). For example, in the Taiwanese country
903 chicken *Gallus gallus domesticus*, mass spectrometry revealed 92 distinct proteins
904 to be differentially expressed in the testes as a result of acute heat stress,
905 potentially linked to a decrease in fertility (Wang et al., 2014). Proteomics has also

906 revealed specific post-translational modifications such as acetylation of lysine can
907 change in response to heat stress in mouse testes (C. Xie et al., 2018).

908

909 Here, we exposed male zebrafish to two-week periods of increased temperature of
910 34°C and compared these to males maintained at 28°C. We performed two
911 experimental blocks, one to collect testes for weight measurements, and one to
912 collect testes for quantitative proteomic profiling using liquid chromatography
913 tandem mass tag spectrometry (TMT LC-MS/MS) to measure the changes in
914 abundance across the testes proteome.

915

916 Tandem Mass Tag (TMT) labelling was selected because it enables multiplexed
917 quantification of peptides across multiple samples within a single LC–MS/MS run,
918 substantially reducing technical variation and improving the accuracy of relative
919 protein abundance measurements (Zhang & Elias, 2017). This workflow was
920 paired with an Orbitrap mass spectrometer, as Orbitrap instruments provide high
921 mass accuracy, high resolving power, and excellent dynamic range, all of which
922 enhance peptide identification confidence and quantification precision (Eliuk &
923 Makarov, 2015). Together, these features make TMT-labelled Orbitrap-based
924 proteomics well suited for detecting subtle shifts in protein expression across
925 biological samples.

926

927 Further analyses including STRING and gene ontology (GO term) were performed
928 to provide evidence at both a proteomic and physiological level that changes to
929 molecular mechanistic regulation are key to the changes observed in sperm
930 function and quality for zebrafish instead of physiological changes in terms of
931 gonad size.

932 **2.3 Methods**

933 **2.3.1 Zebrafish husbandry**

934 We used sexually mature AB wild-type male zebrafish obtained from the European
935 Zebrafish Resource Centre (EZRC) and aged between 18 to 24 months for this
936 study. Prior to experiments, the fish were maintained in 3.5L tanks at a 10:6 male
937 to female sex ratios kept at 28°C for two weeks with a 14:10 light schedule. All fish
938 were kept in a recirculating aquatic system with filtered, UV-treated water and
939 maintained under standard zebrafish husbandry conditions. Fish were fed *ad*
940 *libitum* with a mix of dry feed (ZEBRAFEED 400–600 by SPAROS, Área
941 Empresarial de Marim, Lote C, 8700-221 Olhão, Portugal) and live artemia (Sep-
942 Art Artemia Cysts, Ocean Nutrition). All fish used for experiments were kept under
943 Home Office license P0C37E901.

944

945 **2.3.2 Experimental set up**

946 Male zebrafish were randomly allocated to experimental tanks in the standard 10:6
947 male:female ratio (16 fish per 3.5 L tank). For each experimental run, six tanks
948 were established (three replicate blocks), and within each block, the two tanks
949 were randomly assigned to either the control temperature (28 °C) or the heat-
950 stress treatment (34 °C). To minimise environmental confounds, each treatment
951 tank was physically paired with its corresponding control tank from the same block;
952 paired tanks were positioned adjacent to one another on the same rack and
953 exposed to identical light conditions, room temperature, and flow rate.
954 Submersible heaters were added to both tanks in each pair, activated at 34 °C for
955 treatment tanks or 28°C in control tanks to control for potential heater effects. Fish
956 remained in their assigned conditions for two weeks.

957 For the proteomics analyses, we collected the testes from a total of 60 males and
958 pooled the testes from 10 males kept in the same tank as one replicate sample
959 resulting in a total of three replicates.

960

961 For analysis of the change in testes weight, we used 42 sexually mature ABWT
962 male zebrafish obtained from the Zebrafish International Resource Center (ZIRC)
963 aged one and a half years. Fish were kept in a sex ratio of 6 males to 6 females
964 with 12 fish per 3.5L tank. Prior to the experiment, fish were anaesthetised using
965 metomidate hydrochloride (Aquacalm by Syndel, #9, 4131 Mostar Rd, Nanaimo,
966 BC V9T 6A6 Canada), weighed to the nearest mg, and photographed for
967 identification. Fish were arranged into three replicate blocks, each consisting of
968 one control tank and one heat-treatment tank, positioned adjacent to one another
969 on the same rack and exposed to identical light conditions, room temperature, and
970 flow rate. Following the two-week treatment period, fish IDs were anonymised and
971 fish were euthanised, weighed, photographed for identification and gonads were
972 dissected on ice and weighed. Following data analysis, identification photographs
973 were used to reveal treatment identities and match weights pre- and post-
974 treatment.

975

976 **2.3.3 Protein extraction and LC-MS/MS**

977 Dissected testes were flash frozen in liquid nitrogen upon collection with no added
978 buffer and stored at -80°C prior to extraction. Protein was extracted from pooled
979 testes samples , using an SDC-based in-solution digestion approach (Masuda et
980 al., 2008), by the addition of 500 µL 10% SDS with three cycles of vortexing and
981 boiling at 99°C as well as pestle disruption. The samples were then vortexed and
982 centrifuged to remove debris and Proteins were precipitated using
983 methanol/chloroform and acetone. Protein pellets were resuspended in 2.5%
984 sodium deoxycholate (SDC; Merck) in 0.2 M EPPS-buffer (Merck), pH 8.5, and
985 vortexed under heating for a total of three cycles.

986

987 Protein concentration was estimated using a Direct Detect fluorometric assay
988 (MERCK MILLIPORE, Dorset, UK). Equal amounts of protein for each replicate
989 were reduced, alkylated, and digested with trypsin in the SDC buffer according to
990 standard procedures. After digestion, the SDC was precipitated by adjusting to
991 0.2% TFA, and the clear supernatant subjected to C18 SPE (OMIX tips; Agilent).
992 Peptide concentration was further estimated by running an aliquot of the digests

993 on LCMS. Tandem Mass Tag (TMT) labelling was performed using a TMT™ 6plex
994 kit (Lot VB290974, ThermoFisher Scientific, Hemel Hempstead, UK) according to
995 the manufacturer's instructions with slight modifications; for each sample approx.
996 100 µg of the testes peptides were dissolved in 90 µl of 0.2 M EPPS buffer
997 (MERCK)/10% acetonitrile, and 200 µg TMT reagent dissolved in 22 µl of
998 acetonitrile was added. Samples were assigned to the TMT channels in two
999 separate experiments, as follows: replicates from Control males were run in
1000 channels 126, 127 and 128 and replicates from heat stress males were run in
1001 channels 129, 130 and 131.

1002

1003 After 2 h incubation, aliquots of 1.5 µl from each replicate from each individual
1004 TMT experiment were combined in 500 µl 0.2% TFA, desalted, and analysed on
1005 the mass spectrometer to check the labelling efficiency and estimate total sample
1006 abundances. The sample aliquots were quenched by adding 8 µl of 5%
1007 hydroxylamine and combined to roughly level abundances. The peptides were
1008 desalted using a C18 Sep-Pak cartridge (200 mg, Waters, Wilmslow, UK). The
1009 eluted peptides were dissolved in 500 µl of 25 mM NH₄HCO₃ and fractionated by
1010 high pH reversed phase HPLC.

1011

1012 The replicates were loaded to an XBridge® 5 µm BEH C18 130 Å column (250 x
1013 4.6 mm, Waters). Fractionation was performed on an ACQUITY Arc Bio System
1014 (Waters) with the following gradient of solvents A (water), B (acetonitrile), and C
1015 (25 mM NH₄HCO₃ in water) at a flow rate of 1 ml min⁻¹: solvent C was kept at 10%
1016 throughout the gradient; solvent B: 0-5 min: 5%, 5-10 min: 5-10%, 10-80 min: 10-
1017 45%, 80-90 min: 45-80%, followed by 5 min at 80% B and re-equilibration to 5%
1018 for 24 min. Fractions of 1mL were collected every 1 min and concatenated by
1019 combining fractions of similar peptide concentration to produce 29 final fractions
1020 testis samples for MS analysis.

1021

1022 Aliquots were analysed by nanoLC-MS/MS on an Orbitrap Eclipse™ Tribrid™
1023 mass spectrometer coupled to an UltiMate® 3000 RSLCnano LC system (Thermo
1024 Fisher Scientific, Hemel Hempstead, UK). The samples were loaded onto a trap

1025 cartridge (Pepmap 100, C18, 5um, 0.3x5mm, Thermo) with 0.1% TFA at 15 μ l min⁻¹
1026 for 3 min. The trap column was then switched in-line with the analytical column
1027 (nanoEase M/Z column, HSS C18 T3, 1.8 μ m, 100 \AA , 250 mm x 0.75 μ m, Waters)
1028 for separation using the following gradient of solvents A (water, 0.1% formic acid)
1029 and B (80% acetonitrile, 0.1% formic acid) at a flow rate of 0.2 μ l min⁻¹: 0-3 min
1030 3% B (parallel to trapping); 3-10 min linear increase B to 8 %; 10-75 min increase
1031 B to 37%; 75-90 min linear increase B to 50 %; followed by a ramp to 99% B and
1032 re-equilibration to 3% B.

1033

1034 Data were acquired with the following parameters in positive ion mode: MS1/OT:
1035 resolution 120K, profile mode, mass range *m/z* 400-1800, AGC target 100%, max
1036 inject time 50 ms; MS2/IT: data dependent analysis with the following parameters:
1037 top10 in IT Turbo mode, centroid mode, quadrupole isolation window 0.7 Da,
1038 charge states 2-5, threshold 1.9e4, CID CE = 35, AGC target 1e4, max. inject time
1039 70 ms, dynamic exclusion 1 count for 15 sec mass tolerance of 7 ppm; MS3
1040 synchronous precursor selection (SPS): 10 SPS precursors, isolation window 0.7
1041 Da, HCD fragmentation with CE=65, Orbitrap Turbo TMT and TMTpro resolution
1042 30k, AGC target 1e5, max inject time 105 ms, Real Time Search (RTS): protein
1043 database *Danio rerio* (Uniprot reference proteome UP000000437, August 2022,
1044 46,842 entries), enzyme trypsin, 1 missed cleavage, oxidation (M) as variable,
1045 carbamidomethyl (C) and TMT as fixed modifications, Xcorr = 1, dCn = 0.05.

1046

1047 **2.3.4 Weight data analysis**

1048 Weight data were analysed and visualised using R version 4.4.3 (The R
1049 Foundation for Statistical Computing, Vienna, Austria, URL [https://www.R-](https://www.R-project.org/)
1050 [project.org/](https://www.R-project.org/)) for generalised linear model analysis. Model assumptions were
1051 checked using DHARMA (Florian, 2016). We ran a series of statistical models to
1052 assess the effects of heat treatment on the size of the testes. Assumption
1053 violations in residuals led us to refit all models using Gamma GLMs with a log link,
1054 which better accommodate the positive, right-skewed distribution of testes weight.
1055 DHARMA diagnostics confirmed substantially improved model fit and residual

1056 uniformity for these models. We used stepwise reduction using the AIC as an
1057 indicator of fit to determine the final models.

1058

1059 **2.3.5 Proteome data analysis**

1060 The acquired raw proteome data were processed and quantified in Proteome
1061 Discoverer 3.0 (Thermo) using the incorporated search engines Comet and
1062 CHIMERYS (MSAID, Munich, Germany). The processing workflow for both
1063 engines included recalibration of MS1 spectra (RC), reporter ion quantification by
1064 most confident centroid (20 ppm) and a search on the *Danio rerio* fasta database
1065 (as above) and a common contaminants database. For CHIMERY, the Top N
1066 Peak Filter was used with 20 peaks per 100 Da and parameters were precursor
1067 tolerance 6 ppm, enzyme trypsin with 1 missed cleavage, variable modification
1068 oxidation (M), fixed modifications carbamidomethyl (C) and TMT 6plex on N-
1069 terminus and K. For Comet the version 2019.01 rev. 0 parameter file was used
1070 with default settings except precursor tolerance set to 6 ppm and trypsin missed
1071 cleavages set to 1. Modifications were the same as for CHIMERYS.

1072

1073 The consensus workflow included the following parameters: assigning the three
1074 replicates/channels as described above per condition (cold and heat), only unique
1075 peptides (protein groups) for quantification, intensity-based abundance, TMT
1076 channel correction values applied (Lot VB290974),), co-isolation/SPS matches
1077 thresholds 50%/70%, normalised CHIMERYS Coefficient Threshold 0.8,
1078 normalisation on total peptide abundances, protein abundance-based ratio
1079 calculation, missing values imputation by low abundance resampling, hypothesis
1080 testing by t-test (background based), adjusted p-value calculation by BH-method.
1081 All data filtering was performed in accordance with current proteomics best
1082 practice guidelines (Burger, 2018).

1083

1084 Following data acquisition from the consensus workflow, all identified Uniprot IDs
1085 were re-mapped using the Uniprot ID-mapping software (The UniProt Consortium,
1086 2021) to ensure removal of deprecated and obsolete protein IDs. Processed data

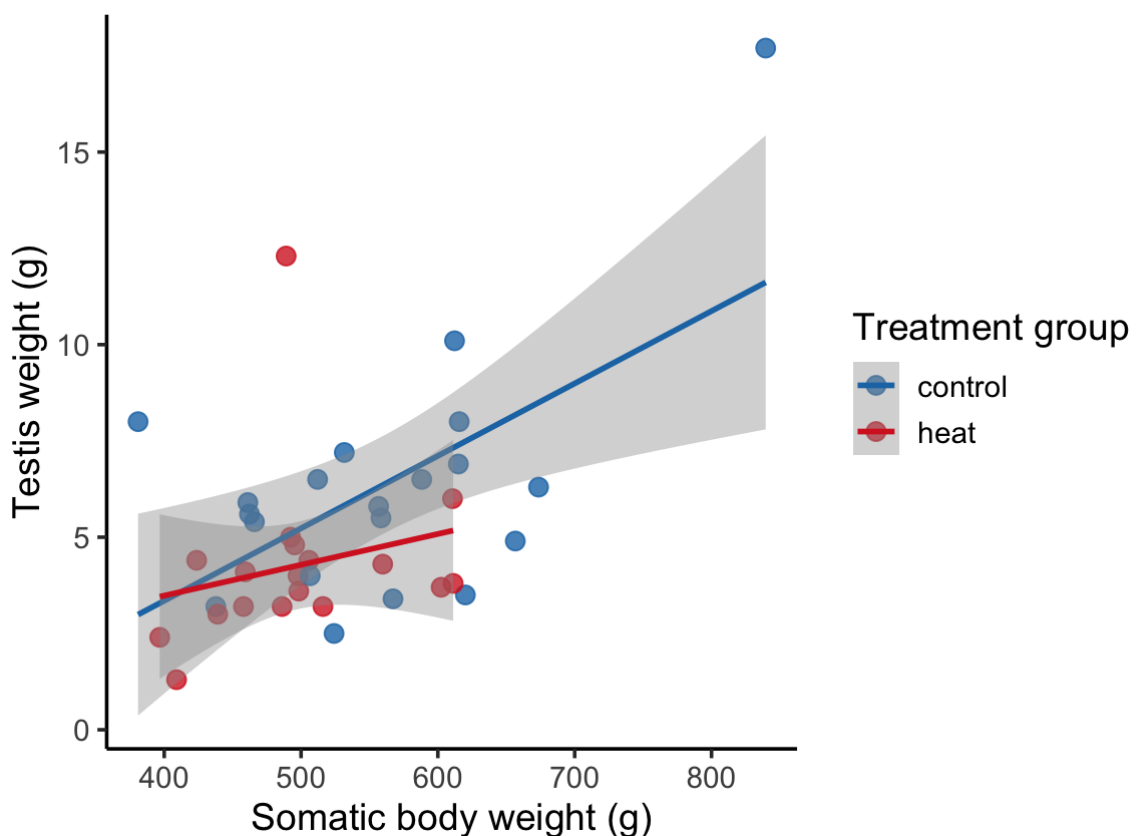
1087 were further analysed and visualised using R version 4.4.3 (The R Foundation for
1088 Statistical Computing, Vienna, Austria, URL <https://www.R-project.org/>), using a
1089 modified Dseq2 differential expression pipeline (Love et al., 2014) to normalize
1090 abundances and determine data significance. Gene Ontology (GO) term analysis
1091 was performed using BioMart (Haw et al., 2011; Smedley et al., 2015) and
1092 Bioconductor (Gentleman et al., 2004) packages through R.

1093 **2.4 Results**

1094 **2.4.1 Relative testes weight**

1095 Visual inspection of the allometric relationship between somatic body weight and
1096 testis mass (Figure 2-1) showed an approximately linear association with variance
1097 increasing at higher testis mass. This supports the suitability of the Gamma GLMs
1098 used to test treatment effects on corrected testes weights.

1099



1100

1101 Figure 2-1: Scatterplot showing the relationship between somatic body weight
1102 (total body mass minus testes; x-axis) and corrected testis mass (y-axis) for
1103 individual males in the control (28°C, blue) and heat-treated (34°C, red) groups.
1104 Points represent individual fish, and coloured lines show group-specific linear
1105 regression fits with 95% confidence intervals.

1106

1107

1108

1109 Across all final Gamma GLMs (Tables 2-1-2-4), the effect of heat treatment on
1110 testes weight was consistently negative, with varying significance depending on
1111 the covariates included. The models included Treatment (Heat vs Control), Batch
1112 (B1–B3), and one of three body-weight covariates (final weight, somatic weight, or
1113 weight change), depending on the model. When controlling for final body mass,
1114 the effect was not significant (Δ Deviance = 3.579, df = 33, p = 0.094, Table 2-1),
1115 but body mass itself was a strong positive predictor of testes weight (p = 0.010). A
1116 similar trend was seen when using post-testes body mass (Δ Deviance = 3.433, df
1117 = 33, p = 0.088, Table 2-2). In contrast, when modelling testes weight as a
1118 proportion of body mass, the treatment effect remained non-significant (Δ
1119 Deviance = 1.258, df = 33, p = 0.089, Table 2-3), suggesting a consistent but
1120 modest reduction in reproductive investment under heat stress.

1121

1122 Table 2-1: Results for Gamma GLM model 1- comparing corrected testes weights
1123 against the final body weight.

Dependent variable: <u>testes_corrected</u>	
Treatment (Heat)	-0.256
t = -1.729	p < 0.1
Weight_T2W	0.002
t = 2.759	p < 0.01
Batch (B2)	-0.025
t = -0.147	
Batch (B3)	0.235
t = 1.380	
Constant	0.496
t = 1.044	
Null deviance	8.848 (df = 37)
Residual deviance	5.269 (df = 33)
Δ Deviance	3.579
Observations	38
Akaike Inf. Crit.	164.359
Note:	* p < 0.1; ** p < 0.05; *** p < 0.01

1124

1125

1126

1127

1128

1129 Table 2-2: Results for Gamma GLM model 2- comparing corrected testes weights
1130 against the adjusted final body weight (with the weight of the testes deducted from
1131 the measured final body weight).

Dependent variable:	testes_corrected
Treatment (Heat)	-0.265
t = -1.759	<i>p < 0.1</i>
Weights_after	0.002
t = 2.593	<i>p < 0.05</i>
Batch (B2)	-0.029
t = -0.172	
Batch (B3)	0.235
t = 1.354	
Constant	0.549
t = 1.131	
Null deviance	8.848 (df = 37)
Residual deviance	5.415 (df = 33)
Δ Deviance	3.433
Observations	38
Akaike Inf. Crit.	165.424
Note:	* <i>p < 0.1</i> ; ** <i>p < 0.05</i> ; *** <i>p < 0.01</i>

1132

1133

1134

1135 Table 2-3: Results for Gamma GLM model 3- comparing proportion of the final
1136 weight that was the testes against adjusted final body weight.

Dependent variable:	Proportion
Treatment (Heat)	-0.269
<i>t</i> = -1.757	<i>p</i> < 0.1
Weights_after	0.0004
<i>t</i> = 0.470	
Batch (B2)	-0.038
<i>t</i> = -0.220	
Batch (B3)	0.228
<i>t</i> = 1.293	
Constant	-4.767
<i>t</i> = -9.639	<i>p</i> < 0.01
Null deviance	8.848 (df = 37)
Residual deviance	5.269 (df = 33)
Δ Deviance	1.258
Observations	38
Akaike Inf. Crit.	-309.107
Note:	* <i>p</i> < 0.1; ** <i>p</i> < 0.05; *** <i>p</i> < 0.01

1137

1138 We also modelled testes weight as a function of weight change during the
1139 experiment. While weight gain was not itself a significant predictor (Δ Deviance =
1140 2.382, df = 33, *p* = 0.187, Table 2-4,), the treatment effect remained significant
1141 (Estimate = -0.396, *p* = 0.016), supporting the interpretation of a direct effect of
1142 heat on testes development, rather than an indirect effect via somatic growth.

1143

1144

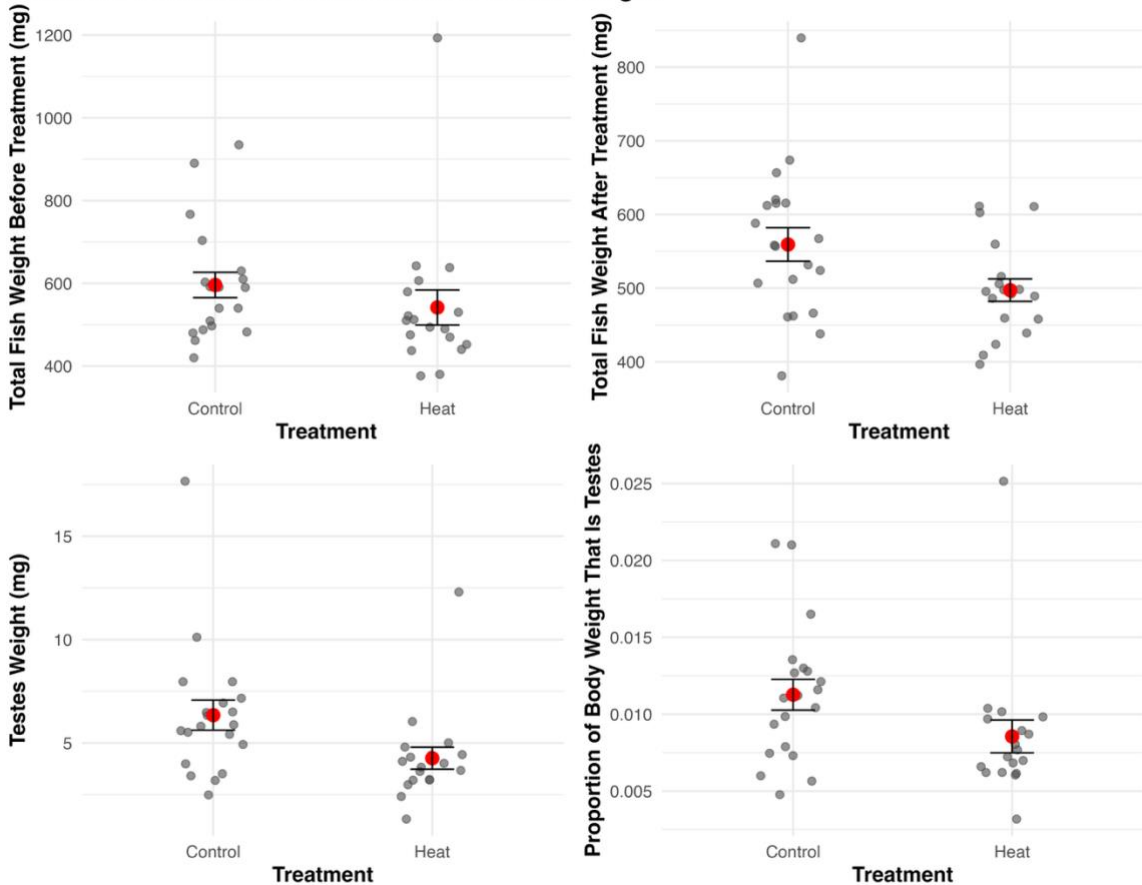
1145 Table 2-4: Results for Gamma GLM model 4- comparing weight of testes
1146 corrected against change in body weight.

Dependent variable:	testes_corrected
Treatment (Heat)	-0.396
t = -2.540	p < 0.05
Weight_dif	0.001
t = 1.348	
Batch (B2)	0.023
t = 0.115	
Batch (B3)	0.191
t = 0.999	
Constant	1.796
t = 12.407	p < 0.01
Null deviance	8.848 (df = 37)
Residual deviance	6.466 (df = 33)
Δ Deviance	2.382
Observations	38
Akaike Inf. Crit.	172.338
Note:	* <i>p</i> < 0.1; ** <i>p</i> < 0.05; *** <i>p</i> < 0.01

1147

1148 Overall, our models consistently show that heat treatment leads to a reduction in
1149 relative testes weight across multiple body size metrics and model structures,
1150 corresponding to an estimated 20–33% decrease in testes mass relative to
1151 controls (Figure 2-2). The magnitude of the effect varies slightly depending on
1152 whether final or adjusted (final weight of the fish with the weight of the testes
1153 deducted) body mass is used, but the direction of the treatment effect is
1154 consistent. Importantly, the observed reduction in testes size persists even after
1155 controlling for variation in somatic growth, supporting the conclusion that elevated
1156 temperature imposes a specific reproductive cost independent of body condition or
1157 size.

Effects of Heat Treatment on Fish and Testes Weight



1158

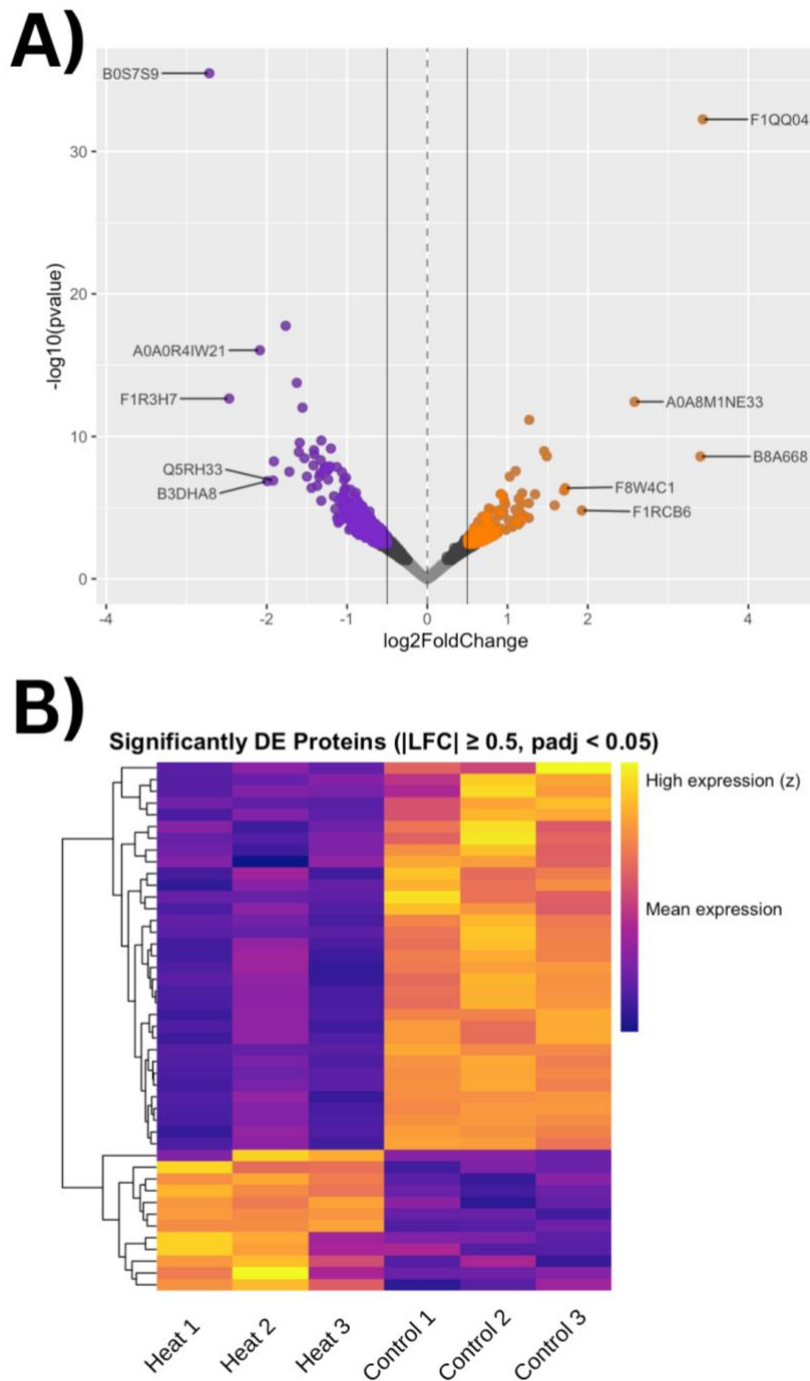
1159 Figure 2-2: Effect of heat treatment on zebrafish body weight and testes weight-
1160 Scatter plots show individual values for control ($n = 21$) and heat-treated fish (n
1161 =21), with red dots indicating the mean and error bars representing standard error
1162 of the mean. A) **total fish** weight before treatment (T_0), B) total somatic weight
1163 after treatment (T_{2W}), calculated as total body weight minus testes, C) testes
1164 weight after treatment and D) proportion of total body weight accounted for by
1165 testes mass.

1166

2.4.2 Testes Proteome

1168 The initial TMT quantitative proteome produced for the six pooled testes samples
1169 resulted in 11,434 peptide matches using Uniprot database version 2022_05.
1170 Following re-mapping of the proteome to the more recent Uniprot database
1171 version 2024_06, and filtering to remove medium and low FDR confidences as
1172 well as entries with unique peptide numbers less than two, a total of 5415 proteins
1173 were confidently identified (Supplementary Table 1). We compared protein

1174 abundance between the two experimental groups using the software *DESeq2*
1175 (Love et al., 2014) of the 5,415 identified proteins with non-zero total read counts,
1176 a total of 414 proteins (7.6%) were identified as significantly differentially abundant
1177 ($p_{adj} < 0.05$) between testes of males kept at 28°C and 34°C (Supplementary
1178 Table 2). Of these, 146 proteins (2.7%) were significantly more abundant in heat
1179 treated testes (\log_2 fold change > 0), and 268 proteins (4.9%) were significantly
1180 less abundant in heat treated testes (\log_2 fold change < 0). No outliers were
1181 detected based on Cook's distance, and no features were filtered out due to low
1182 counts (mean count < 410), as determined by independent filtering in *DESeq2*. We
1183 added an additional filtering step to retain only proteins with an absolute \log_2 fold
1184 change ($|LFC| \geq 0.5$) to ensure only proteins that substantially changed as a result
1185 of treatment are included. This produced a final list of 377 proteins that showed
1186 significantly different abundances between the heat treated and control testes, of
1187 which 244 were found to be significantly more abundant in Control testes, and 133
1188 were significantly more abundant in heat-treated testes (Figure 2-3).



1189

1190 Figure 2-3- Heatmap and Volcano plot of differences in testes proteome as a
 1191 result of heat stress. (A) Volcano plot showing the 5415 identified proteins, with
 1192 significantly more abundant proteins in heat treated testes ($p_{adj} < 0.05$, $LFC > 0.5$)
 1193 shown in orange, whilst significantly less abundant proteins in heat treated testes
 1194 ($p_{adj} < 0.05$, $LFC < -0.5$) shown in violet. (B) A heatmap with all 5415 identified
 1195 proteins $LFC > 0.5$ and $p_{adj} < 0.05$.

1196 The five proteins with most significantly lower abundance in testes of heat-treated
1197 males were F1R3H7, Q5RH33, A0A0R4IW21, B0S7S9, and B3DHA8 (Figure 2-
1198 3A). Of these, F1R3H7 and Q5RH33 correspond to annotated proteins (RIB43A-
1199 like with coiled-coils protein 1, and FYVE, RhoGEF and PH domain-containing 6,
1200 respectively), while the remaining three were listed as uncharacterised or identified
1201 via Sanger codes.

1202

1203 The five proteins with most significantly higher abundance in testes of heat-treated
1204 males were F1QQ04, A0A8M1NE33, B8A668, F8W4C1, and F1RCB6 (Figure 2-
1205 3A). Based on UniProt annotation, these correspond to Serpin H1 (collagen-
1206 binding protein), Heat shock cognate 71 kDa protein, Calponin, Myelin basic
1207 protein, and Actin alpha cardiac muscle 1a, respectively.

1208

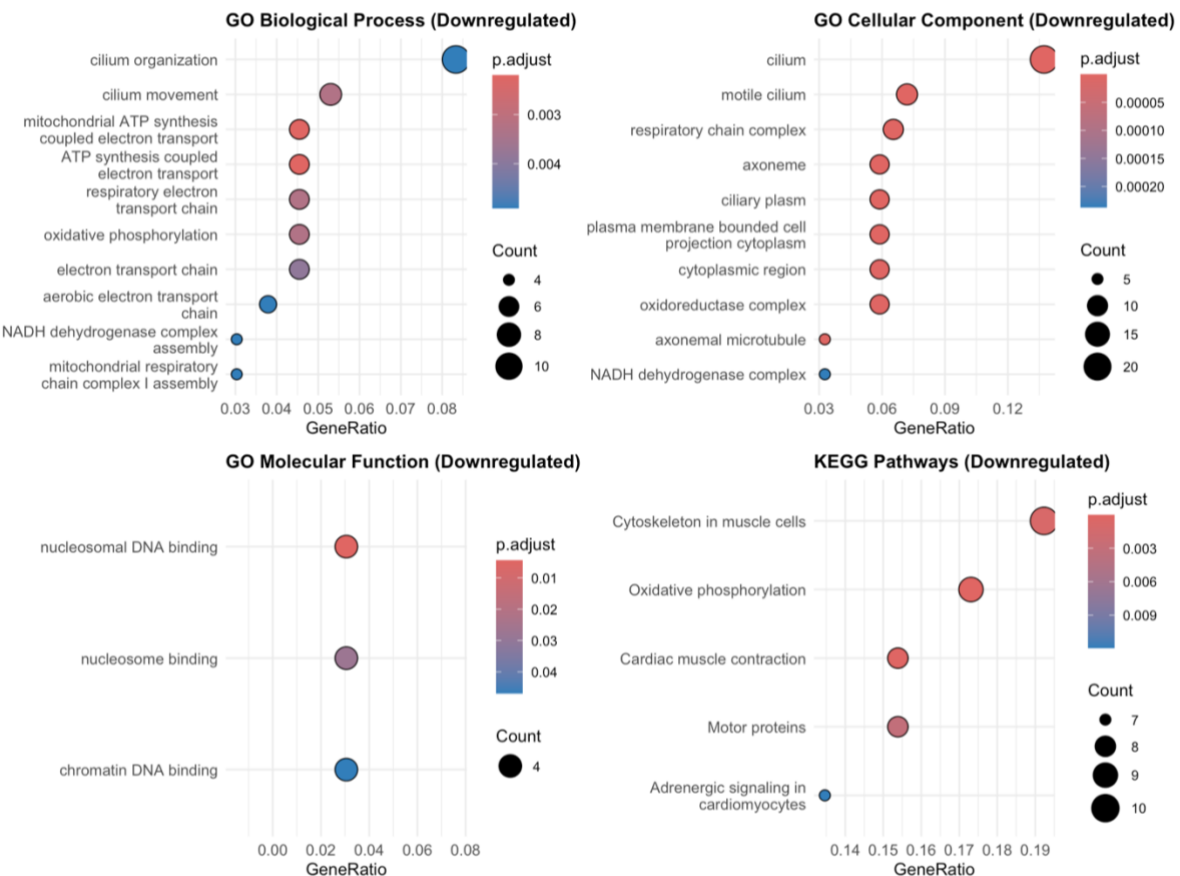
1209 **2.4.3 The GO terms and STRING analysis**

1210 Protein IDs were mapped using *BioMart* (Smedley et al., 2015) to retrieve
1211 corresponding Ensembl and Entrez gene identifiers for both significantly
1212 upregulated and downregulated proteins in the heat-treated testes proteome,
1213 compared to Controls. The resulting gene IDs were analysed for functional
1214 enrichment using the full zebrafish genome as the background. Enriched Gene
1215 Ontology (GO) terms were identified across the categories of Biological Process,
1216 Cellular Component, and Molecular Function, along with KEGG pathways
1217 (Supplementary Tables 3 & 4).

1218

1219 Gene ontology (GO) enrichment analysis of proteins with lower abundance in
1220 heat-treated testes identified significant enrichment for biological processes
1221 including cilium organization, cilium movement, oxidative phosphorylation, electron
1222 transport chain, and mitochondrial complex I assembly (Figure 2-4).
1223 Corresponding cellular component terms included cilium, motile cilium, axoneme,
1224 respiratory chain complex, and NADH dehydrogenase complex. Molecular function
1225 terms were enriched for nucleosomal DNA binding and nucleosome binding.
1226 KEGG pathway analysis highlighted downregulation of oxidative phosphorylation,

1227 cardiac muscle contraction, cytoskeletal elements, motor proteins, and adrenergic
1228 signalling in cardiomyocytes (Figure 2-4).



1229

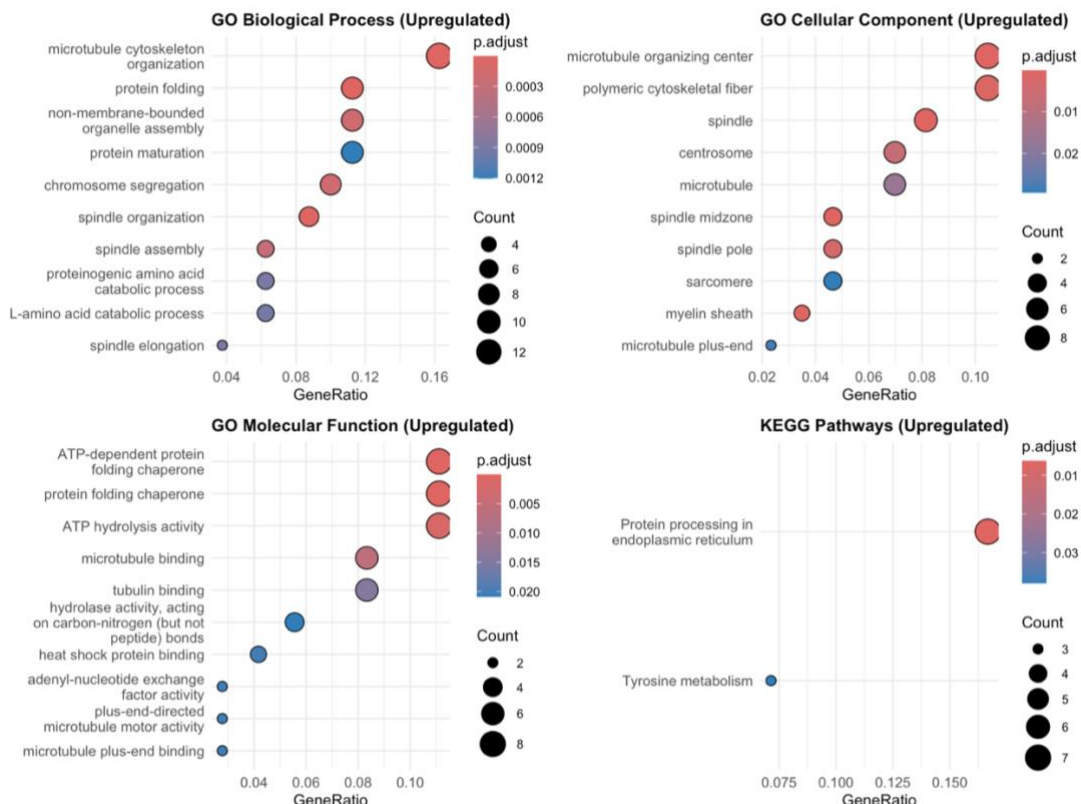
1230 Figure 2-4: GO terms of genes linked to proteins that are downregulated in heat-
1231 stressed zebrafish testes. Dot plots showing the top 10 terms for each GO
1232 analysis (biological processes, cellular components and molecular function) and
1233 KEGG pathways enriched for proteins that were less abundant in heat treated
1234 testes compared to control testes. The GO terms were calculated against a
1235 background of the entire zebrafish genome.

1236

1237 For proteins with higher abundance in heat-treated testes, enriched GO biological
1238 processes included microtubule cytoskeleton organization, protein folding, spindle
1239 assembly and organization, chromosome segregation, and organelle assembly
1240 (Figure 2-5). Cellular component terms included centrosome, spindle, microtubule,
1241 and sarcomere, while molecular function terms were enriched for ATP-dependent
1242 protein folding chaperones, ATP hydrolysis activity, and microtubule binding.

1243 KEGG pathway analysis identified enrichment for protein processing in the
1244 endoplasmic reticulum and tyrosine metabolism (Figure 2-5).

1245

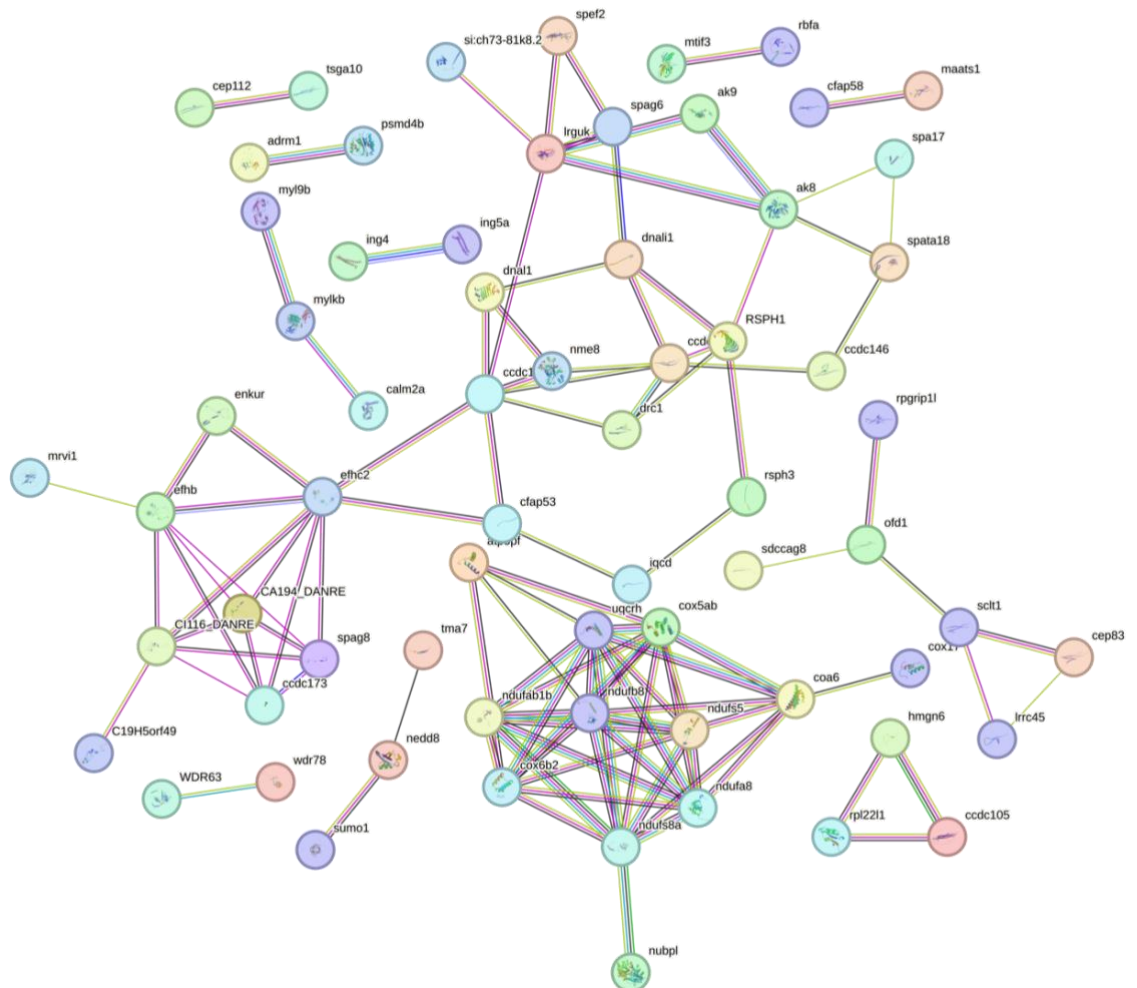


1246

1247 Figure 2-5: GO terms of genes linked to proteins that are upregulated in heat-
1248 stressed zebrafish testes. Dot plots showing the top 10 terms for each GO term
1249 (biological processes, cellular components and molecular function) and KEGG
1250 pathways enriched for proteins that were more abundant in heat treated testes
1251 compared to control testes. These GO terms were calculated against a
1252 background of the entire zebrafish genome.

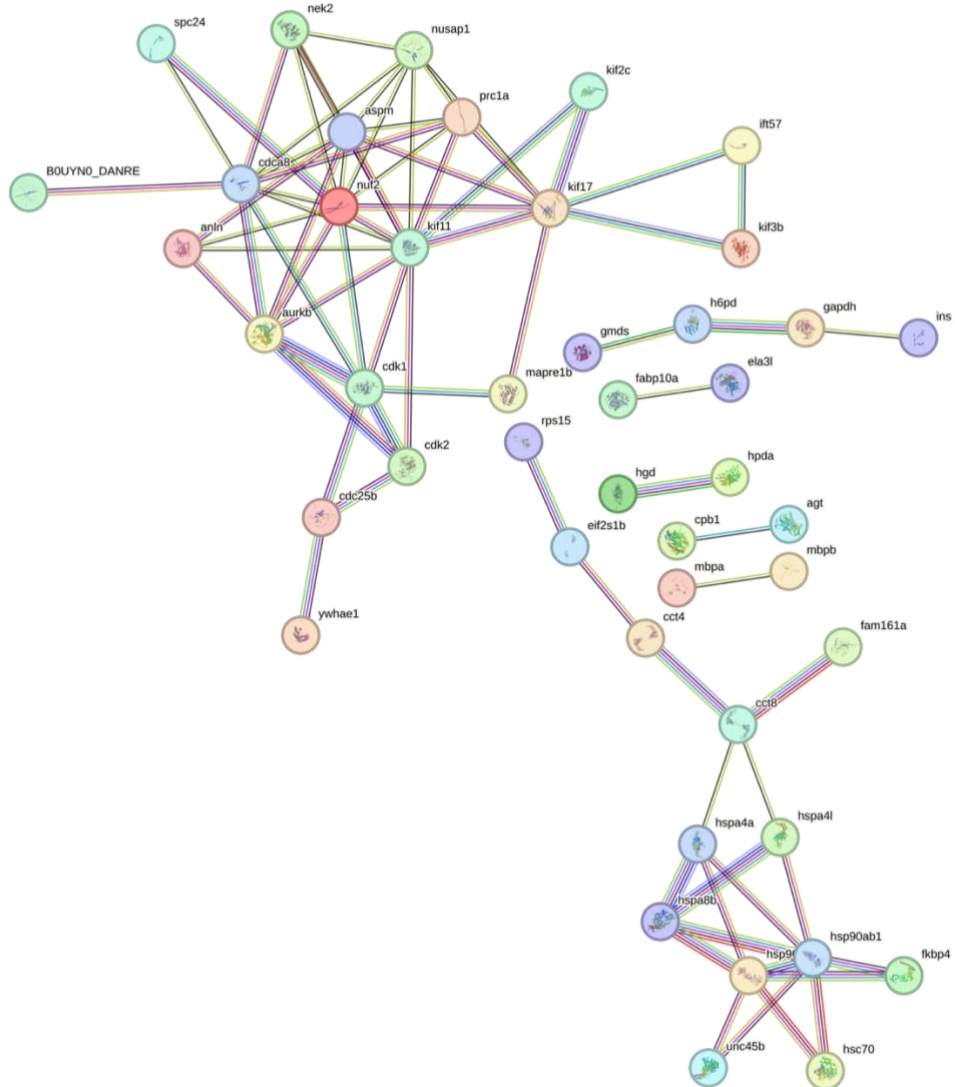
1253

1254 STRING network analysis of downregulated proteins revealed a cluster of
1255 interactions among oxidative phosphorylation-related proteins, including
1256 cytochrome c oxidase subunit (Cox6b2) and multiple components of the NADH
1257 dehydrogenase (Nduf) complex (Figure 2-6). In the network of upregulated
1258 proteins, two main clusters were detected: one comprising heat shock proteins
1259 (including Hsp90) and another comprising kinesin-like proteins (kif11, kif17)
1260 (Figure 2-7).



1262

1263 Figure 2-6- STRING network of protein–protein interactions for proteins
 1264 significantly less abundant in testes of heat-treated males ($p_{adj} < 0.05$, LFC ≤ -0.5). Nodes represent proteins and are colour-coded according to STRING
 1265 functional enrichment clusters. Each node contains the predicted tertiary structure
 1266 generated by the STRING/PDB model. Edges represent protein–protein
 1267 associations, with edge colours indicating the evidence source; known
 1268 interactions: curated databases (light blue), experimentally determined (pink),
 1269 predicted interactions: gene neighbourhood (green), gene fusions (red), gene co-
 1270 occurrence (blue), other evidence: text mining (yellow), co-expression (black),
 1271 protein homology (purple). A minimum interaction confidence score of 0.7 (high
 1272 confidence) was applied, and all disconnected proteins were hidden.



1274
 1275 Figure 2-7- STRING network of protein–protein interactions for proteins
 1276 significantly more abundant in testes of heat-treated males ($p_{adj} < 0.05$, LFC ≥ 0.5).
 1277 Nodes represent proteins and are colour-coded according to STRING functional
 1278 enrichment clusters. Each node contains the predicted tertiary structure of the
 1279 protein, as generated by the STRING/PDB modelling pipeline. Edges represent
 1280 predicted or known protein–protein associations, and edge colours correspond to
 1281 the specific underlying evidence source: known interactions: curated databases
 1282 (light blue), experimentally determined (pink), predicted interactions: gene
 1283 neighbourhood (green), gene fusions (red), gene co-occurrence (blue), other
 1284 evidence sources: text mining (yellow), co-expression (black), protein homology
 1285 (purple). A minimum interaction confidence score of 0.7 (high confidence) was
 1286 applied. Disconnected proteins were hidden to improve clarity of the interaction
 1287 network.

1288 **2.5 Discussion**

1289 **2.5.1 The global zebrafish testes proteome**

1290 Previous global proteomes of zebrafish testes identified 2214 proteins (Groh et al.,
1291 2011a) compared to 5,415 proteins identified in our study. However, these
1292 previous results were published 14 years before the analysis of our data and whilst
1293 similar methods of LC-MS/MS were used, the technology for identification of lower
1294 abundance proteins has greatly improved, leading to the increase in proteins
1295 identified in our study. Similarly in more recent targeted proteomic analyses of the
1296 zebrafish testes response to microplastic exposure, 1347 proteins were identified
1297 (Li et al., 2024), however, the number of fish per pool used in the recently
1298 published paper was lower than our study, potentially suggesting that our data
1299 provide a broader snapshot of the testes proteome. Although our data do not
1300 classify or characterise the proteins identified within this proteome in depth, the
1301 addition of these proteins to the confirmed zebrafish testes proteome can act as a
1302 resource for continued research.

1303

1304 Comparable upregulation of molecular chaperones and cytoskeletal regulators has
1305 been reported in the testes of other ectothermic species exposed to thermal
1306 stress, including tilapia (*Oreochromis niloticus*), common carp (*Cyprinus carpio*),
1307 and rainbow trout (*Oncorhynchus mykiss*), indicating a conserved protective
1308 strategy to maintain spermatogenic function (Deane & Woo, 2011). These
1309 parallels suggest that activation of protein-folding and cytoskeletal stabilization
1310 pathways represents a general vertebrate response to elevated temperature,
1311 rather than one unique to zebrafish.

1312

1313 **2.5.2 The effects of heat stress on the testes proteome**

1314 Among the top five proteins with significantly lower abundance in heat stressed
1315 testes, F1R3H7 is a RIB43A-like protein with coiled-coils protein 1, which has
1316 been linked to the formation and function of cilia or flagella-like structures in both
1317 humans and zebrafish (Frohnhofer et al., 2016). The second identifiable protein
1318 was Q5RH33, which is a FYVE, RhoGEF and PH domain-containing 6 protein.

1319 This protein has been previously identified as important in embryogenesis
1320 although the exact role has not been investigated (Lo et al., 2003). These proteins
1321 would suggest that the formation of flagella and therefore the processes of
1322 spermatogenesis may be decreased in zebrafish testes in response to prolonged
1323 heat exposure.

1324

1325 The highest-ranked protein by LFC was Serpin H1 (F1QQ04), also known as Heat
1326 shock protein 47 (HSP47), which functions as a molecular chaperone involved in
1327 the biosynthesis and proper folding of collagen, a role which is conserved across
1328 many aquatic species including rainbow trout *Oncorhynchus mykiss*, and zebrafish
1329 . In addition to its role in collagen maturation, HSP47 contributes to the
1330 preservation of cellular architecture and function under stress conditions including
1331 thermal stress and hypoxia (Lim & Bernier, 2022). Another highly-ranked protein
1332 by LFC A0A8M1NE33 is commonly known as heat shock 70 kDa protein-like and
1333 has a role as a molecular chaperone in maintaining cellular functions during stress
1334 response, in a highly conserved process across aquatic species such as the Nile
1335 tilapia *Oreochromis niloticus*, with both proteins regulated through the heat-shock
1336 factor 1 pathway (Delaney & Klesius, 2004). The presence of these two heat-
1337 shock proteins among the most strongly upregulated in heat-treated testes
1338 indicates a substantial cellular investment in molecular repair and stress mitigation
1339 mechanisms compared to the control group.

1340

1341 The third most upregulated protein, Calponin (B8A668), is an actin-binding protein
1342 that regulates actomyosin interactions and smooth muscle contraction. Calponin
1343 has been implicated in cytoskeletal reorganization and cell motility, processes that
1344 may be particularly important under stress conditions where structural stability of
1345 the testes is compromised (Q. Zhu et al., 2004). The fourth, Myelin basic protein
1346 (F8W4C1), is a structural protein previously noted in the nervous system of
1347 zebrafish (Brösamle & Halpern, 2002), but it may participate in membrane
1348 stabilization and signalling during spermatogenesis, as it has previously been
1349 identified in the testes of *Xenopus laevis* (Nanba et al., 2010). Finally, Actin alpha
1350 cardiac muscle 1a (F1RCB6) is a cytoskeletal protein central to contractile and

1351 structural integrity, with expression in multiple tissue types (Arora et al., 2023).
1352 Upregulation of this isoform of actin may suggest effects on the ability for the
1353 testes to contract and expand during ejaculation.

1354

1355 Together, these proteins highlight a combined response to heat stress in zebrafish
1356 testes that involves both canonical molecular chaperones (HSP47, HSP70-like)
1357 and structural or cytoskeletal elements (Calponin, Myelin basic protein, and Actin),
1358 pointing to a coordinated effort to preserve testicular architecture and maintain
1359 spermatogenic potential under elevated temperatures.

1360

1361 **2.5.3 The effects of heat stress on testes size**

1362 To determine if changes in the testes proteome reflected a general reduction in
1363 testes size or a more specific disruption of processes such as spermatogenesis,
1364 body weights were measured pre- and post-treatment and testes weights
1365 measured post-treatment. Our analysis showed a reduction in relative testes size
1366 in heat-treated males. Therefore, the reduction in sperm yield is likely to reflect
1367 both impaired spermatogenesis and a measurable decrease in gonad size under
1368 heat stress. These findings echo results found in other species such as red flour
1369 beetles, where up to a 40% reduction in testes volume were found after sublethal
1370 heat treatment (Cole et al., 2025). In Nile tilapia (*Oreochromis niloticus*), exposure
1371 to elevated temperatures (36–37 °C) led to pronounced testicular atrophy,
1372 vacuolization and the loss of spermatogenic germ cells, although partial recovery
1373 was observed after return to control temperatures (Jin et al., 2019). Similar
1374 reductions in testes size under elevated temperatures have been documented in
1375 the European bullhead (*Cottus gobio*), where thermal stress impaired reproductive
1376 physiology and reduced gonadal investment (Dorts et al., 2012).

1377

1378 Our findings align with a growing body of research showing that heat stress can
1379 directly impair spermatogenesis in ectothermic taxa. In freshwater ectotherms
1380 such as guppies (*Poecilia reticulata*), experimental heatwaves have been shown to
1381 reduce testis size, sperm number, and sperm velocity, resulting in a cumulative
1382 deterioration of reproductive performance (Breedveld et al., 2023). Similarly,

1383 comparative reviews of teleost fishes highlight that elevated temperatures disrupt
1384 gametogenesis at multiple levels, from germ cell proliferation to spawning output,
1385 with consequences for population dynamics under climate change scenarios (Alix
1386 et al., 2020).

1387

1388 **2.5.4 The GO terms and STRING analyses of heat-stressed testes**

1389 The idea that the heat-treated testes show decreased spermatogenesis and
1390 increased stress response compared to the control testes is further supported by
1391 GO term analysis (Figure 2-3, 2-4). The terms noted for GO terms related to less
1392 abundant proteins are mainly directly related to both the function of mature sperm
1393 and the processes of spermatogenesis which suggests that not only was
1394 spermatogenesis decreased in heat-treated testes, but the overall number of
1395 mature sperm was lower as well. Decreases in spermatogenic output as a
1396 response to heat stress have been widely observed across teleost species. For
1397 example, in medaka *Oryzias latipes* with a loss of developing sperm cells being
1398 noted alongside the importance of the Notch pathway in maintaining
1399 spermatogonial stem cells (and therefore spermatogenesis) during the application
1400 of thermal stress (Moreno Acosta et al., 2023).

1401

1402 The GO terms related to higher abundance proteins in the heat-treated testes are
1403 suggestive of cellular repair and stress response. Notably the upregulation of
1404 cellular repair, as well as the higher abundance of HSP47 and HSP70 is contrary
1405 to patterns that have previously been reported. It has previously been reported
1406 that other teleost including the minnow *Puntius sophore* demonstrate a
1407 downregulation of HSP proteins in the gonads in response to thermal stress,
1408 possibly due to an increase in testes apoptosis (Mahanty et al., 2019). In contrast,
1409 the combination of upregulated repair-associated GO terms and elevated HSP
1410 expression in our dataset suggests that the zebrafish in this study may possess a
1411 greater reproductive tolerance to elevated temperatures, mounting a repair
1412 response rather than entering a degenerative state. This interpretation is further
1413 supported by the fact that testes weight was reduced in heat-treated males, with

1414 some of this change potentially attributable to overall somatic effects and
1415 spermatogenic reduction instead of direct gonadal destruction.

1416

1417 These GO term sets are supported by STRING analysis of the significantly more
1418 and less abundant proteins (Figures 2-6 and 2-7). The STRING analysis of
1419 significantly less abundant proteins in heat-treated testes includes cytochrome c
1420 oxidase subunit (Cox6b2) and several components of the NADH dehydrogenase
1421 (Nduf) complex, both key elements of the oxidative phosphorylation pathway. This
1422 finding suggests a reduction in oxidative phosphorylation activity in the heat-
1423 treated testes, which may reflect a state of oxidative stress in the testes. The direct
1424 link between heat stress and oxidative stress has previously been shown in mice,
1425 with developing round spermatids being directly vulnerable to these stressors
1426 (Houston et al., 2018). The vulnerability of developing spermatids to both heat and
1427 oxidative stress further implicates that the processes of spermatogenesis and
1428 sperm maturation are likely to be highly affected by thermal stress, reducing the
1429 spermatogenic output of testes.

1430

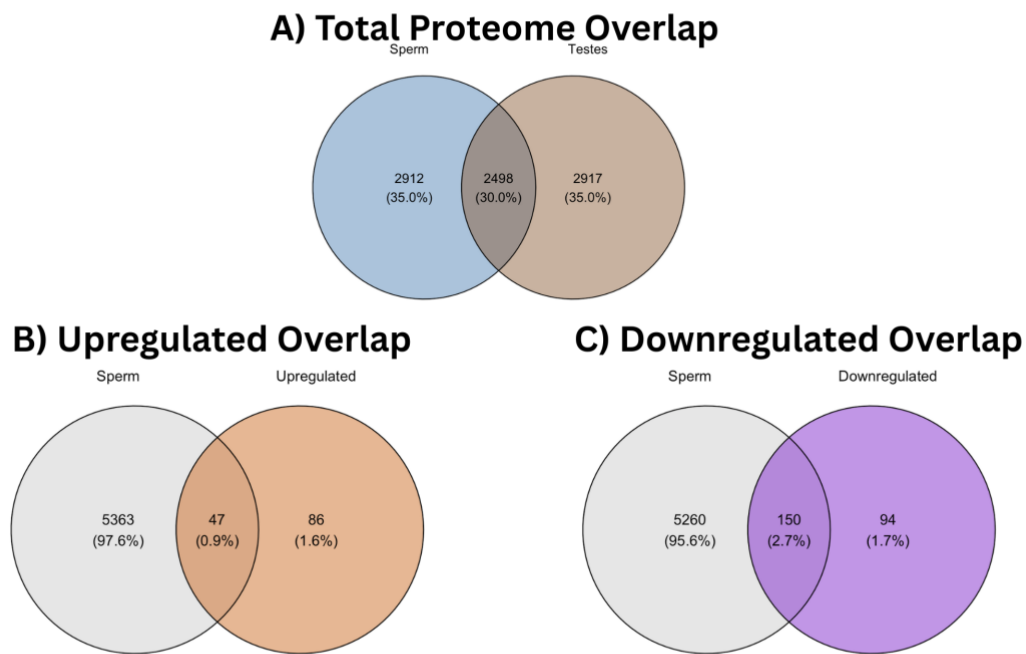
1431 The STRING analysis of the more abundant proteins also supports the
1432 mechanisms presented by the GO terms, with nodes containing two Hsp90
1433 proteins, suggestive of a heat-stress response and another node containing both
1434 kif11 and kif17 (kinesin-like proteins) which is suggestive of cellular proliferation
1435 and repair, similarly to the GO terms. Kinesins and kinesin-like proteins have
1436 previously been reported to be heavily involved in spermatogenesis, with kif17
1437 implicated in chromatoid body movement and RNA metabolism (Ma et al., 2017).
1438 This seems counter-intuitive to the reduction in spermatogenesis noted earlier,
1439 however, these proteins are also capable of forming complexes with HSP proteins
1440 and are therefore also integral to the thermal stress response (Hirokawa &
1441 Tanaka, 2015).

1442

1443 Another line of evidence supporting the hypothesis that heat-stressed testes
1444 undergo reduced spermatogenesis comes from the overlap between the zebrafish
1445 sperm proteome (Chapter 3) and the testicular proteome presented here. Notably,

1446 the sperm proteome was generated from sperm stripped directly from the same
1447 testes used in this study. However, due to difficulties in collecting sperm from heat-
1448 treated males, primarily due to low sperm counts and small ejaculate volume, no
1449 treatment-based comparison could be made within the sperm proteome dataset.
1450 Despite this limitation, the comparison of protein overlap is revealing: 150 proteins
1451 of lower abundance in the heat-treated testes overlapped with the sperm
1452 proteome, compared to only 47 proteins of higher abundance (Figure 2-8). This
1453 suggests that many of the proteins reduced in abundance in heat-stressed testes
1454 are likely sperm-associated, further supporting the idea of reduced spermatogenic
1455 output under heat stress.

1456



1457

1458 Figure 2-8: Venn diagrams comparing the zebrafish testes proteome and zebrafish
1459 sperm proteome (Chapter 3). (A) Venn diagram representing the overall overlap
1460 between the zebrafish sperm proteome (Chapter 3) with the combined zebrafish
1461 testes proteome. (B) Venn diagram showing the overlap of the sperm proteome
1462 (Chapter 3) with the significant proteins of higher abundance in the heat-treated
1463 testes. (C) Venn diagram showing the overlap of the sperm proteome (Chapter 3)
1464 with the significant proteins of lower abundance in the heat-treated testes.

1465 The continued evidence of a reduction in spermatogenesis in the testes in
1466 response to thermal stress directly links to previous data showing decreased
1467 fertility in male zebrafish in response to the same heat stress parameters (Irish et
1468 al., 2024). However, the upregulation of repair-associated proteins in the testes
1469 shown here may help explain the lack of observed effects on offspring quality in
1470 those same experiments. This suggests that while spermatogenesis was impaired,
1471 active cellular repair mechanisms may have mitigated the production or release of
1472 damaged sperm, thereby buffering against downstream reproductive
1473 consequences.

1474

1475 **2.5.5 Conclusion**

1476 Overall, our study provides both a comprehensive global proteomic profile of the
1477 zebrafish testes and protein-level evidence for the physiological effects of heat
1478 stress on the male gonads. These effects include clear signatures of impaired
1479 spermatogenesis and heightened stress-induced cellular repair. Notably, the most
1480 differentially abundant proteins included classical heat shock proteins such as
1481 Hsp70 and Serpin H1 (HSP47), consistent with the activation of protective
1482 chaperone systems in response to thermal insult. In contrast, GO terms
1483 associated with proteins of significantly lower abundance in heat-treated testes
1484 were enriched for processes related to cilia formation and motility, functions
1485 strongly linked to mature sperm cells.

1486

1487 Importantly, the hypothesis that molecular differences were solely due to reduced
1488 testis size in heat-treated males was not supported. Although gonad size
1489 decreased by 20–33% in heat-treated fish, this morphological change alone is
1490 unlikely to explain all the molecular alterations detected. This strengthens the
1491 conclusion that heat stress directly impairs the cellular and molecular processes of
1492 spermatogenesis, rather than causing changes through generalised shrinkage of
1493 the gonad.

1494

1495 Taken together, our findings offer a detailed insight into the molecular and
1496 physiological impacts of heat stress on male zebrafish reproduction, with broader

1497 implications for understanding thermal sensitivity in teleost fish. This dataset lays
1498 important groundwork for future studies into reproductive resilience under climate
1499 change and may help predict the reproductive consequences of rising water
1500 temperatures for externally fertilising species.

1501

1502 **3 The Zebrafish Sperm Proteome**

1503 This chapter is based on the following published manuscript:

1504 Cohen-Krais, J., Martins, C., Bartram, J., Crighton, Z., de Coriolis, J.-C., Godden,
1505 A., Marcu, D., Robak, W., Saalbach, G. and Immler, S. (2025), The Zebrafish
1506 Sperm Proteome. *Proteomics*, 25:

1507 e202400310. <https://doi.org/10.1002/pmic.202400310> (Appendix 1)

1508 **3.1 Abstract**

1509 One of the key processes that forms the basis of fertilisation is the tight interaction
1510 between sperm and egg. Both sperm and egg proteomes are known to evolve and
1511 diverge rapidly even between closely related species. Understanding the sperm
1512 proteome therefore provides key insights into the proteins that underpin the
1513 mechanisms involved during fertilisation and the fusion between sperm and egg,
1514 and how they can differ across individuals of the same species. Despite being a
1515 commonly used model organism for reproductive research, little is currently
1516 understood about the sperm proteome of the zebrafish *Danio rerio*. We performed
1517 proteomics analysis using nanoLC-MS/MS after off-line sample fractionation with
1518 six pooled samples containing sperm from ten males each. A total of 5410 proteins
1519 were confidently identified, from which a total of 3900 GenelIDs were generated
1520 leading to 1720 Gene Ontology terms. A high abundance of histone proteins was
1521 noted, with 8 identified within the top 25 most abundant proteins. This proteome
1522 also provides evidence of the retention of proteins that have previously been
1523 identified as important for spermatogenesis.

1524

1525 **3.2 Introduction**

1526 Sperm are highly complex cells with key functions essential for successful
1527 reproduction and fertility. The proteome of sperm provides insight into functional
1528 aspects such as motility, capacitation, and fertilisation (Amaral, Castillo, et al.,
1529 2014). Sperm morphology, and therefore the sperm proteome, shows
1530 considerable variation not only across species and individuals but also between
1531 ejaculates from the same individual, influenced by factors such as age (Kleshchev
1532 et al., 2023), environmental conditions (Kleshchev et al., 2021), and overall health
1533 status (Morrow & Gage, 2001). Identifying and quantifying the proteins present in
1534 sperm can therefore help pinpoint potential biomarkers associated with male
1535 reproductive performance and fertility.

1536

1537 According to Web of Science (Clarivate (Web of Science). Clarivate 2024. All
1538 rights reserved.), “sperm proteomes” have been described in 891 papers,
1539 including 34 human papers and 857 papers on other species. The current total
1540 number of proteins identified in the human sperm proteome is 6871 combined
1541 across all accessible human sperm proteomics datasets, with a maximum of 5685
1542 identified from a single experiment (Luo et al., 2022). Similarly, in the domestic
1543 bull *Bos taurus*, proteomic analyses of high and low motility sperm populations
1544 revealed that 498 proteins differed between high and low fertility bulls (D’Amours
1545 et al., 2019a). Furthermore, the number of proteins identified in sperm proteomes
1546 differ by up to 21.6% across three mouse species (Aitken et al., 2007; Baker,
1547 Hetherington, Reeves, Müller, et al., 2008; Chauvin et al., 2012; Vicens et al.,
1548 2017), exhibiting divergent mating systems thought to drive the evolution in the
1549 sperm proteome. In the oyster *Crassostrea hongkongensis*, the sperm proteome
1550 was used to establish the molecular mechanisms underlying species-specific
1551 sperm and oocyte binding in free-spawning organisms (Mu et al., 2020), and
1552 similarly, high levels of variation in the sperm proteome have been identified
1553 across marine mussel species *Mytilus edulis* and *Mytilus galloprovincialis* (Romero
1554 et al., 2019).

1555

1556 Previous studies highlight the diversity and rapid divergence of sperm proteomes
1557 even between closely related species as an indicator of their key role in
1558 reproduction (Vicens et al., 2017). In teleost fish species such as the rainbow
1559 trout *Oncorhynchus mykiss*, 206 proteins have been identified in sperm (Nynca et
1560 al., 2014), whereas in carp *Cyprinus carpio*, 348 proteins were identified (Dietrich
1561 et al., 2014). This variation in protein numbers is likely not only due to biological
1562 differences between species but also the analytical methods used to determine the
1563 proteomes. More accurate data are therefore needed to allow further research into
1564 the role of the sperm proteome in sperm function and sperm-egg interactions.

1565

1566 The zebrafish *Danio rerio* is a popular model organism for biomedical research
1567 ranging from ecotoxicology, evolutionary and developmental biology, cancer and
1568 neurodegenerative diseases, and ageing (Hajam et al., 2021). As an externally
1569 fertilising vertebrate, collection of gametes and *in vitro* fertilisation is particularly
1570 easy and can be performed mimicking natural conditions, rendering the zebrafish
1571 a prime model organism to study fertility and reproduction (Meyers, 2018).
1572 Proteomic profiles have been developed for a wide range of zebrafish tissues
1573 including the testes (2214 described proteins) and the ovaries (1379 described
1574 proteins) (Groh et al., 2011b). In addition, the zebrafish oocyte proteome has been
1575 described with 1568 proteins differing between mature and immature oocytes (C.
1576 Ge et al., 2017) and the proteome profiling of zebrafish embryos has been used to
1577 study the effects of environmental stressors such as toxins (Vieira et al., 2020).
1578 The available proteomic profile of the zebrafish currently includes 53,918 proteins
1579 on the NCBI Refseq protein database (O'Leary et al., 2016). However, despite the
1580 proliferation of proteomic profiling of zebrafish tissues and cell types, the global
1581 proteomic profiling of zebrafish sperm is currently lacking.

1582

1583 Here, the global proteomic profile of zebrafish sperm was obtained through
1584 tandem liquid chromatography-mass spectrometry (LC-MS/MS) and analysed
1585 through the comparison of relative peptide abundance as well as Gene Ontology.

1586

1587 **3.3 Methods**

1588 **3.3.1 Zebrafish husbandry and experimental set up**

1589 Sperm were collected from sexually mature ABWT (AB Wild Type strain) male
1590 zebrafish, originally obtained from the Zebrafish International Resource Center
1591 (ZIRC, Oregon) and maintained at the Controlled Environment Facility at the
1592 University of East Anglia, UK. The males were between 1 and 1.5 years old and at
1593 the peak of reproductive age. All fish were kept in a recirculating aquatic system
1594 with filtered, UV-treated water and maintained under standard zebrafish husbandry
1595 conditions. Prior to gamete collection, the fish were maintained in 3.5 L tanks at a
1596 10:6 male to female sex ratio kept at 28°C (standard temperature) or 34°C (high
1597 temperature) to test for a potential role of environmental factors shaping the sperm
1598 proteome with a 14:10 light schedule and fed ad libitum with a mix of dry feed
1599 (ZEBRAFEED 400–600 by SPAROS, Área Empresarial de Marim, Lote C, 8700-
1600 221 Olhão, Portugal) and live *Artemia* (Sep-Art Artemia Cysts, Ocean Nutrition).
1601 All fish used for experiments were kept under Home Office license P0C37E901.

1602
1603 Males were housed as part of a three-block design, with each block consisting of
1604 one control tank (28 °C) and one heat-treatment tank (34 °C). Fish were randomly
1605 distributed into tanks in the standard 10:6 male:female ratio (16 fish per 3.5 L
1606 tank). Within each block, control and heat-treatment tanks were positioned
1607 adjacent to one another on the same rack to ensure identical light, flow, and
1608 environmental conditions. Submersible heaters were added to all tanks activated
1609 at 34 °C for treatment tanks or 28°C in control tanks to control for potential heater
1610 effects. Fish were maintained under their assigned temperature for two weeks
1611 prior to sperm collection.

1612
1613 Following anaesthesia using metomidate hydrochloride (Aquacalm by Syndel, #9,
1614 4131 Mostar Rd, Nanaimo, BC V9T 6A6 Canada), males were stripped for sperm
1615 through gentle squeezing in a cranio-caudal direction and the ejaculates were
1616 collected immediately into a microcapillary tube. Due to the low number of cells
1617 produced in a single zebrafish ejaculate, sperm samples from ten males were
1618 pooled into one replicate sample to ensure sufficient material for mass

1619 spectrometry, and we collected a total of six biological replicates (60 males).
1620 These sperm pools were washed in Hanks' Balanced Salt Solution to remove
1621 seminal fluid and pelleted through centrifugation for 8 min at 8000 rpm, before
1622 freezing in N₂, followed by storage at -80°C.

1623

1624 **3.3.2 Proteomics**

1625 After thawing, sperm pool pellets were precipitated in acetone (50 µL + 900 µL,
1626 10 mM NaCl) under vortexing on ice for 2 h. The pellets were then resuspended in
1627 50 µL of SDC buffer (2.5% sodium deoxycholate (SDC; Merck) in 0.2 M EPPS-
1628 buffer (Merck), pH 8.5) and vortexed under heating, using an SDC-based in-
1629 solution digestion approach (Masuda et al., 2008). Aiming at 50 µg protein per
1630 sample, estimated by a Direct Detect fluorometric assay (MERCK MILLIPORE,
1631 Dorset, UK), equal amounts of protein per sample were reduced, alkylated, and
1632 digested with trypsin in the SDC buffer according to standard procedures adapted
1633 from Shevchenko et al. (Shevchenko et al., 2006). After the digest, the SDC was
1634 precipitated by adding an equal volume of 0.4% TFA, and the clear supernatant
1635 subjected to C18 SPE (OMIX tips; Agilent). Peptide concentration was further
1636 estimated by analysing a small aliquot of the digests by LCMS, as described
1637 below, to estimate the total peptide abundance per sample. Sample aliquots
1638 corresponding to estimated equal peptide abundances were used for TMT
1639 labelling using a TMT 6plex kit (Lot VB290974, ThermoFisher Scientific, Hemel
1640 Hempstead, UK) according to the manufacturer's instructions with slight
1641 modifications. However, this labelling was not used for quantification and is not
1642 relevant for the analysis presented in this paper. Six differently labelled samples
1643 were pooled and desalted using a C18 Sep-Pak cartridge (200 mg, Waters,
1644 Wilmslow, UK). The eluted peptides were dissolved in 500 µL of 25 mM
1645 NH₄HCO₃ and fractionated by high pH reversed phase HPLC. For this, the
1646 samples were loaded to an XBridge 3.5 µm C18 column (150 × 3.0 mm, Waters).

1647

1648 Fractionation was performed on an ACQUITY Arc Bio System (Waters) with the
1649 following gradient of solvents A (water), B (acetonitrile), and C (25 mM
1650 NH₄HCO₃ in water) at a flow rate of 0.5 mL/min: solvent C was kept at 10%

1651 throughout the gradient; solvent B: 0–5 min: 5%, 5–10 min: 5%–10%, 10–60 min:
1652 10%–40%, 60–75 min: 40%–80%, followed by 5 min at 80% B and re-equilibration
1653 to 5% for 24 min. Fractions of 0.5 mL were collected every 1 min and
1654 concatenated by combining fractions of similar peptide concentration to produce
1655 19 final fractions of the sperm samples for MS analysis. Aliquots were analysed by
1656 nanoLC-MS/MS on an Orbitrap Eclipse Tribrid mass spectrometer coupled to an
1657 UltiMate 3000 RSLCnano LC system (Thermo Fisher Scientific, Hemel
1658 Hempstead, UK). The samples were loaded onto a trap cartridge (Pepmap 100,
1659 C18, 5 μ m, 0.3 \times 5 mm, Thermo) with 0.1% TFA at 15 μ L/min for 3 min. The trap
1660 column was then switched in-line with the analytical column (nanoEase M/Z
1661 column, HSS C18 T3, 1.8 μ m, 100 \AA , 250 mm \times 0.75 μ m, Waters) for separation
1662 using the following gradient of solvents A (water, 0.1% formic acid) and B (80%
1663 acetonitrile, 0.1% formic acid) at a flow rate of 0.2 μ L/min: 0–3 min 3% B (parallel
1664 to trapping); 3–10 min linear increase B to 8%; 10–75 min increase B to 37%; 75–
1665 90 min linear increase B to 50%; followed by a ramp to 99% B and re-equilibration
1666 to 3% B. Data were acquired with the following parameters in positive ion mode:
1667 MS1/OT: resolution 120K, profile mode, mass range *m/z* 400–1800, AGC target
1668 100%, max inject time 50 ms; MS2/IT: data dependent analysis with the following
1669 parameters: top10 in IT Turbo mode, centroid mode, quadrupole isolation window
1670 0.7 Da, charge states 2–5, threshold 1.9e4, CID CE = 35, AGC target 1e4, max.
1671 inject time 70 ms, dynamic exclusion 1 count for 15 s mass tolerance of 7 ppm;
1672 MS3 synchronous precursor selection (SPS): 10 SPS precursors, isolation window
1673 0.7 Da, HCD fragmentation with CE = 65, Orbitrap Turbo TMT and TMTpro
1674 resolution 30k, AGC target 1e5, max inject time 105 ms, Real Time Search (RTS):
1675 protein database *D. rerio* (Uniprot reference proteome UP000000437, August
1676 2022, 46,842 entries), enzyme trypsin, 1 missed cleavage, oxidation (M) as
1677 variable, carbamidomethyl (C) and TMT as fixed modifications, Xcorr = 1, dCn =
1678 0.05. The LCMS analysis was done in 2022 using the database available at that
1679 time. The final processing reported here was done in 2024 using the updated
1680 database from 2024.

1681

1682 **3.3.3 Data analysis**

1683 The acquired raw data from the 19 HPLC fractions were processed and quantified
1684 using peptide peak intensities in Proteome Discoverer 3.1 (Thermo); all mentioned
1685 tools of the following workflows are nodes of the proprietary Proteome Discoverer
1686 (PD) software. The *D. rerio* fasta database (Uniprot
1687 UP000000437_Danio_7955.fasta, April 2024, 25,991 entries) was imported into
1688 PD adding a reversed sequence database for decoy searches. The processing
1689 workflow included Minora Feature Detection with min. trace length 7, S/N 5, PSM
1690 confidence high, and Top N Peak Filter with 20 peaks per 100 Da. For the
1691 database search the CHIMERS search engine (MSAID, Munich, Germany) was
1692 used with the inferys_3.0.0_fragmentation prediction model with FDR targets 0.01
1693 (strict) and 0.05 (relaxed), a fragment tolerance of 0.3 Da, enzyme trypsin with one
1694 missed cleavage, variable modification oxidation (M), fixed modifications
1695 carbamidomethyl (C), and TMT 6plex on N-terminus and K.
1696 The consensus workflow was set up to quantify peptides and proteins based on
1697 their ion count intensity combined from all HPLC fractions of the six pooled
1698 samples. For identification, an FDR of 0.01 was used as strict threshold. Protein
1699 abundance was calculated using the top three most abundant peptides unique to
1700 protein groups. The results were exported into a Microsoft Excel table including
1701 data for protein abundances, number of peptides, protein coverage, the search
1702 identification score and other important values. All data filtering was performed in
1703 accordance with current proteomics best practice guidelines (Burger, 2018).
1704
1705 Processed data were then further analysed and visualised using R version 4.0.3
1706 (The R Foundation for Statistical Computing, Vienna, Austria,
1707 URL <https://www.R-project.org/>). ID mapping was performed using Uniprot
1708 (Bateman et al., 2023) as well as the STRING database (Szklarczyk et al., 2023).
1709 Gene Ontology (GO) term analysis was performed using ShinyGO 0.76.2 (S. Ge
1710 et al., 2020).

1711

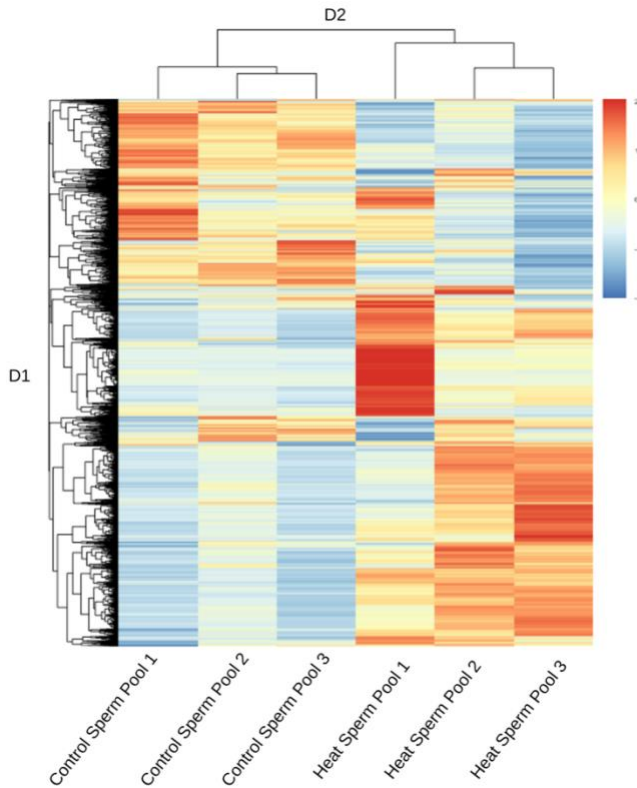
1712 **3.4 Results**

1713 Initial mass-spectrometry runs had been designed to compare the sperm
1714 proteomes of males from 28 °C and 34 °C treatments. However, preliminary
1715 quality-control assessments showed that individual tank-level samples displayed
1716 high preparation-related variability, including elevated CV values and unstable
1717 adjusted p-values. This variability made differential expression analysis unreliable
1718 and indicated that the dataset was better suited to generating a high-confidence
1719 global sperm proteome rather than testing for temperature effects.

1720 To maximise protein coverage and increase depth of identification, we pooled all
1721 six tank replicates to produce a combined dataset. The observed variation in the
1722 34 °C samples most likely reflected a combination of biological heterogeneity and
1723 technical noise during sample preparation, further supporting the decision to
1724 combine the dataset into one global proteome rather than pursue treatment-level
1725 comparisons.

1726
1727 Following filtering to remove any single peptide matches and potential
1728 contaminants, a total of 5410 proteins could be confidently identified from the
1729 combined six pooled sperm samples (Supplementary Table 5). Of these, 4168
1730 could be quantified, while 1242 could not be quantified, (Figure 3-1).

1731



1732

1733 Figure 3-1: Heatmap comparing heat-treated and control sperm proteomes,
1734 showing the 4168 quantifiable proteins identified. Log scale.

1735

1736 The Uniprot UP000000437_Danio_7955.fasta reference proteome of the zebrafish
1737 used in this study contains one protein per gene (25,991 entries) [19]. The
1738 GRCz11 reference genome [22] for zebrafish includes a total of 25,545 coding
1739 genes. In this study, 5410 proteins were detected, which suggests that roughly
1740 20% of the potential zebrafish gene products were detected.

1741

1742 According to the Uniprot ID database (Bateman et al., 2023), of the 5410 proteins
1743 that were confidently identified in this dataset, 3449 (63.8%) were listed as having
1744 previously been identified with evidence at the protein level, 1042 (19.3%) were
1745 found at the transcript level, 473 (8.7%) were inferred from homology, and 446
1746 (8.2%) were predicted from the zebrafish genome but have no previously recorded
1747 protein evidence.

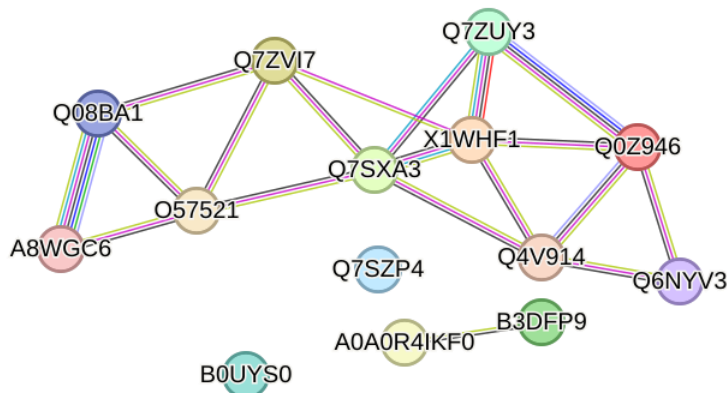
1748

1749 The top 25 most abundant proteins from the sample pools include eight different
1750 histone related proteins including Histone H3-like (*A0A8M6Z1M4*), H1.0 linker
1751 histone (*Q6NYV3*), Histone H2B (*X1WHF1*), Histone H1-like (*A0A8M6Z7Z5*),
1752 Histone H1-like (*Q568D0*), Histone H2A (*Q0Z946*), Histone H2AX (*Q7ZUY3*), and
1753 Core histone macro-H2A (*Q4V914*).

1754

1755 These top 25 proteins were also mapped with the STRING database (Szklarczyk
1756 et al., 2023) (Figure 3-2), and while 11 of these could not be identified, the largest
1757 continuous network determined by this database included five of the histone
1758 related proteins mentioned above as well as the alpha (Q08BA1) and beta
1759 (A8WGC6) subunits of ATP-synthase and heat shock protein HSP 90- beta
1760 (O57521).

1761



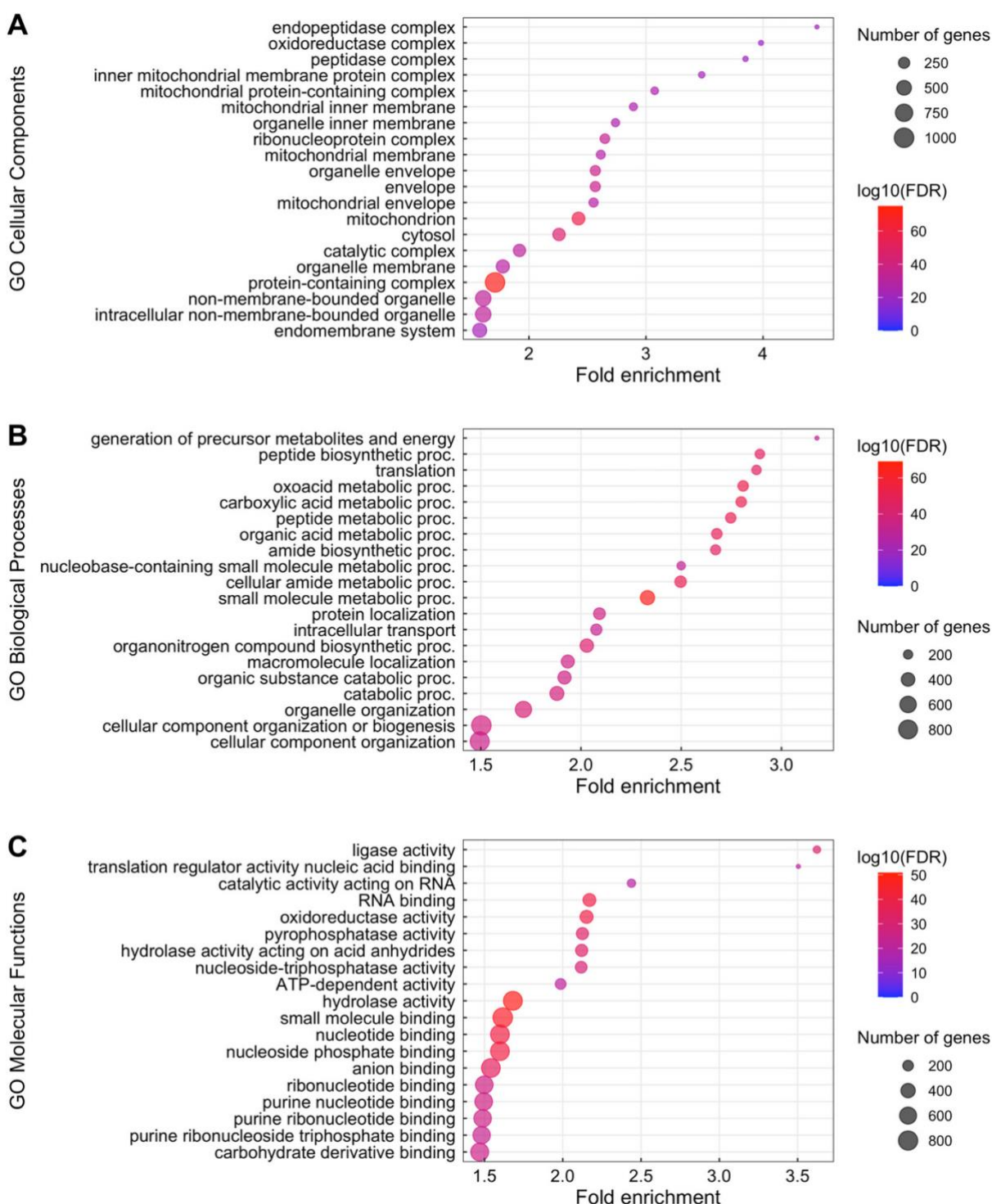
1762

1763 Figure 3-2: The STRING database map generated through the input of the protein
1764 accession ID of the 25 most abundant proteins detected in this data.

1765

1766 The 5410 proteins were matched to 4844 NCBI GeneIDs using the Uniprot ID
1767 mapping software. A total of 566 proteins could not be assigned NCBI GeneIDs.
1768 Using the assigned GeneIDs, a total of 1919 GO terms were identified among the
1769 three categories of GO terms, including 395 cellular components (Figure 3-3A),
1770 1001 biological processes (Figure 3-3B), and 523 molecular functions (Figure 3-
1771 3C). Two of the most fold-enriched cellular component GO terms were the
1772 endopeptidase and peptidase complexes. Of the top 20 cellular component GO
1773 terms, six were mitochondria related. The biological processes included in the top

1774 20 GO terms by fold-enrichment include a number of biosynthetic processes for
 1775 molecules such as peptides and amides as well as the establishment of protein
 1776 localisation. The highest fold-enrichment molecular function GO term was ligase
 1777 activity, and nine of the top 20 molecular functions were molecular binding terms
 1778 such as anion binding and small molecule binding.



1779
 1780 Figure 3-3: Top 20 GO terms ranked by fold-enrichment for the zebrafish sperm
 1781 proteome, based on the 4844 assigned GenIDs for (A) cellular component GO

1782 terms, (B) biological process GO terms and (C) molecular function GO terms for
1783 the sperm proteome.

1784

1785 **3.5 Discussion**

1786 Initial TMT-based proteomic analysis revealed no significantly differentially
1787 expressed proteins between sperm from males maintained at 28°C or 34°C ($p_{adj} <$
1788 0.05), likely due to substantial biological variability among the high-temperature
1789 replicates. As a result, all six pooled sperm samples were combined for
1790 downstream interpretation. After filtering to exclude single-peptide identifications
1791 and contaminants, 5410 proteins were confidently identified, representing
1792 approximately 20% of the predicted protein-coding genes in the zebrafish genome.
1793 Of these, 4168 proteins were quantifiable. According to UniProt classification,
1794 most identified proteins had existing protein- or transcript-level evidence, while
1795 ~8% were predicted with no prior protein-level confirmation. The most abundant
1796 proteins included multiple histone variants, with STRING analysis revealing a
1797 central interaction network comprising histones, ATP-synthase subunits, and heat
1798 shock proteins. GO annotation of the mapped proteins (n = 4844) identified
1799 enrichment in mitochondrial components, biosynthetic processes, and molecular
1800 binding functions, highlighting key functional themes in the zebrafish sperm
1801 proteome.

1802

1803 Despite the inability to compare temperature treatments directly, the combined
1804 dataset provides valuable insight into the zebrafish sperm proteome under
1805 standard laboratory conditions. Compared to previous studies in other teleost fish,
1806 the depth of coverage achieved here is substantially higher. For example,
1807 proteomic profiling in rainbow trout (*Oncorhynchus mykiss*) sperm identified 206
1808 proteins using a combined SDS-PAGE and LC-MS/MS method (Nynca et al.,
1809 2014), while a similar study in carp (*Cyprinus carpio L*) spermatozoa identified 348
1810 proteins (Dietrich et al., 2014). In contrast, our study confidently identified 5410
1811 proteins, of which 4168 were quantified. These differences are likely attributable to
1812 methodological advancements, including the use of tandem mass tag (TMT)
1813 labelling, deeper mass spectrometry acquisition, and a more complete zebrafish

1814 reference genome and proteome. This expanded proteome offers a valuable
1815 resource for understanding zebrafish sperm biology and represents one of the
1816 most comprehensive teleost sperm proteomes to date.

1817

1818 Even when compared to proteomic profiles of other tissue types from zebrafish,
1819 our study presents a more complete proteomic profile. For example, proteomic
1820 profiles of other zebrafish organs identified ~1300 proteins in muscle tissue (5% of
1821 gene products), ~1500 proteins in skin tissue (6% of gene products) and ~2400
1822 proteins in gill tissue (9% of gene products) resulting in a total of over 5000
1823 proteins across all tissues (Nolte et al., 2014). In contrast, the present study
1824 identified 5410 proteins in zebrafish sperm alone.

1825

1826 Supporting the idea of a functionally distinct and complex sperm proteome, eight
1827 histone variants were among the 25 most abundant proteins identified. The high
1828 abundance of histones in zebrafish sperm is to be expected due to the lack of
1829 protamine-replacement and maintenance of histone packaging during sperm
1830 chromatin condensation during spermatogenesis (González-Rojo et al., 2018a).
1831 This contrasts with the protamine-based DNA compaction observed in many other
1832 species, including mammals such as humans and mice, where histones are
1833 replaced to achieve tighter genome condensation (Elango et al., 2022).

1834

1835 One key process shared by the sperm of many species is capacitation.
1836 Capacitation refers to the physiological changes sperm undergo such as changes
1837 to the membrane, motility patterns, and protein phosphorylation states, in order to
1838 become able to fertilise an oocyte (Bailey, 2010). While capacitation is a common
1839 process amongst sperm, the exact mechanisms and activation triggers can vary
1840 greatly across species, especially dependent on the internal or external mode of
1841 fertilisation used. In mammals, capacitation typically occurs post-ejaculation within
1842 the female reproductive tract (Stival et al., 2016). In contrast, in many fish species,
1843 sperm capacitation is activated in response to environmental cues such as
1844 osmotic shock (Alavi & Cosson, 2006). Therefore, while zebrafish (*Danio rerio*) are
1845 often regarded as a useful model for human reproductive biology due to their
1846 ~70% genetic homology with humans (Howe et al., 2013), differences in key

1847 reproductive processes such as capacitation, differences in reproduction due to
1848 internal vs external environments, and reproductive strategy must be carefully
1849 considered. This may provide some explanation as to the differences noted
1850 between mammalian sperm DNA compaction and the histone-rich compaction
1851 observed in zebrafish.

1852
1853 The STRING network generated from the top 25 most abundant proteins (Figure
1854 3-2) further supports the central role of histones in zebrafish sperm biology. The
1855 largest interaction cluster consisted predominantly of core histones and histone
1856 variants, reflecting their dominance among the most abundant proteins in the
1857 dataset and reinforcing the histone-based chromatin organisation characteristic of
1858 this species. Notably, most mammalian sperm contains DNA that has been
1859 repackaged from histones to protamines during spermatogenesis to increase DNA
1860 compaction (Moritz & Hammoud, 2022), although this repackaging does not occur
1861 in zebrafish. The presence of ATP synthase subunits and the heat shock protein
1862 HSP90-beta within the same network suggests that proteins involved in
1863 mitochondrial energy production and protein stabilisation are also maintained at
1864 high abundance in mature sperm. These findings highlight the dual importance of
1865 chromatin structure and protein stabilisation or stress response in the functional
1866 proteome of zebrafish sperm.

1867
1868 GO term analysis of the identified proteins further reinforced the importance of
1869 chromatin structure, mitochondrial function, and protein processing in mature
1870 zebrafish sperm. Among the top fold-enriched cellular component GO terms
1871 (Figure 3-3 A) were the endopeptidase and peptidase complexes, both of which
1872 are known to be important in sperm motility due to their roles in mediating protein–
1873 protein interactions in response to activation stimuli (Ren et al., 2023). Six of the
1874 top ten highly enriched cellular component GO terms were associated with
1875 mitochondrial components including; mitochondrion, mitochondrial membrane,
1876 mitochondrial envelope, mitochondrial inner membrane, inner mitochondrial
1877 membrane protein complex, and mitochondrial protein-containing complex ,
1878 consistent with the role of mitochondria in ATP production required for flagellar
1879 movement (Kumar, 2022). In zebrafish sperm specifically, mitochondria are known

1880 to undergo ultrastructural changes during activation including bursting of the
1881 plasma membrane, further underscoring their importance in motility (Sáez-
1882 Espinosa et al., 2022). These ultrastructural effects, specifically changes in the
1883 plasma membrane, may be reflected as four of the top 10 highly enriched cellular
1884 component GO terms were directly linked to mitochondrial membranes.

1885

1886 Since this proteome was generated from mature sperm, many of the biological
1887 process terms may reflect proteins retained from earlier stages of
1888 spermatogenesis (Figure 3-3B), including organelle organisation, cellular
1889 component localisation or biosynthesis, and protein localization. This raises the
1890 possibility that proteins initially involved in spermatogenic processes may have
1891 alternative or residual roles in the mature sperm cell. For example, enriched
1892 molecular function terms (Figure 3-3C) included ligase activity and various binding
1893 functions, such as anion and small molecule binding, which may relate to the
1894 known role of ion flux in sperm activation. Zebrafish sperm are activated by a
1895 hypo-osmotic shock triggered by a drop in extracellular potassium upon
1896 ejaculation into water, initiating rapid changes in membrane potential and motility
1897 (Sáez-Espinosa et al., 2022; Wilson-Leedy et al., 2009). The presence of proteins
1898 associated with these functions supports the idea that the mature zebrafish sperm
1899 proteome is primed for environmental responsiveness and rapid activation.

1900

1901 The initial experimental design for this study aimed to compare the sperm
1902 proteomes of samples extracted from the same testes used to generate the
1903 proteomic dataset presented in Chapter 2, with males grouped in pools of ten by
1904 tank and treatment. However, this temperature-based comparison was ultimately
1905 not possible due to both high variability and low sperm availability in samples from
1906 males kept at 34°C. As shown by the GO term analysis in Chapter 2,
1907 spermatogenesis appeared to be downregulated in the testes following heat
1908 treatment. This likely resulted in reduced sperm output, and it is possible that the
1909 limited sperm produced were also more susceptible to damage under thermal
1910 stress, contributing to the high variation observed across samples. Other studies
1911 have previously reported measurable differences in sperm proteomes as a result
1912 of heat stress, for example in *Drosophila melanogaster* where 96 proteins were

1913 found to differ in abundance between multigenerational heat stress groups,
1914 although this approach was not quantitative (Khan & Mishra, 2024). This suggests
1915 that higher sample sizes may help identify more subtle differences in sperm
1916 proteomes between temperature conditions, and future studies will be needed to
1917 address this question in greater detail.

1918

1919 The quality and reliability of the dataset were further supported by the levels of
1920 existing evidence associated with the identified proteins. Of the 5410 proteins
1921 confidently identified, 63.8% had previously been validated at the protein level,
1922 while an additional 19.3% had transcript-level evidence. A smaller proportion were
1923 inferred from homology (8.7%) or predicted from genome annotations without prior
1924 empirical support (8.2%). These proportions reflect a high level of agreement with
1925 existing zebrafish proteomic and transcriptomic resources and indicate that the
1926 dataset is both comprehensive and robust, with the potential to highlight novel or
1927 under-characterised sperm-specific proteins.

1928

1929 In conclusion, quantitative mass spectrometry-based profiling of zebrafish sperm
1930 yielded a comprehensive dataset of 5410 proteins. The high abundance of histone
1931 variants reflects the distinctive chromatin architecture of zebrafish sperm, which
1932 lacks protamine-based DNA compaction. In addition, many proteins associated
1933 with earlier stages of spermatogenesis appear to be retained in mature sperm, as
1934 suggested by the enrichment of relevant biological process GO terms. Enrichment
1935 of cellular component and molecular function terms related to mitochondrial
1936 activity, protein complexes, and binding functions further highlights the importance
1937 of energy production and environmental responsiveness in sperm activation.
1938 Together, these findings provide a valuable resource for future protein-level
1939 investigations of zebrafish sperm biology and reinforce the utility of this species as
1940 a model for reproductive proteomics.

1941

1942 **4 The Proteomic Biomarkers of Human**

1943 **Sperm Quality**

1944 **4.1 Abstract**

1945 Sperm quality plays a critical role in male fertility, yet much remains unknown
1946 about the molecular mechanisms that determine which sperm are most
1947 functionally competent. Previous work has shown that haploid selection within
1948 ejaculates, where selection acting upon phenotypic differences among genetically
1949 distinct sperm to influence fertilisation outcomes, can impact offspring fitness.
1950 While genomics and transcriptomics have provided insight into sperm
1951 development and gene expression, proteomics offers a direct window into
1952 functional cellular mechanisms. In particular, identifying proteins associated with
1953 sperm motility and longevity can enable the discovery of biomarkers for sperm
1954 quality, with potential applications in diagnostics and assisted reproductive
1955 technologies.

1956

1957 This study investigates the proteomic signatures underlying sperm quality in
1958 humans by identifying protein biomarkers associated with motility and longevity.
1959 Using Tandem Mass Tag (TMT)-based quantitative proteomics, sperm
1960 subpopulations were isolated from the same ejaculate via methyl cellulose and
1961 swim-up assays, methods that respectively select for high motility and prolonged
1962 viability. Comparative proteomic analysis identified 4,616 high-confidence proteins,
1963 with 1,178 showing differential abundance between selected and unselected
1964 sperm. Proteins with lower abundance in selected sperm were strongly enriched
1965 for markers of cellular immaturity and stress, such as those involved in RNA
1966 processing and immune signalling. Whereas proteins with higher abundance in
1967 selected sperm were associated with structural and functional components critical
1968 for motility and membrane stability. A shortlist of 68 candidate biomarkers was
1969 generated, with OLFM4 emerging as the most consistently downregulated protein
1970 in high-quality sperm. These findings provide a molecular foundation for

1971 developing non-destructive diagnostic tools for sperm selection, with implications
1972 for improving male fertility assessments and assisted reproduction outcomes.

1973

1974 **4.2 Introduction**

1975 The effects of competition between individuals during sexual reproduction as a
1976 driving force for evolution forms the basis of the theory of sexual selection (Darwin,
1977 1871). This theory was later expanded to include competition between the sperm
1978 of different males, termed sperm competition (Parker, 1970). More recently, this
1979 framework has been extended to recognise that competition can also occur within
1980 a single ejaculate, where genetically distinct sperm from the same male vary in
1981 their capacity to fertilise an egg (Wigby & Chapman, 2004). The concept of haploid
1982 selection extends the framework of sexual selection to the gametic stage,
1983 proposing that genetically distinct gametes within an ejaculate can differ in
1984 fertilisation success, allowing selection to act at the haploid stage even in primarily
1985 diploid organisms (Immler & Otto, 2018; Joseph & Kirkpatrick, 2004).

1986

1987 However, the concept of haploid selection has previously been overlooked in
1988 evolutionary theories, as haploid sperm were assumed to be transcriptionally and
1989 translationally inactive (Hecht, 1998). At the time, the regulation of sperm
1990 phenotype was thought to be entirely determined by the diploid male during
1991 spermatogenesis, and differences observed among mature spermatozoa were
1992 generally attributed to random developmental variation rather than a reflection of
1993 genetic variation and a possible target of selection (Immler, 2019).

1994

1995 Contrary to earlier assumptions, mature sperm are not merely passive carriers of
1996 paternal DNA. Post-meiotic sperm can be highly varied, and haploid selection acts
1997 as an important evolutionary tool in removing deleterious alleles from a population
1998 (Alavioon et al., 2017; Immler, 2019; Immler & Otto, 2018). Molecular studies have
1999 shown that sperm retain a diverse repertoire of RNAs and proteins, many of which
2000 are functionally active and can influence fertilisation and early embryogenesis
2001 (Miller & Ostermeier, 2006; Ostermeier et al., 2004). This variation provides a

2002 direct link between haploid genotype and phenotype, making sperm legitimate
2003 targets of natural selection. Rather than representing developmental noise,
2004 heterogeneity among spermatozoa can therefore have adaptive consequences,
2005 both for immediate fertilisation success and for the genetic quality of subsequent
2006 offspring (Sendler et al., 2013).

2007

2008 Growing empirical evidence supports the idea that haploid selection is not just a
2009 theoretical possibility, but an observable process across a wide range of taxa
2010 (Immler, 2019; Immler & Otto, 2018). Previous work in zebrafish (*Danio rerio*)
2011 provided evidence that haploid selection operates within a single ejaculate, with
2012 sperm longevity linked to consistent effects on offspring phenotype (Alavioon et
2013 al., 2017, 2019). Comparable evidence has been reported in Atlantic salmon
2014 (*Salmo salar*), where genetic variation among sperm influences fertilisation
2015 success, indicating that haploid selection can act during external fertilisation in
2016 natural populations (Immler et al., 2014). Evidence from mammals further
2017 supports that the haploid sperm genotype plays a role in shaping sperm function
2018 and fertilisation ability (Ramón et al., 2014). In cattle (*Bos taurus*), comparisons
2019 between X- and Y-chromosome-bearing sperm have revealed consistent
2020 differences in several mitochondrial proteins, including enzymes central to
2021 oxidative phosphorylation and energy metabolism (Scott et al., 2018). These
2022 observations suggest that variation at the haploid genome level can influence
2023 metabolic performance, a functional trait directly tied to motility and therefore
2024 fertilisation potential. Other studies have shown that sperm genotype can have a
2025 direct effect on the ability of a sperm to overcome selective barriers to reach the
2026 oocyte during natural conception (Nixon et al., 2023). In mice (*Mus musculus*) for
2027 example, sperm that reached the oviduct exhibited lower levels of DNA
2028 fragmentation than those that did not (Hourcade et al., 2010), while in boar (*Sus*
2029 *scrofa*), sperm with compromised chromatin integrity were under-represented
2030 among those capable of penetrating oocytes (Ardon et al., 2008). Collectively,
2031 these findings indicate that mammalian sperm with higher genetic quality are more
2032 likely to reach later stages of fertilisation, consistent with haploid selection acting
2033 within the ejaculate.

2034

2035 Following previous research, genomic studies in humans identified parallel
2036 signatures of haploid selection, with longevity-based sperm selection also being
2037 found to be associated with genomic divergence and improvements in key sperm
2038 traits such as motility, morphology, and DNA integrity (Marcu, 2024). The
2039 implications of sperm selection extend beyond evolutionary theory and are highly
2040 relevant to fertility in both humans and animals. Assisted reproductive
2041 technologies (ART) currently rely on criteria such as morphology and motility to
2042 select sperm, but these measures are poor predictors of fertilisation and
2043 pregnancy success (Ribas-Maynou et al., 2021). As a result, embryos generated
2044 through ART may carry a higher genetic load, reducing implantation rates,
2045 increasing miscarriage risk, and potentially compromising offspring health (van
2046 Oosterhout et al., 2022).

2047

2048 Incorporating principles of within-ejaculate sperm selection could help to address
2049 the limitations of current ART methods by favouring sperm that demonstrate better
2050 function, and therefore possibly a lower genetic load, thereby lowering the
2051 transmission of deleterious alleles. Recent conceptual work has argued that
2052 developing non-destructive molecular markers for sperm quality would be
2053 transformative, improving both diagnostic assessment of male infertility and the
2054 efficiency of clinical procedures such as IVF and ICSI (Alavioon et al., 2021).

2055

2056 High throughput approaches such as genomics, transcriptomics, and proteomics
2057 have provided important insights into sperm biology (Amaral, Castillo, et al., 2014;
2058 Cannarella et al., 2020). Proteomics complements both genomic and
2059 transcriptomic approaches by directly measuring all proteins present within a cell
2060 at the time of study, providing a more accurate depiction of cellular function and
2061 phenotype (Aebersold & Mann, 2003). Methods such as Tandem Mass Tag (TMT)
2062 quantitative proteomics allow for the measurement of specific protein abundances
2063 (Pagel et al., 2021), which offers critical insights into the actual biological
2064 processes occurring within the cell, making it a useful tool for understanding the
2065 molecular mechanisms underlying sperm function and haploid selection.

2066

2067 Proteomic studies have provided important insights into the molecular basis of
2068 human male infertility, firstly by comparing ejaculates from men with different
2069 clinical diagnoses (Cannarella et al., 2020). Contrasts between normozoospermic
2070 and asthenozoospermic human samples exhibit consistent differences in proteins
2071 associated with metabolism, motility, oxidative stress, and structural integrity
2072 (Martínez-Heredia et al., 2008; Saraswat et al., 2017). While these studies have
2073 advanced understanding of infertility, they treat ejaculates as homogeneous units
2074 and overlook the substantial heterogeneity that exists among sperm from the
2075 same individual. More recent work started to focus on this heterogeneity by
2076 examining subpopulations within single ejaculates where distinct proteomic
2077 signatures have been identified between functional states of sperm from the same
2078 ejaculate (Parkes & Garcia, 2024). Sequential analyses before and after
2079 capacitation and the acrosome reaction revealed dynamic changes in protein
2080 abundance in human sperm (Castillo et al., 2023; Secciani et al., 2009), while
2081 comparisons of mature versus immature sperm within a single sample showed
2082 distinct molecular profiles (Cui et al., 2016).

2083

2084 In this chapter, two distinct selection methods were used to select for human
2085 sperm subpopulations from the same ejaculate. The first was a methyl cellulose
2086 assay, which enriched for progressively motile sperm through migration within a
2087 viscous medium over four hours. The second approach involved a swim-up assay,
2088 allowing comparison of sperm that were motile both before and after a four-hour
2089 incubation, thus differentiating between shorter- and longer-lived sperm. These
2090 subpopulations were analysed using TMT-based quantitative proteomics to
2091 characterise the sperm proteome and to detect differences in protein abundance
2092 between subpopulations from the same ejaculate. The aim was to determine
2093 whether proteomic differences could be detected between sperm subpopulations
2094 isolated from the same ejaculate, and to identify candidate molecular markers
2095 associated with sperm motility and longevity.

2096

2097 **4.3 Methods**

2098 **4.3.1 Sperm parameter analysis**

2099 Samples were collected from two self-reported healthy donors at the University of
2100 East Anglia, UK, under ethics permit no. ETH2324-0997, and two self-reported
2101 healthy donors from Cape Town, South Africa (ZA). Following collection, samples
2102 were warmed to 37°C in a Midi 40 CO₂ incubator (Thermo Fisher, UK).
2103 Measurements of volume and pH were taken. Sperm concentration, motility and
2104 velocity parameters were assessed with the motility module of Integrated Semen
2105 Analysis System (ISAS) v1 (Poiser, Spain), and the data was captured with an
2106 ISAS 782M camera connected to a UB203i microscope with a 10x phase contrast
2107 objective and a pre-heated stage. Preheated (37°C) disposable 75 mm x 25 mm
2108 glass chamber slides with 20-micron depth chambers (Cytonix, USA) were loaded
2109 with 2µl of sample and at least 200 sperm were analysed from at least two fields
2110 for one second at 50 frames per second (f/s). Kinematics parameters recorded for
2111 each sample included: curvilinear velocity (VCL), straight-line velocity (VSL),
2112 average path velocity (VAP), linearity (LIN) = (VSL/ VCL)*100, straightness (STR)
2113 = (VSL/ VAP)*100, wobble (WOB) = (VAP/ VCL)*100, amplitude of lateral head
2114 displacement (ALH) and beat cross frequency (BCF).

2115

2116 **4.3.2 Sperm selection assays**

2117 For the two samples collected at UEA, methyl cellulose (MC) assays were
2118 conducted by using a 10 cm-diameter watch glass filled with 10 mL of 1% (w/v)
2119 methylcellulose (Sigma, Denmark), distributed evenly up to a 4 cm radius. Raw
2120 ejaculate (300 µL) was carefully pipetted into the centre, forming a central deposit
2121 of approximately 0.5 cm in diameter. For each donor, five watch glasses were
2122 prepared in parallel to allow recovery of sufficient cell numbers. Samples were
2123 incubated at 37°C under 5% CO₂ for two hours in a Midi 40 CO₂ incubator
2124 (Thermo Fisher, UK). Motile sperm were collected from the outer edge of the
2125 methylcellulose dome at radii ranging from 2 to 3.5 cm from the centre depending
2126 on relative sperm density. Sperm density at different radii was determined by
2127 taking 2 µL samples from each measured point on the radius of the dish and
2128 examining using CASA (ISAS v1 Poiser, Spain). The furthest point with at least 10

2129 visible sperm per field of view was selected, and 4mL of sperm were collected
2130 using extra-long bevelled 200 μ L pipette tips and pooled. A 2 mL sample of sperm
2131 that did not pass the selection criteria was taken from the central point of the dish,
2132 also using extra-long bevelled 200 μ L pipette tips, avoiding debris at the bottom
2133 and without touching the dish. To extract sperm from the viscous methyl cellulose,
2134 1 μ L of cellulase was added per 1 mL of collected sample, mixed, and incubated at
2135 50°C for two hours with shaking at 50 rpm using a Thermomixer C (Eppendorf,
2136 Germany). The samples were centrifuged at 14,000 rpm for 5 minutes.
2137 Supernatant was discarded and sperm pellets were stored at -80°C until protein
2138 extraction.

2139

2140 For the two sperm samples collected in South Africa and subjected to swim up
2141 (SW) assays, aliquots of 1 mL raw ejaculate were mixed 1:1 with human tubal fluid
2142 (HTF) medium and incubated at 37°C in 5% CO₂ for 4 hours. At both T0 (prior to
2143 incubation) and T4 (following the 4 hour incubation) a 0.5 mL aliquot was removed
2144 from the sample, was gently placed under 1 mL of fresh HTF in a new tube and
2145 incubated for 60 minutes to allow motile sperm to swim up. The top 0.5 mL were
2146 collected using a 1 mL Pasteur pipette, centrifuged at 700 x g for 10 minutes at
2147 room temperature, and resuspended in HTF. The samples were then centrifuged
2148 at 14000 rpm for 5 minutes. Supernatant was discarded and sperm pellets were
2149 stored at -80°C until protein extraction.

2150

2151 **4.3.3 Sample preparation for proteomics**

2152 Sperm sub-population pellets collected from the methyl cellulose and swim-up
2153 assays were washed in HTF and resuspended in 200 μ L HTF. Two samples per
2154 donor were used for proteomic comparison: one representing the less motile or
2155 unselected population (Centre (MC) or T0 (SW) and one representing the motile,
2156 selected population (Edge (MC) or T4 (SW)). All samples were stored at -80°C.

2157

2158 **4.3.4 Protein extraction and peptide preparation**

2159 Frozen sperm pellets were thawed and precipitated with 450 μ L acetone, vortexed
2160 for 15 minutes, and centrifuged at 10,000 rpm for 10 minutes at room temperature.
2161 Samples were then prepared using an SDC-based in-solution digestion approach
2162 (Masuda et al., 2008). Wherein, after removal of the supernatant, 500 μ L acetone
2163 was added, and samples were gently mixed, centrifuged at 10,000 rpm for 10
2164 minutes, and air-dried at room temperature. Pellets were resuspended in 100 μ L
2165 2.5% sodium deoxycholate (SDC) in 0.2 M EPPS buffer (pH 8.5). Samples were
2166 reduced with dithiothreitol, alkylated with iodoacetamide, and digested with trypsin.
2167 SDC was removed by acid precipitation, and peptides were desalted by C18 solid-
2168 phase extraction.

2169

2170 **4.3.5 TMT labelling and fractionation**

2171 Peptides were quantified and labelled using an 8-plex TMT10 kit (ThermoFisher
2172 Scientific). Each sample was dissolved in EPPS/acetonitrile, labelled with 200 μ g
2173 TMT reagent, and combined after a 2-hour incubation. Aliquots were checked for
2174 labelling efficiency via LC-MS. Samples were quenched with hydroxylamine,
2175 desalted using C18 Sep-Pak cartridges, and fractionated by high pH reverse-
2176 phase HPLC. Fractions were concatenated into 20 final pools. Each sample
2177 replicate was fractionated using a Pierce High pH Fractionation kit to yield 7
2178 fractions.

2179

2180 **4.3.6 Mass spectrometry Acquisition**

2181 Samples were analysed on an Orbitrap Eclipse Tribrid mass spectrometer with
2182 FAIMS Pro Duo and UltiMate 3000 RSLCnano LC. Samples were loaded on a
2183 C18 trap cartridge and separated on an Aurora Frontier UHPLC column. A
2184 detailed gradient of increasing acetonitrile (0-105 min) was used for peptide
2185 elution. MS acquisition included MS1 at 120K resolution, FAIMS CVs of -35V, -
2186 50V, and -65V, MS2 CID fragmentation with rapid mode acquisition, and SPS-
2187 MS3 detection for quantification. The sample for donor 3 (SW) was repeated due
2188 to issues with initial data acquisition.

2189 **4.3.7 Data processing and protein identification**

2190 Raw data files were analysed in Proteome Discoverer 3.1 using CHIMERS and
2191 Comet search engines against the UP000005640_human_2024_9606.fasta
2192 database. Recalibration, quantification, and database searching were performed
2193 with fixed (carbamidomethylation, TMT) and variable (oxidation) modifications.
2194 Peptide-spectrum matches were filtered at 1% FDR. Quantification was performed
2195 using intensity-based abundance with correction for co-isolation, missing value
2196 imputation, and t-tests with BH correction.

2197

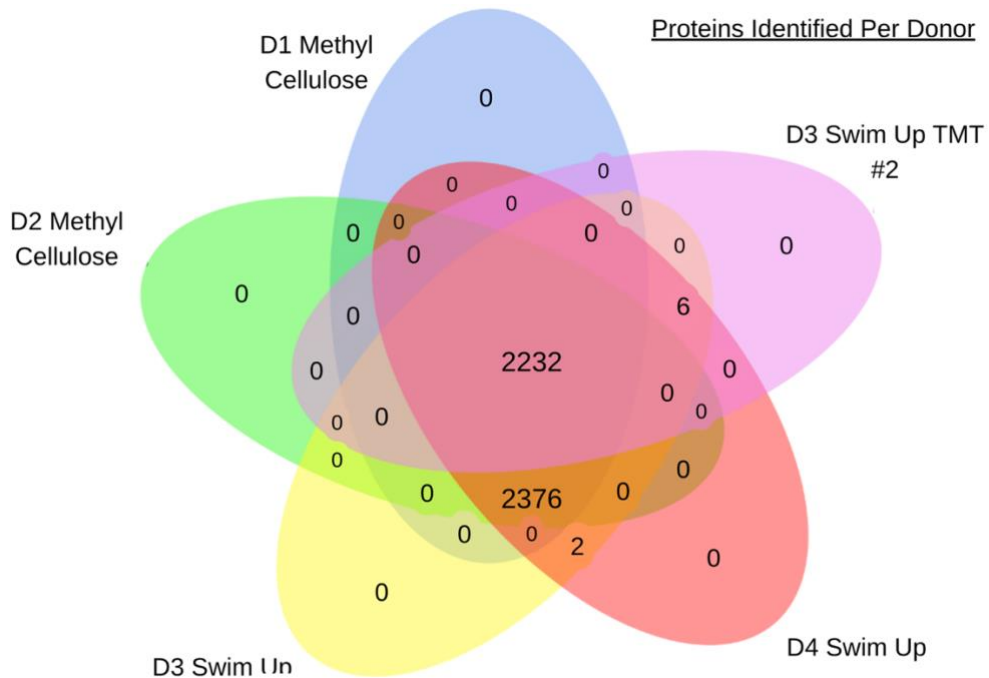
2198 **4.3.8 Filtering and structural analysis**

2199 Proteins with fewer than two unique peptides (excluding NAs) or detected in fewer
2200 than three of five samples (four donors with donor 3 repeated) were excluded.
2201 Structural models for shortlisted proteins were visualised using PyMOL (version
2202 3.1.5.1) (Schrödinger, LLC, 2015). All data filtering was performed in accordance
2203 with current proteomics best practice guidelines (Burger, 2018). Gene Ontology
2204 (GO) term analysis was performed using BioMart (Haw et al., 2011; Smedley et
2205 al., 2015) and Bioconductor (Gentleman et al., 2004) packages through R.

2206

2207 **4.4 Results**

2208 A total of 8,161 peptide matches were initially identified across all sperm samples
2209 using TMT-labelled LC-MS/MS. To ensure confidence in protein identification, the
2210 dataset was filtered to retain only proteins supported by at least two unique
2211 peptides per experiment and detected in a minimum of three donors. This resulted
2212 in a high-confidence dataset of 4,616 proteins (Figure 4-1, Supplementary Table
2213 6), which was carried forward for downstream comparative analyses.



2214

2215 Figure 4-1: Overlap of confidently identified proteins across all donors.

2216 Venn diagram showing the intersection of proteins identified in each of the five
 2217 human donors following TMT-labelled LC-MS/MS. Proteins were retained in the
 2218 final dataset if they were supported by at least two unique peptides and detected
 2219 in a minimum of three donors, resulting in a high-confidence proteome of 4,616
 2220 proteins used for downstream comparative and enrichment analyses.

2221

2222 The high-confidence protein dataset was then analysed for differences in
 2223 abundance between selected sperm samples (T4, Edge) and unselected samples
 2224 (T0, Centre) to investigate the effects of selection on the sperm proteome. Filtering
 2225 criteria required a consistent twofold change in the same direction across at least
 2226 three donors, and a $p_{adj} < 0.05$ in at least one donor. This analysis identified 634
 2227 proteins with significantly lower abundance and 544 proteins with significantly
 2228 higher abundance in selected sperm.

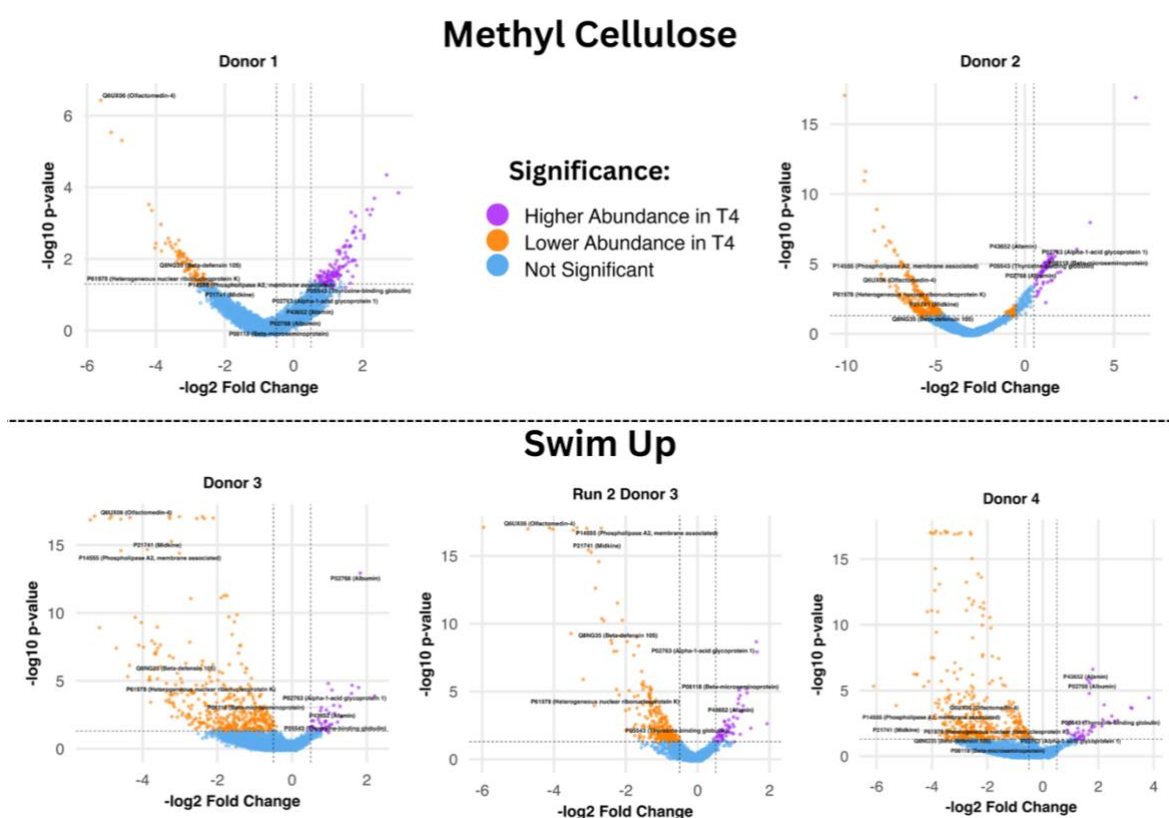
2229

2230 The combined set of 1,178 proteins showing differential abundance was further
 2231 refined to generate shortlists of candidate biomarkers. For proteins with lower
 2232 abundance in selected sperm, more stringent filtering was applied due to the
 2233 strength of observed directional change. This resulted in a shortlist of 62 proteins.

2234 In contrast, although 544 proteins were initially identified with significantly higher
2235 abundance, these changes were less consistent across donors. Therefore, a
2236 looser criterion was applied, including only proteins with a fold-change ratio above
2237 2 in at least two donors, and significance in at least one donor. This added a
2238 further six proteins to the shortlist (Supplementary Table 7).

2239

2240 From the combined shortlist of 68 proteins, top candidates were selected using
2241 additional criteria. The top five proteins with lower abundance in selected sperm
2242 were present in all five samples (four donors with one repeated), statistically
2243 significant in at least four donors, and had a median fold-change ratio below 0.2.
2244 Similarly, the top four proteins with higher abundance were present in all five
2245 donors, significant in at least four donors, and had a median fold-change ratio
2246 above 2 (Figure 4-2).



2247

2248 Figure 4-2: Volcano plots showing differential protein abundance between selected
2249 and unselected sperm pools. The plots display the $-\log_2$ fold-change in protein
2250 abundance (x-axis) against the $-\log_{10} p_{adj}$ (y-axis) for each donor, comparing
2251 selected (T4/Edge) and unselected (T0/Centre) sperm subpopulations. Proteins

2252 with significantly higher (right, purple) or lower (left, orange) abundance in selected
2253 sperm are highlighted. The top candidate proteins, shortlisted based on
2254 consistency across donors and magnitude of change, are labelled on each plot.
2255 Cut-off thresholds for differential abundance included a minimum twofold change
2256 across at least three donors and a $p_{adj} < 0.05$ in at least one donor.

2257
2258 Following the identification of differentially abundant proteins across the whole
2259 dataset, changes in abundance were also analysed within each experimental
2260 replicate. For each experiment, proteins were considered to be higher in
2261 abundance if the fold-change ratio was greater than one in both donors, and lower
2262 in abundance if the ratio was below one. Proteins that were not statistically
2263 significant in both donors were excluded.

2264
2265 This filtering identified 52 proteins with higher abundance and 425 with lower
2266 abundance in the methyl cellulose assay (donors 1–2), 33 higher and 594 lower in
2267 the first swim-up assay (donors 3 & 4), and 59 higher and 276 lower in the second
2268 swim-up TMT replicate (donor 3). When considered separately, the number of
2269 significant proteins per donor ranged from 43–113 higher and 86–431 lower
2270 abundance proteins (Table 4–1). These experiment- and donor-specific protein
2271 lists were then annotated with Entrez Gene IDs and used for Gene Ontology (GO)
2272 enrichment analysis against the full human genome background.

2273

2274

2275 Table 4-1: Number of Proteins of significantly higher and lower abundance in
2276 selected sperm by donor.

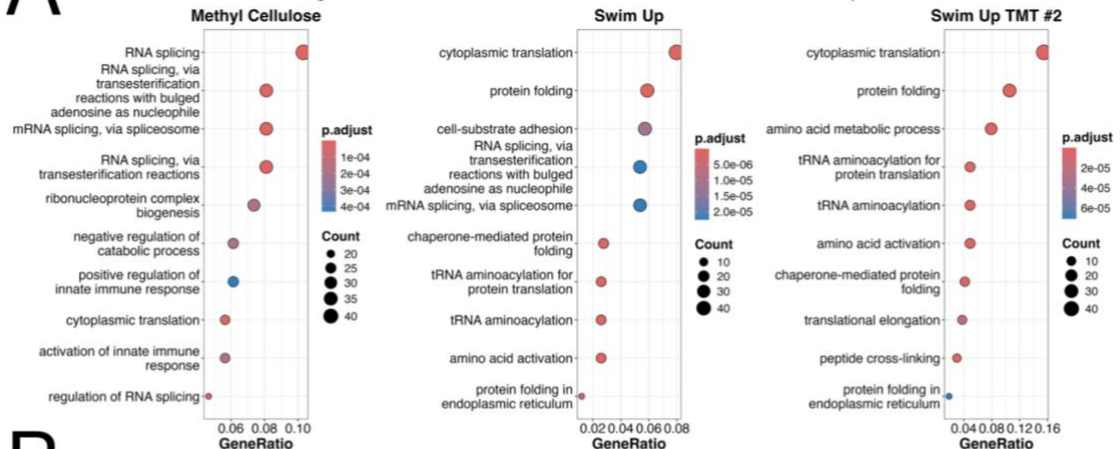
Donor and Experiment	Proteins Significantly Higher in Selected Sperm	Proteins Significantly Lower in Selected Sperm
Donor 1 Methyl Cellulose	113	86
Donor 2 Methyl Cellulose	101	430
Donor 3 Swim Up	43	427
Donor 4 Swim Up	45	431
Donor 5 Swim Up TMT 2	59	276

2277

2278 We performed enrichment analyses for proteins with significantly different
2279 abundances between sperm pools for biological processes, cellular components,
2280 molecular functions, and KEGG pathways (Figures 4-3–4-6). Gene Ontology
2281 enrichment of biological processes for proteins less abundant in selected sperm
2282 were strongly associated with RNA processing and protein translation (Figure 4-
2283 3A). In contrast, proteins more abundant in selected sperm were enriched for
2284 biological processes related to membrane remodelling and regulation of enzymatic
2285 activity following selection via methyl cellulose. The first swim up TMT enriched for
2286 lipid transport and cholesterol efflux pathways characteristic of capacitation, whilst
2287 the second TMT for swim up enriched for motility and membrane organisation.
2288 (Figure 4-3B).

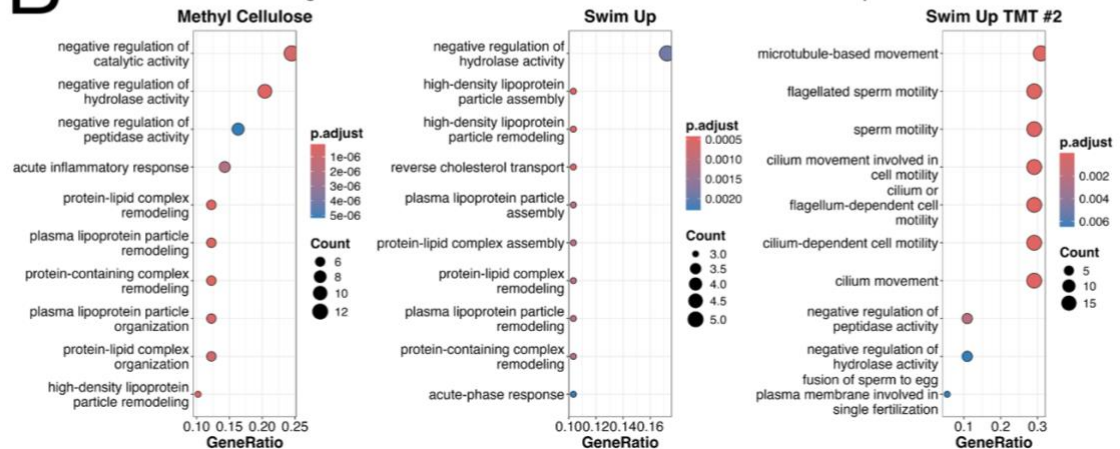
A

GO: Biological Processes Enrichment – Proteins Less Abundant in Selected Sperm



B

GO: Biological Processes Enrichment – Proteins More Abundant in Selected Sperm



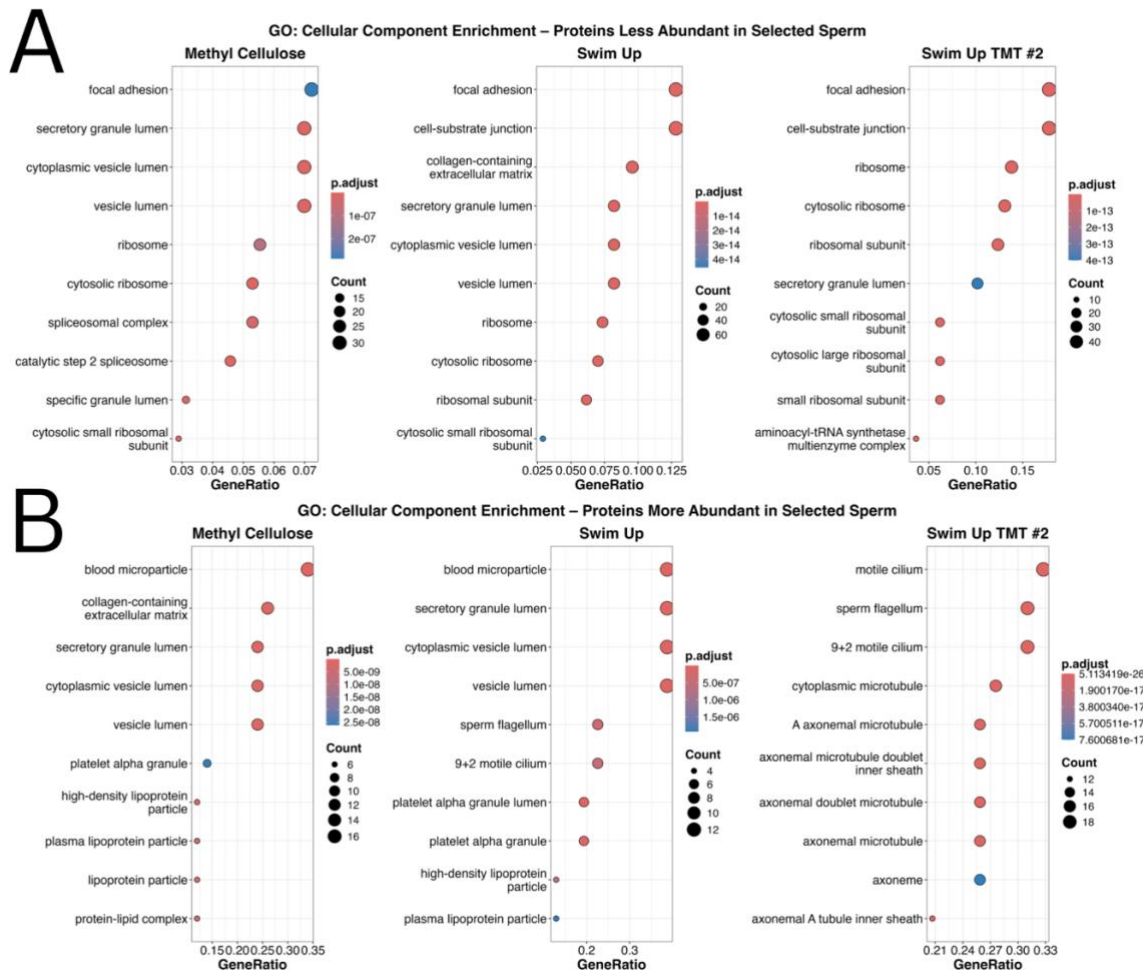
2289

2290 Figure 4-3: A) Bubble plot showing the top 10 significantly enriched GO Biological
 2291 Process terms among proteins with lower abundance in selected sperm compared
 2292 to unselected sperm. B) Bubble plot showing the top 10 significantly enriched GO
 2293 Biological Process terms among proteins with higher abundance in selected sperm
 2294 compared to unselected sperm. Gene Ontology (GO) term analysis was performed
 2295 using BioMart (Haw et al., 2011; Smedley et al., 2015) and Bioconductor
 2296 (Gentleman et al., 2004) packages through R.

2297

2298 For cellular component terms, proteins depleted in selected sperm were
 2299 associated with ribosomal and spliceosomal structures, including “cytosolic
 2300 ribosome,” “ribosomal subunit,” and “spliceosomal complex” (Figure 4-4A).
 2301 Proteins enriched in selected sperm mapped to structures such as “sperm

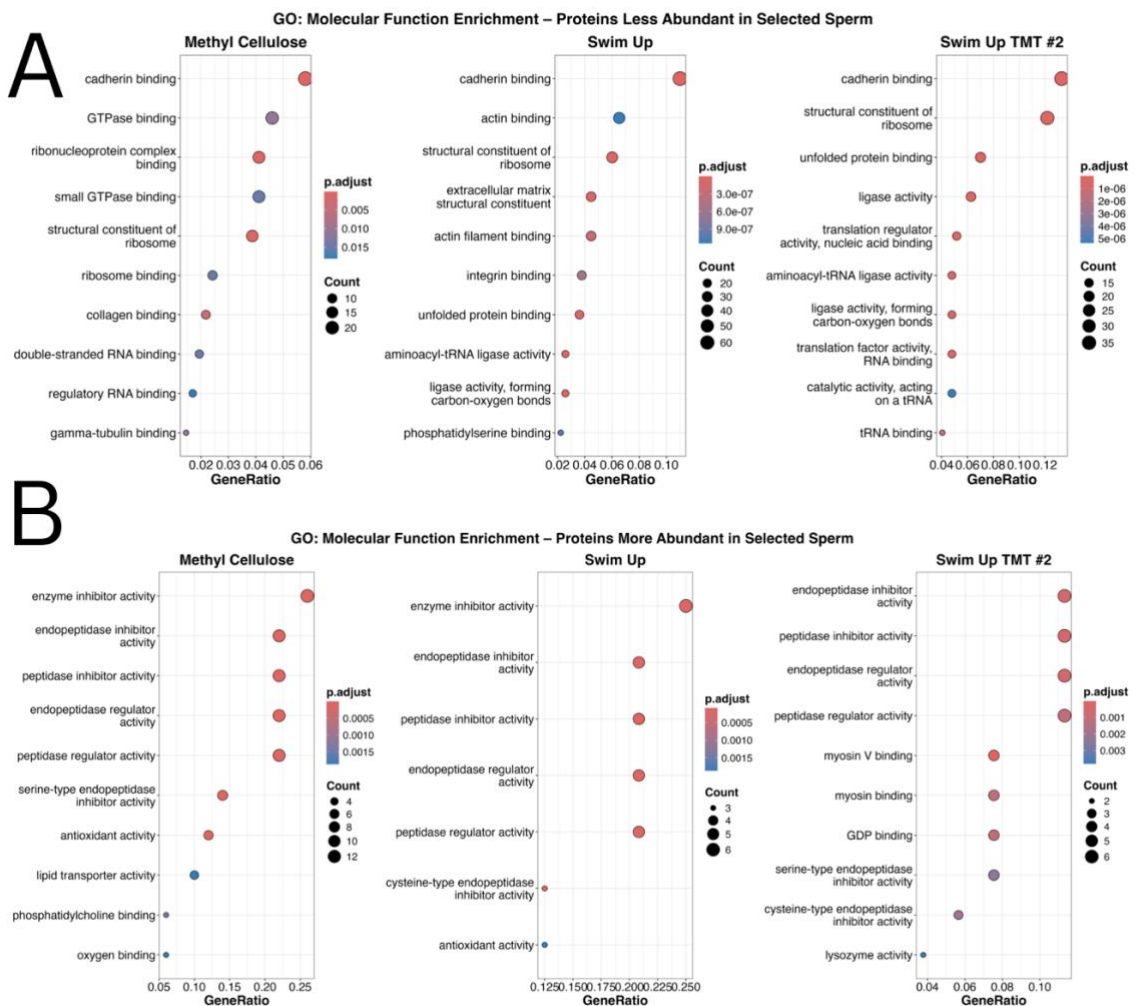
2302 flagellum," "motile cilium," and "axoneme," with strong signals in swim-up replicate
 2303 2 (Figure 4-4B).



2304
 2305 Figure 4-4: A) Bubble plot displaying the top 10 GO Cellular Component
 2306 enrichment for proteins with lower abundance in selected sperm. B) Bubble plot
 2307 displaying the top 10 GO Cellular Component enrichment for proteins with higher
 2308 abundance in selected sperm. Gene Ontology (GO) term analysis was performed
 2309 using BioMart (Haw et al., 2011; Smedley et al., 2015) and Bioconductor
 2310 (Gentleman et al., 2004) packages through R.

2311
 2312 Molecular function analysis showed that proteins less abundant in selected sperm
 2313 were enriched for RNA- and ribosome-binding activities, including
 2314 "ribonucleoprotein complex binding" and "structural constituent of ribosome"
 2315 (Figure 4-5A). Adhesion-related terms such as "collagen binding" and "cell-

2316 substrate junction" were also observed. Proteins more abundant in selected sperm
 2317 were enriched for functions related to enzyme inhibition and structural support,
 2318 including "endopeptidase inhibitor activity," "peptidase regulator activity," and
 2319 "antioxidant activity" (Figure 4-5B).



2320

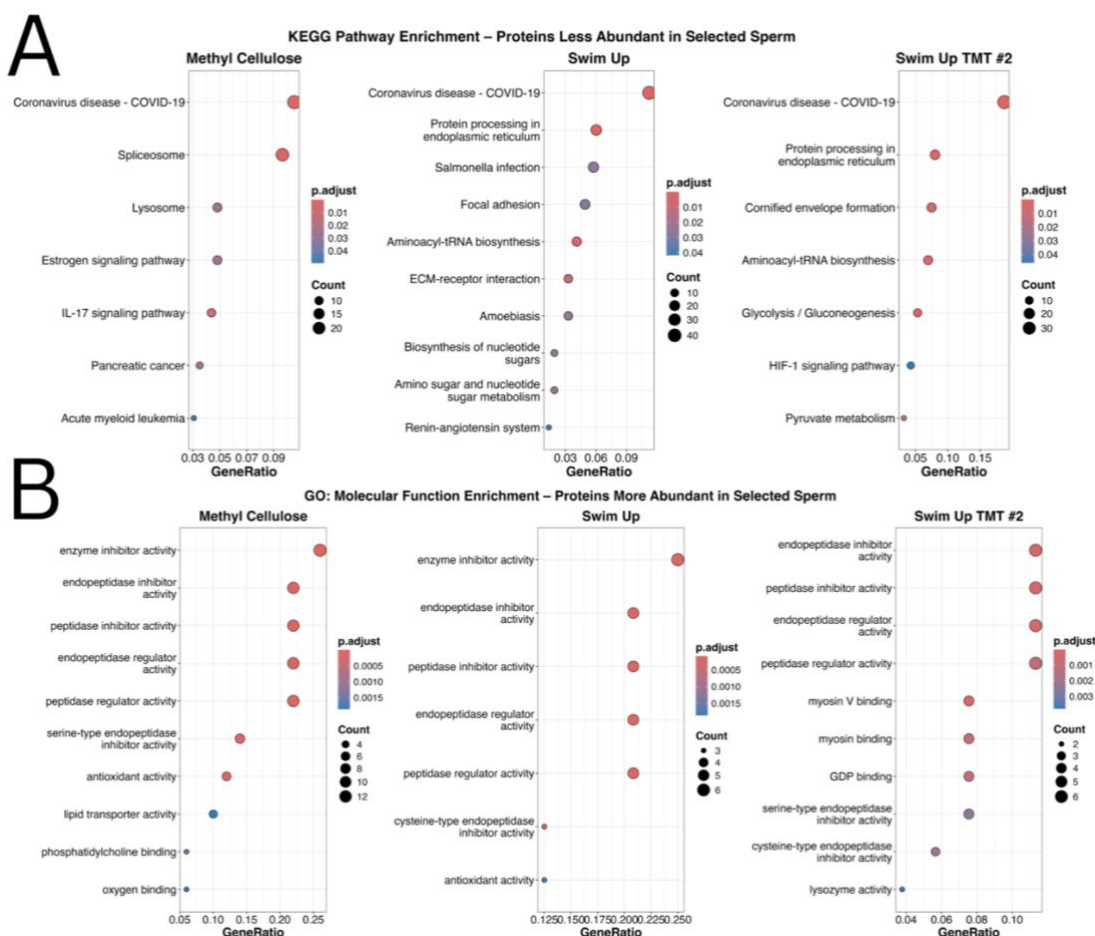
2321 Figure 4-5: A) Bubble plot displaying the top 10 GO Molecular Function
 2322 enrichment for proteins with lower abundance in selected sperm. B) Bubble plot
 2323 displaying the top 10 GO Molecular Function enrichment for proteins with higher
 2324 abundance in selected sperm. Gene Ontology (GO) term analysis was performed
 2325 using BioMart (Haw et al., 2011; Smedley et al., 2015) and Bioconductor
 2326 (Gentleman et al., 2004) packages through R.

2327

2328 KEGG pathway analysis of proteins depleted in selected sperm revealed
 2329 enrichment for "spliceosome," "ribosome," "protein processing in endoplasmic

2330 reticulum," and "aminoacyl-tRNA biosynthesis" (Figure 4-6A). In contrast, proteins
2331 enriched in selected sperm were associated with pathways including "cholesterol
2332 metabolism," "complement and coagulation cascades," and "thyroid hormone
2333 synthesis" (Figure 4-6B).

2334



2335

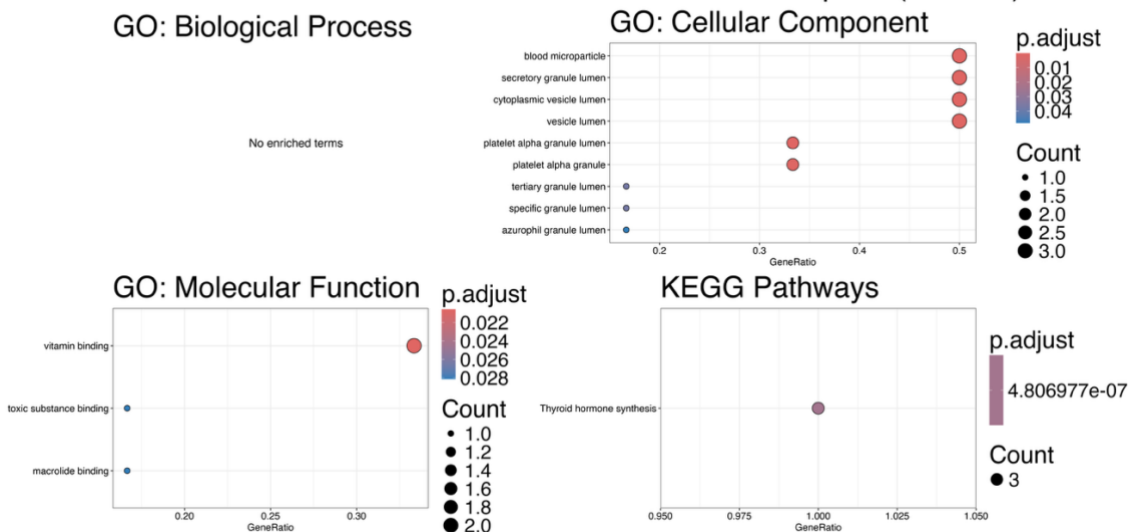
2336 Figure 4-6: A) Bubble plot displaying the top 10 KEGG pathway enrichment for
2337 proteins with lower abundance in selected sperm. B) Bubble plot displaying the top
2338 10 KEGG pathway enrichment for proteins with higher abundance in selected
2339 sperm. Gene Ontology (GO) term analysis was performed using BioMart (Haw et
2340 al., 2011; Smedley et al., 2015) and Bioconductor (Gentleman et al., 2004)
2341 packages through R.

2342

2343 Analysis of shortlisted proteins showed no significant enrichment for biological
2344 processes among the six proteins more abundant in selected sperm, although

2345 Cellular Component terms such as “secretory granule lumen” and “platelet alpha
 2346 granule” were identified, together with Molecular Function terms including “vitamin
 2347 binding” and “toxic substance binding” (Figure 4-7). By contrast, the 62 proteins
 2348 with lower abundance in selected sperm showed consistent enrichment across all
 2349 GO categories, including “RNA splicing,” “mRNA processing,” “regulatory RNA
 2350 binding,” and “helicase activity,” alongside significant enrichment for the KEGG
 2351 pathway “Spliceosome” (Figure 4-8).

Functional Enrichment – Proteins More Abundant in Selected Sperm (Shortlist)



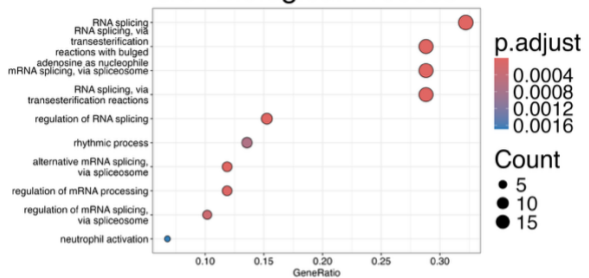
2352

2353 Figure 4-7: Bubble plots displaying the top 10 GO terms enriched for Biological
 2354 Processes, Cellular Components, Molecular Functions and KEGG Pathways for
 2355 shortlisted proteins higher in abundance in selected sperm. Gene Ontology (GO)
 2356 term analysis was performed using BioMart (Haw et al., 2011; Smedley et al.,
 2357 2015) and Bioconductor (Gentleman et al., 2004) packages through R.

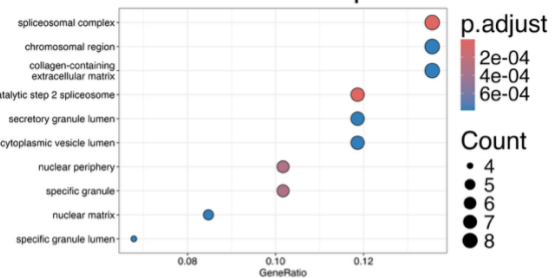
2358

Functional Enrichment – Proteins Less Abundant in Selected Sperm (Shortlist)

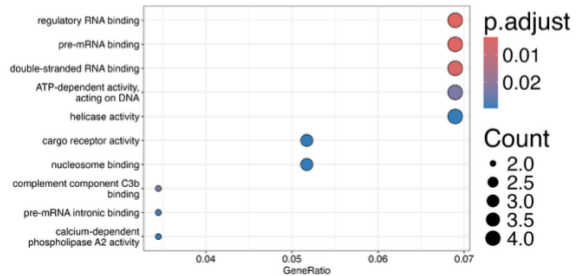
GO: Biological Process



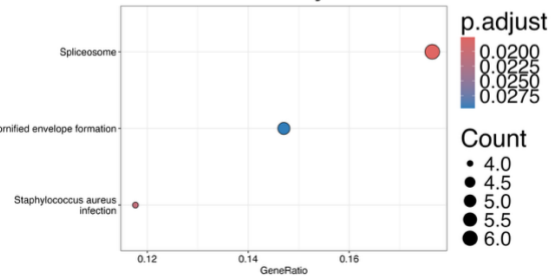
GO: Cellular Component



GO: Molecular Function



KEGG Pathways



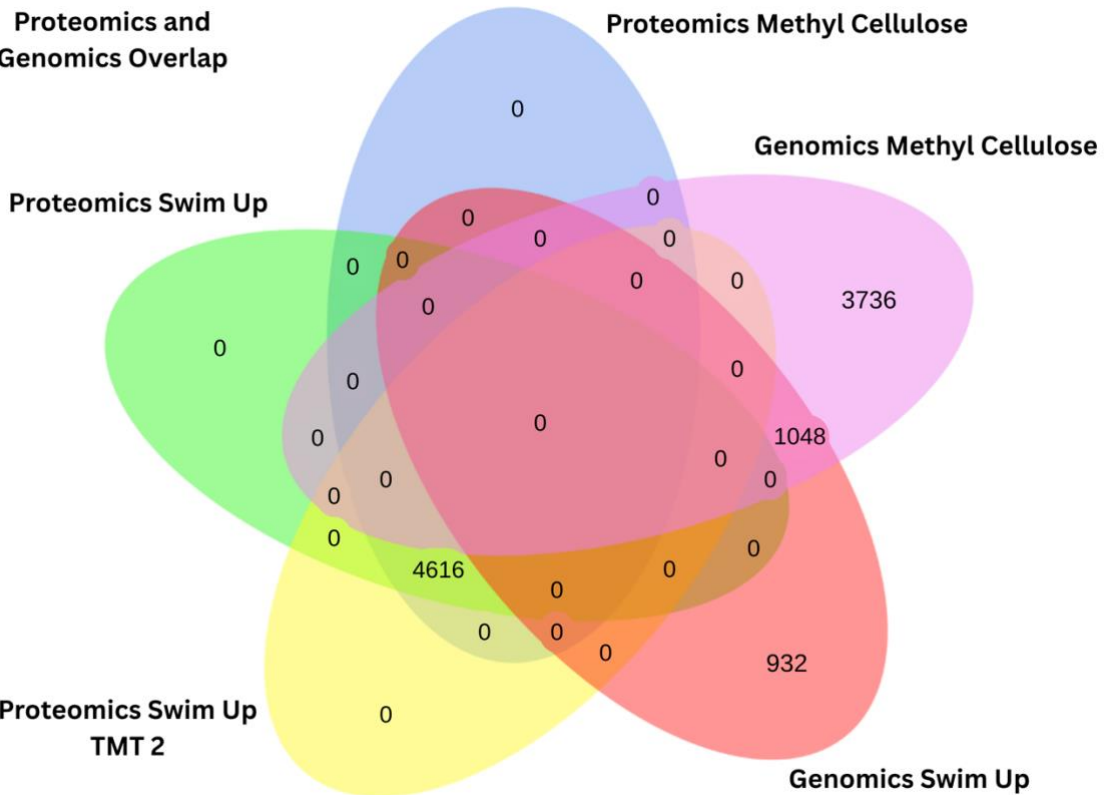
2359

2360 Figure 4-8: Bubble plots displaying the top 10 GO terms enriched for Biological
2361 Processes, Cellular Components, Molecular Functions and KEGG Pathways for
2362 shortlisted proteins lower in abundance in selected sperm. Gene Ontology (GO)
2363 term analysis was performed using BioMart (Haw et al., 2011; Smedley et al.,
2364 2015) and Bioconductor (Gentleman et al., 2004) packages through R.

2365

2366 Comparison of proteomic data (4,616 confidently identified proteins) to previously
2367 generated genomic datasets from methyl cellulose and swim-up assays revealed
2368 no overlap between the two (Figure 4-9).

2369



2370

2371 Figure 4-9: Overlap of confidently identified proteins across the three TMT
2372 experiments and two genomics datasets (*Marcu, 2024*). Venn diagram showing
2373 the intersection of proteins identified in each of the three TMT-labelled LC-MS/MS.
2374 Protein IDs were converted to Entrez IDs which were compared with the Entrez
2375 IDs determined by *Marcu et al. 2024*.

2376

2377 4.5 Discussion

2378 4.5.1 Overview of findings and proteomic depth

2379 We show that selection for sperm subpopulations based on sperm quality from the
2380 same ejaculate is associated with consistent proteomic differences. Across four
2381 donors, quantitative proteomic analysis identified 1,178 proteins with altered
2382 abundance between selected and unselected sperm. The most consistent signal
2383 was a depletion of proteins involved in RNA processing and translation in selected
2384 sperm, while proteins linked to motility and membrane organisation were enriched.
2385 Refinement of the dataset yielded a shortlist of 68 candidate biomarkers, including
2386 nine top candidates present across all donors. These findings provide direct
2387 molecular evidence that functionally distinct sperm subpopulations within a single

2388 ejaculate differ in their proteomic profiles. Of the 1,178 proteins with consistent
2389 differential abundance across all donors, 634 proteins were less abundant and 544
2390 more abundant in selected sperm. Notably, the magnitude of the fold-change ratio
2391 and consistency of lower abundance were stronger, with many proteins showing
2392 fold-change ratios < 0.2 across multiple donors.

2393

2394 A total of 4,616 proteins were confidently identified from human sperm samples
2395 using TMT-labelled quantitative proteomics. While this number is lower than the
2396 ~6,000 proteins reported across the full known human mature sperm proteome, it
2397 is important to note that the larger figure was compiled through meta-analyses of
2398 multiple studies rather than a single dataset (Castillo et al., 2023). In contrast, the
2399 current dataset was derived from only four biological replicates yet still captures
2400 over 75% of the known human sperm proteome, demonstrating substantial depth
2401 and coverage.

2402

2403 **4.5.2 Comparison of selection methods**

2404 Differences between the methyl cellulose and swim up selection methods
2405 influenced both the number and identity of proteins with significantly different
2406 abundances between sperm pools. The more mechanically stringent methyl
2407 cellulose assay likely selects for sperm with enhanced motility traits, as migration
2408 through viscous media requires high progressive motility and is correlated with
2409 fertilisation competence in vivo (Quill et al., 2003; Suarez & Pacey, 2006). In
2410 contrast, the swim-up assay selects sperm that are both progressively motile in a
2411 less viscous medium and able to maintain that motility over extended incubation.
2412 Several studies have shown that swim up assays isolate sperm with improved
2413 morphology, DNA integrity, and fertilising potential compared to the raw ejaculate
2414 (Henkel & Schill, 2003). The requirement for sustained swimming over time means
2415 that swim up fractions are enriched for sperm with increased longevity and
2416 resilience, traits directly linked to higher fertilisation rates (McDowell et al., 2014).

2417

2418 This difference in selective pressures between the two methods is demonstrated
2419 by the differences observed in the GO terms generated for proteins more

2420 abundant in selected sperm, with the swim-up experiments enriched for “cillum
2421 motility” and related terms, consistent with previous evidence that sperm flagellar
2422 beating and ciliary function are central determinants of fertilising ability (Amaral et
2423 al., 2013; Lindemann & Lesich, 2016). By contrast, In the methyl cellulose
2424 experiments, enrichment for terms such as “oxygen binding” is consistent with the
2425 importance of redox regulation for sperm quality, as oxygen-binding proteins can
2426 support mitochondrial respiration while protecting against reactive oxygen species
2427 (ROS), which are key modulators of capacitation and fertilisation but detrimental in
2428 excess (O’Flaherty & Matsushita-Fournier, 2017). Lipid–protein interactions are
2429 also critical for capacitation, acrosome exocytosis, and membrane fusion with the
2430 oocyte, with cholesterol efflux and lipid remodelling representing established
2431 hallmarks of sperm functional maturation (Gadella & Luna, 2014). Together, these
2432 functional enrichments highlight that the two assays isolate sperm populations with
2433 distinct molecular signatures: swim-up favouring motility and longevity, and methyl
2434 cellulose selecting for resilience in viscous environments and optimal metabolic
2435 and membrane properties.

2436

2437 **4.5.3 Candidate biomarkers**

2438 The most consistently and significantly less abundant protein in selected sperm
2439 across all donors and experiments was Olfactomedin-4 (*OLFM4*, Q6UX06).
2440 *OLFM4* is a glycoprotein that has been found to be implicated in cell adhesion,
2441 immune regulation, and apoptotic resistance in the context of the gastrointestinal
2442 epithelium and cancer biology (Wei et al., 2024). The presence of *OLFM4* in
2443 mammalian spermatozoa and epididymal vesicles has been previously reported,
2444 suggesting a role in sperm maturation or intercellular signalling within the
2445 reproductive tract (Zmudzinska et al., 2022). Its lower abundance in sperm that
2446 successfully passed through our selection assays may indicate that elevated
2447 levels of *OLFM4* are deleterious to sperm function or structural integrity, potentially
2448 interfering with motility due to inappropriate cell adhesion. Given its consistent
2449 significance across donors and the lowest observed median fold-change ratio,
2450 *OLFM4* may represent a key marker of poor-quality sperm.

2451

2452 Two of the other most significantly less abundant proteins were phospholipase A2
2453 (*PLA2G2A*, P14555) and Midkine (*MDK*, P21741), which also showed consistent
2454 and notable depletion in selected sperm. Phospholipase A2 is a secretory enzyme,
2455 known to be present in human seminal plasma, and also known to be closely
2456 related to various male reproductive malignancies including penile, prostate and
2457 testicular cancer (Dahiya et al., 2023). Midkine is a protein growth factor classically
2458 involved in embryonic development, tissue regeneration, and inflammatory
2459 signalling. Many studies have focussed on the importance of midkine during
2460 fertilisation (Torabi et al., 2017). This makes the lower abundance of midkine in
2461 selected sperm surprising although it has also been implicated as a potential
2462 prognostic biomarker for embryonal carcinoma (Jono & Ando, 2010). The lower
2463 abundance of both phospholipase A2 and midkine in the selected sperm
2464 population further supports the previous evidence that sperm that survive selective
2465 pressures may relate to increased health benefits in the offspring (Alavioon et al.,
2466 2019).

2467

2468 The final two proteins in the top five are Beta-defensin 105 (*DEFB105A*, Q8NG35) and
2469 Heterogeneous nuclear ribonucleoprotein K (*HNRNPK*, P61978). Beta-defensin
2470 105 is an antimicrobial peptide that has previously been identified in the mouse
2471 epididymis (Yamaguchi et al., 2002), with some members of the beta-defensin
2472 protein family believed to be positive markers of human fertility (Solanki et al.,
2473 2023), although the exact impact of beta-defensin 105 has not been categorised.
2474 Heterogeneous nuclear ribonucleoprotein K has previously been identified in the
2475 human sperm nucleus (de Mateo et al., 2011), and mutations in the gene
2476 responsible for this protein have previously been identified in men with impaired
2477 spermatogenesis (Westerveld et al., 2004). Both heterogeneous nuclear
2478 ribonucleoprotein K and beta-defensin 105 have been implicated as having
2479 positive effects on male fertility (Solanki et al., 2023; Westerveld et al., 2004) so
2480 their conserved lower abundance between selected sperm samples of different
2481 donors is puzzling. This trend and the exact effects of these proteins abundances
2482 on mature sperm require more investigation to determine what molecular effects
2483 are conferred and if they may act as suitable biomarkers of sperm quality.

2484

2485 Among the six proteins (Thyroxine-binding globulin, Afamin, Beta-
2486 microseminoprotein, Alpha-1-acid glycoprotein 1, Albumin, and Transthyretin)
2487 shortlisted as higher in abundance in selected sperm, four met the additional
2488 selection criteria of being detected across all donors, significant in at least four,
2489 and with a median fold-change ratio above 2. However, due to variability across
2490 individuals, none of these proteins were consistently identified in more than two
2491 donors within the initial discovery set. As a result, their utility as biomarker
2492 candidates remains uncertain, but they could warrant further investigation in larger
2493 cohorts where inter-individual variation can be more robustly accounted for.

2494

2495 Proteins selected for downstream validation by flow cytometry (Chapter 5) were
2496 chosen based on their strong and consistent differential expression, predicted or
2497 known membrane localisation, and potential relevance to sperm function or
2498 fertility. The combination of differential abundance, biological plausibility, and
2499 accessibility in intact sperm made these candidates suitable for further study.

2500

2501 **4.5.4 Functional enrichment analysis**

2502 Functional enrichment analyses revealed two broad and consistent patterns.
2503 Firstly, proteins linked to RNA processing were consistently depleted. This aligns
2504 with previous work showing that translational and splicing activity are features of
2505 immature sperm and are typically absent in fully mature, high-quality spermatozoa
2506 (Nixon et al., 2023). The depletion of these proteins in selected fractions therefore
2507 supports the interpretation that sperm surviving the assays represent a more
2508 functionally mature population.

2509

2510 Secondly, proteins more abundant in selected sperm were enriched for terms
2511 related to motility. These included components of the flagellum and cilium,
2512 consistent with evidence that flagellar structure and activity are central to sperm
2513 motility and fertilisation competence (Lindemann & Lesich, 2016). Other enriched
2514 functions included lipid metabolism and membrane-associated protein complexes,
2515 processes closely linked to capacitation and the regulation of membrane fluidity
2516 (Gadella & Luna, 2014). Enrichment for antioxidant and enzyme inhibitor activities

2517 is also consistent with the requirement to withstand oxidative and proteolytic stress
2518 during transit through the female tract, factors well known to compromise fertility
2519 when unregulated (Bisht et al., 2017; Cesari et al., 2010).

2520

2521 KEGG pathways reinforced these patterns, linking less abundant proteins to
2522 translational machinery and more abundant proteins to lipid metabolism and
2523 hormonal regulation. Specific KEGG pathways mentioned such as cholesterol
2524 efflux and membrane fluidity have been recognised hallmarks of capacitation
2525 (Cross, 1998), while thyroid hormones are known to modulate testicular and
2526 epididymal function, with downstream effects on sperm quality (Jasim, 2021).

2527

2528 Taken together, these enrichment results suggest that sperm selection favours
2529 cells with molecular profiles optimised for motility, membrane remodelling, and
2530 stress resistance, while excluding sperm that retain features of immaturity or
2531 dysregulation. This provides further support for the idea that within-ejaculate
2532 variation in sperm function is reflected at the proteomic level and can be detected
2533 by differential selection assays.

2534

2535 **4.5.5 Integration with genomic data**

2536 Comparison of the proteomic dataset (4,616 confidently identified proteins) with
2537 previously generated genomic datasets from methyl cellulose and swim-up assays
2538 revealed no direct overlap between the two (Figure 4-9). This is expected, as
2539 genomic and proteomic analyses capture different but complementary layers of
2540 haploid selection: variation at the DNA sequence level versus the resulting
2541 functional phenotypes at the protein level. Importantly, however, both approaches
2542 converge on the same biological signal. In the genomic study, selected sperm
2543 showed a reduced representation of alleles associated with human disease,
2544 consistent with haploid selection filtering out genetically compromised cells (Marcu
2545 et al., 2024). In the present proteomic dataset, several of the top five proteins
2546 depleted in selected sperm are annotated as disease biomarkers, suggesting that
2547 sperm excluded during selection also carry molecular signatures linked to
2548 pathological processes. Together, these independent lines of evidence support the

2549 conclusion that haploid selection reduces the transmission of deleterious or
2550 disease-associated variants, with implications both for reproductive success and
2551 for the genetic health of offspring.

2552

2553 **4.5.6 Experimental design limitations**

2554 It should also be noted that due to logistical constraints, the swim-up assays were
2555 performed on donor samples obtained in Cape Town, South Africa, while the
2556 methyl cellulose assays were carried out on samples collected in Norwich, United
2557 Kingdom. Rather than limiting the study, this design was chosen to avoid
2558 restricting the dataset to a single age group or ethnic background, thereby
2559 capturing a broader range of variation in sperm proteomes. In line with this, each
2560 donor was treated as an independent experiment and overlaps in protein changes
2561 across donors and assays provide evidence for robust signals and promising
2562 biomarker candidates. The observed variation between donors and between
2563 assays likely reflects both biological differences among individuals and assay-
2564 specific selective pressures. Such variation between donors is well documented,
2565 with previous proteomic studies showing extensive inter-individual differences in
2566 protein composition and abundance (Amaral, et al., 2014 ; Saraswat et al., 2017).
2567 Importantly, the presence of this variation emphasises the need to investigate
2568 sperm function at the level of the individual ejaculate, since pooling or averaging
2569 across donors could obscure meaningful haploid-level differences.

2570

2571 Another limitation is the current inability to define the sperm cell surface proteome.
2572 Although biomarkers should ideally be surface expressed to enable non-
2573 destructive selection, distinguishing true surface proteins from intracellular
2574 components remains technically challenging. single-cell proteomics of sperm is not
2575 yet feasible, and many of the proteins identified to date lack functional annotation
2576 or localisation data. Furthermore, functional predictions are often based on
2577 somatic data, which may not accurately reflect sperm biology. This uncertainty
2578 limits the ability to distinguish surface-expressed candidates from intracellular
2579 proteins, highlighting the need for further studies that combine proteomics with
2580 imaging or biochemical validation of protein localisation.

2581

2582 **4.5.7 Conclusion**

2583 Our findings provide proteomic evidence that within-ejaculate sperm selection is
2584 associated with systematic molecular differences, identifying candidate biomarkers
2585 that distinguish higher-quality sperm from those of lower quality. By showing that
2586 sperm excluded during selection are enriched for proteins linked to immaturity,
2587 dysregulation, and disease processes, this study demonstrates that haploid
2588 selection acts at the protein level to shape sperm quality. These insights move
2589 beyond descriptive catalogues of the sperm proteome and establish a functional
2590 link between molecular composition and selective fertilisation potential. Future
2591 work to validate the localisation and function of these candidates, particularly
2592 those expressed at the sperm surface, will be essential for translating these
2593 findings into clinical tools. Incorporating proteomic biomarkers into assisted
2594 reproduction technologies would provide a non-destructive means of identifying
2595 sperm with superior functional capacity and lower genetic risk, improving both
2596 fertility treatment outcomes and the long-term health of offspring. More broadly,
2597 the integration of genomic, transcriptomic, and proteomic layers will be key to
2598 building a comprehensive understanding of haploid selection in humans and its
2599 evolutionary and biomedical significance.

2600

2601

2602 **5 Validation of Cell Surface Biomarkers**

2603 **for Sperm Longevity and Fitness**

2604 **5.1 Abstract**

2605 Within-ejaculate variation in sperm quality presents both a biological challenge for
2606 understanding male fertility, and a clinical opportunity for improved selection in
2607 assisted reproductive technologies (ART). In Chapter 4, 68 candidate sperm
2608 surface biomarkers were identified via Tandem Mass Tag (TMT)-based
2609 quantitative proteomics in sperm selected in two assays selecting for sustained
2610 motility and longevity, thereby serving as a functional proxy for sperm quality. To
2611 validate these candidates and assess their potential functional relevance, three
2612 biomarkers were selected for further investigation: Olfactomedin-4 (OLFM4),
2613 junction plakoglobin (JUP/CTNG), and Amine oxidase copper containing 3
2614 (AOC3). These markers were prioritised based on their consistent and statistically
2615 significant differential abundance between selected and unselected sperm
2616 fractions, predicted surface localisation, and the availability of validated antibodies
2617 suitable for flow cytometry in human tissue. Imaging flow cytometry was employed
2618 using the BD FACSDiscovery S8 system to assess marker expression and
2619 localisation on sperm from 5 donors. Sperm were sorted following incubation for
2620 longevity, with the addition of viability dye prior to fixing. This approach enabled
2621 single-cell analysis of fluorescence intensity in both long- and short-lived sperm
2622 subpopulations. OLFM4 and CTNG were predicted to have lower fluorescence
2623 intensity in long-lived sperm, while AOC3 was selected as a contrasting marker
2624 predicted to show increased abundance in selected sperm. The aim was to
2625 confirm the membrane localisation of these markers and assess their utility in
2626 reliably distinguishing sperm subpopulations, contributing to the development of
2627 surface-based biomarkers for sperm quality. Both OLFM4 and CTNG were
2628 validated as potential biomarkers of sperm fitness with a consistent trend of higher
2629 marker fluorescence in short-lived sperm. In contrast, AOC3 was not found to be a
2630 suitable biomarker due to the highly variable trend between donor samples. This
2631 work provides an essential step toward developing molecularly guided sperm
2632 selection strategies for improving ART outcomes.

2633 **5.2 Introduction**

2634 One of the largest advances in reproductive medicine was the invention of
2635 Assisted Reproductive Technologies (ART). The first of these was in vitro
2636 fertilisation (IVF), in which multiple sperm are co-incubated with an oocyte in a
2637 culture dish, allowing fertilisation to occur outside the body under controlled
2638 laboratory conditions (Steptoe & Edwards, 1978). A second milestone came with
2639 the development of Intra-Cytoplasmic Sperm Injection (ICSI), in which a single
2640 sperm is selected and injected directly into the cytoplasm of the oocyte using
2641 micromanipulation techniques (G. Palermo et al., 1992). Both, IVF and ICSI are
2642 now routine clinical practice, together accounting for estimates of around 3–6% of
2643 all births in high-income countries and more than 10 million births worldwide since
2644 the first IVF child was born (Adamson et al., 2025)

2645

2646 Despite their widespread use, ART procedures remain associated with significant
2647 challenges. Even with technical improvements, the chance of a live birth per
2648 treatment cycle remains below 30% in most age groups, and miscarriage rates are
2649 approximately 20–30%, compared with around 10–15% in natural conceptions
2650 (Szamatowicz & Szamatowicz, 2023; van Oosterhout et al., 2022). Women
2651 undergoing treatment face substantial physical and emotional burdens, including
2652 repeated cycles of ovarian stimulation, invasive oocyte retrieval, and the stress of
2653 variable outcomes (Szamatowicz & Szamatowicz, 2023). While much of the focus
2654 has been on maternal factors, growing evidence suggests that paternal
2655 contributions, including sperm DNA fragmentation, chromosomal abnormalities,
2656 and epigenetic alterations, can play a role in early embryo loss and adverse
2657 pregnancy outcomes (Alavioon et al., 2021; van Oosterhout et al., 2022). These
2658 challenges underscore that ART, while transformative, still has substantial room
2659 for improvement in order to increase success rates and reduce the physical and
2660 emotional burden on patients.

2661

2662 A key concern is that both IVF and, to an even greater extent, ICSI circumvent
2663 many of the natural barriers that normally regulate fertilisation. In vivo, sperm must
2664 undergo capacitation, migrate through the female reproductive tract, interact with

2665 the zona pellucida, and complete the acrosome reaction before fusing with the
2666 oocyte (Kim et al., 2008). Each of these steps functions as a stringent filter that
2667 reduces the probability of fertilisation by sperm carrying DNA damage,
2668 chromosomal abnormalities, or compromised morphology (Alavioon et al., 2021).
2669 By bypassing these checkpoints, ART relaxes natural selection on sperm quality,
2670 which may increase the genetic load passed to offspring. Genetic load refers to
2671 the accumulation of deleterious mutations or other heritable defects within a
2672 population that reduce overall fitness (van Oosterhout et al., 2022). This relaxed
2673 selection may partly explain the elevated miscarriage rates observed in ART
2674 pregnancies, as well as raise concerns about the long-term consequences of
2675 transmitting hidden defects to the next generation.

2676

2677 Recognising that ART bypasses many of the natural filters of fertilisation raises a
2678 fundamental question: which characteristics define a sperm that would normally
2679 succeed in passing these barriers, and how do such sperm differ from the rest of
2680 the ejaculate? Traditional semen analysis focuses on concentration, motility, and
2681 morphology (Nixon et al., 2023). While these parameters are useful for diagnosing
2682 severe cases of male infertility, they have limited ability to predict fertilisation,
2683 embryo development, or live birth outcomes in ART (Villani et al., 2022). Beyond
2684 these basic measures, studies have suggested that traits such as sperm longevity
2685 (Alavioon et al., 2017), progressive motility (Kumar & Singh, 2021), and intact DNA
2686 integrity (Alahmar et al., 2022) provide better indications of reproductive potential.
2687 However, methods for separating sperm on the basis of these traits remain
2688 technically challenging.

2689

2690 A number of assays have been developed to enrich for sperm with presumed
2691 superior fertilisation potential. The most widely used approaches are density
2692 gradient centrifugation and swim-up (Amano et al., 2024), both of which select for
2693 sperm with greater motility and reduced levels of cellular debris or dead cells.
2694 More recent methods, such as microfluidic devices (Doostabadi et al., 2022),
2695 attempt to mimic aspects of the female reproductive tract by favouring sperm with
2696 intact membranes or more mature functional profiles. However, none of these

2697 approaches consistently predicts treatment outcomes, and their ability to reduce
2698 miscarriage or improve live birth rates remains uncertain.

2699

2700 Given the limitations of current selection methods, one major area of research has
2701 focused on identifying reliable biomarkers of sperm quality. The aim is to find
2702 molecular or cellular features that distinguish sperm most capable of supporting
2703 fertilisation and embryo development from the rest of the population. For example,
2704 studies of sperm surface biomarkers such as Heat Shock Protein A2 (HSPA2),
2705 Parkinsonism-associated protein DJ-1 (DJ-1), and Serum Amyloid P component
2706 (SAP), examined how these markers correlated with sperm quality across 114
2707 donors with either normal or abnormal spermograms (Amaral, Paiva, et al., 2014).
2708 However, these markers were assessed at the level of whole ejaculate populations
2709 and were primarily explored as diagnostic tools for distinguishing between fertile
2710 and infertile men.

2711

2712 Before candidate biomarkers can be advanced for intensive clinical investigation,
2713 they must undergo a structured development process that includes analytical
2714 validation to assess their reliability, reproducibility, and specificity for the intended
2715 application (McShane et al., 2013). One widely used analytical method is
2716 immunohistochemistry (IHC), which relies on antibody-based detection of protein
2717 targets in fixed tissue samples (Ramos-Vara et al. 2014). This technique typically
2718 uses enzyme-linked or chromogenic systems to visualise antigen–antibody
2719 complexes, although fluorescent conjugates may also be employed in
2720 immunofluorescence-based approaches.

2721

2722 A more recently developed platform that can be applied to biomarker validation is
2723 imaging flow cytometry, which combines high-throughput single-cell fluorescence
2724 analysis with microscopic imaging (Harte et al., 2024). This approach allows highly
2725 targeted detection using a wide range of antibodies, either through premade
2726 antibody–fluorophore conjugates or via secondary antibody labelling strategies.
2727 Importantly, imaging flow cytometry can be coupled with flow-assisted cell sorting

2728 (FACS), enabling the non-destructive separation of sperm populations based on
2729 biomarker expression for downstream analysis.

2730

2731 Flow cytometry has already been established as a powerful platform for biomarker
2732 detection in clinical settings. In reproductive biology for example, sperm
2733 aneuploidy testing by Fluorescence In Situ Hybridisation (FISH) coupled with flow
2734 cytometric analysis has been used to assess chromosomal abnormalities in men
2735 with severe infertility, providing diagnostic information that can guide ART
2736 decisions (de Lima Rosa et al., 2023). Although not yet widely standardised, such
2737 assays demonstrate the feasibility of applying flow-based methods to sperm
2738 biomarker detection. Beyond reproduction, flow cytometry is routinely employed in
2739 clinical haematology, where immunophenotyping of leukocytes using antibody-
2740 labelled surface markers is a cornerstone of diagnosing and monitoring blood
2741 cancers such as leukaemia and lymphoma (Brestoff, 2023). These established
2742 examples highlight how flow cytometry-based biomarker assays can move from
2743 research to clinical application, supporting its potential utility in the development of
2744 sperm-specific biomarkers.

2745

2746 Whereas previous biomarker studies have largely aimed to stratify fertility status
2747 across individuals (Blaurock et al., 2022), this study focuses on identifying and
2748 separating potentially less-fit sperm within a single ejaculate. This shift in
2749 emphasis is motivated by evidence that sperm populations are highly
2750 heterogeneous, with only a small proportion typically capable of successful
2751 fertilisation under natural conditions (van Oosterhout et al., 2022). By targeting this
2752 within-ejaculate variation, it may be possible to exclude sperm carrying DNA
2753 damage or other hidden defects and thereby enrich for those with the greatest
2754 developmental potential (Alavioon et al., 2021). Such an approach has the
2755 potential to improve reproductive outcomes, even in cases where infertility has
2756 already been diagnosed, by providing a means to optimise sperm selection
2757 beyond conventional semen analysis or bulk biomarker assays.

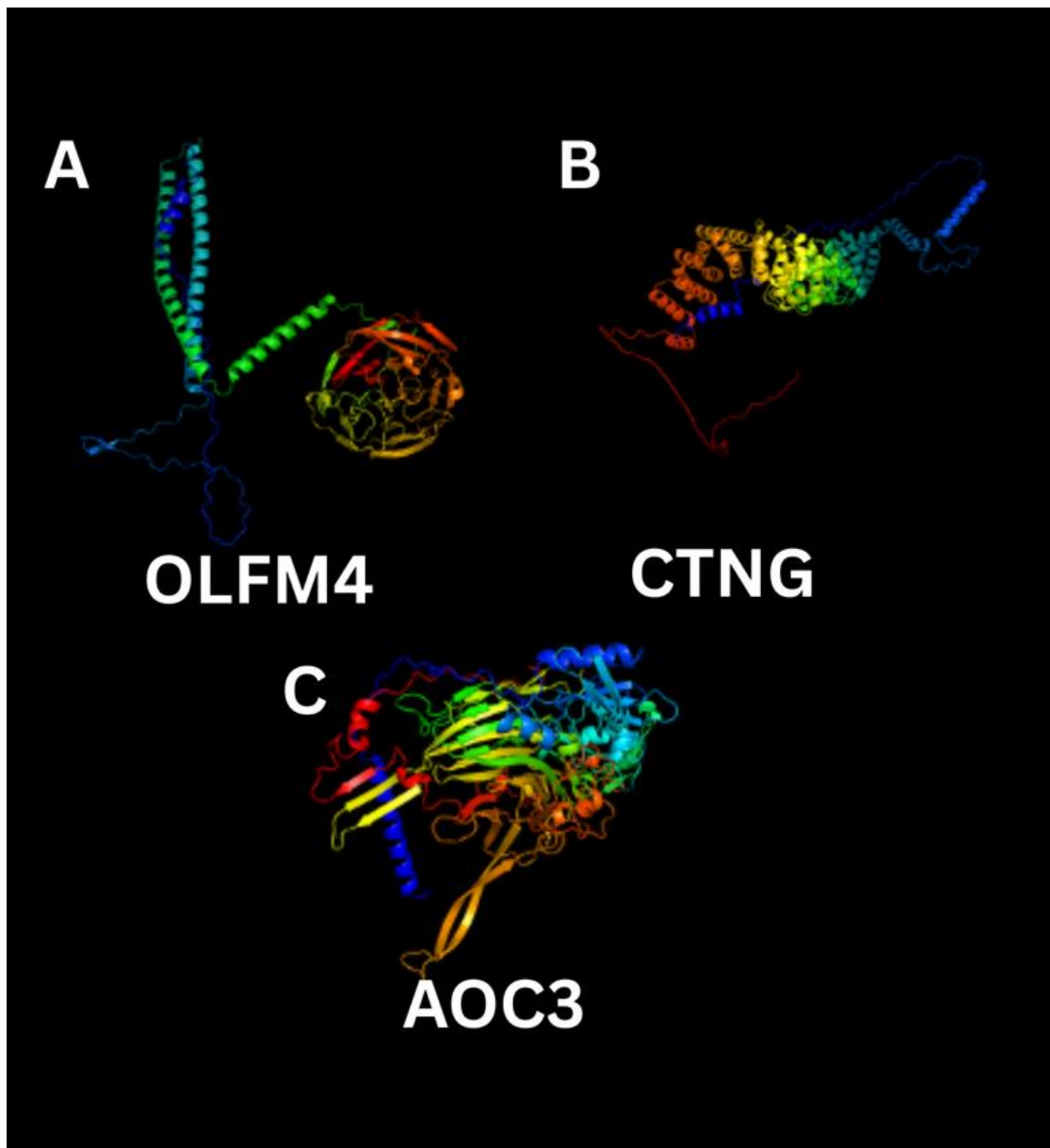
2758

2759 Following the proteomic profiling of intra-ejaculate variation in sperm fitness
2760 presented in Chapter 4, and the identification of 68 candidate surface biomarkers,
2761 it became necessary to validate the presence, trends, and localisation of these
2762 proteins on live spermatozoa. Proteomic data alone cannot establish whether such
2763 markers are accessible at the cell surface, nor whether they exhibit sufficient
2764 variability within an ejaculate to permit targeted selection. Because of these
2765 constraints, three candidate biomarkers were selected from the shortlist generated
2766 in Chapter 4. These markers were prioritised based on both their high median
2767 abundance ratios and statistically significant p-values in the proteomic dataset, as
2768 well as the commercial availability of antibodies validated for use in human
2769 tissues.

2770

2771 The first of these biomarkers chosen for further validation, is Olfactomedin-4
2772 (OLFM4), which was found to have statistically significantly lower abundance in
2773 the T4/edge selected samples across all measured donors and mass spectrometry
2774 analysis (Chapter 4). OLFM4 (Figure 5-1A) is a glycoprotein that has previously
2775 been found in neutrophil granules, intestinal crypts and prostate tissue (Kobayashi
2776 et al., 2007). This protein has been previously described as a biomarker for
2777 disease severity in conditions such as sepsis, viral infections, and malaria (W. Liu
2778 et al., 2010). Similarly, OLFM4 has been described to modulate inflammation and
2779 tissue repair by inhibiting the antimicrobial and pro-inflammatory functions of
2780 neutrophil cationic proteins (Vandenbergh-Dürr et al., 2024). The ability to
2781 regulate immune responses and interact with other surface proteins suggests that
2782 it may play a role in cellular viability and stress responses and therefore may be
2783 relevant to sperm viability and longevity under selection pressures.

2784



2785

2786 Figure 5-1: Predicted tertiary structures of OLFM4, CTNG, and AOC3.

2787 A-C) Three-dimensional protein structures visualised in PyMOL using the
2788 corresponding Protein Data Bank (PDB) entries retrieved via UniProt. Each
2789 structure is colour-coded by protein chain/domain, where each colour represents
2790 an individual polypeptide chain or structural domain within the protein.
2791 A) OLFM4 (Olfactomedin-4): coloured by chain to illustrate the organisation of the
2792 olfactomedin domain relative to the N-terminal region.
2793 B) CTNG (Junction plakoglobin / γ -catenin): coloured by chain to highlight the
2794 arrangement of its armadillo repeats and domain layout.
2795 C) AOC3 (Amine oxidase, copper-containing 3): coloured by chain to visualise the
2796 enzyme's dimeric architecture and domain structure.

2797 The second selected candidate biomarker is junction plakoglobin (JUP) also
2798 known as γ -catenin (CTNG) (Figure 5-1B). This is a cell adhesion molecule in the
2799 armadillo family, homologous to β -catenin, and acts as a critical component of
2800 desmosomes and adherens junctions, anchoring cadherins to the cytoskeleton
2801 and helping maintain tissue integrity (Ding et al., 2025). Previous research has
2802 found that the dysregulation of CTNG is associated with various cancers, and
2803 overexpression of CTNG has been linked to increased proliferation, migration, and
2804 invasion in oral squamous cell carcinoma (Fang et al., 2020). Whilst the function of
2805 CTNG in sperm has not been widely studied, it is likely that the established
2806 membrane localisation and role in cell–cell adhesion suggest it may contribute to
2807 sperm structural integrity, interactions with Sertoli cells and response to membrane
2808 stress or survival.

2809

2810 The final selected candidate protein for validation was Amine Oxidase, Copper
2811 Containing 3 (AOC3), also known as vascular adhesion protein-1 (VAP-1). This
2812 protein was chosen to investigate potential biomarkers that were found to increase
2813 in abundance in T4 and edge selected sperm populations, as a contrast to CTNG
2814 and OLFM4. AOC3 (Figure 5-1C) is a membrane-bound surface protein with dual
2815 roles of a monoamine oxidase- producing aldehydes, ammonia, and hydrogen
2816 peroxide from primary amines, and as an adhesion molecule where it facilitates
2817 leukocyte binding and transmigration at inflamed endothelial sites (Boyer et al.,
2818 2021). AOC3 has been found to be highly expressed on vascular endothelium,
2819 myofibroblasts, and inflammatory tissues, and has been identified as a biomarker
2820 for myofibroblasts (Hsia et al., 2016). Whilst, as with OLFM4 and CTNG, AOC3
2821 has not previously been studied in sperm, its consistent membrane localisation
2822 and roles in redox biology and cellular adhesion suggest a potential contribution to
2823 sperm membrane integrity or oxidative stress response.

2824

2825 To validate these candidates, the BD FACSDiscovery S8 spectral imaging flow
2826 cytometry system was employed to examine their surface expression on live
2827 spermatozoa. Each marker was assessed using separate antibody staining
2828 protocols to ensure specificity, and all samples were processed without cell

2829 permeabilization to maintain membrane integrity and confirm surface localisation.
2830 This strategy enabled single-cell resolution of marker expression on both live and
2831 dead spermatozoa, allowing direct comparison of fluorescence intensity across
2832 sperm longevity subpopulations and supporting the identification of consistent,
2833 surface-accessible biomarkers.

2834

2835 Together, OLFM4, CTNG, and AOC3 represent three surface proteins with distinct
2836 biological functions and contrasting expression patterns in the proteomic dataset.
2837 Their analysis in this chapter provides both validation of proteomic findings and a
2838 proof-of-concept for applying spectral imaging flow cytometry to biomarker
2839 detection in sperm. This approach represents a key step toward developing
2840 clinically relevant tools for sperm selection in ART.

2841

2842 **5.3 Methods**

2843 **5.3.1 Biomarker candidate selection**

2844 Based on the 68 shortlisted candidate cell surface biomarkers identified in Chapter
2845 4, a refined selection of OLFM4, CTNG, and AOC3 was chosen for validation.
2846 Selection criteria included: (i) predicted surface availability to enable antibody
2847 access, (ii) statistical significance and consistent trends in the proteomic dataset,
2848 and (iii) the commercial availability of validated antibodies suitable for flow
2849 cytometry. Fluorophore-conjugated antibodies were selected where possible, and
2850 fluorophore choice together with panel design was optimised using the
2851 IntelliPanel™ tool available through FluoroFinder (FluoroFinder, Boulder, CO,
2852 USA).

2853

2854 **5.3.2 Biomarker titration and experimental design**

2855 Fluorophores were selected to minimise spectral overlap with the eFluor™ 520
2856 fixable viability dye (eBioscience, Invitrogen). As the surface abundance of the
2857 candidate markers had not been previously quantified, the brightest available
2858 fluorophore conjugates were chosen to maximise detection sensitivity. Due to time
2859 constraints, a fixation-based method was employed.

2860

2861 Antibody titration was performed for each candidate marker (OLFM4–PE, CTNG–
2862 mFluor Violet 450, AOC3–AF594) using both sperm samples and UltraComp
2863 eBeads (Thermo Fisher). Frozen sperm samples (T0/mid and T4/edge fractions;
2864 16×10^6 cells per fraction) were thawed, counted, and aliquoted at 1×10^6 cells
2865 in 100 μL of flow staining buffer per tube. For each antibody, three concentrations
2866 were tested (5 μL , 7.5 μL , 10 μL), in both T0 and T4 samples, with fully unstained
2867 and Fc-blocked controls included. Parallel bead controls were stained under
2868 identical conditions to assess non-specific binding.

2869

2870 Samples were incubated at room temperature for 30 min in the dark with gentle
2871 vortexing, washed in flow buffer, pelleted at 1,300 rpm for 5 min, and resuspended
2872 in 200 μL buffer for storage at 4 °C until acquisition. Titration outcomes were
2873 evaluated by assessing fluorescence intensity and background in both sperm and
2874 bead controls, with optimal antibody concentrations determined as those providing
2875 maximal signal-to-noise ratio without evidence of nonspecific staining.

2876

2877 **5.3.3 Sample collection and preparation**

2878 Samples were collected from five self-reported healthy donors at the University of
2879 East Anglia, UK, under ethics permit no. ETH2324-0997 and giving full consent.
2880 Following collection, samples were warmed to 37 °C and measurements of volume
2881 and pH were taken. Sperm concentration, motility and velocity parameters were
2882 assessed using Computer Assisted Sperm Analysis (CASA) with the motility
2883 module of Integrated Semen Analysis System (ISAS) v1 (Poiser, Spain), and the
2884 data was captured with an ISAS 782M camera connected to a UB203i microscope
2885 with a 10x phase contrast objective and a pre-heated stage. Preheated (37°C)
2886 disposable 75 mm x 25 mm glass chamber slides with 20-micron depth chambers
2887 (Cytonix, USA) were loaded with 2 μl of sample and at least 200 sperm were
2888 analysed from at least two fields for one second at 50 frames per second (f/s).
2889 Kinematics parameters recorded for each sample included: curvilinear velocity
2890 (VCL), straight-line velocity (VSL), average path velocity (VAP), linearity (LIN) =
2891 (VSL/ VCL)*100, straightness (STR) = (VSL/ VAP)*100, wobble (WOB) = (VAP/

2892 VCL)*100, amplitude of lateral head displacement (ALH) and beat cross frequency
2893 (BCF).

2894

2895 Samples were then aliquoted to approximately 1.5 million cells in 1 mL of human
2896 tubal fluid (HTF) medium. Aliquots were incubated for 4 hours at 37 °C with 5%
2897 CO₂ prior to antibody staining. Following incubation, sperm samples were
2898 reassessed for motility and cell number using CASA, then immediately stained
2899 with eFluor™ 520 fixable viability dye (eBioscience, Invitrogen) according to the
2900 manufacturer's protocol. After viability staining, cells were fixed in 4%
2901 paraformaldehyde (PFA) at 4 °C.

2902

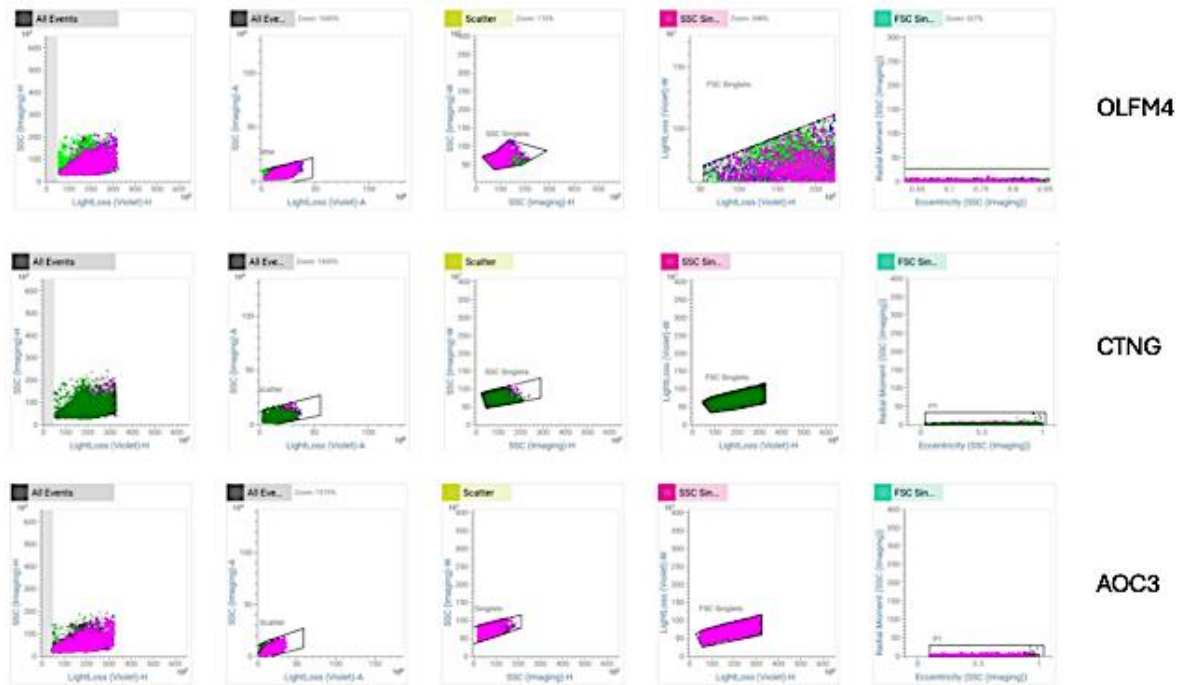
2903 Fixed cells were then blocked using Human Fc Receptor Blocking Solution
2904 (eBioscience, Invitrogen) to minimise non-specific antibody binding. Fluorophore-
2905 conjugated primary antibodies were subsequently added and incubated under
2906 standard conditions. The following antibodies were used: anti-OLFM4 clone 12,
2907 conjugated to R-phycoerythrin (PE), at a 1:10 dilution (Novus Biologicals, NBP3-
2908 06415PE); anti-CTNG (CTNG/2155R), conjugated to mFluor Violet 450 SE, at
2909 1:10 dilution (Novus Biologicals, NBP3-08485MFV450); and anti-AOC3
2910 (VAP1/AOC3 - TK8-14), conjugated to Alexa Fluor 594, at 1:10 dilution (Bio-
2911 Techne, NBP2-81043AF594.). Throughout staining, cells underwent minimal
2912 washing steps to preserve cell numbers and were stored overnight at 4 °C prior to
2913 flow cytometry analysis.

2914

2915 **5.3.4 Flow cytometry**

2916 Samples were analysed using the BD FACSDiscover™ S8 Cell Sorter (BD
2917 Biosciences), operated in fully spectral mode. No cell sorting was performed.
2918 Imaging and fluorescence data were acquired simultaneously for each sample with
2919 fixable viability dye (eFluor™ 520) detected using imaging laser B1 to allow for
2920 imaging. Events were gated to isolate the sperm population (P1), based on
2921 forward and side scatter properties (Figure 5-2). All subsequent data acquisition
2922 and analysis were restricted to this P1 population. For each antibody-stained

2923 sample, between 5,000 and 50,000 individual events within the P1 gate were
2924 recorded, depending on sample quality and cell availability.



2925
2926 Figure 5-1: Gating strategy used for imaging flow cytometry acquisition.
2927 Graphs generated using BD FACSChorus software illustrating the gating strategy
2928 used during sample acquisition on the BD FACSDiscovery S8 imaging flow
2929 cytometer. Gating was performed to identify a P1 population of single sperm cells
2930 based on forward and side scatter properties, and to exclude debris and
2931 aggregates. Gates were validated using the images generated on the S8.

2932

2933 **5.3.5 Data analysis and statistical modelling**

2934 Spectral unmixing was performed using BD FACSChorus™ software (BD
2935 Biosciences), based on single-stained controls (fluorescence minus one) for each
2936 fluorophore-conjugated antibody and the fixable viability dye. An unstained sperm
2937 sample was included in experiment set to control for cellular autofluorescence
2938 during unmixing. Compensation and unmixing matrices were applied prior to
2939 further analysis.

2940

2941 Flow cytometry image files were merged with the primary fluorescence data using
2942 BD CellView™ Image Extractor. The resulting datasets were processed in R

2943 v4.4.3 (R Core Team, 2017). Data were normalised using the CytoNorm package
2944 (Van Gassen et al., 2020), and quality control was performed using PeacoQC
2945 (Emmeneel et al., 2022) to identify and remove anomalous events. Gated and
2946 cleaned data were subsequently analysed in FlowJo v 10.10.0 (BD Life Sciences –
2947 FlowJo, LLC, Ashland, OR, USA. <https://www.flowjo.com>), with all events
2948 restricted to the P1 sperm population (see Figure 5-2 for gating strategy).

2949

2950 Statistical modelling of marker expression in live and dead cell populations was
2951 conducted in R v4.4.3 (R Core Team, 2017), with residual diagnostics simulated
2952 using the DHARMA package (Hartig et al., 2024) to evaluate model fit and
2953 distribution assumptions..

2954

2955 **5.4 Results**

2956 **5.4.1 OLFM4**

2957 The potential biomarker identified as both consistently and significantly reduced in
2958 higher fitness sperm, and likely to be expressed on the cell surface, was OLFM4.
2959 Five samples were stained with both eFluor 520 (fixable viability dye) and an anti-
2960 OLFM4 antibody conjugated to the fluorophore PE. During data acquisition,
2961 doublets and aggregates were excluded through gating, ensuring that only single-
2962 cell events within the P1 population were analysed (Figure 5-2).

2963

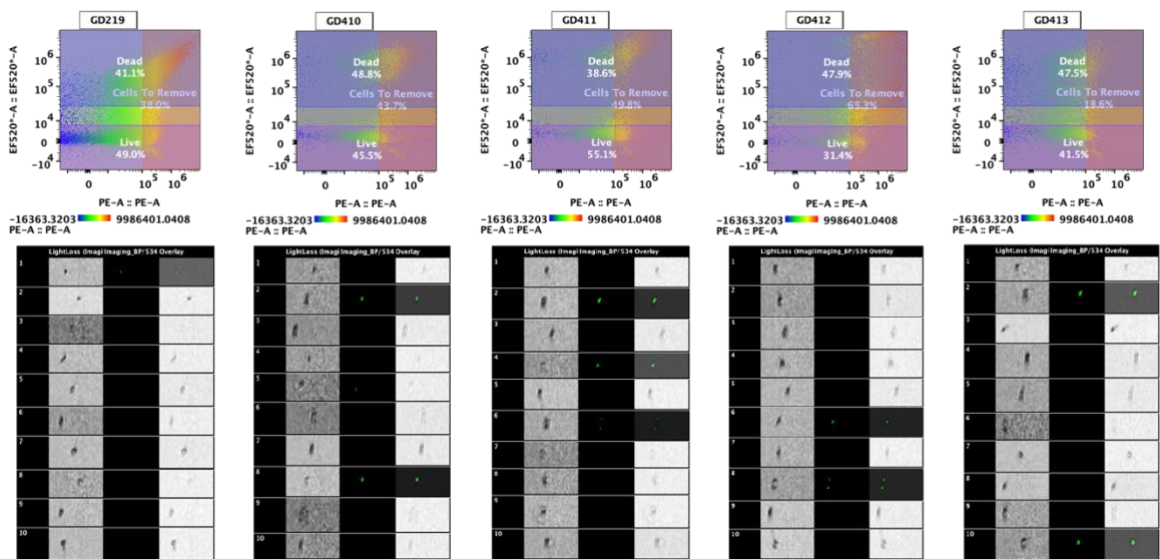
2964 Following data acquisition, gating was initially applied using one representative
2965 sample (GD219) to separate live and dead cells. The eFluor 520 signal enabled
2966 clear resolution between these populations. A distinct band of cells located
2967 between the live and dead gates was observed; these likely represent apoptotic
2968 cells at the time of fixation, exhibiting intermediate staining intensity.

2969

2970 To define OLFM4 marker positivity, a heatmap colour scale was applied to the
2971 OLFM4 signal, and a fluorescence intensity threshold of 10^5 was selected to
2972 distinguish OLFM4-positive cells. Cells with a fluorescence intensity above this

value were classified as OLFM4 positive (Figure 5-3). While this cut-off was not formally validated, it allowed for clear discrimination of marker-positive cells within the observed fluorescence range. Across all donors, approximately 40–50% of spermatozoa were classified as dead, with the remaining 30–55% viable at the time of analysis. OLFM4 staining was detected in both live and dead populations, though the proportion of positive cells varied between donors (Table 5-1). Percentages do not sum to 100% because a small proportion of events could not be confidently classified as live or dead due to ambiguous or low-intensity fluorescence signals and were therefore excluded from the summary. In most samples, 10–25% of dead sperm and 7–20% of live sperm were OLFM4-positive, with GD411 showing the highest proportion of live OLFM4+ cells (22.5%) and GD413 the lowest (6.6%).

2985



2986

2987 Figure 5-2: OLFM4 staining results across donors. Biexponential flow cytometry
2988 plots displaying OLFM4 staining on spermatozoa from each donor, with eFluor 520
2989 viability staining on the y-axis and OLFM4-PE fluorescence on the x-axis. Each
2990 plot represents a single donor sample. The first ten cell images from each sample,
2991 captured using the BD FACSDiscovery S8 imaging system, are shown below the
2992 corresponding plot to illustrate representative staining patterns and cell
2993 morphology. Gating was applied to distinguish live and dead sperm cells, and to
2994 assess OLFM4 surface expression under non-permeabilised conditions. Three
2995 gating populations, live cells, dead cells, and OLFM4-positive cells, were applied
2996 for all samples to support standardised comparison across donors.

2997 Table 5-1: Proportion of cells within live/dead gates and above the threshold of 10^5
 2998 (OLFM4 Positive). Flow-cytometry-derived cell counts and percentages for each
 2999 OLFM4-stained sample. “Total Dead” and “Total Live” correspond to events falling
 3000 within the viability gates; cells that fell between gates and could not be classified
 3001 were therefore excluded from the dataset. “Dead + Positive” and “Live + Positive”
 3002 represent the subsets within each viability gate that were OLFM4-positive.
 3003 Percentages are shown relative to P1 (all confirmed singlet sperm cells). “Total
 3004 cell count” reflects all recorded events within P1.

Sample	Total Dead	Total Dead (%P1)	Dead + Positive	Dead + Positive (%P1)	Total Live	Total Live (%) P1)	Live + Positive	Live + Positive (%P1)	Total cell count
OLFM4 GD219	1873	41.1	11124	24.4	2237	49	5211	11.4	4563
OLFM4 GD410	4881	48.8	2931	29.3	4548	45.5	1134	11.3	1000
OLFM4 GD411	3860	38.6	2434	24.3	5507	55.1	2253	22.5	1000
OLFM4 GD412	4794	47.9	4123	41.2	3139	31.4	1354	13.5	1000
OLFM4 GD413	4752	47.5	1064	10.6	4151	41.5	660	6.6	1000

3005
 3006 Across all five samples, the proportion of OLFM4-positive cells was significantly
 3007 higher in the dead population compared to the live population. This was tested
 3008 using a binomial generalised linear mixed model with the proportion of OLFM4-
 3009 positive cells as the response variable, live/dead status as a fixed effect, and
 3010 sample ID as a random intercept (Table 5-2 ; $z = -67.67$, estimate = -0.888 , $p <$
 3011 0.01). Model diagnostics performed using the DHARMA package (Hartig et al.,
 3012 2024) indicated no evidence of overdispersion, zero-inflation, or model
 3013 misspecification.

3014 Table 5-2: Results from a generalised linear mixed-effects model (GLMM)
3015 comparing OLFM4 expression on live versus dead sperm cells.

3016

Dependent variable: Marker Positive (Proportion)	
Intercept (Dead Cells)	-1.098
<i>z</i> = -5.033	<i>p</i> < 0.01
Live Cells vs Dead	-0.888
<i>z</i> = -67.674	<i>p</i> < 0.01
Observations	10
Log Likelihood	-549.810
Akaike Inf. Crit.	1,105.620
Bayesian Inf. Crit.	1,106.528
Note:	* <i>p</i> < 0.1; ** <i>p</i> < 0.05; *** <i>p</i> < 0.01

3017

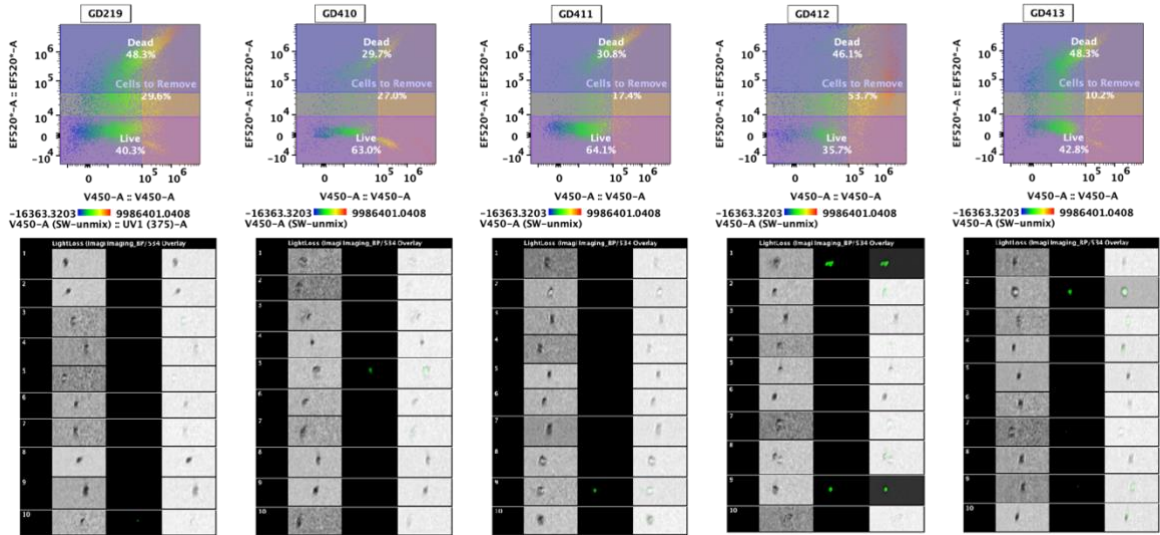
3018 These findings further support the proteomic results presented in Chapter 4, where
3019 OLFM4 was found to be significantly more abundant in lower-fitness sperm. Taken
3020 together, this strengthens the case for OLFM4 as a potential negative biomarker of
3021 sperm quality.

3022

3023 **5.4.2 CTNG**

3024 The second candidate biomarker selected for validation was CTNG. The same five
3025 donor samples were stained with eFluor™ 520 and an anti-CTNG antibody
3026 conjugated to mFluor Violet 450. Doublets and aggregates were similarly excluded
3027 during acquisition, and only single-cell events within the P1 sperm population were
3028 retained for analysis (Figure 5-4). Following the same method as was applied to
3029 the OLFM4 stained cells, gating to distinguish live and dead cells was initially
3030 defined using sample GD219 as a template with the eFluor 520 signal again
3031 providing clear separation. As with OLFM4, a distinct population of apoptotic cells
3032 was observed between the live and dead gates.

3033



3034

3035 Figure 5-3: CTNG staining results across donors. Biexponential flow cytometry
 3036 plots displaying CTNG staining on spermatozoa from each donor, with eFluor 520
 3037 viability staining on the y-axis and CTNG-V450 fluorescence on the x-axis. Each
 3038 plot represents a single donor sample. The first ten cell images from each sample,
 3039 captured using the BD FACSDiscovery S8 imaging system, are shown below the
 3040 corresponding plot to illustrate representative staining patterns and cell
 3041 morphology. Gating was applied to distinguish live and dead sperm cells, and to
 3042 assess CTNG surface expression under non-permeabilised conditions. Three
 3043 gating populations, live cells, dead cells, and CTNG-positive cells, were applied for
 3044 all samples to support standardised comparison across donors.

3045

3046 A fluorescence intensity threshold of 10^5 was selected for CTNG positivity, based
 3047 on visual inspection of the heatmap colour scale. Cells with intensities above this
 3048 value were classified as CTNG-positive (Figure 5-4). This threshold was not
 3049 formally validated but allowed for clear visual discrimination across the dataset.
 3050 Across donors, 30–50% of spermatozoa were non-viable at the time of staining,
 3051 with the remaining 35–65% classified as live (Table 5-3). CTNG staining was
 3052 predominantly detected in dead cells, with 6–38% of non-viable sperm positive for
 3053 CTNG across samples. In contrast, the live fraction generally exhibited very low
 3054 CTNG positivity (<5%), except for donor GD410, which displayed a notably higher
 3055 proportion of live CTNG+ sperm (13.4%). Overall, CTNG expression appeared
 3056 largely restricted to dead sperm populations.

3057

3058 Table 5-3: Proportion of cells within live/dead gates and above the threshold of 10^5
3059 (CTNG Positive). Flow-cytometry-derived cell counts and percentages for each
3060 CTNG-stained sample. “Total Dead” and “Total Live” correspond to events falling
3061 within the viability gates; cells that fell between gates and could not be classified
3062 were therefore excluded from the dataset. “Dead + Positive” and “Live + Positive”
3063 represent the subsets within each viability gate that were CTNG- positive.
3064 Percentages are shown relative to P1 (all confirmed singlet sperm cells). “Total
3065 cell count” reflects all recorded events within P1.

3066

Sample	Total Dead	Total Dead (%P1)	Dead + Positive	Dead + Positive (% P1)	Total Live	Total Live (%)	Live + Positive	Live + Positive (% P1)	Total cell count
CTNG GD219	12149	48.3	5858	23.3	10146	40.3	1111	4.41	25165
CTNG GD410	1703	29.7	704	12.3	3607	63	767	13.4	5729
CTNG GD411	3080	30.8	1441	14.4	6410	64.1	217	2.17	10000
CTNG GD412	4613	46.1	3815	38.1	3571	35.7	624	6.24	10000
CTNG GD413	4831	48.3	662	6.62	4282	42.8	254	2.54	10000

3067

3068 Across all five samples, the proportion of CTNG-positive cells was higher in the
3069 dead population compared to the live population, as assessed by a binomial
3070 generalised linear mixed model with live/dead status as a fixed effect and sample
3071 ID as a random intercept (Table 5-4; $z = -76.786$, estimate = -1.657 , $p < 0.01$). The

3072 effect was significant, with a $p < 0.001$. DHARMa diagnostic plots indicated a well-
3073 fitted model with no violations of model assumptions.

3074

3075 Table 5-4: Generalised linear model (GLMM) results comparing CTNG expression
3076 on live versus dead sperm cells.

3077

Dependent variable: Marker Positive (Proportion)	
Intercept (Dead Cells)	-1.505
$z = -5.339$	$p < 0.01$
Live Cells vs Dead	-1.657
$z = -76.786$	$p < 0.01$
Observations	10
Log Likelihood	-679.799
Akaike Inf. Crit.	1,365.598
Bayesian Inf. Crit.	1,366.505
Note:	$*p < 0.1$; $**p < 0.05$; $***p < 0.01$

3078

3079 These findings are also in line with the proteomic data from Chapter 4, where
3080 CTNG was more abundant in lower-fitness sperm. Therefore, CTNG can be
3081 considered a strong second candidate to act as a biomarker for lower sperm
3082 fitness within an ejaculate.

3083

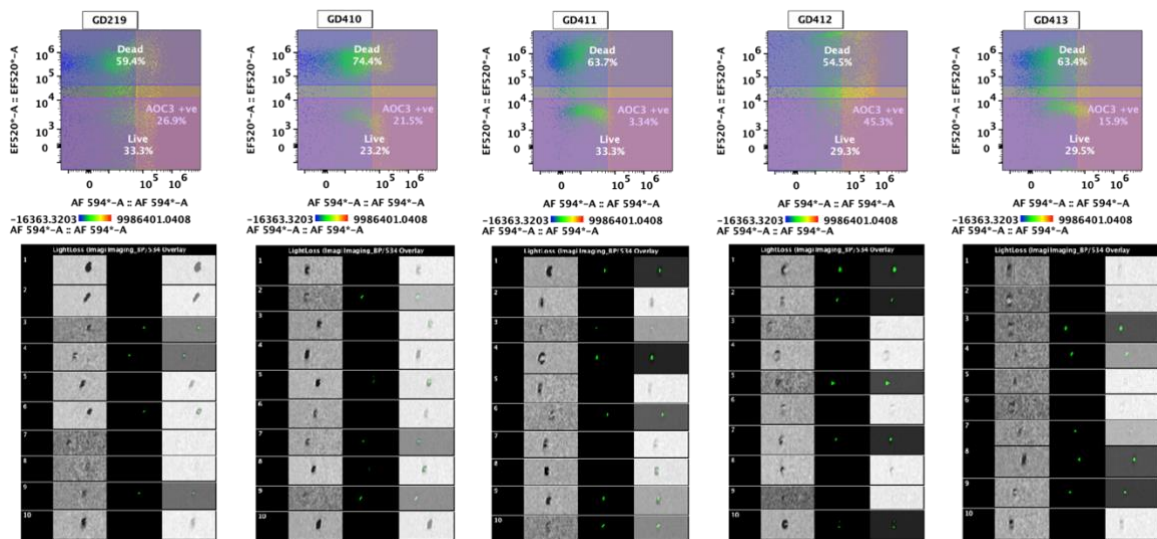
3084 **5.4.3 AOC3**

3085 The third candidate biomarker selected for validation was amine oxidase copper-
3086 containing 3 (AOC3), which was identified in Chapter 4 as being significantly more
3087 abundant in higher-fitness sperm and predicted to localise to the cell surface. This
3088 candidate was selected due to its potential to function with inverse action in
3089 selection compared to OLFM4 and CTNG. The same five donor samples were
3090 stained with eFluor™ 520 and an anti-AOC3 antibody conjugated to Alexa Fluor
3091 594 and gated for single-cell events within the P1 sperm population (Figure 5-2).
3092 Live and dead cells were gated using the same approach as described for OLFM4
3093 and CTNG, with eFluor 520 providing clear separation. A population of cells with
3094 intermediate staining was again observed and excluded from further analysis.

3095

3096 A fluorescence intensity threshold of around $10^{4.5}$ was selected based on visual
3097 inspection of the heatmap colour scale to distinguish AOC3-positive cells (Figure
3098 5-5). Across all donors, 55–75% of spermatozoa were non-viable, with 23–33%
3099 classified as live (Table 5-5). AOC3 staining was detected in both live and dead
3100 populations, though the proportion of positive cells varied between donors. Among
3101 dead sperm, AOC3 positivity ranged from 1–28%, whereas in live cells, 2–13%
3102 were AOC3-positive. Donor GD219 displayed the highest proportion of live AOC3+
3103 sperm (13%), while GD411 exhibited minimal staining in both live and dead
3104 fractions (<2%).

3105



3106

3107 Figure 5-4: AOC3 staining results across donors. Biexponential flow cytometry
3108 plots displaying AOC3 staining on spermatozoa from each donor, with eFluor 520
3109 viability staining on the y-axis and AOC3-AF594 fluorescence on the x-axis. Each
3110 plot represents a single donor sample. The first ten cell images from each sample,
3111 captured using the BD FACSDiscovery S8 imaging system, are shown below the
3112 corresponding plot to illustrate representative staining patterns and cell
3113 morphology. Gating was applied to distinguish live and dead sperm cells, and to
3114 assess AOC3 surface expression under non-permeabilised conditions.

3115

3116

3117

3118

3119

3120 Table 5-5: Proportion of cells within live/dead gates and above the threshold of 10^5
3121 (AOC3 Positive). Flow-cytometry-derived cell counts and percentages for each
3122 AOC3-stained sample. “Total Dead” and “Total Live” correspond to events falling
3123 within the viability gates; cells that fell between gates and could not be classified
3124 were therefore excluded from the dataset. “Dead + Positive” and “Live + Positive”
3125 represent the subsets within each viability gate that were AOC3-positive.
3126 Percentages are shown relative to P1 (all confirmed singlet sperm cells). “Total
3127 cell count” reflects all recorded events within P1.

3128

Sample	Total Dead	Total Dead (%P1)	Dead + Positive	Dead + Positiv e (% P1)	Total Live	Total Live (% P1)	Live + Positiv e	Live + Positive (% P1)	Total cells
AOC3 GD219	5944	59.4	1222	12.2	3334	33.3	1299	13	10000
AOC3 GD410	7442	74.4	1159	11.6	2322	23.2	947	9.47	10000
AOC3 GD411	6366	63.7	149	1.49	3326	33.3	176	1.76	10000
AOC3 GD412	5451	54.5	2780	27.8	2934	29.3	1120	11.2	10000
AOC3 GD413	6336	63.4	703	7.03	2953	29.5	820	8.2	10000

3129
3130 Whilst statistical modelling using a **binomial generalised linear mixed model**
3131 indicated a significant effect of live/dead status on AOC3 expression (Table 5-6; z
3132 $=-17.040$, $estimate = -0.364$, $p < 0.01$), with a higher proportion of AOC3-positive
3133 cells observed in the dead population, this trend was not consistent across all five
3134 samples. In some individuals, the proportion of AOC3-positive cells was nearly
3135 identical between live and dead populations, while in others the trend was
3136 opposite to that predicted based on the proteomic data from Chapter 4.

3137
3138
3139
3140
3141
3142
3143
3144

3145 Table 5-6: Results from a generalised linear mixed effects model (GLMM)
3146 comparing AOC3 expression on live versus dead sperm cells.

Dependent variable: Marker Positive (Proportion)	
Intercept (Dead Cells)	-2.248
$z = -5.505$	$p < 0.01$
Live Cells vs Dead	-0.364
$z = -17.040$	$p < 0.01$
Observations	10
Log Likelihood	-379.681
Akaike Inf. Crit.	765.363
Bayesian Inf. Crit.	766.270
Note:	$*p < 0.1$; $**p < 0.05$; $***p < 0.01$

3147

3148 These findings suggest that while AOC3 may exhibit differential expression in bulk
3149 proteomic datasets, its surface expression in individual sperm cells does not follow
3150 a consistent live/dead pattern. As such, AOC3 does not appear to be a reliable
3151 marker of sperm viability or quality in this context and may not be suitable for use
3152 as a single-cell biomarker.

3153

3154 **5.5 Discussion**

3155 One of the fundamental requirements for biomarker validation is the determination
3156 of cellular localisation. For all three markers tested here, the expected binding site
3157 for the antibodies was the sperm cell surface. The presence of these biomarkers
3158 on the cell surface was confirmed, as cells were not permeabilised prior to staining
3159 and the expected fluorescence signals were observed. This was further supported
3160 by the fluorescence minus one (FMO) controls, which were used to ensure the
3161 correct spectral unmixing had been applied and indicated that the detected signals
3162 were unlikely to result from non-specific binding. All three markers were also
3163 detected on both live and dead cells. This suggests that cell structure was well
3164 preserved following fixation, and that antibody binding was maintained across both
3165 populations. Together, these results support the conclusion that the staining
3166 patterns observed accurately reflect true marker localisation on the sperm surface.

3167

3168 Whilst the results for both OLFM4 and CTNG matched the expected surface
3169 binding patterns predicted by the proteomics data, the pattern observed for AOC3
3170 did not align with these predictions. The proteomics results for AOC3 had already
3171 indicated variability between donors, both in abundance trends between T0 and T4
3172 and in whether AOC3 was detectable at all. This suggests that AOC3 abundance,
3173 particularly at the cell surface, varies substantially among individuals. The
3174 biomarker validation results further support this, demonstrating high variability in
3175 AOC3 expression across the five donors tested. Such inconsistency indicates that
3176 AOC3 is not a suitable biomarker for sperm fitness assessment.

3177 In contrast, despite natural donor-to-donor variation, OLFM4 and CTNG showed
3178 consistent surface binding patterns across all donors. This stability supports their
3179 potential as reliable biomarkers of sperm fitness, as the expected biological
3180 variability among individuals did not disrupt the overall expression patterns of
3181 these markers.

3182
3183 Whilst this study represents an early-stage investigation, it provides an important
3184 step toward bridging the gap between descriptive sperm proteomics and functional
3185 sperm selection. Previous biomarker studies in reproductive biology have primarily
3186 sought to differentiate between fertile and infertile individuals (Amaral, Paiva, et
3187 al., 2014; Castillo et al., 2019), identifying proteins such as AKAP4, SEMG1, and
3188 HSPA2 as indicators of general sperm quality (Amaral, Paiva, et al., 2014).
3189 However, these approaches treat the ejaculate as a homogenous population. In
3190 contrast, the present work targets within-ejaculate variation, building on evidence
3191 that sperm populations exhibit functional heterogeneity even within a single
3192 sample (Alavioon et al., 2021; van Oosterhout et al., 2022). By identifying and
3193 validating biomarkers linked to sperm longevity and structural integrity, this study
3194 shifts focus from diagnostic classification toward the selective enrichment of viable
3195 sperm for assisted conception.

3196
3197 The potential applications of such biomarkers lie primarily in sperm selection for
3198 ART. Current ART procedures such as IVF and ICSI rely on relatively crude
3199 selection strategies, swim-up, density gradient centrifugation, or simple

3200 morphological assessment, that do not account for molecular indicators of sperm
3201 competence (Nixon et al., 2023). Biomarker-guided selection could theoretically
3202 enable the exclusion of sperm carrying DNA damage, oxidative stress markers, or
3203 defective membrane proteins before fertilisation occurs, thereby reducing
3204 miscarriage risk and improving embryo quality (van Oosterhout et al., 2022).
3205 However, these methods have not translated into routine clinical use due to
3206 variable specificity and technical demands. The present validation of OLFM4 and
3207 CTNG adds to this growing body of evidence suggesting that molecular-level
3208 selection is feasible when coupled to modern imaging and sorting technologies.
3209 However, the routine use of FACS or spectral flow cytometry in a clinical setting
3210 remains limited by cost, infrastructure, and the technical complexity of sample
3211 preparation and instrument operation. In addition, regulatory constraints around
3212 the manipulation of human gametes currently restrict the use of such techniques to
3213 research contexts rather than clinical fertilisation procedures.

3214

3215 In the longer term, the most viable translational pathway may involve adapting
3216 these validated biomarkers for use with non-cytometric selection platforms.
3217 Antibodies or ligands targeting surface markers such as OLFM4 or CTNG could be
3218 immobilised onto microfluidic filters, magnetic bead systems, or size-exclusion
3219 matrices to selectively capture or enrich viable sperm expressing the desired
3220 molecular profile. Alternative approaches using biotinylated antibodies and
3221 streptavidin-coated columns have already been demonstrated for cell-surface
3222 sample separation in other contexts such as separating metastatic tumour cells
3223 from other cancer cells (Karhemo et al., 2012), suggesting that similar principles
3224 could be applied to sperm. Such antibody-based filtration systems could bridge the
3225 gap between laboratory-scale validation and clinically deployable sperm selection
3226 tools, offering a practical route for translation into ART workflows.

3227

3228 Before clinical translation can be considered, several limitations must be
3229 addressed. Firstly, although OLFM4 and CTNG have been validated as sperm
3230 surface markers and consistent trends have been observed across two analytical
3231 platforms, the sample size remains limited to nine donors. Future studies involving

3232 a larger and more diverse donor population, including individuals with varied
3233 fertility outcomes, will be essential. Secondly, this study employed fixed sperm,
3234 which may potentially alter protein architecture; given that live sperm are required
3235 for fertilisation in ART, replication of these findings using live, non-fixed sperm is
3236 critical. Co-localisation studies would also be beneficial to determine the spatial
3237 distribution of these markers relative to each other and to key fertilisation proteins
3238 such as IZUMO1, to understand any potential for antibodies binding these markers
3239 to interfere with fertilisation. Finally, prior to clinical application, it would be
3240 necessary to assess both the fertilisation and developmental competence of
3241 sperm selected by these biomarkers, to ensure no detrimental effects and to verify
3242 whether "higher fitness" sperm confer tangible benefits to offspring health.

3243

3244 Another limitation on the validation of the candidate biomarkers identified in
3245 Chapter 4 was the availability of antibodies to the identified proteins. As flow
3246 cytometry has traditionally been applied primarily to immunological research, non-
3247 immunologically relevant antibodies are less common. Whilst it is possible to
3248 create new antibodies if there is a lack of commercially available options, the time
3249 and expense required to both produce these and validate that they are binding the
3250 intended target often renders this approach impractical. In future, recombinant
3251 antibody libraries and phage-display technologies may offer a route to rapidly
3252 generate high-specificity reagents for sperm surface proteins. Integration of
3253 antibody-based sorting with microfluidic sperm handling devices may also provide
3254 a clinically scalable path forward, allowing for biomarker-based enrichment without
3255 high-speed sorting of live gametes.

3256

3257 In conclusion, this study validates OLFM4 and CTNG as sperm surface
3258 biomarkers that are enriched in sperm cells failing to survive longevity selection,
3259 as initially predicted by TMT mass spectrometry. In contrast, AOC3 was found to
3260 be an unsuitable biomarker due to its inconsistency across donors and with
3261 proteomics predictions. These findings provide a promising foundation for the
3262 development of novel sperm selection strategies in ART; however, substantial
3263 further research is required before clinical implementation can be realised.

3264 **6 General Discussion**

3265 Sexual reproduction is widespread yet inefficient because it halves genetic
3266 contribution per parent, requires costly mate search and mating behaviours, and
3267 entails the production and maintenance of specialised gametes and reproductive
3268 tissues (Gibson et al., 2017; Lively & Morran, 2014). A defining feature of many
3269 sexually reproducing eukaryotes is a brief haploid phase embedded within an
3270 otherwise diploid life cycle, creating the potential for selection to act directly on
3271 phenotypes expressed by haploid genotypes before fertilisation (Immler, 2019;
3272 Mable & Otto, 1998). This process, termed haploid selection, was long considered
3273 minor in animals because gametes were thought to be largely transcriptionally
3274 silent (Joseph & Kirkpatrick, 2004), gene products were believed to be equalised
3275 through intercellular bridges (Dym & Fawcett, 1971; Greenbaum et al., 2011;
3276 Weber & Russell, 1987), and in some taxa fertilisation can occur even with
3277 anucleate sperm (Lindsley & Grell, 1969), all of which were thought to limit haploid
3278 individuality and opportunity for selection (Caldwell & Handel, 1991; Joseph &
3279 Kirkpatrick, 2004).

3280

3281 Recent work has challenged this view by demonstrating post-meiotic gene
3282 expression and incomplete sharing among spermatids, measurable genotype–
3283 phenotype associations within ejaculates, and offspring consequences of selecting
3284 specific sperm phenotypes, establishing haploid selection as a plausible and
3285 consequential evolutionary force (Alavioon et al., 2017, 2019; Bhutani et al., 2021).
3286 In humans, within-ejaculate genomic shifts consistent with haploid selection have
3287 been reported (Marcu et al., 2024), directly precipitating the questions addressed
3288 in this thesis. Building on these findings, recent reviews argue that recognising
3289 haploid-stage filtering has implications for both evolutionary theory and clinical
3290 practice, including assisted reproductive technologies (ART) (Alavioon et al., 2021;
3291 van Oosterhout et al., 2022).

3292

3293 Against this backdrop, the overarching goal of the thesis was to discover sperm
3294 biomarkers with clinical potential to separate higher-fitness from lower-fitness cells

3295 within an ejaculate using approaches that are realistic for translation into ART
3296 workflows. This goal was developed into four connected research aims:

3297

3298 Aim 1. Determine how dynamically the testicular proteome responds to a defined
3299 selective pressure via environmental variation, and whether such perturbations
3300 leave molecular “legacy” signatures with potential functional relevance for sperm
3301 production. Motivated by prior evidence that environmental challenges can have
3302 lasting effects on sperm and offspring (Irish et al., 2024), I used prolonged mild
3303 thermal stress in zebrafish to quantify pathway-level proteome remodelling in
3304 testes (Chapter 2).

3305

3306 Aim 2. Assess whether comparable proteomic signatures are detectable in mature
3307 sperm produced by the same testes analysed in Aim 1. Due to technical
3308 constraints that precluded statistically significant comparison of heat-treated and
3309 control sperm proteomes, this aim was reframed to generate a high-coverage
3310 global sperm proteome as a cross-species reference and as a molecular baseline
3311 for subsequent within-ejaculate work in humans (Chapter 3).

3312

3313 Aim 3. Test whether established functional selection methods that enrich for
3314 higher-quality human sperm, namely swim-up and methyl-cellulose migration,
3315 produce measurable proteomic differences among sperm from the same ejaculate
3316 (Chapter 4), and evaluate whether any of these differences include surface-
3317 exposed molecules that could serve as candidate biomarkers of sperm fitness
3318 (Marcu et al., 2024).

3319

3320 Aim 4. Validate shortlisted biomarkers of sperm quality at single-cell resolution and
3321 assess translational feasibility (Chapter 5). Spectral imaging flow cytometry on
3322 non-permeabilised human sperm, with fluorescence minus one controls and
3323 viability gating, was used to confirm surface localisation and accessibility of
3324 candidate biomarkers and to test whether marker intensity reflects sperm longevity
3325 and survival.

3326 **6.1 Evidence of the Effect of Environmental Stress on**
3327 **Sperm Production**

3328 In Chapter 2, tandem mass tag (TMT) proteomics was used to profile zebrafish
3329 (*Danio rerio*) testes following prolonged mild heat exposure and identified 5,415
3330 proteins. Of these, 377 were significantly differentially abundant between heat-
3331 treated and control groups, with 133 increased and 244 decreased in heat-
3332 stressed testes. Enrichment analyses highlighted depletion of cilium movement,
3333 axonemal dynein complex, microtubule-based process, motile cilium, and
3334 oxidative phosphorylation, alongside increased abundance of proteostasis factors
3335 including HSP70 family proteins and SERPINH1/HSP47. A gamma generalised
3336 linear model showed that shifts in testis mass during exposure were not explained
3337 by body mass alone, indicating intrinsic germline responses rather than general
3338 condition effects. Together, these patterns provide protein-level evidence for
3339 reduced spermatogenesis with a concurrent shift toward cellular protection and
3340 repair.

3341

3342 Thermal stress is a pervasive disruptor of male reproduction in ectotherms, and
3343 comparable tissue-level outcomes are reported across teleosts. In medaka
3344 (*Oryzias latipes*), elevated temperature increases TUNEL-positive germ cells, and
3345 elevates HSP70 and HSP90, consistent with apoptosis and proteotoxic stress
3346 (Furukawa et al., 2019). In tilapia (*Oreochromis niloticus*), heat reduces
3347 spermatogonial proliferation and contracts elongating spermatid pools, with
3348 mitochondrial dysfunction and unfolded-protein-response activation that mirror the
3349 proteostasis and energy-metabolism shifts observed here (Alvarenga & França,
3350 2009; Jin et al., 2019). In salmonids including *Salmo salar* and *Salmo trutta*, warm-
3351 water anomalies impair spermatogenesis, lower milt quality, and reduce sperm
3352 motility in parallel with altered antioxidant enzymes and ATP metabolism in testes
3353 and sperm (Lahnsteiner, 2012; Pankhurst & Munday, 2011). The depletion of
3354 dyneins, radial-spoke and intraflagellar-transport components together with
3355 increased chaperones observed in Chapter 2 matches these histological and
3356 functional outcomes, indicating that temperature primarily targets the flagellar

3357 biogenesis toolkit and energy homeostasis needed to produce competent, motile
3358 sperm.

3359

3360 Mechanistically, convergent pathways recur across models. Proteotoxic stress
3361 activates HSF1-driven chaperone induction that stabilises misfolded proteins;
3362 mitochondrial dysfunction elevates reactive oxygen species and compromises
3363 ATP supply, membranes and DNA; and microtubule-based assembly defects
3364 impair manchette dynamics and axoneme formation essential for spermiogenesis
3365 (Boni, 2019; Houston et al., 2018; Robinson et al., 2023; Widlak & Vydra, 2017).
3366 The enriched and depleted proteins reported in Chapter 2 map onto this triad,
3367 indicating a coordinated pause in spermatid maturation with activation of protective
3368 programs. Environmentally induced “legacy” signatures can persist into mature
3369 sperm, including altered protein cargo and small RNAs with effects on early
3370 development, which provides a plausible conduit from testis stress to embryo-level
3371 consequences and frames testis-proteome plasticity as an upstream driver of
3372 within-ejaculate sperm (Godden et al., 2025).

3373

3374 Morphological responses in tissue structure and size are often subtle early and
3375 become pronounced with sustained stress across taxa. In the red flour beetle
3376 (*Tribolium castaneum*), testis mass modelled against body mass shows that sub-
3377 lethal chronic warming produces a treatment-specific reduction in testis volume
3378 independent of somatic growth, consistent with an intrinsic testicular response
3379 trajectory under heat stress (Cole et al., 2025). Comparable heat sensitivity is
3380 evident in parasitoid wasps such as *Nasonia vitripennis*, where elevated
3381 developmental temperature reduces testis size and sperm reserves with
3382 downstream losses in male fertility (Nguyen et al., 2013), and in fruit flies
3383 (*Drosophila melanogaster*), where sustained heat induces testicular atrophy,
3384 meiotic arrest, and depletion of elongating spermatids before whole-body condition
3385 declines (David et al., 2005; Rohmer et al., 2004). Taken together, these data
3386 support interpreting the present combination of modest mass change and strong
3387 proteomic reprogramming as an early or partially reversible phase in which
3388 functional disruption precedes gross anatomical change.

3389 These results support three broad conclusions. The zebrafish testis proteome is
3390 highly dynamic under heat, shifting coordinated functional enrichment rather than
3391 isolated proteins. Biologically meaningful disruption of spermatogenesis can occur
3392 without large organ-size changes, implying that proteome-level readouts capture
3393 earlier phases of dysfunction. Selective depletion of axonemal and ciliary
3394 components provides a plausible molecular mechanism for the reduced
3395 spermatogenic output observed in heat-stressed testes.

3396

3397 Future work should resolve these responses by cell type and time: histology and
3398 immunostaining to localise stage-specific arrests; sorting enriched germ-cell
3399 fractions for targeted proteomics or single-cell transcriptomics; and time-course
3400 and recovery designs to discriminate reversible programs from irreversible loss.
3401 Coupling testis proteomics directly to CASA-based motility, ATP measurements,
3402 and fertilisation assays for the testes measured would link environment to tissue
3403 and gamete function, while ecologically realistic warming and heatwave regimes
3404 would connect laboratory findings to climate-related risk in wild and cultured fish
3405 populations.

3406

3407 **6.2 Evidence of Phenotypic Variation Between** 3408 **Ejaculates**

3409 In Chapter 3, a high-depth zebrafish sperm proteome was generated. Across three
3410 pooled sperm samples from independent male groups, 5,410 proteins were
3411 confidently identified and 4,168 were quantified using TMT-multiplexed nanoLC–
3412 Orbitrap MS/MS. This represents one of the most complete teleost sperm
3413 proteomes to date and provides a baseline catalogue for functional and
3414 comparative studies of male fertility.

3415

3416 Depth and cross-species context support the completeness of this dataset. The
3417 zebrafish catalogue corresponds to roughly twenty percent of predicted protein-
3418 coding genes in the GRCz11 reference, which is unusually broad for a mature
3419 haploid cell type. Published sperm proteomes in other species are typically

3420 smaller, for example about 2,850 proteins in epididymal sperm from house mouse
3421 (*Mus musculus*) using earlier discovery pipelines (Baker, Hetherington, Reeves, &
3422 Aitken, 2008), 348 in common carp (*Cyprinus carpio*) with 2D-gel workflows
3423 (Dietrich et al., 2014), and 744 in koala (*Phascolarctos cinereus*) from limited
3424 material (Skerrett-Byrne et al., 2021). Several factors likely explain the larger
3425 catalogue here, including higher input and pooling per TMT channel, modern
3426 Orbitrap acquisition, and well-curated zebrafish databases that improve peptide-to-
3427 protein assignment.

3428

3429 The functional composition aligns with known sperm biology. Network analysis of
3430 the most abundant proteins highlighted multiple histone variants together with
3431 chromatin-associated factors, consistent with histone retention and lack of
3432 protamine usage in zebrafish sperm chromatin organisation (González-Rojo et al.,
3433 2018b). Cellular-component enrichment showed strong mitochondrial signals and
3434 abundant axonemal and dynein components, matching the energetic and
3435 structural demands of motility in teleost sperm and the reliance on oxidative
3436 phosphorylation and glycolysis to power the flagellum (Inaba, 2011). Biological-
3437 process terms such as organelle organisation, cellular component localisation, and
3438 protein localisation suggest that mature ejaculated sperm retain a subset of late
3439 spermatogenic and maturation proteins, a pattern also reported in human and
3440 livestock datasets that differentiate fertile from subfertile males and high- from low-
3441 motility samples (Amaral, Paiva, et al., 2014; D'Amours et al., 2019b; Guo et al.,
3442 2019; Selvam et al., 2019).

3443

3444 With respect to between-ejaculate differences, the present design maximised
3445 proteome depth by analysing pooled material, which strengthens coverage but
3446 limits direct inference on inter-male variance because dispersion cannot be
3447 estimated per individual. Nevertheless, the magnitude of variation observed in the
3448 zebrafish sperm proteome, together with literature showing substantial variation
3449 among males in motility, morphology, metabolism, and fertilisation outcomes,
3450 indicate that ejaculate-level proteomic differences are likely to be biologically

3451 meaningful and potentially predictive of fertility phenotypes across individuals and
3452 species (Amaral, Castillo, et al., 2014; Cannarella et al., 2020).

3453

3454 Future work should retain depth while restoring individual resolution. Practical
3455 options remain limited with current technology however, designs that sample pre-
3456 and post-exposure within the same male will help control baseline differences, and
3457 gentle, detergent-free processing can preserve surface proteins relevant to
3458 selection and downstream biomarker discovery for ART translation.

3459

3460 **6.3 Evidence of Within-Ejaculate Sperm Variation**

3461 In Chapter 4, selected sperm pools from human ejaculates were fractionated to
3462 test whether functional heterogeneity among sperm from the same male is
3463 reflected in molecular differences. Two complementary assays were used: a
3464 methyl-cellulose migration assay that enriches for sperm capable of sustained
3465 progression through a viscous medium, and a swim-up that enriches for
3466 progressively motile, longer-lived sperm. Tandem mass tag (TMT) proteomics
3467 across five donors identified 4,616 proteins, of which 1,178 showed consistent
3468 differential abundance between selected and unselected fractions within each
3469 assay. Gene ontology analyses converged on the same broad picture across all
3470 donors and assays: selected sperm pools were enriched for axonemal, dynein and
3471 mitochondrial enrichments and for process terms related to cilium movement,
3472 sperm motility and membrane lipid remodelling, whereas unselected sperm pools
3473 were enriched for protein folding, RNA splicing and spliceosomal components,
3474 consistent with incomplete spermiogenesis and a stress-response state. At the
3475 single-protein level, OLFM4 was consistently lower in selected sperm across
3476 donors, whereas several adhesion and stress-signalling proteins were higher in
3477 unselected fractions.

3478

3479 These patterns align with extensive functional evidence that sperm from a single
3480 male are not equivalent and that subtle performance differences bias fertilisation.
3481 In externally fertilising Atlantic salmon (*Salmo salar*), within-ejaculate variation in

3482 velocity predicts competitive fertilisation success and drives differences in embryo
3483 development and size (Gage et al., 2004). In domestic fowl (*Gallus gallus*
3484 *domesticus*), a simple sperm mobility assay predicts both competitive and non-
3485 competitive fertility, linking progressive motility to paternity outcomes (Froman et
3486 al., 2002). In mice, variation in morphology and kinematics among sperm from the
3487 same male influences the probability of reaching the oocyte in vivo (Firman &
3488 Simmons, 2010). Together with zebrafish experiments showing that selecting
3489 long-lived sperm within an ejaculate improves embryo viability and adult
3490 reproductive performance (Alavioon et al., 2017, 2019), these data indicate that
3491 performance-based enrichment maps onto fitness-relevant outcomes across taxa.

3492
3493 To assess the technical repeatability of the TMT proteomics workflow, one human
3494 sperm sample analysed in TMT Set 2 was re-run independently in TMT Set 3.
3495 Comparison of protein identifications between experiments showed extremely high
3496 concordance: 7,414 proteins were shared between the 7,498 proteins detected in
3497 Set 2 and the 7,486 proteins detected in Set 3, corresponding to 98.9% and 99.0%
3498 overlap respectively. This level of agreement is consistent with published
3499 estimates of Orbitrap–TMT technical repeatability, in which replicate injections or
3500 repeated multiplexed analyses typically show >90–95% overlap in identified
3501 proteins and tightly correlated reporter-ion intensities (Casey et al., 2017). These
3502 results confirm that the depth and composition of the human sperm proteome
3503 reported here are not artefacts of run-to-run variation but reflect a stable molecular
3504 profile of mature human sperm.

3505
3506 The proteomic signatures observed here are also consistent with comparative
3507 sperm proteomics in humans and livestock. Studies differentiating fertile from
3508 subfertile men, or high- from low-motility ejaculates, repeatedly report higher
3509 abundance of axonemal motors, radial-spoke proteins and energy-metabolism
3510 enzymes in better-performing samples, together with increased chaperones and
3511 RNA-processing machinery in poorer samples (Amaral, Castillo, et al., 2014). In
3512 boar (*Sus scrofa*), high-fertility ejaculates show enrichment of glycolytic and
3513 mitochondrial proteins that support sustained flagellar beating, whereas low-fertility
3514 samples are enriched for proteins associated with stress responses and defective

3515 maturation (Noguchi et al., 2015). In cattle (*Bos taurus*), quantitative proteomics
3516 links sperm freezability and field fertility to dynein heavy chains, outer-dense fibre
3517 proteins and oxidative phosphorylation, again tying energetic and axonemal
3518 capacity to functional competence (D'Amours et al., 2019). The same proteomic
3519 signatures emerge in the selected human fractions here, suggesting that the
3520 molecular correlates of “better” sperm are conserved.

3521

3522 The methyl-cellulose assay adds a useful dimension by mimicking viscous
3523 microenvironments. Traversing viscous media requires specific membrane
3524 biophysical properties and metabolic tuning, including lipid-domain remodelling,
3525 cholesterol efflux and efficient ATP supply, which are reflected in the enrichment of
3526 lipid-handling and catalytic-regulation terms in the methyl-cellulose–selected
3527 fractions (Suarez & Pacey, 2006). By contrast, swim-up exerts a simpler kinematic
3528 filter, and the dominant enrichments for sperm motility and cilium movement in
3529 swim-up–selected fractions match this expectation (Magdanz et al., 2019). The
3530 convergence across assays on mitochondrial and axonemal enrichment, despite
3531 their different mechanical challenges, strengthens the inference that core motility
3532 and energy pathways underpin within-ejaculate performance differences.

3533

3534 Markers of immaturity were a consistent feature of unselected fractions.
3535 Enrichment for RNA splicing, spliceosomal components and protein folding points
3536 to persistence of earlier spermatogenic machinery, which is frequently observed in
3537 asthenozoospermic ejaculates and in ejaculates with retained cytoplasmic droplets
3538 and defective chromatin condensation (Amaral et al., 2014; Saraswat et al., 2017).
3539 Cellular-component and molecular-function terms such as focal adhesion, collagen
3540 binding and cell–substrate junction suggest a propensity for inappropriate
3541 adhesion or agglutination that can impede progressive movement, a phenomenon
3542 reported in subfertile human samples and linked to altered surface composition
3543 and antisperm factors (Barratt et al., 2011). Against this backdrop, the consistently
3544 lower abundance of OLFM4 in selected fractions is notable. OLFM4 is a
3545 glycoprotein implicated in cell–cell interactions and immune modulation in
3546 neutrophils and epithelia; elevated levels in unselected fractions may reflect a

3547 stress-response or adhesive state that is incompatible with sustained motility and
3548 longevity, making OLFM4 a plausible negative marker of functional competence
3549 pending direct functional tests.

3550

3551 The broader literature on sperm selection technologies helps situate these
3552 findings. Classical enrichment by swim-up or density gradients improves motility
3553 and reduces debris but does not reliably remove sperm with DNA damage or
3554 epigenetic defects, and clinical gains are inconsistent (Said & Land, 2011).
3555 Microfluidic devices and viscous-media filters can reduce DNA fragmentation and
3556 oxidative damage and improve blastocyst quality in some studies, but outcomes
3557 vary and standardisation is limited (Beckham et al., 2018; Doostabadi et al., 2022).
3558 Ligand-based approaches such as zona-pellucida binding or annexin-V magnetic
3559 sorting enrich for sperm with lower DNA fragmentation and better morphology,
3560 again with mixed translation to live-birth rates (Huszar et al., 2007). The present
3561 proteomic contrasts provide a molecular rationale for why some modalities
3562 succeed in specific contexts and argue for combining physical selection with
3563 molecular readouts to target genuinely “functional” sperm.

3564

3565 The data presented in Chapter 4 therefore does two things. Firstly, provide
3566 molecular evidence that subpopulations within a single human ejaculate differ in
3567 ways that map onto fitness-relevant traits such as motility, longevity and
3568 membrane competence. Secondly, they deliver a shortlist of surface-accessible
3569 candidates, including OLFM4 and CTNG, that can be developed into non-
3570 destructive enrichment tools more compatible with clinical workflows than high-
3571 speed sorting. The immediate next steps are to increase cohort size, obtain paired
3572 methyl-cellulose and swim-up fractions from the same ejaculate to partition assay-
3573 specific from donor-specific effects, and couple TMT depth to functional readouts
3574 such as CASA kinematics, oxidative status, DNA integrity and time-to-blastocyst in
3575 appropriate model systems. Ultimately, integrating performance-based selection
3576 with biomarker-guided capture will allow tests of whether enriching for specific
3577 molecular states translates into higher embryo viability and live-birth rates, the key
3578 clinical end points.

3579

3580 **6.4 Validation of Biomarkers of Sperm Fitness**

3581 In Chapter 5, imaging spectral flow cytometry was used to validate three surface
3582 candidate sperm quality biomarkers from Chapter 4, namely OLFM4, CTNG/JUP
3583 and AOC3, on non-permeabilised human sperm. Five donor ejaculates were
3584 incubated for selection on longevity, stained with a fixable viability dye (eFluor
3585 520), and probed in separate panels with fluorophore-conjugated antibodies
3586 (OLFM4-PE, CTNG-mFluor Violet 450, AOC3-Alexa Fluor 594). Data were
3587 acquired on the BD FACSDiscover S8 in fully spectral mode with simultaneous
3588 bright field imaging. Spectral unmixing used single-stained and fluorescence-
3589 minus-one controls, gates isolated single sperm (P1), and viability gates separated
3590 live and dead cells. At single cell resolution, OLFM4 and CTNG signals localised
3591 to the sperm surface and were consistently higher in the short-lived fraction across
3592 donors, whereas AOC3 showed marked inter-individual variability and no
3593 consistent association with longevity. Binomial generalised linear mixed models
3594 confirmed the enrichment of OLFM4-positive and CTNG-positive events among
3595 dead relative to live cells. Together these results verify surface availability for
3596 OLFM4 and CTNG, link their abundance to within-ejaculate fitness proxies, and
3597 indicate that AOC3 is unsuitable as a robust marker in this context.

3598

3599 Discovery proteomics can nominate dozens of putative sperm markers, but clinical
3600 or evolutionary relevance hinges on three questions: is the epitope truly on the cell
3601 surface in intact sperm, does its single-cell distribution track functional
3602 heterogeneity within an ejaculate, and is the pattern reproducible across men.
3603 Imaging spectral flow cytometry addresses exactly this translation gap by
3604 quantifying marker localisation and intensity in tens of thousands of individual,
3605 non-permeabilised sperm while simultaneously recording morphology and viability,
3606 thereby converting bulk trends into cell-resolved evidence that can be coupled to
3607 performance phenotypes such as longevity or motility (Cannarella et al., 2020;
3608 Intasqui et al., 2018).

3609

3610 Viewed against established sperm surface biology, the two validated candidates
3611 here, OLFM4 and CTNG/JUP, fall into a class of markers that appear enriched on
3612 short-lived, low-fitness cells and thus operate as negative selection cues rather
3613 than positive tags for elite sperm. That logic mirrors prior work where surface
3614 composition predicts function: for example, the IZUMO1–JUNO pair is essential for
3615 gamete fusion and quantitative or spatial differences in IZUMO1 bear on
3616 fertilisation competence (Bianchi et al., 2014) and the mucin-like glycoprotein
3617 DEFB126 facilitates passage through cervical mucus, where common human
3618 deletions reduce paternity odds despite normal semen parameters (Tollner et al.,
3619 2011). Beyond proteins, deficits in PLC ζ , the sperm oocyte-activation factor, are
3620 linked to fertilisation failure in both human and mouse, underscoring how single
3621 molecules can set a hard ceiling on embryo development even when motility is
3622 adequate (Kashir, 2020). In that landscape, the association of OLFM4 with cell–cell
3623 interactions and inflammatory signalling, and the role of CTNG/JUP in junctional
3624 architecture, make their enrichment on short-lived cells biologically plausible as
3625 indicators of stress-biased or adhesion-prone surface states that are incompatible
3626 with sustained progression through the female tract.

3627

3628 Methodologically, imaging flow confers specific advantages for sperm. It permits
3629 visual verification of gating and dye localisation in a cell type with unusual size,
3630 shape and intrinsic autofluorescence, and it quantifies heterogeneous, non-
3631 Gaussian marker distributions that bulk assays average away. Using non-
3632 permeabilised cells ensures that signals correspond to surface-available epitopes,
3633 a prerequisite for downstream affinity capture or depletion in workflows that are
3634 more compatible with IVF/ICSI than high-speed sorting of live gametes (Intasqui et
3635 al., 2018).

3636

3637 Important caveats remain. Fixation can alter epitope accessibility for a subset of
3638 targets; sample size was modest; and associations were made to longevity rather
3639 than to fertilisation and embryo development. The immediate path forward is clear:
3640 extend to live, non-fixed preparations using gentle antibody formats, increase
3641 donor numbers, pair pre-enrichment modalities within the same ejaculate to test

3642 assay-specific robustness, and couple staining with orthogonal functional readouts
3643 in the same cells, such as DNA-integrity assays, mitochondrial potential and
3644 capacitation markers, before moving to embryo-level endpoints in suitable animal
3645 models or prospective clinical cohorts (Codina et al., 2015; McShane et al., 2013).
3646 If these steps confirm consistency, OLFM4 and CTNG/JUP are well positioned as
3647 depletion targets for immuno-microfluidic filters or bead-based capture to remove
3648 low-fitness sperm, complementing existing motility-based selection and addressing
3649 a long-standing gap between “moving” and “functionally competent” sperm.

3650

3651 **6.5 Molecular evidence supporting haploid selection**

3652 A central aim of this thesis was to test whether molecular heterogeneity among
3653 sperm within a single ejaculate provides a substrate for selection acting at the
3654 haploid stage. The human proteomics data showed reproducible differences
3655 between selected (higher longevity and motility) and unselected subpopulations
3656 across donors. Selected sperm were enriched for proteins and pathways
3657 consistent with superior performance, including enrichments linked to axonemal
3658 function, energy metabolism, and oxidative stress resilience, whereas unselected
3659 sperm showed signatures of incomplete maturation, RNA processing, and
3660 inappropriate adhesion. These patterns are consistent with selection acting on
3661 phenotypes expressed during the haploid phase rather than a homogeneous
3662 output of the diploid male genotype (Immler, 2019; Sutter & Immler, 2020).

3663

3664 Single-cell validation with spectral imaging flow cytometry confirmed cell surface
3665 localisation and within-ejaculate trends for two candidates. OLFM4 and CTNG
3666 were consistently more abundant on short-lived, low-quality sperm and reduced on
3667 long-lived, higher-quality cells, aligning with the discovery proteomes. These
3668 findings confirm that at least some quality-linked molecular features are externally
3669 accessible on intact sperm and measurable at single-cell resolution, which is a
3670 prerequisite for functional selection or clinical screening.

3671

3672 Direct one-to-one correspondence between proteomic and genomic signals is not
3673 expected, because proteins integrate post-meiotic gene regulation, selective
3674 protein retention, and epigenetic programming. Nevertheless, the overall picture
3675 aligns with emerging genomic and transcriptomic evidence for allele-biased
3676 expression and genotype–phenotype coupling among haploid sperm within a
3677 male, supporting the biological plausibility of haploid selection in animals (Bhutani
3678 et al., 2021; Marcu et al., 2024).

3679

3680 Taken together, these findings indicate that sperm are not biologically equivalent.
3681 Functionally relevant molecular variation exists within ejaculates, can be detected
3682 on the cell surface, and tracks phenotypes that matter for fertilisation potential.
3683 This supports a model in which selection can act among haploid gametes prior to
3684 fusion and provides a molecular basis for future causal tests in models where
3685 embryo and offspring outcomes can be measured (Alavioon et al., 2017, 2019).

3686

3687 **6.6 Cross-species translation and model choice**

3688 Direct experimental tests of whether specific sperm produce healthier embryos or
3689 offspring cannot be performed in humans for ethical and legal reasons, which
3690 makes model organisms essential for connecting sperm phenotype to
3691 developmental outcomes (Hoo et al., 2016; Meyers, 2018). Zebrafish is an
3692 effective discovery platform because external fertilisation, high fecundity, and
3693 optical access to embryos allow controlled selection regimes and prospective tests
3694 of viability that are not possible in humans. Extensive genomic resources,
3695 transgenesis, CRISPR, and single-cell methods enable causal interrogation of
3696 pathways highlighted by proteomics, while waterborne exposures make
3697 temperature and contaminant studies ecologically realistic for aquatic systems
3698 (Hoo et al., 2016).

3699

3700 Important physiological differences limit direct one-to-one translation. Teleost
3701 sperm are activated by external osmolality rather than undergoing mammalian-
3702 style capacitation in an oviduct, many teleosts lack a classical acrosome, and

3703 chromatin packaging relies more on histones and species-specific basic proteins
3704 than on protamines, all of which shift baseline proteomes and selection filters
3705 relative to humans (Immler, 2019; Suarez & Pacey, 2006). Testis organisation,
3706 thermal biology, and post-testicular maturation also differ across taxa, which must
3707 be considered when inferring clinical relevance.

3708

3709 A tiered strategy mitigates these gaps. Discovery is performed in zebrafish to
3710 identify conserved axes of sperm performance such as mitochondrial function,
3711 redox homeostasis, and axonemal integrity. Orthologue mapping and targeted
3712 assays are then applied to human ejaculates to confirm cell surface availability
3713 and within-ejaculate trends using spectral imaging flow cytometry. Where female-
3714 tract biology and acrosome function are critical, mammalian models such as
3715 mouse for mechanism and bovine or porcine systems for ART-relevant handling
3716 provide complementary validation. Nonhuman primates are reserved for late-stage
3717 translational questions where justified (Stouffer & Woodruff, 2017b; Suarez &
3718 Pacey, 2006).

3719

3720 This triangulation treats zebrafish as a hypothesis generator, mammals as
3721 mechanistic validators, and human ejaculates as the final clinical filter. Conserved
3722 features that recur across taxa are most likely to generalise, whereas model-
3723 specific signals guide species-tailored applications (Hoo et al., 2016; Immler,
3724 2019).

3725

3726 **6.7 Broader Implications**

3727 **6.7.1 Evolutionary significance**

3728 These results support an updated view of sexual reproduction as a multi-level
3729 selection process. Evidence for functionally meaningful molecular heterogeneity
3730 within ejaculates, coupled with single-cell validation of fitness-linked cell surface
3731 features, is consistent with selection acting among haploid gametes prior to
3732 fertilisation. This complements classic frameworks of anisogamy and the biphasic
3733 life cycle by showing that the brief haploid phase can express phenotypes with

3734 consequences for fertilisation and potentially for offspring performance (Immler,
3735 2019; Mable & Otto, 1998; Parker et al., 1972).

3736

3737 The data also refine models of sperm competition. Traditional models emphasise
3738 numbers and motility while assuming within-male homogeneity. The present
3739 findings indicate that internal competition within an ejaculate can favour sperm that
3740 express specific molecular traits such as enhanced membrane integrity, oxidative
3741 stress resistance, and robust axonemal architecture, adding a purifying component
3742 to selection before zygote formation (Lüpold & Pitnick, 2018; Sutter & Immler,
3743 2020). This provides empirical grounding for theoretical models that incorporate
3744 allele-biased expression, post-meiotic regulation, and selective protein retention as
3745 mechanisms enabling haploid selection in “diploid” organisms (Bhutani et al.,
3746 2021; Immler, 2019).

3747

3748 **6.7.2 Relevance to human fertility and ART**

3749 Clinically, these results argue for moving beyond morphology and gross motility
3750 toward molecularly informed, functionally validated sperm assessment.

3751 Conventional selection methods such as swim-up and density gradients enrich for
3752 movement but do not reliably exclude sperm with DNA damage, epigenetic
3753 abnormalities, or membrane defects, and they remain poor predictors of embryo
3754 viability or live birth (Said & Land, 2011). The identification of cell surface markers
3755 that track within-ejaculate longevity and survival, combined with spectral imaging
3756 flow cytometry on non-permeabilised cells, provides proof of concept for minimally
3757 invasive screening and enrichment of higher-fitness sperm that is compatible with
3758 ART workflows (Oseguera-López et al., 2019).

3759

3760 Near-term translational steps include larger multi-centre validations of OLFM4 and
3761 CTNG trends across clinical cohorts, development of rapid cell surface assays or
3762 microfluidic capture using antibodies against validated targets, and prospective
3763 studies that relate marker-guided selection to fertilisation, embryo quality,
3764 implantation, and live birth. Such tools are especially pertinent for unexplained
3765 infertility and repeated ART failure, where standard semen parameters lack

3766 predictive power. A molecularly informed selection paradigm has the potential to
3767 improve outcomes while reducing the emotional and financial burden of repeated
3768 cycles (Barratt et al., 2011; Said & Land, 2011).

3769

3770 **6.8 Critical reflections and limitations**

3771 While this thesis advances understanding of sperm heterogeneity, haploid
3772 selection, and male fertility, several limitations should be acknowledged to
3773 contextualise the inferences and to guide next steps. These relate to sample size,
3774 pooling, reagent constraints, experimental design, and generalisability.

3775

3776 First, sample sizes in the human work were modest, often five or fewer donors per
3777 experiment. Mixed-effects models and within-ejaculate contrasts helped control for
3778 inter-individual variability, but statistical power and external validity remain
3779 constrained. Donor-specific patterns, such as variability in AOC3, underline the
3780 need for larger cohorts to distinguish stable biological heterogeneity from sampling
3781 noise.

3782

3783 Second, pooled materials were required for high-depth proteomics in zebrafish
3784 testes and sperm. Pooling enabled robust protein identification and quantification
3785 but averages away individual-level structure, limiting direct linkage between
3786 organismal traits and molecular profiles. Tank replicates and standardised pooling
3787 mitigate this to an extent, yet one-to-one genotype–phenotype mapping was not
3788 possible.

3789

3790 Third, reagent availability and specimen handling bounded the scope of single-cell
3791 validation. Only candidates with reliable, surface-accessible antibodies could be
3792 tested, and several promising targets were excluded due to lack of suitable
3793 reagents for non-permeabilised sperm. The use of fixation in imaging flow
3794 cytometry safeguarded morphology and gating but may alter epitope conformation
3795 or membrane accessibility, potentially biasing signal magnitude.

3796

3797 Fourth, the thesis establishes associations between molecular signatures and
3798 sperm fitness proxies such as longevity and motility, rather than causal links to
3799 fertilisation or developmental outcomes. Direct tests of fertilisation success and
3800 offspring phenotypes are not feasible in humans and were beyond scope in
3801 zebrafish. Future functional assays in tractable models will be required to confirm
3802 whether depleting or enriching specific surface-defined subpopulations shifts
3803 embryo viability or offspring performance.

3804

3805 Finally, cross-species inference should be cautious. Core pathways related to
3806 oxidative stress, metabolism, and flagellar function appear conserved between
3807 zebrafish and humans, but species differences in spermatogenesis, maturation
3808 environments, and reproductive strategy may shape effect sizes and marker
3809 performance. Clinical translation will require validation in human cohorts and under
3810 clinically relevant workflows.

3811

3812 Despite these constraints, the combination of multi-species designs,
3813 complementary proteomic and single-cell readouts, and convergent within-
3814 ejaculate patterns provides a strong evidential base. Stating these limitations
3815 delineates the bounds of inference and clarifies priorities for future work: larger
3816 human cohorts, unpooled designs where feasible, expanded reagent development
3817 for live-cell assays, and prospective tests of biomarker-guided enrichment against
3818 fertilisation and embryo outcomes.

3819

3820 **6.9 Future directions**

3821 Building on the findings of this thesis, a number of promising research directions
3822 emerge that could clarify unresolved mechanisms, validate functional relevance,
3823 and translate molecular discoveries into clinical tools. While the evidence
3824 presented here establishes key associations between sperm phenotypes,
3825 molecular profiles, and functional potential, several areas require deeper
3826 investigation to fully understand the biological implications and therapeutic
3827 opportunities.

3828

3829 A primary next step involves the functional validation of candidate sperm
3830 biomarkers in model organisms. While this thesis demonstrated consistent
3831 associations between certain surface proteins and sperm fitness traits such as
3832 motility and longevity, causality has not yet been established. *In vivo* fertilisation
3833 experiments using model organisms such as zebrafish or mice could directly test
3834 whether sperm expressing or lacking specific markers differ in fertilisation success
3835 or influence downstream embryo viability and offspring outcomes. Controlled
3836 breeding experiments, where sperm are sorted based on biomarker expression
3837 before fertilisation, would allow a more definitive assessment of how molecular
3838 variation translates to reproductive performance.

3839

3840 Another important direction involves improving the resolution of sperm
3841 phenotyping through single-cell or live-cell molecular profiling. While high-
3842 throughput proteomics has revealed biologically meaningful variation, it is
3843 inherently a bulk technique and therefore obscures cell-level heterogeneity.
3844 Recent advances in single-cell mass spectrometry and live-cell barcoding could
3845 allow researchers to examine molecular differences between individual sperm
3846 cells with greater precision. Coupling live-cell sorting techniques to downstream
3847 omics analyses, such as transcriptomics or targeted proteomics, would also offer
3848 the opportunity to study dynamic processes such as capacitation, acrosome
3849 reaction, and mitochondrial activation in real time.

3850

3851 In human reproductive research, longitudinal outcome studies are needed to
3852 evaluate the clinical relevance of the molecular traits identified here. While this
3853 thesis focused on associations with sperm motility and viability, future studies
3854 should examine whether these markers predict fertilisation success, embryo
3855 development, implantation rates, or live birth outcomes in ART contexts. Cohort
3856 studies involving patients undergoing IVF or ICSI could provide valuable real-world
3857 data linking molecular biomarkers to treatment success. Such studies would also
3858 offer insight into inter-individual variability, a recurring theme throughout this
3859 thesis, and help identify which molecular features are robust across populations.

3860

3861 The development of non-invasive sperm selection technologies also represents a
3862 key translational goal. Building on the flow cytometry work presented in this thesis,
3863 novel technologies could be designed to sort or enrich for sperm lacking markers
3864 associated with low fitness. These technologies must preserve cell viability and
3865 functionality for use in ART, but may include microfluidic devices, optical imaging-
3866 based sorters, or label-free selection methods that exploit biophysical differences
3867 such as refractive index or dielectric properties. The integration of such tools into
3868 fertility clinics would mark a major shift from morphology-based to molecularly
3869 informed sperm selection.

3870

3871 Another important area for exploration is the genetic and epigenetic basis of sperm
3872 heterogeneity. Although this thesis inferred that functional variation may be
3873 shaped by haploid gene expression or selective protein retention, the specific
3874 genetic mechanisms remain unclear. Technologies such as single-cell RNA
3875 sequencing, allele-specific expression analysis, and methylation profiling could
3876 reveal how genetic variants or epigenetic marks influence the molecular
3877 phenotype of individual sperm cells. This could also provide insight into how
3878 environmental factors, such as stress or toxin exposure, shape gamete quality
3879 across developmental time.

3880

3881 Finally, the broader implications of sperm heterogeneity for offspring health
3882 warrant further investigation. Emerging evidence suggests that sperm molecular
3883 quality may influence not only fertilisation but also embryonic development and
3884 long-term health outcomes. Whether sperm surface markers or proteomic profiles
3885 can predict disease risk, developmental robustness, or transgenerational effects
3886 remains an open and compelling question.

3887

3888 Together, these future directions outline a clear path from the discovery of sperm
3889 heterogeneity to the mechanistic understanding and clinical application of this
3890 phenomenon. Interdisciplinary research combining molecular biology, reproductive
3891 physiology, evolutionary theory, and clinical practice will be essential to advancing

3892 this field. The continued exploration of sperm phenotypes at the molecular level
3893 offers an opportunity to deepen our understanding of sexual reproduction while
3894 improving reproductive outcomes for patients.

3895

3896 **6.10 Conclusions**

3897 This thesis demonstrates that sperm fitness is molecularly encoded,
3898 phenotypically expressed, and subject to selection. Through a combination of
3899 high-resolution proteomics, sperm subpopulation analysis, and single-cell
3900 validation, the work provides strong evidence that sperm are not functionally
3901 equivalent and that their phenotypic variation has biological and potentially clinical
3902 significance. Variation occurs not only between males, but also within individual
3903 ejaculates, and this variation can be traced to differences in protein expression
3904 that relate to key fitness traits such as motility and longevity.

3905

3906 The findings support and refine evolutionary models of gamete competition and
3907 suggest that selection can act at the haploid stage of the reproductive cycle,
3908 challenging long-held assumptions about the passivity of sperm cells. This work
3909 also lays the foundation for new clinical approaches to diagnosing and treating
3910 male infertility. By identifying functionally relevant molecular markers, it offers a
3911 path forward for improving sperm selection methods in ART and better predicting
3912 fertilisation outcomes.

3913

3914 More broadly, this thesis underscores the value of applying evolutionary theory to
3915 clinical fertility problems. It shows that understanding the origins and
3916 consequences of sperm heterogeneity is not only a matter of basic science, but a
3917 practical necessity for enhancing human reproductive health. This work sets the
3918 stage for future efforts to harness molecular variation in the service of more
3919 effective, personalised fertility care.

3920

3921

3922 **Appendix**

3923 Appendix 1: The Zebrafish Sperm Proteome Published Manuscript.

3924 Please see supplied PDF file “The Zebrafish Sperm Proteome 2024.pdf”

3925

3926 Supplementary Table 1: The complete zebrafish testes proteome.

3927 Please see supplied Excel file “Supplementary Table 1.xlsx”

3928

3929 Supplementary Table 2: Proteins with significantly different abundance between
3930 heat-treated and control testes

3931 Please see supplied Excel file “Supplementary Table 2.xlsx”

3932

3933 Supplementary Table 3: GO terms for proteins significantly less abundant in heat
3934 treated testes

3935 Please see supplied Excel file “Supplementary Table 3.xlsx”

3936

3937 Supplementary Table 4: GO terms for proteins significantly more abundant in heat
3938 treated testes

3939 Please see supplied Excel file “Supplementary Table 4.xlsx”

3940

3941 Supplementary Table 5: The zebrafish sperm proteome

3942 Please see supplied Excel file “Supplementary Table 5.xlsx”

3943

3944 Supplementary Table 6: The human sperm proteome

3945 Please see supplied Excel file “Supplementary Table 6.xlsx”

3946

3947 Supplementary Table 7: Biomarker shortlist

3948 Please see supplied Excel file “Supplementary Table 7.xlsx”

3949 **References**

3950 Adamson, G. D., Creighton, P., de Mouzon, J., Zegers-Hochschild, F., Dyer, S., & Chambers, G. M.
3951 (2025). How many infants have been born with the help of assisted reproductive
3952 technology? *Fertility and Sterility*, 124(1), 40–50.
3953 <https://doi.org/10.1016/j.fertnstert.2025.02.009>

3954 Aebersold, R., & Mann, M. (2003). Mass spectrometry-based proteomics. *Nature*, 422(6928), 198–
3955 207. <https://doi.org/10.1038/nature01511>

3956 Ahmad, R., & Budnik, B. (2023). A review of the current state of single-cell proteomics and future
3957 perspective. *Analytical and Bioanalytical Chemistry*, 415(28), 6889–6899.
3958 <https://doi.org/10.1007/s00216-023-04759-8>

3959 Aitken, R. J., Nixon, B., Lin, M., Koppers, A. J., Lee, Y. H., & Baker, M. A. (2007). Proteomic changes
3960 in mammalian spermatozoa during epididymal maturation. *Asian Journal of Andrology*,
3961 9(4), 554–564. <https://doi.org/10.1111/j.1745-7262.2007.00280.X>

3962 Alahmar, A. T., Singh, R., & Palani, A. (2022). Sperm DNA Fragmentation in Reproductive
3963 Medicine: A Review. *Journal of Human Reproductive Sciences*, 15(3), 206–218.
3964 https://doi.org/10.4103/jhrs.jhrs_82_22

3965 Alavi, S. M. H., & Cosson, J. (2006). Sperm motility in fishes. (II) Effects of ions and osmolality: A
3966 review. *Cell Biology International*, 30(1), 1–14.
3967 <https://doi.org/10.1016/j.cellbi.2005.06.004>

3968 Alavioon, G., Cabrera Garcia, A., LeChatelier, M., Maklakov, A. A., & Immler, S. (2019). Selection
3969 for longer lived sperm within ejaculate reduces reproductive ageing in offspring. *Evolution
3970 Letters*, 3(2), 198–206. <https://doi.org/10.1002/evl3.101>

3971 Alavioon, G., Hotzy, C., Nakhro, K., Rudolf, S., Scofield, D. G., Zajitschek, S., Maklakov, A. A., &
3972 Immler, S. (2017). Haploid selection within a single ejaculate increases offspring fitness.

3973 *Proceedings of the National Academy of Sciences of the United States of America*, 114(30),
3974 8053–8058. <https://doi.org/10.1073/pnas.1705601114>

3975 Alavioon, G., Marcu, D., & Immler, S. (2021). Within-Ejaculate Sperm Selection and Its Implications
3976 for Assisted Reproduction Technologies. In L. Björndahl, J. Flanagan, R. Holmberg, & U.
3977 Kvist (Eds), *XIIIth International Symposium on Spermato*logy (pp. 127–133). Springer
3978 International Publishing. https://doi.org/10.1007/978-3-030-66292-9_20

3979 Alfonso, S., Gesto, M., & Sadoul, B. (2021). Temperature increase and its effects on fish stress
3980 physiology in the context of global warming. *Journal of Fish Biology*, 98(6), 1496–1508.
3981 <https://doi.org/10.1111/jfb.14599>

3982 Alix, M., Kjesbu, O. S., & Anderson, K. C. (2020). From gametogenesis to spawning: How climate-
3983 driven warming affects teleost reproductive biology. *Journal of Fish Biology*, 97(3), 607–
3984 632. <https://doi.org/10.1111/jfb.14439>

3985 Alvarenga, É. R. de, & França, L. R. de. (2009). Effects of Different Temperatures on Testis
3986 Structure and Function, with Emphasis on Somatic Cells, in Sexually Mature Nile Tilapias
3987 (*Oreochromis niloticus*)1. *Biology of Reproduction*, 80(3), 537–544.
3988 <https://doi.org/10.1095/biolreprod.108.072827>

3989 Amano, K., Oigawa, S., Ichizawa, K., Tokuda, Y., Unagami, M., Sekiguchi, M., Furui, M., Nakaoka,
3990 K., Ito, A., Hayashi, R., Tamaki, Y., Hayashi, Y., Fukuda, Y., Katagiri, Y., Nakata, M., &
3991 Nagao, K. (2024). Swim-up method is superior to density gradient centrifugation for
3992 preserving sperm DNA integrity during sperm processing. *Reproductive Medicine and*
3993 *Biology*, 23(1), e12562. <https://doi.org/10.1002/rmb2.12562>

3994 Amaral, A., Castillo, J., Ramalho-Santos, J., & Oliva, R. (2014). The combined human sperm
3995 proteome: Cellular pathways and implications for basic and clinical science. *Human*
3996 *Reproduction Update*, 20(1), 40–62. <https://doi.org/10.1093/HUMUPD/DMT046>

3997 Amaral, A., Lourenço, B., Marques, M., & Ramalho-Santos, J. (2013). *Mitochondria functionality*
3998 *and sperm quality*. <https://doi.org/10.1530/REP-13-0178>

3999 Amaral, A., Paiva, C., Attardo Parrinello, C., Estanyol, J. M., Ballescà, J. L., Ramalho-Santos, J., &
4000 Oliva, R. (2014). Identification of Proteins Involved in Human Sperm Motility Using High-
4001 Throughput Differential Proteomics. *Journal of Proteome Research*, 13(12), 5670–5684.
4002 <https://doi.org/10.1021/pr500652y>

4003 Ardon, F., Helms, D., Sahin, E., Bollwein, H., Topfer-Petersen, E., & Waberski, D. (2008).
4004 Chromatin-unstable boar spermatozoa have little chance of reaching oocytes in vivo.
4005 *Reproduction*, 135(4), 461–470. <https://doi.org/10.1530/REP-07-0333>

4006 Arora, A. S., Huang, H.-L., Singh, R., Narui, Y., Suchenko, A., Hatano, T., Heissler, S. M.,
4007 Balasubramanian, M. K., & Chinthalapudi, K. (2023). Structural insights into actin isoforms.
4008 *eLife*, 12, e82015. <https://doi.org/10.7554/eLife.82015>

4009 Bahat, A., & Eisenbach, M. (2006). Sperm thermotaxis. *Molecular and Cellular Endocrinology*,
4010 252(1), 115–119. <https://doi.org/10.1016/j.mce.2006.03.027>

4011 Bailey, J. L. (2010). Factors Regulating Sperm Capacitation. *Systems Biology in Reproductive
4012 Medicine*, 56(5), 334–348. <https://doi.org/10.3109/19396368.2010.512377>

4013 Baker, M. A., Hetherington, L., Reeves, G. M., & Aitken, R. J. (2008). The mouse sperm proteome
4014 characterized via IPG strip prefractionation and LC-MS/MS identification. *PROTEOMICS*,
4015 8(8), 1720–1730. <https://doi.org/10.1002/PMIC.200701020>

4016 Barbarossa, V., Bosmans, J., Wanders, N., King, H., Bierkens, M. F. P., Huijbregts, M. A. J., &
4017 Schipper, A. M. (2021). Threats of global warming to the world's freshwater fishes. *Nature
4018 Communications*, 12(1), 1701. <https://doi.org/10.1038/s41467-021-21655-w>

4019 Barratt, C. L., Mansell, S., Beaton, C., Tardif, S., & Oxenham, S. K. (2011). Diagnostic tools in male
4020 infertility—The question of sperm dysfunction. *Asian Journal of Andrology*, 13(1), 53–58.
4021 <https://doi.org/10.1038/aja.2010.63>

4022 Barreau, C., Benson, E., & White-Cooper, H. (2008). Comet and cup genes in Drosophila
4023 spermatogenesis: The first demonstration of post-meiotic transcription. *Biochemical
4024 Society Transactions*, 36(3), 540–542. <https://doi.org/10.1042/BST0360540>

4025 Bateman, A., Martin, M. J., Orchard, S., Magrane, M., Ahmad, S., Alpi, E., Bowler-Barnett, E. H.,
4026 Britto, R., Bye-A-Jee, H., Cukura, A., Denny, P., Dogan, T., Ebenezer, T. G., Fan, J., Garmiri,
4027 P., da Costa Gonzales, L. J., Hatton-Ellis, E., Hussein, A., Ignatchenko, A., ... Zhang, J.
4028 (2023). UniProt: The Universal Protein Knowledgebase in 2023. *Nucleic Acids Research*,
4029 51(D1), D523–D531. <https://doi.org/10.1093/NAR/GKAC1052>

4030 Beckham, J., Alam, F., Omojola, V., Scherr, T., Guitreau, A., Melvin, A., Park, D. S., Choi, J.-W.,
4031 Tiersch, T. R., & Todd Monroe, W. (2018). *A microfluidic device for motility and osmolality*
4032 *analysis of zebrafish sperm*. <https://doi.org/10.1007/s10544-018-0308-2>

4033 Beukeboom, L. W., & Perrin, N. (2014). *The Evolution of Sex Determination*. Oxford University
4034 Press. <https://doi.org/10.1093/acprof:oso/9780199657148.001.0001>

4035 Bhutani, K., Stansifer, K., Ticau, S., Bojic, L., Villani, A.-C., Slisz, J., Cremers, C. M., Roy, C., Donovan,
4036 J., Fiske, B., & Friedman, R. C. (2021). Widespread haploid-biased gene expression enables
4037 sperm-level natural selection. *Science*, eabb1723–eabb1723.
4038 <https://doi.org/10.1126/science.abb1723>

4039 Bianchi, E., Doe, B., Goulding, D., & Wright, G. J. (2014). Juno is the egg Izumo receptor and is
4040 essential for mammalian fertilization. *Nature*, 508(7497), 483–487.
4041 <https://doi.org/10.1038/nature13203>

4042 Bisht, S., Faiq, M., Tolahunase, M., & Dada, R. (2017). Oxidative stress and male infertility. *Nature*
4043 *Reviews Urology*, 14(8), 470–485. <https://doi.org/10.1038/nrurol.2017.69>

4044 Blaurock, J., Baumann, S., Grunewald, S., Schiller, J., & Engel, K. M. (2022). Metabolomics of
4045 Human Semen: A Review of Different Analytical Methods to Unravel Biomarkers for Male
4046 Fertility Disorders. *International Journal of Molecular Sciences* 2022, Vol. 23, Page 9031,
4047 23(16), 9031–9031. <https://doi.org/10.3390/IJMS23169031>

4048 Boni, R. (2019). Heat stress, a serious threat to reproductive function in animals and humans.
4049 *Molecular Reproduction and Development*, 86(10), 1307–1323.
4050 <https://doi.org/10.1002/MRD.23123>

4051 Borowsky, R., Luk, A., He, X., & Kim, R. S. (2018). Unique sperm haplotypes are associated with
4052 phenotypically different sperm subpopulations in *Astyanax* fish. *BMC Biology*, 16(1), 72.
4053 <https://doi.org/10.1186/s12915-018-0538-z>

4054 Boyer, D. S., Rippmann, J. F., Ehrlich, M. S., Bakker, R. A., Chong, V., & Nguyen, Q. D. (2021). Amine
4055 oxidase copper-containing 3 (AOC3) inhibition: A potential novel target for the
4056 management of diabetic retinopathy. *International Journal of Retina and Vitreous*, 7(1),
4057 30. <https://doi.org/10.1186/s40942-021-00288-7>

4058 Breedveld, M. C., Devigili, A., Borgheresi, O., & Gasparini, C. (2023). Reproducing in hot water:
4059 Experimental heatwaves deteriorate multiple reproductive traits in a freshwater
4060 ectotherm. *Functional Ecology*, 37(4), 989–1004. <https://doi.org/10.1111/1365->
4061 2435.14279

4062 Brestoff, J. R. (2023). Full spectrum flow cytometry in the clinical laboratory. *International Journal
4063 of Laboratory Hematology*, 45(S2), 44–49. <https://doi.org/10.1111/ijlh.14098>

4064 Brösamle, C., & Halpern, M. E. (2002). Characterization of myelination in the developing zebrafish.
4065 *Glia*, 39(1), 47–57. <https://doi.org/10.1002/glia.10088>

4066 Burger, T. (2018). Gentle Introduction to the Statistical Foundations of False Discovery Rate in
4067 Quantitative Proteomics. *Journal of Proteome Research*, 17(1), 12–22.
4068 <https://doi.org/10.1021/acs.jproteome.7b00170>

4069 Caballero, A., & García-Dorado, A. (2013). Allelic diversity and its implications for the rate of
4070 adaptation. *Genetics*, 195(4), 1373–1384. <https://doi.org/10.1534/genetics.113.158410>

4071 Caldwell, K. A., & Handel, M. A. (1991). Protamine transcript sharing among postmeiotic
4072 spermatids. *Proceedings of the National Academy of Sciences*, 88(6), 2407–2411.
4073 <https://doi.org/10.1073/pnas.88.6.2407>

4074 Cannarella, R., Condorelli, R. A., Calogero, A. E., & La Vignera, S. (2020). Novel Insights on the Role
4075 of the Human Sperm Proteome. *Protein & Peptide Letters*, 27(12), 1181–1185.
4076 <https://doi.org/10.2174/0929866527666200505215921>

4077 Canosa, L. F., & Bertucci, J. I. (2023). The effect of environmental stressors on growth in fish and
4078 its endocrine control. *Frontiers in Endocrinology*, 14.
4079 <https://doi.org/10.3389/fendo.2023.1109461>

4080 Carvalho, M. G., Silva, K. M., Aristizabal, V. H. V., Ortiz, P. E. O., Paranzini, C. S., Melchert, A.,
4081 Amaro, J. L., & Souza, F. F. (2021). Effects of Obesity and Diabetes on Sperm Cell
4082 Proteomics in Rats. *Journal of Proteome Research*, 20(5), 2628–2642.
4083 <https://doi.org/10.1021/acs.jproteome.0c01044>

4084 Casey, T. M., Khan, J. M., Bringans, S. D., Koudelka, T., Takle, P. S., Downs, R. A., Livk, A., Syme, R.
4085 A., Tan, K.-C., & Lipscombe, R. J. (2017). Analysis of Reproducibility of Proteome Coverage
4086 and Quantitation Using Isobaric Mass Tags (iTRAQ and TMT). *Journal of Proteome
4087 Research*, 16(2), 384–392. <https://doi.org/10.1021/acs.jproteome.5b01154>

4088 Castillo, J., Bogle, O. A., Jodar, M., Torabi, F., Delgado-Dueñas, D., Estanyol, J. M., Ballescà, J. L.,
4089 Miller, D., & Oliva, R. (2019). Proteomic Changes in Human Sperm During Sequential in
4090 vitro Capacitation and Acrosome Reaction. *Frontiers in Cell and Developmental Biology*, 7.
4091 <https://doi.org/10.3389/fcell.2019.00295>

4092 Castillo, J., de la Iglesia, A., Leiva, M., Jodar, M., & Oliva, R. (2023). Proteomics of human
4093 spermatozoa. *Human Reproduction*, 38(12), 2312–2320.
4094 <https://doi.org/10.1093/humrep/dead170>

4095 Cesari, A., Monclus, M. de los A., Tejón, G. P., Clementi, M., & Fornes, M. W. (2010). Regulated
4096 serine proteinase lytic system on mammalian sperm surface: There must be a role.
4097 *Theriogenology*, 74(5), 699-711.e5. <https://doi.org/10.1016/j.theriogenology.2010.03.029>

4098 Chalmel, F., & Rolland, A. D. (2015). *Linking transcriptomics and proteomics in spermatogenesis*.
4099 <https://doi.org/10.1530/REP-15-0073>

4100 Chand, D., & Lovejoy, D. A. (2011). Stress and reproduction: Controversies and challenges. *General
4101 and Comparative Endocrinology*, 171(3), 253–257.
4102 <https://doi.org/10.1016/j.ygcen.2011.02.022>

4103 Chauvin, T., Xie, F., Liu, T., Nicora, C. D., Yang, F., Camp, D. G., Smith, R. D., & Roberts, K. P. (2012).

4104 A systematic analysis of a deep mouse epididymal sperm proteome. *Biology of*
4105 *Reproduction*, 87(6). <https://doi.org/10.1095/BIOLREPROD.112.104208>

4106 Cheng, L., von Schuckmann, K., Abraham, J. P., Trenberth, K. E., Mann, M. E., Zanna, L., England,
4107 M. H., Zika, J. D., Fasullo, J. T., Yu, Y., Pan, Y., Zhu, J., Newsom, E. R., Bronselaer, B., & Lin,
4108 X. (2022). Past and future ocean warming. *Nature Reviews Earth & Environment*, 3(11),
4109 776–794. <https://doi.org/10.1038/s43017-022-00345-1>

4110 Codina, M., Estanyol, J. M., Fidalgo, M. J., Ballescà, J. L., & Oliva, R. (2015). Advances in sperm
4111 proteomics: Best-practise methodology and clinical potential. *Expert Review of*
4112 *Proteomics*, 12(3), 255–277. <https://doi.org/10.1586/14789450.2015.1040769>

4113 Cole, B., Vasudeva, R., Dragoi, K., Hibble, J., King, J., Maklakov, A. A., Chapman, T., & Gage, M. J. G.
4114 (2025). Short experimental heatwaves have sublethal impacts on male reproduction in a
4115 model insect. *Journal of Experimental Biology*, 228(15), jeb250555.
4116 <https://doi.org/10.1242/jeb.250555>

4117 Cross, N. L. (1998). Role of Cholesterol in Sperm Capacitation1. *Biology of Reproduction*, 59(1), 7–
4118 11. <https://doi.org/10.1095/biolreprod59.1.7>

4119 Cui, Z., Sharma, R., & Agarwal, A. (2016). Proteomic analysis of mature and immature ejaculated
4120 spermatozoa from fertile men. *Asian Journal of Andrology*, 18(5), 735.
4121 <https://doi.org/10.4103/1008-682X.164924>

4122 Dahiya, K., Dhankhar, R., Singh, P., Sethi, J., Dhankhar, K., Ahlawat, R., & Gupta, M. (2023).
4123 Phospholipase A2 in male reproductive cancers. In S. Chakraborti (Ed.), *Phospholipases in*
4124 *Physiology and Pathology* (pp. 209–217). Academic Press. <https://doi.org/10.1016/B978-0-323-95697-0.00001-7>

4125 D'Amours, O., Calvo, É., Bourassa, S., Vincent, P., Blondin, P., & Sullivan, R. (2019a). Proteomic
4126 markers of low and high fertility bovine spermatozoa separated by Percoll gradient.

4128 *Molecular Reproduction and Development*, 86(8), 999–1012.

4129 <https://doi.org/10.1002/mrd.23174>

4130 Darwin, C. (1871). *The descent of man, and selection in relation to sex*. J. Murray.

4131 <https://doi.org/10.5962/bhl.title.2092>

4132 Davalieva, K., Rusevski, A., Velkov, M., Noveski, P., Kubelka-Sabit, K., Filipovski, V., Plaseski, T.,

4133 Dimovski, A., & Plaseska-Karanfilska, D. (2022). Comparative proteomics analysis of

4134 human FFPE testicular tissues reveals new candidate biomarkers for distinction among

4135 azoospermia types and subtypes. *Journal of Proteomics*, 267, 104686.

4136 <https://doi.org/10.1016/j.jprot.2022.104686>

4137 David, J. R., Araripe, L. O., Chakir, M., Legout, H., Lemos, B., Pétavy, G., Rohmer, C., Joly, D., &

4138 Moreteau, B. (2005). Male sterility at extreme temperatures: A significant but neglected

4139 phenomenon for understanding *Drosophila* climatic adaptations. *Journal of Evolutionary*

4140 *Biology*, 18(4), 838–846. <https://doi.org/10.1111/j.1420-9101.2005.00914.x>

4141 De Jonge, C., & Barratt, C. I. R. (2019). The present crisis in male reproductive health: An urgent

4142 need for a political, social, and research roadmap. *Andrology*, 7(6), 762–768.

4143 <https://doi.org/10.1111/andr.12673>

4144 de Kretser, D. M., Loveland, K. L., Meinhardt, A., Simorangkir, D., & Wreford, N. (1998).

4145 Spermatogenesis. *Human Reproduction*, 13(suppl_1), 1–8.

4146 https://doi.org/10.1093/humrep/13.suppl_1.1

4147 de Lima Rosa, J., de Paula Freitas Dell'Aqua, C., de Souza, F. F., Missassi, G., & Kempinas, W. D. G.

4148 (2023). Multiple flow cytometry analysis for assessing human sperm functional

4149 characteristics. *Reproductive Toxicology*, 117, 108353.

4150 <https://doi.org/10.1016/j.reprotox.2023.108353>

4151 de Mateo, S., Castillo, J., Estanyol, J. M., Ballescà, J. L., & Oliva, R. (2011). Proteomic

4152 characterization of the human sperm nucleus. *PROTEOMICS*, 11(13), 2714–2726.

4153 <https://doi.org/10.1002/pmic.201000799>

4154 de Siqueira-Silva, D. H., dos Santos Silva, A. P., Ninhaus-Silveira, A., & Veríssimo-Silveira, R. (2015).

4155 The effects of temperature and busulfan (Myleran) on the yellowtail tetra *Astyanax*
4156 *altiparanae* (Pisces, Characiformes) spermatogenesis. *Theriogenology*, 84(6), 1033–1042.

4157 <https://doi.org/10.1016/j.theriogenology.2015.06.004>

4158 Deane, E. E., & Woo, N. Y. S. (2011). Advances and perspectives on the regulation and expression
4159 of piscine heat shock proteins. *Reviews in Fish Biology and Fisheries*, 21(2), 153–185.
4160 <https://doi.org/10.1007/s11160-010-9164-8>

4161 Delaney, M. A., & Klesius, P. H. (2004). Hypoxic conditions induce Hsp70 production in blood,
4162 brain and head kidney of juvenile Nile tilapia *Oreochromis niloticus* (L.). *Aquaculture*,
4163 236(1), 633–644. <https://doi.org/10.1016/j.aquaculture.2004.02.025>

4164 Dietrich, M. A., Arnold, G. J., Fröhlich, T., & Ciereszko, A. (2014). In-depth proteomic analysis of
4165 carp (*Cyprinus carpio* L) spermatozoa. *Comparative Biochemistry and Physiology Part D:*
4166 *Genomics and Proteomics*, 12, 10–15. <https://doi.org/10.1016/J.CBD.2014.09.003>

4167 Ding, W., Sun, J., Song, S., Cui, Y., Chen, F., Yuan, Q., & Shang, W. (2025). Junction Plakoglobin – A
4168 Dual-Role Player in Cancer Biology. *International Journal of Surgery*,
4169 10.1097/JS9.0000000000002365. <https://doi.org/10.1097/JS9.0000000000002365>

4170 Doostabadi, M. R., Mangoli, E., Marvast, L. D., Dehghanpour, F., Maleki, B., Torkashvand, H., &
4171 Talebi, A. R. (2022). Microfluidic devices employing chemo- and thermotaxis for sperm
4172 selection can improve sperm parameters and function in patients with high DNA
4173 fragmentation. *Andrologia*, 54(11), e14623. <https://doi.org/10.1111/and.14623>

4174 Dorts, J., Grenouillet, G., Douxfils, J., Mandiki, S. N. M., Milla, S., Silvestre, F., & Kestemont, P.
4175 (2012). Evidence that elevated water temperature affects the reproductive physiology of
4176 the European bullhead *Cottus gobio*. *Fish Physiology and Biochemistry*, 38(2), 389–399.
4177 <https://doi.org/10.1007/s10695-011-9515-y>

4178 Dym, M., & Fawcett, D. W. (1971). Further Observations on the Numbers of Spermatogonia,
4179 Spermatocytes, and Spermatids Connected by Intercellular Bridges in the Mammalian

4180 Testis1. *Biology of Reproduction*, 4(2), 195–215.

4181 <https://doi.org/10.1093/biolreprod/4.2.195>

4182 Elango, K., Kumaresan, A., Talluri, T. R., Raval, K., Paul, N., Peter, E. S. K. J., Sinha, M. K., Patil, S., &

4183 Verma, A. (2022). Impact of sperm protamine on semen quality and fertility. *Journal of*

4184 *Reproductive Healthcare and Medicine*, 3. https://doi.org/10.25259/JRHM_2_2022

4185 Elisio, M., Chalde, T., & Miranda, L. A. (2012). Effects of short periods of warm water fluctuations

4186 on reproductive endocrine axis of the pejerrey (*Odontesthes bonariensis*) spawning.

4187 *Comparative Biochemistry and Physiology Part A: Molecular & Integrative Physiology*,

4188 163(1), 47–55. <https://doi.org/10.1016/j.cbpa.2012.05.178>

4189 Eliuk, S., & Makarov, A. (2015). Evolution of Orbitrap Mass Spectrometry Instrumentation. *Annual*

4190 *Review of Analytical Chemistry*, 8(1), 61–80. <https://doi.org/10.1146/annurev-anchem-071114-040325>

4192 Emmaneel, A., Quintelier, K., Sichien, D., Rybakowska, P., Marañón, C., Alarcón-Riquelme, M. E.,

4193 Van Isterdael, G., Van Gassen, S., & Saeys, Y. (2022). PeacoQC: Peak-based selection of

4194 high quality cytometry data. *Cytometry. Part A: The Journal of the International Society for*

4195 *Analytical Cytology*, 101(4), 325–338. <https://doi.org/10.1002/cyto.a.24501>

4196 Esteves, S. C., Gosálvez, J., López-Fernández, C., Núñez-Calonge, R., Caballero, P., Agarwal, A., &

4197 Fernández, J. L. (2015). Diagnostic accuracy of sperm DNA degradation index (DDSi) as a

4198 potential noninvasive biomarker to identify men with varicocele-associated infertility.

4199 *International Urology and Nephrology*, 47(9), 1471–1477.

4200 <https://doi.org/10.1007/s11255-015-1053-6>

4201 European IVF Monitoring Consortium (EIM), for the E. S. of H. R. and E. (ESHRE), Wyns, C., De

4202 Geyter, C., Calhaz-Jorge, C., Kupka, M. S., Motrenko, T., Smeenk, J., Bergh, C., Tandler-

4203 Schneider, A., Rugescu, I. A., & Goossens, V. (2022). ART in Europe, 2018: Results

4204 generated from European registries by ESHRE†. *Human Reproduction Open*, 2022(3),

4205 hoac022. <https://doi.org/10.1093/hropen/hoac022>

4206 Fang, J., Xiao, L., Zhang, Q., Peng, Y., Wang, Z., & Liu, Y. (2020). Junction plakoglobin, a potential
4207 prognostic marker of oral squamous cell carcinoma, promotes proliferation, migration
4208 and invasion. *Journal of Oral Pathology & Medicine*, 49(1), 30–38.
4209 <https://doi.org/10.1111/jop.12952>

4210 Fenkes, M., Fitzpatrick, J. L., Ozolina, K., Shiels, H. A., & Nudds, R. L. (2017). Sperm in hot water:
4211 Direct and indirect thermal challenges interact to impact on brown trout sperm quality.
4212 *Journal of Experimental Biology*, 220(14), 2513–2520.
4213 <https://doi.org/10.1242/JEB.156018/262533/AM/SPERM-IN-HOT-WATER-DIRECT-AND->
4214 INDIRECT-THERMAL

4215 Firman, R. C., & Simmons, L. W. (2010). EXPERIMENTAL EVOLUTION OF SPERM QUALITY VIA
4216 POSTCOPULATORY SEXUAL SELECTION IN HOUSE MICE. *Evolution*, 64(5), 1245–1256.
4217 <https://doi.org/10.1111/j.1558-5646.2009.00894.x>

4218 Firman, R. C., & Simmons, L. W. (2015). Gametic interactions promote inbreeding avoidance in
4219 house mice. *Ecology Letters*, 18(9), 937–943. <https://doi.org/10.1111/ele.12471>

4220 Florian, H. (2016). DHARMA: Residual Diagnostics for Hierarchical (Multi-Level / Mixed) Regression
4221 Models. *CRAN: Contributed Packages*. <https://doi.org/10.32614/cran.package.dharma>

4222 Frohnhöfer, H. G., Geiger-Rudolph, S., Pattky, M., Meixner, M., Huhn, C., Maischein, H.-M.,
4223 Geisler, R., Gehring, I., Maderspacher, F., Nüsslein-Volhard, C., & Irion, U. (2016).
4224 Spermidine, but not spermine, is essential for pigment pattern formation in zebrafish.
4225 *Biology Open*, 5(6), 736–744. <https://doi.org/10.1242/bio.018721>

4226 Froman, D. P., Pizzari, T., Feltmann, A. J., Castillo-Juarez, H., & Birkhead, T. R. (2002). Sperm
4227 mobility: Mechanisms of fertilizing efficiency, genetic variation and phenotypic
4228 relationship with male status in the domestic fowl, *Gallus gallus domesticus*. *Proceedings
4229 of the Royal Society of London. Series B: Biological Sciences*, 269(1491), 607–612.
4230 <https://doi.org/10.1098/rspb.2001.1925>

4231 Furukawa, F., Hamasaki, S., Hara, S., Uchimura, T., Shiraishi, E., Osafune, N., Takagi, H., Yazawa, T.,

4232 Kamei, Y., & Kitano, T. (2019). Heat shock factor 1 protects germ cell proliferation during

4233 early ovarian differentiation in medaka. *Scientific Reports*, 9(1), 6927.

4234 <https://doi.org/10.1038/s41598-019-43472-4>

4235 Gadella, B. M., & Luna, C. (2014). Cell biology and functional dynamics of the mammalian sperm

4236 surface. *Theriogenology*, 81(1), 74–84.

4237 <https://doi.org/10.1016/j.theriogenology.2013.09.005>

4238 Gage, M. J. G., Macfarlane, C. P., Yeates, S., Ward, R. G., Searle, J. B., & Parker, G. A. (2004).

4239 Spermatozoal Traits and Sperm Competition in Atlantic Salmon: Relative Sperm Velocity Is

4240 the Primary Determinant of Fertilization Success. *Current Biology*, 14(1), 44–47.

4241 <https://doi.org/10.1016/j.cub.2003.12.028>

4242 Gardner, D. K., Meseguer, M., Rubio, C., & Treff, N. R. (2015). Diagnosis of human preimplantation

4243 embryo viability. *Human Reproduction Update*, 21(6), 727–747.

4244 <https://doi.org/10.1093/humupd/dmu064>

4245 Ge, C., Lu, W., & Chen, A. (2017). Quantitative proteomic reveals the dynamic of protein profile

4246 during final oocyte maturation in zebrafish. *Biochemical and Biophysical Research*

4247 *Communications*, 490(3), 657–663. <https://doi.org/10.1016/j.bbrc.2017.06.093>

4248 Ge, S., Jung, D., & Yao, R. (2020). ShinyGO. 2628–2629.

4249 Gentleman, R. C., Carey, V. J., Bates, D. M., Bolstad, B., Dettling, M., Dudoit, S., Ellis, B., Gautier, L.,

4250 Ge, Y., Gentry, J., Hornik, K., Hothorn, T., Huber, W., Iacus, S., Irizarry, R., Leisch, F., Li, C.,

4251 Maechler, M., Rossini, A. J., ... Zhang, J. (2004). Bioconductor: Open software

4252 development for computational biology and bioinformatics. *Genome Biology*, 5(10), R80.

4253 <https://doi.org/10.1186/gb-2004-5-10-r80>

4254 Gibson, A. K., Delph, L. F., & Lively, C. M. (2017). The two-fold cost of sex: Experimental evidence

4255 from a natural system. *Evolution Letters*, 1(1), 6–15. <https://doi.org/10.1002/evl3.1>

4256 Gjedrem, T., & Baranski, M. (2009). The Success of Selective Breeding in Aquaculture. In T.
4257 Gjedrem & M. Baranski (Eds), *Selective Breeding in Aquaculture: An Introduction* (pp. 13–
4258 23). Springer Netherlands. https://doi.org/10.1007/978-90-481-2773-3_3

4259 Godden, A. M., Silva, W. T. A. F., Kiehl, B., Jolly, C., Folkes, L., Alavioon, G., & Immler, S. (2025).
4260 Environmentally induced variation in sperm sRNAs is linked to gene expression and
4261 transposable elements in zebrafish offspring. *Heredity*, 134(3), 234–246.
4262 <https://doi.org/10.1038/s41437-025-00752-2>

4263 Godmann, M., Lambrot, R., & Kimmins, S. (2009). The dynamic epigenetic program in male germ
4264 cells: Its role in spermatogenesis, testis cancer, and its response to the environment.
4265 *Microscopy Research and Technique*, 72(8), 603–619. <https://doi.org/10.1002/jemt.20715>

4266 González-Rojo, S., Fernández-Díez, C., Lombó, M., & Herráez, M. P. (2018a). Distribution of DNA
4267 damage in the sperm nucleus: A study of zebrafish as a model of histone-packaged
4268 chromatin. *Theriogenology*, 122, 109–115.
4269 <https://doi.org/10.1016/j.theriogenology.2018.08.017>

4270 Greenbaum, M. P., Iwamori, T., Buchold, G. M., & Matzuk, M. M. (2011). Germ Cell Intercellular
4271 Bridges. *Cold Spring Harbor Perspectives in Biology*, 3(8), a005850.
4272 <https://doi.org/10.1101/cshperspect.a005850>

4273 Griesinger, G., & Larsson, P. (2023). Conventional outcome reporting per IVF cycle/embryo
4274 transfer may systematically underestimate chances of success for women undergoing
4275 ART: Relevant biases in registries, epidemiological studies, and guidelines. *Human
4276 Reproduction Open*, 2023(2), hoad018. <https://doi.org/10.1093/hropen/hoad018>

4277 Groh, K. J., Nesatyy, V. J., Segner, H., Eggen, R. I. L., & Suter, M. J.-F. (2011a). Global proteomics
4278 analysis of testis and ovary in adult zebrafish (*Danio rerio*). *Fish Physiology and
4279 Biochemistry*, 37(3), 619–647. <https://doi.org/10.1007/s10695-010-9464-x>

4280 Guan, Y., Chen, Y., Huang, Q., He, Y., Li, X., Zhu, Z., Xiong, Y., Ouyang, J., Jiang, G., Zhang, Y., &
4281 Wang, C. (2025). Exploring heat stress responses and heat tolerance in rice in the

4282 reproductive stage: A dual omics approach. *Plant Growth Regulation*.

4283 <https://doi.org/10.1007/s10725-025-01352-0>

4284 Guo, Y., Jiang, W., Yu, W., Niu, X., Liu, F., Zhou, T., Zhang, H., Li, Y., Zhu, H., Zhou, Z., Sha, J., Guo, X., & Chen, D. (2019). Proteomics analysis of asthenozoospermia and identification of

4285 glucose-6-phosphate isomerase as an important enzyme for sperm motility. *Journal of*

4286 *Proteomics*, 208, 103478–103478. <https://doi.org/10.1016/J.JPROT.2019.103478>

4287 Hajam, Y. A., Rani, R., Sharma, P., Kumar, R., Verma, S. K., Hajam, Y. A., Rani, R., Sharma, P.,

4288 Kumar, R., & Verma, S. K. (2021). Zebrafish (*Danio rerio*): A Versatile Model for

4289 Reproductive Biology. *Recent Updates in Molecular Endocrinology and Reproductive*

4290 *Physiology of Fish*, 105–120. https://doi.org/10.1007/978-981-15-8369-8_8

4291 Harte, D. S. G., Lynch, A. M., Verma, J., Rees, P., Filby, A., Wills, J. W., & Johnson, G. E. (2024). A

4292 multi-biomarker micronucleus assay using imaging flow cytometry. *Archives of Toxicology*,

4293 98(9), 3137–3153. <https://doi.org/10.1007/s00204-024-03801-7>

4294 Hartig, F., Lohse, L., & leite, M. de S. (2024). *DHARMa: Residual Diagnostics for Hierarchical (Multi-*

4295 *Level / Mixed) Regression Models* (Version 0.4.7) [Computer software]. <https://cran.r-project.org/web/packages/DHARMa/index.html>

4296

4297

4298 Hashemita, M., Sabbagh, S., Orazizadeh, M., Ghadiri, A., & Bahmanzadeh, M. (2015). A

4299 proteomic analysis on human sperm tail: Comparison between normozoospermia and

4300 asthenozoospermia. *Journal of Assisted Reproduction and Genetics*, 32(6), 853–863.

4301 <https://doi.org/10.1007/s10815-015-0465-7>

4302 Haw, R. A., Croft, D., Yung, C. K., Ndegwa, N., D'Eustachio, P., Hermjakob, H., & Stein, L. D. (2011).

4303 The Reactome BioMart. *Database: The Journal of Biological Databases and Curation*,

4304 2011, bar031. <https://doi.org/10.1093/database/bar031>

4305 Hecht, N. B. (1998). Molecular mechanisms of male germ cell differentiation. *BioEssays*, 20(7),

4306 555–561. [https://doi.org/10.1002/\(SICI\)1521-1878\(199807\)20:7%253C555::AID-BIES6%253E3.0.CO;2-J](https://doi.org/10.1002/(SICI)1521-1878(199807)20:7%253C555::AID-BIES6%253E3.0.CO;2-J)

4308 Henkel, R. R., & Schill, W.-B. (2003). Sperm preparation for ART. *Reproductive Biology and*
4309 *Endocrinology*, 1(1), 108. <https://doi.org/10.1186/1477-7827-1-108>

4310 HFEA: UK fertility regulator. (2022). Human Fertilisation & Embryology Authority (HFEA).
4311 https://www.hfea.gov.uk/about-us/publications/research-and-data/fertility-treatment-2022-preliminary-trends-and-figures/?utm_source=chatgpt.com

4313 Hirokawa, N., & Tanaka, Y. (2015). Kinesin superfamily proteins (KIFs): Various functions and their
4314 relevance for important phenomena in life and diseases. *Experimental Cell Research*,
4315 334(1), 16–25. <https://doi.org/10.1016/j.yexcr.2015.02.016>

4316 Hoang-Thi, A. P., Dang-Thi, A. T., Phan-Van, S., Nguyen-Ba, T., Truong-Thi, P. L., Le-Minh, T.,
4317 Nguyen-Vu, Q. H., & Nguyen-Thanh, T. (2022). The Impact of High Ambient Temperature
4318 on Human Sperm Parameters: A Meta-Analysis. *Iranian Journal of Public Health*, 51(4),
4319 710–710. <https://doi.org/10.18502/IJPH.V51I4.9232>

4320 Hoo, J. Y., Kumari, Y., Shaikh, M. F., Hue, S. M., & Goh, B. H. (2016). Zebrafish: A Versatile Animal
4321 Model for Fertility Research. *BioMed Research International*, 2016(1), 9732780.
4322 <https://doi.org/10.1155/2016/9732780>

4323 Hourcade, J. D., Pérez-Crespo, M., Fernández-González, R., Pintado, B., & Gutiérrez-Adán, A.
4324 (2010). Selection against spermatozoa with fragmented DNA after postovulatory mating
4325 depends on the type of damage. *Reproductive Biology and Endocrinology*, 8(1), 9.
4326 <https://doi.org/10.1186/1477-7827-8-9>

4327 Houston, B. J., Nixon, B., Martin, J. H., De Iuliis, G. N., Trigg, N. A., Bromfield, E. G., McEwan, K. E.,
4328 & Aitken, R. J. (2018). Heat exposure induces oxidative stress and DNA damage in the
4329 male germ line. *Biology of Reproduction*, 98(4), 593–606.
4330 <https://doi.org/10.1093/biolre/roy009>

4331 Howe, K., Clark, M. D., Torroja, C. F., Torrance, J., Berthelot, C., Muffato, M., Collins, J. E.,
4332 Humphray, S., McLaren, K., Matthews, L., McLaren, S., Sealy, I., Caccamo, M., Churcher,
4333 C., Scott, C., Barrett, J. C., Koch, R., Rauch, G. J., White, S., ... Stemple, D. L. (2013). The

4334 zebrafish reference genome sequence and its relationship to the human genome. *Nature*,
4335 496(7446), 498–503. <https://doi.org/10.1038/NATURE12111>

4336 Hsia, L., Ashley, N., Ouaret, D., Wang, L. M., Wilding, J., & Bodmer, W. F. (2016). Myofibroblasts
4337 are distinguished from activated skin fibroblasts by the expression of AOC3 and other
4338 associated markers. *Proceedings of the National Academy of Sciences*, 113(15), E2162–
4339 E2171. <https://doi.org/10.1073/pnas.1603534113>

4340 Hu, L., Du, J., Lv, H., Zhao, J., Chen, M., Wang, Y., Wu, F., Liu, F., Chen, X., Zhang, J., Ma, H., Jin, G.,
4341 Shen, H., Chen, L., Ling, X., & Hu, Z. (2018). Influencing factors of pregnancy loss and
4342 survival probability of clinical pregnancies conceived through assisted reproductive
4343 technology. *Reproductive Biology and Endocrinology : RB&E*, 16, 74.
4344 <https://doi.org/10.1186/s12958-018-0390-6>

4345 Hughes, J. S., & Otto, S. P. (1999). Ecology and the evolution of biphasic life cycles. *American
4346 Naturalist*, 154(3), 306–320.
4347 <https://doi.org/10.1086/303241/ASSET/IMAGES/LARGE/FG5.JPG>

4348 Huszar, G., Jakab, A., Sakkas, D., Ozenci, C.-C., Cayli, S., Delpiano, E., & Ozkavukcu, S. (2007).
4349 Fertility testing and ICSI sperm selection by hyaluronic acid binding: Clinical and genetic
4350 aspects. *Reproductive BioMedicine Online*, 14(5), 650–663.
4351 [https://doi.org/10.1016/S1472-6483\(10\)61060-7](https://doi.org/10.1016/S1472-6483(10)61060-7)

4352 Immler, S. (2019). Haploid Selection in ‘diploid’ Organisms. *Annual Review of Ecology, Evolution,
4353 and Systematics*, 50, 219–236. <https://doi.org/10.1146/annurev-ecolsys-110218-024709>

4354 Immler, S., Hotzy, C., Alavioon, G., Petersson, E., & Arnqvist, G. (2014). Sperm variation within a
4355 single ejaculate affects offspring development in atlantic salmon. *Biology Letters*, 10(2).
4356 <https://doi.org/10.1098/rsbl.2013.1040>

4357 Immler, S., & Otto, S. P. (2018). The evolutionary consequences of selection at the haploid
4358 gametic stage. *American Naturalist*, 192(2), 241–249.
4359 <https://doi.org/10.1086/698483/ASSET/IMAGES/LARGE/FG1.JPG>

4360 Inaba, K. (2011). Sperm flagella: Comparative and phylogenetic perspectives of protein
4361 components. *Molecular Human Reproduction*, 17(8), 524–538.
4362 <https://doi.org/10.1093/molehr/gar034>

4363 Intasqui, P., Agarwal, A., Sharma, R., Samanta, L., & Bertolla, R. P. (2018). Towards the
4364 identification of reliable sperm biomarkers for male infertility: A sperm proteomic
4365 approach. *Andrologia*, 50(3), e12919. <https://doi.org/10.1111/and.12919>

4366 Irish, S. D., Sutter, A., Pinzoni, L., Sydney, M. C., Travers, L., Murray, D., de Coriolis, J.-C., & Immler,
4367 S. (2024). Heatwave-Induced Paternal Effects Have Limited Adaptive Benefits in Offspring.
4368 *Ecology and Evolution*, 14(10), e70399. <https://doi.org/10.1002/ece3.70399>

4369 Jasim, S. (2021). Thyroid Hormones in Male Reproduction and Fertility. *AACE Clinical Case Reports*,
4370 7(1), 1.

4371 Jayakodi, M., Lee, S.-C., & Yang, T.-J. (2019). Comparative transcriptome analysis of heat stress
4372 responsiveness between two contrasting ginseng cultivars. *Journal of Ginseng Research*,
4373 43(4), 572–579. <https://doi.org/10.1016/j.jgr.2018.05.007>

4374 Jenkins, C. D., & Kirkpatrick, M. (1995). DELETERIOUS MUTATION AND THE EVOLUTION OF
4375 GENETIC LIFE CYCLES. *Evolution*, 49(3), 512–520. [5646.1995.TB02283.X](https://doi.org/10.1111/J.1558-
4376 5646.1995.TB02283.X)

4377 Jenkins, T. G., & Carrell, D. T. (2012). The sperm epigenome and potential implications for the
4378 developing embryo. *REPRODUCTION*, 143(6), 727–734. [https://doi.org/10.1530/REP-11-0450](https://doi.org/10.1530/REP-11-
4379 0450)

4380 Jin, Y. H., Davie, A., & Migaud, H. (2019). Temperature-induced testicular germ cell loss and
4381 recovery in Nile tilapia *Oreochromis niloticus*. *General and Comparative Endocrinology*,
4382 283, 113227. <https://doi.org/10.1016/j.ygcen.2019.113227>

4383 Jono, H., & Ando, Y. (2010). Midkine: A Novel Prognostic Biomarker for Cancer. *Cancers*, 2(2),
4384 Article 2. <https://doi.org/10.3390/cancers2020624>

4385 Joseph, S. B., & Kirkpatrick, M. (2004). Haploid selection in animals. *Trends in Ecology & Evolution*,
4386 19(11), 592–597. <https://doi.org/10.1016/J.TREE.2004.08.004>

4387 Kalra, S. K., & Molinaro, T. A. (2008). The association of in vitro fertilization and perinatal
4388 morbidity. *Seminars in Reproductive Medicine*, 26(5), 423–435. <https://doi.org/10.1055/s-0028-1087108>

4390 Karhemo, P.-R., Ravela, S., Laakso, M., Ritamo, I., Tatti, O., Mäkinen, S., Goodison, S., Stenman, U.-
4391 H., Hölttä, E., Hautaniemi, S., Valmu, L., Lehti, K., & Laakkonen, P. (2012). An optimized
4392 isolation of biotinylated cell surface proteins reveals novel players in cancer metastasis.
4393 *Journal of Proteomics*, 77, 87–100. <https://doi.org/10.1016/j.jprot.2012.07.009>

4394 Kashir, J. (2020). Increasing associations between defects in phospholipase C zeta and conditions
4395 of male infertility: Not just ICSI failure? *Journal of Assisted Reproduction and Genetics*,
4396 37(6), 1273–1293. <https://doi.org/10.1007/s10815-020-01748-z>

4397 Kastelic, J. P., & Rizzoto, G. (2021). Thermoregulation of the Testes. In *Bovine Reproduction* (pp.
4398 40–46). John Wiley & Sons, Ltd. <https://doi.org/10.1002/9781119602484.ch4>

4399 Khan, S., & Mishra, R. K. (2024). Multigenerational Effect of Heat Stress on the *Drosophila*
4400 *melanogaster* Sperm Proteome. *Journal of Proteome Research*, 23(6), 2265–2278.
4401 <https://doi.org/10.1021/acs.jproteome.4c00205>

4402 Kim, E., Yamashita, M., Kimura, M., Honda, A., Kashiwabara, S., & Baba, T. (2008). Sperm
4403 penetration through cumulus mass and zona pellucida. *The International Journal of
4404 Developmental Biology*, 52(5–6), 677–682. <https://doi.org/10.1387/ijdb.072528ek>

4405 Kincaid, H. L. (1983). Inbreeding in fish populations used for aquaculture. *Aquaculture*, 33(1), 215–
4406 227. [https://doi.org/10.1016/0044-8486\(83\)90402-7](https://doi.org/10.1016/0044-8486(83)90402-7)

4407 Kleshchev, M., Osadchuk, A., & Osadchuk, L. (2021). Impaired semen quality, an increase of sperm
4408 morphological defects and DNA fragmentation associated with environmental pollution in
4409 urban population of young men from Western Siberia, Russia. *PLOS ONE*, 16(10),
4410 e0258900. <https://doi.org/10.1371/journal.pone.0258900>

4411 Kleshchev, M., Osadchuk, L., & Osadchuk, A. (2023). Age-Related Changes in Sperm Morphology
4412 and Analysis of Multiple Sperm Defects. *Frontiers in Bioscience-Scholar*, 15(3), 12.
4413 <https://doi.org/10.31083/j.fbs1503012>

4414 Kobayashi, D., Koshida, S., Moriai, R., Tsuji, N., & Watanabe, N. (2007). Olfactomedin 4 promotes
4415 S-phase transition in proliferation of pancreatic cancer cells. *Cancer Science*, 98(3), 334–
4416 340. <https://doi.org/10.1111/j.1349-7006.2007.00397.X>

4417 Kropp, J., Carrillo, J. A., Namous, H., Daniels, A., Salih, S. M., Song, J., & Khatib, H. (2017). Male
4418 fertility status is associated with DNA methylation signatures in sperm and transcriptomic
4419 profiles of bovine preimplantation embryos. *BMC Genomics*, 18(1), 280.
4420 <https://doi.org/10.1186/s12864-017-3673-y>

4421 Krueger-Hadfield, S. A. (2024). Let's talk about sex: Why reproductive systems matter for
4422 understanding algae. *Journal of Phycology*, 60(3), 581–597.
4423 <https://doi.org/10.1111/jpy.13462>

4424 Kumar, N. (2022). Sperm Mitochondria, the Driving Force Behind Human Spermatozoa Activities:
4425 Its Functions and Dysfunctions—A Narrative Review. *Current Molecular Medicine*, 23(4),
4426 332–340. <https://doi.org/10.2174/156652402266220408104047>

4427 Kumar, N., & Singh, A. K. (2021). The anatomy, movement, and functions of human sperm tail: An
4428 evolving mystery. *Biology of Reproduction*, 104(3), 508–520.
4429 <https://doi.org/10.1093/biolre/ioaa213>

4430 Lahnsteiner, F. (2012). Thermotolerance of brown trout, *Salmo trutta*, gametes and embryos to
4431 increased water temperatures. *Journal of Applied Ichthyology*, 28(5), 745–751.
4432 <https://doi.org/10.1111/j.1439-0426.2012.01934.x>

4433 Lefebvre, R., & Suarez, S. S. (1996). Effect of Capacitation on Bull Sperm Binding to Homologous
4434 Oviductal Epithelium1. *Biology of Reproduction*, 54(3), 575–582.
4435 <https://doi.org/10.1095/biolreprod54.3.575>

4436 Levine, H., Jørgensen, N., Martino-Andrade, A., Mendiola, J., Weksler-Derri, D., Jolles, M., Pinotti,
4437 R., & Swan, S. H. (2023). Temporal trends in sperm count: A systematic review and meta-
4438 regression analysis of samples collected globally in the 20th and 21st centuries. *Human
4439 Reproduction Update*, 29(2), 157–176. <https://doi.org/10.1093/humupd/dmac035>

4440 Li, Z., Xian, H., Ye, R., Zhong, Y., Liang, B., Huang, Y., Dai, M., Guo, J., Tang, S., Ren, X., Bai, R., Feng,
4441 Y., Deng, Y., Yang, X., Chen, D., Yang, Z., & Huang, Z. (2024). Gender-specific effects of
4442 polystyrene nanoplastic exposure on triclosan-induced reproductive toxicity in zebrafish
4443 (*Danio rerio*). *Science of The Total Environment*, 932, 172876.
4444 <https://doi.org/10.1016/j.scitotenv.2024.172876>

4445 Liang, J., Zheng, Y., Zeng, W., Chen, L., Yang, S., Du, P., Wang, Y., Yu, X., & Zhang, X. (2021).
4446 Comparison of proteomic profiles from the testicular tissue of males with impaired and
4447 normal spermatogenesis. *Systems Biology in Reproductive Medicine*, 67(2), 127–136.
4448 <https://doi.org/10.1080/19396368.2020.1846822>

4449 Lim, M. Y.-T., & Bernier, N. J. (2022). Zebrafish parental progeny investment in response to cycling
4450 thermal stress and hypoxia: Deposition of heat shock proteins but not cortisol. *Journal of
4451 Experimental Biology*, 225(21), jeb244715. <https://doi.org/10.1242/jeb.244715>

4452 Lindemann, C. B., & Lesich, K. A. (2016). Functional anatomy of the mammalian sperm flagellum.
4453 *Cytoskeleton*, 73(11), 652–669. <https://doi.org/10.1002/cm.21338>

4454 Lindsley, D. L., & Grell, E. H. (1969). Spermiogenesis without chromosomes in *Drosophila
4455 melanogaster*. *Genetics*, 61(1), Suppl:69–78.

4456 Lismér, A., & Kimmins, S. (2023). Emerging evidence that the mammalian sperm epigenome
4457 serves as a template for embryo development. *Nature Communications*, 14(1), 2142.
4458 <https://doi.org/10.1038/s41467-023-37820-2>

4459 Liu, F., Qiu, Y., Zou, Y., Deng, Z.-H., Yang, H., & Liu, D. Y. (2011). Use of zona pellucida-bound
4460 sperm for intracytoplasmic sperm injection produces higher embryo quality and

4461 implantation than conventional intracytoplasmic sperm injection. *Fertility and Sterility*,
4462 95(2), 815–818. <https://doi.org/10.1016/j.fertnstert.2010.09.015>

4463 Liu, W., Lee, H. W., Liu, Y., Wang, R., & Rodgers, G. P. (2010). Olfactomedin 4 is a novel target
4464 gene of retinoic acids and 5-aza-2'-deoxycytidine involved in human myeloid leukemia cell
4465 growth, differentiation, and apoptosis. *Blood*, 116(23), 4938–4947.
4466 <https://doi.org/10.1182/BLOOD-2009-10-246439>

4467 Lively, C. M., & Morran, L. T. (2014). The ecology of sexual reproduction. *Journal of Evolutionary
4468 Biology*, 27(7), 1292–1303. <https://doi.org/10.1111/jeb.12354>

4469 Lo, J., Lee, S., Xu, M., Liu, F., Ruan, H., Eun, A., He, Y., Ma, W., Wang, W., Wen, Z., & Peng, J.
4470 (2003). 15000 unique zebrafish EST clusters and their future use in microarray for profiling
4471 gene expression patterns during embryogenesis. *Genome Research*, 13(3), 455–466.
4472 <https://doi.org/10.1101/gr.885403>

4473 López-Galindo, L., Juárez, O. E., Larios-Soriano, E., Vecchio, G. D., Ventura-López, C., Lago-Lestón,
4474 A., & Galindo-Sánchez, C. (2019). Transcriptomic analysis reveals insights on male
4475 infertility in octopus maya under chronic thermal stress. *Frontiers in Physiology*, 9,
4476 428692–428692. [https://doi.org/10.3389/FPHYS.2018.01920/BIBTEX](https://doi.org/10.3389/FPHYS.2018.01920)

4477 Love, M. I., Huber, W., & Anders, S. (2014). Moderated estimation of fold change and dispersion
4478 for RNA-seq data with DESeq2. *Genome Biology*, 15(12), 550.
4479 <https://doi.org/10.1186/s13059-014-0550-8>

4480 Luo, M., Su, T., Wang, S., Chen, J., Lin, T., Cheng, Q., Chen, Y., Gong, M., Yang, H., Li, F., & Zhang, Y.
4481 (2022). Proteomic Landscape of Human Spermatozoa: Optimized Extraction Method and
4482 Application. *Cells*, 11(24), Article 24. <https://doi.org/10.3390/cells11244064>

4483 Lüpold, S., & Pitnick, S. (2018). *Sperm form and function: What do we know about the role of
4484 sexual selection?* <https://doi.org/10.1530/REP-17-0536>

4485 Lyon, M. F., Glenister, P. H., & Hawker, S. G. (1972). Do the H-2 and T-Loci of the Mouse have a
4486 Function in the Haploid Phase of Sperm ? *Nature*, 240(5377), 152–153.
4487 <https://doi.org/10.1038/240152b0>

4488 Ma, D.-D., Wang, D.-H., & Yang, W.-X. (2017). Kinesins in spermatogenesis†. *Biology of*
4489 *Reproduction*, 96(2), 267–276. <https://doi.org/10.1095/biolreprod.116.144113>

4490 Mable, B. K., & Otto, S. P. (1998). The evolution of life cycles with haploid and diploid phases.
4491 *BioEssays*, 20, 453–462. [https://doi.org/10.1002/\(SICI\)1521-1878\(199806\)20:6](https://doi.org/10.1002/(SICI)1521-1878(199806)20:6)

4492 Mable, B. K., & Otto, S. P. (2001). Masking and purging mutations following EMS treatment in
4493 haploid, diploid and tetraploid yeast (*Saccharomyces cerevisiae*). *Genet. Res., Camb*, 77,
4494 9–26. <https://doi.org/10.1017/S0016672300004821>

4495 Magdanz, V., Boryshpolets, S., Ridzewski, C., Eckel, B., & Reinhardt, K. (2019). The motility-based
4496 swim-up technique separates bull sperm based on differences in metabolic rates and tail
4497 length. *PLoS One*, 14(10), e0223576. <https://doi.org/10.1371/journal.pone.0223576>

4498 Mahanty, A., Purohit, G. K., Mohanty, S., & Mohanty, B. P. (2019). Heat stress–induced alterations
4499 in the expression of genes associated with gonadal integrity of the teleost *Puntius*
4500 *sophore*. *Fish Physiology and Biochemistry*, 45(4), 1409–1417.
4501 <https://doi.org/10.1007/s10695-019-00643-4>

4502 Marcu, D. (2024). *Linking sperm genotype to phenotype: Exploring the underlying mechanisms of*
4503 *haploid gametic selection* [Doctoral, University of East Anglia. School of Biological
4504 Sciences]. <https://ueaepprints.uea.ac.uk/id/eprint/95705/>

4505 Marcu, D., Cohen-Krais, J., Godden, A., Alavioon, G., Martins, C., Almstrup, K., Saalbach, G., &
4506 Immller, S. (2024). *Within-ejaculate haploid selection reduces disease biomarkers in human*
4507 *sperm* (p. 2024.10.08.617222). bioRxiv. <https://doi.org/10.1101/2024.10.08.617222>

4508 Martin-DeLeon, P. A. (2006). Epididymal SPAM1 and its impact on sperm function. *Molecular and*
4509 *Cellular Endocrinology*, 250(1), 114–121. <https://doi.org/10.1016/j.mce.2005.12.033>

4510 Martínez-Heredia, J., de Mateo, S., Vidal-Taboada, J. M., Ballescà, J. L., & Oliva, R. (2008).
4511 Identification of proteomic differences in asthenozoospermic sperm samples. *Human*
4512 *Reproduction*, 23(4), 783–791. <https://doi.org/10.1093/humrep/den024>

4513 Masuda, T., Tomita, M., & Ishihama, Y. (2008). Phase transfer surfactant-aided trypsin digestion
4514 for membrane proteome analysis. *Journal of Proteome Research*, 7(2), 731–740.
4515 <https://doi.org/10.1021/pr700658q>

4516 McDowell, S., Kroon, B., Ford, E., Hook, Y., Glujsovsky, D., & Yazdani, A. (2014). Advanced sperm
4517 selection techniques for assisted reproduction. *The Cochrane Database of Systematic*
4518 *Reviews*, 10, CD010461. <https://doi.org/10.1002/14651858.CD010461.pub2>

4519 McShane, L. M., Cavenagh, M. M., Lively, T. G., Eberhard, D. A., Bigbee, W. L., Williams, P. M.,
4520 Mesirov, J. P., Polley, M.-Y. C., Kim, K. Y., Tricoli, J. V., Taylor, J. M. G., Shuman, D. J.,
4521 Simon, R. M., Doroshow, J. H., & Conley, B. A. (2013). Criteria for the use of omics-based
4522 predictors in clinical trials. *Nature*, 502(7471), 317–320.
4523 <https://doi.org/10.1038/nature12564>

4524 Meyers, J. R. (2018). Zebrafish: Development of a Vertebrate Model Organism. *Current Protocols*
4525 *in Essential Laboratory Techniques*, 16(1), 1–26. <https://doi.org/10.1002/cpet.19>

4526 Michod, R. E., & Gayley, T. W. (1992). Masking of Mutations and the Evolution of Sex.
4527 [Https://Doi.Org/10.1086/285354](https://doi.org/10.1086/285354), 139(4), 706–734. <https://doi.org/10.1086/285354>

4528 Miller, D., & Ostermeier, G. C. (2006). Towards a better understanding of RNA carriage by
4529 ejaculate spermatozoa. *Human Reproduction Update*, 12(6), 757–767.
4530 <https://doi.org/10.1093/humupd/dml037>

4531 Moreno Acosta, O. D., Boan, A. F., Hattori, R. S., & Fernandino, J. I. (2023). Notch pathway is
4532 required for protection against heat stress in spermatogonial stem cells in medaka. *Fish*
4533 *Physiology and Biochemistry*, 49(3), 487–500. <https://doi.org/10.1007/s10695-023-01200->
4534 w

4535 Moritz, L., & Hammoud, S. S. (2022). The Art of Packaging the Sperm Genome: Molecular and
4536 Structural Basis of the Histone-To-Protamine Exchange. *Frontiers in Endocrinology*, 13.
4537 <https://doi.org/10.3389/fendo.2022.895502>

4538 Morrow, E. H., & Gage, M. J. G. (2001). Consistent significant variation between individual males
4539 in spermatozoal morphometry. *Journal of Zoology*, 254(2), 147–153.
4540 <https://doi.org/10.1017/S0952836901000656>

4541 Mu, H., Ke, S., Zhang, D., Zhang, Y., Song, X., Yu, Z., Zhang, Y., & Qiu, J. (2020). The Sperm
4542 Proteome of the Oyster *Crassostrea hongkongensis*. *PROTEOMICS*, 20(19–20), 2000167–
4543 2000167. <https://doi.org/10.1002/pmic.202000167>

4544 Muller, H. J., & Settles, F. (1927). The non-functioning of the genes in spermatozoa. *Zeitschrift Für
4545 Induktive Abstammungs- Und Vererbungslehre*, 43(1), 285–312.
4546 <https://doi.org/10.1007/BF01741012>

4547 Nanba, R., Fujita, N., & Nagata, S. (2010). Structure and expression of *myelin basic protein* gene
4548 products in *Xenopus laevis*. *Gene*, 459(1), 32–38.
4549 <https://doi.org/10.1016/j.gene.2010.03.010>

4550 Naqvi, S. M. K., Kumar, D., Paul, R. Kr., & Sejian, V. (2012). Environmental Stresses and Livestock
4551 Reproduction. In V. Sejian, S. M. K. Naqvi, T. Ezeji, J. Lakritz, & R. Lal (Eds), *Environmental
4552 Stress and Amelioration in Livestock Production* (pp. 97–128). Springer.
4553 https://doi.org/10.1007/978-3-642-29205-7_5

4554 Nguyen, T. M., Bressac, C., & Chevrier, C. (2013). Heat stress affects male reproduction in a
4555 parasitoid wasp. *Journal of Insect Physiology*, 59(3), 248–254.
4556 <https://doi.org/10.1016/j.jinsphys.2012.12.001>

4557 Nixon, B., Schjenken, J. E., Burke, N. D., Skerrett-Byrne, D. A., Hart, H. M., De Iuliis, G. N., Martin, J.
4558 H., Lord, T., & Bromfield, E. G. (2023). New horizons in human sperm selection for assisted
4559 reproduction. *Frontiers in Endocrinology*, 14.
4560 <https://doi.org/10.3389/fendo.2023.1145533>

4561 Noguchi, M., Yoshioka, K., Hikono, H., Iwagami, G., Suzuki, C., & Kikuchi, K. (2015). Centrifugation
4562 on Percoll density gradient enhances motility, membrane integrity and in vitro fertilizing
4563 ability of frozen–thawed boar sperm. *Zygote*, 23(1), 68–75.
4564 <https://doi.org/10.1017/S0967199413000208>

4565 Nolte, H., Konzer, A., Ruhs, A., Jungblut, B., Braun, T., & Krüger, M. (2014). Global Protein
4566 Expression Profiling of Zebrafish Organs Based on in Vivo Incorporation of Stable Isotopes.
4567 *Journal of Proteome Research*, 13(4), 2162–2174. <https://doi.org/10.1021/pr5000335>

4568 Nynca, J., Arnold, G. J., Fröhlich, T., Otte, K., & Ciereszko, A. (2014). Proteomic identification of
4569 rainbow trout sperm proteins. *Proteomics*, 14(12), 1569–1573.
4570 <https://doi.org/10.1002/PMIC.201300521>

4571 Oatley, J. M., & Brinster, R. L. (2012). The Germline Stem Cell Niche Unit in Mammalian Testes.
4572 *Physiological Reviews*, 92(2), 577–595. <https://doi.org/10.1152/physrev.00025.2011>

4573 O’Flaherty, C., & Matsushita-Fournier, D. (2017). Reactive oxygen species and protein
4574 modifications in spermatozoa†. *Biology of Reproduction*, 97(4), 577–585.
4575 <https://doi.org/10.1093/biolre/iox104>

4576 O’Leary, N. A., Wright, M. W., Brister, J. R., Ciufo, S., Haddad, D., McVeigh, R., Rajput, B.,
4577 Robbertse, B., Smith-White, B., Ako-Adjei, D., Astashyn, A., Badretdin, A., Bao, Y.,
4578 Blinkova, O., Brover, V., Chetvernin, V., Choi, J., Cox, E., Ermolaeva, O., ... Pruitt, K. D.
4579 (2016). Reference sequence (RefSeq) database at NCBI: current status, taxonomic
4580 expansion, and functional annotation. *Nucleic Acids Research*, 44(D1), D733–D745.
4581 <https://doi.org/10.1093/NAR/GKV1189>

4582 Oseguera-López, I., Ruiz-Díaz, S., Ramos-Ibeas, P., & Pérez-Cerezales, S. (2019). Novel Techniques
4583 of Sperm Selection for Improving IVF and ICSI Outcomes. *Frontiers in Cell and
4584 Developmental Biology*, 7. <https://doi.org/10.3389/fcell.2019.00298>

4585 Ostermeier, G. C., Miller, D., Huntriss, J. D., Diamond, M. P., & Krawetz, S. A. (2004). Delivering
4586 spermatozoan RNA to the oocyte. *Nature*, 429(6988), 154–154.
4587 <https://doi.org/10.1038/429154a>

4588 Otto, S. P., & Goldstein, D. B. (1992). Recombination and the evolution of diploidy. *Genetics*,
4589 131(3), 745–751. <https://doi.org/10.1093/GENETICS/131.3.745>

4590 Otto, S. P., & Lenormand, T. (2002). Resolving the paradox of sex and recombination. *Nature
4591 Reviews Genetics*, 3(4), 252–261. <https://doi.org/10.1038/nrg761>

4592 Otto, S. P., & Marks, J. C. (1996). Mating systems and the evolutionary transition between
4593 haploidy and diploidy. *Biological Journal of the Linnean Society*, 57(3), 197–218.
4594 <https://doi.org/10.1111/j.1095-8312.1996.tb00309.x>

4595 Pagel, O., Kollipara, L., & Sickmann, A. (2021). Tandem Mass Tags for Comparative and Discovery
4596 Proteomics. In K. Marcus, M. Eisenacher, & B. Sitek (Eds), *Quantitative Methods in
4597 Proteomics* (pp. 117–131). Springer US. https://doi.org/10.1007/978-1-0716-1024-4_9

4598 Palermo, G. D., O'Neill, C. L., Chow, S., Cheung, S., Parrella, A., Pereira, N., & Rosenwaks, Z. (2017).
4599 Intracytoplasmic sperm injection: State of the art in humans. *Reproduction (Cambridge,
4600 England)*, 154(6), F93–F110. <https://doi.org/10.1530/REP-17-0374>

4601 Palermo, G., Joris, H., Devroey, P., & Van Steirteghem, A. C. (1992). Pregnancies after
4602 intracytoplasmic injection of single spermatozoon into an oocyte. *The Lancet*, 340(8810),
4603 17–18. [https://doi.org/10.1016/0140-6736\(92\)92425-F](https://doi.org/10.1016/0140-6736(92)92425-F)

4604 Pandruvada, S., Royzman, R., Shah, T. A., Sindhwan, P., Dupree, J. M., Schon, S., & Avidor-Reiss, T.
4605 (2021). Lack of trusted diagnostic tools for undetermined male infertility. *Journal of
4606 Assisted Reproduction and Genetics*, 38(2), 265–276. [https://doi.org/10.1007/s10815-020-02037-5](https://doi.org/10.1007/s10815-
4607 020-02037-5)

4608 Pankhurst, N. W., & Munday, P. L. (2011). Effects of climate change on fish reproduction and early
4609 life history stages. *Marine and Freshwater Research*, 62(9), 1015–1026.
4610 <https://doi.org/10.1071/MF10269>

4611 Panner Selvam, M. K., Baskaran, S., & Agarwal, A. (2019). Chapter Six - Proteomics of
4612 reproduction: Prospects and perspectives. In G. S. Makowski (Ed.), *Advances in Clinical*
4613 *Chemistry* (Vol. 92, pp. 217–243). Elsevier. <https://doi.org/10.1016/bs.acc.2019.04.005>

4614 Parker, G. A. (1970). Sperm Competition and Its Evolutionary Consequences in the Insects.
4615 *Biological Reviews*, 45(4), 525–567. <https://doi.org/10.1111/j.1469-185X.1970.tb01176.x>

4616 Parker, G. A. (1982). Why are there so many tiny sperm? Sperm competition and the maintenance
4617 of two sexes. *Journal of Theoretical Biology*, 96(2), 281–294.
4618 [https://doi.org/10.1016/0022-5193\(82\)90225-9](https://doi.org/10.1016/0022-5193(82)90225-9)

4619 Parker, G. A., Baker, R. R., & Smith, V. G. F. (1972). The origin and evolution of gamete
4620 dimorphism and the male-female phenomenon. *Journal of Theoretical Biology*, 36(3),
4621 529–553. [https://doi.org/10.1016/0022-5193\(72\)90007-0](https://doi.org/10.1016/0022-5193(72)90007-0)

4622 Parkes, R., & Garcia, T. X. (2024). Bringing proteomics to bear on male fertility: Key lessons. *Expert*
4623 *Review of Proteomics*, 21(4), 181–203. <https://doi.org/10.1080/14789450.2024.2327553>

4624 Paul, C., Murray, A. A., Spears, N., & Saunders, P. T. K. (2008). A single, mild, transient scrotal heat
4625 stress causes DNA damage, subfertility and impairs formation of blastocysts in mice.
4626 *Reproduction (Cambridge, England)*, 136(1), 73–84. <https://doi.org/10.1530/REP-08-0036>

4627 Pérez-Cerezales, S., Laguna-Barraza, R., de Castro, A. C., Sánchez-Calabuig, M. J., Cano-Oliva, E., de
4628 Castro-Pita, F. J., Montoro-Buils, L., Pericuesta, E., Fernández-González, R., & Gutiérrez-
4629 Adán, A. (2018). Sperm selection by thermotaxis improves ICSI outcome in mice. *Scientific*
4630 *Reports*, 8(1), 2902. <https://doi.org/10.1038/s41598-018-21335-8>

4631 Perrot, V., Richerd, S., & Valéro, M. (1991). Transition from haploidy to diploidy. *Nature* 1991
4632 351:6324, 351(6324), 315–317. <https://doi.org/10.1038/351315a0>

4633 Pini, T., Parks, J., Russ, J., Dzieciatkowska, M., Hansen, K. C., Schoolcraft, W. B., & Katz-Jaffe, M.
4634 (2020). Obesity significantly alters the human sperm proteome, with potential
4635 implications for fertility. *Journal of Assisted Reproduction and Genetics*, 37(4), 777–787.
4636 <https://doi.org/10.1007/S10815-020-01707-8/FIGURES/2>

4637 Purchase, C. F., Evans, J. P., & Roncal, J. (2021). *Integrating natural and sexual selection across the*
4638 *biphasic life cycle*. 1–33. <https://doi.org/10.32942/OSF.IO/EU3AM>

4639 Quill, T. A., Sugden, S. A., Rossi, K. L., Doolittle, L. K., Hammer, R. E., & Garbers, D. L. (2003).

4640 Hyperactivated sperm motility driven by CatSper2 is required for fertilization. *Proceedings*
4641 *of the National Academy of Sciences of the United States of America*, 100(25), 14869–
4642 14874. <https://doi.org/10.1073/pnas.2136654100>

4643 R Core Team. (2017). *R: The R Project for Statistical Computing*. <https://www.r-project.org/>

4644 Rahman, M. B., Schellander, K., Luceño, N. L., & Van Soom, A. (2018). Heat stress responses in
4645 spermatozoa: Mechanisms and consequences for cattle fertility. *Theriogenology*, 113,
4646 102–112. <https://doi.org/10.1016/j.theriogenology.2018.02.012>

4647 Ramón, M., Jiménez-Rabadán, P., García-Álvarez, O., Maroto-Morales, A., Soler, A., Fernández-
4648 Santos, M., Pérez-Guzmán, M., & Garde, J. (2014). Understanding Sperm Heterogeneity:
4649 Biological and Practical Implications. *Reproduction in Domestic Animals*, 49(s4), 30–36.
4650 <https://doi.org/10.1111/rda.12404>

4651 Ren, C., Chen, Y., Tang, J., Wang, P., Zhang, Y., Li, C., Zhang, Z., & Cheng, X. (2023). TMT-Based
4652 Comparative Proteomic Analysis of the Spermatozoa of Buck (*Capra hircus*) and Ram (*Ovis*
4653 *aries*). *Genes*, 14(5), Article 5. <https://doi.org/10.3390/genes14050973>

4654 Ribas-Maynou, J., Yeste, M., Becerra-Tomás, N., Aston, K. I., James, E. R., & Salas-Huetos, A.
4655 (2021). Clinical implications of sperm DNA damage in IVF and ICSI: Updated systematic
4656 review and meta-analysis. *Biological Reviews*, 96(4), 1284–1300.
4657 <https://doi.org/10.1111/brv.12700>

4658 Rizzoto, G., Boe-Hansen, G., Klein, C., Thundathil, J. C., & Kastelic, J. P. (2020). Acute mild heat
4659 stress alters gene expression in testes and reduces sperm quality in mice. *Theriogenology*,
4660 158, 375–381. <https://doi.org/10.1016/J.THERIOGENOLOGY.2020.10.002>

4661 Robinson, B. R., Netherton, J. K., Ogle, R. A., & Baker, M. A. (2023). Testicular heat stress, a
4662 historical perspective and two postulates for why male germ cells are heat sensitive.
4663 *Biological Reviews*, 98(2), 603–622. <https://doi.org/10.1111/brv.12921>

4664 Robles, V., Herráez, P., Labbé, C., Cabrita, E., Pšenička, M., Valcarce, D. G., & Riesco, M. F. (2017).
4665 Molecular basis of spermatogenesis and sperm quality. *General and Comparative*
4666 *Endocrinology*, 245, 5–9. <https://doi.org/10.1016/j.ygcen.2016.04.026>

4667 Rohmer, C., David, J. R., Moreteau, B., & Joly, D. (2004). Heat induced male sterility in *Drosophila*
4668 *melanogaster*: Adaptive genetic variations among geographic populations and role of the
4669 Y chromosome. *Journal of Experimental Biology*, 207(16), 2735–2743.
4670 <https://doi.org/10.1242/jeb.01087>

4671 Romero, M. R., Pérez-Figueroa, A., Carrera, M., Swanson, W. J., Skibinski, D. O. F., & Diz, A. P.
4672 (2019). RNA-seq coupled to proteomic analysis reveals high sperm proteome variation
4673 between two closely related marine mussel species. *Journal of Proteomics*, 192, 169–187.
4674 <https://doi.org/10.1016/J.JPROT.2018.08.020>

4675 Sáez-Espinosa, P., Franco-Escalapez, C., Robles-Gómez, L., Silva, W. T. A. F., Romero, A., Immel, S.,
4676 & Gómez-Torres, M. J. (2022). Morphological and ultrastructural alterations of zebrafish
4677 (*Danio rerio*) spermatozoa after motility activation. *Theriogenology*, 188, 108–115.
4678 <https://doi.org/10.1016/j.theriogenology.2022.05.025>

4679 Said, T. M., & Land, J. A. (2011). Effects of advanced selection methods on sperm quality and ART
4680 outcome: A systematic review. *Human Reproduction Update*, 17(6), 719–733.
4681 <https://doi.org/10.1093/humupd/dmr032>

4682 Samardzija, M., Karadjole, M., Getz, I., Makek, Z., Cergolj, M., & Dobranic, T. (2006). Effects of
4683 bovine spermatozoa preparation on embryonic development in vitro. *Reproductive*
4684 *Biology and Endocrinology*, 4(1), 58. <https://doi.org/10.1186/1477-7827-4-58>

4685 Saraswat, M., Joenväärä, S., Jain, T., Tomar, A. K., Sinha, A., Singh, S., Yadav, S., & Renkonen, R.
4686 (2017). Human spermatozoa quantitative proteomic signature classifies normo-and

4687 asthenozoospermia. *Molecular and Cellular Proteomics*, 16(1), 57–72.

4688 <https://doi.org/10.1074/MCP.M116.061028/ATTACHMENT/03DDE3B4-73B5-4382-B3AB-83F09A407B08/MMC2.PDF>

4689

4690 Schreck, C. B. (2010). Stress and fish reproduction: The roles of allostasis and hormesis. *General*

4691 *and Comparative Endocrinology*, 165(3), 549–556.

4692 <https://doi.org/10.1016/j.ygcen.2009.07.004>

4693 Schrödinger, LLC. (2015). *The PyMOL Molecular Graphics System, Version 1.8*.

4694 Scott, C., de Souza, F. F., Aristizabal, V. H. V., Hethrington, L., Krisp, C., Molloy, M., Baker, M. A., &

4695 Dell'Aqua, J. A. (2018). Proteomic profile of sex-sorted bull sperm evaluated by SWATH-

4696 MS analysis. *Animal Reproduction Science*, 198, 121–128.

4697 <https://doi.org/10.1016/j.anireprosci.2018.09.010>

4698 Sebkova, N., Ded, L., Vesela, K., & Dvorakova-Hortova, K. (2014). *Progress of sperm IZUMO1*

4699 *relocation during spontaneous acrosome reaction*. <https://doi.org/10.1530/REP-13-0193>

4700 Secciani, F., Bianchi, L., Ermini, L., Cianti, R., Armini, A., La Sala, G. B., Focarelli, R., Bini, L., & Rosati,

4701 F. (2009). Protein Profile of Capacitated versus Ejaculated Human Sperm. *Journal of*

4702 *Proteome Research*, 8(7), 3377–3389. <https://doi.org/10.1021/pr900031r>

4703 Selvam, M. K. P., Agarwal, A., Pushparaj, P. N., Baskaran, S., & Bendou, H. (2019). Sperm Proteome

4704 Analysis and Identification of Fertility-Associated Biomarkers in Unexplained Male

4705 Infertility. *Genes 2019, Vol. 10, Page 522*, 10(7), 522–522.

4706 <https://doi.org/10.3390/GENES10070522>

4707 Sendler, E., Johnson, G. D., Mao, S., Goodrich, R. J., Diamond, M. P., Hauser, R., & Krawetz, S. A.

4708 (2013). Stability, delivery and functions of human sperm RNAs at fertilization. *Nucleic*

4709 *Acids Research*, 41(7), 4104–4117. <https://doi.org/10.1093/nar/gkt132>

4710 Sengupta, P., Dutta, S., Tusimin, M. B., Irez, T., & Krajewska-Kulak, E. (2018). Sperm counts in

4711 Asian men: Reviewing the trend of past 50 years. *Asian Pacific Journal of Reproduction*,

4712 7(2), 87. <https://doi.org/10.4103/2305-0500.228018>

4713 Sengupta, P., Nwagha, U., Dutta, S., Krajewska-Kulak, E., & Izuka, E. (2017). Evidence for
4714 decreasing sperm count in African population from 1965 to 2015. *African Health Sciences*,
4715 17(2), 418–427. <https://doi.org/10.4314/ahs.v17i2.16>

4716 Sharma, R., Agarwal, A., Mohanty, G., Hamada, A. J., Gopalan, B., Willard, B., Yadav, S., & du
4717 Plessis, S. (2013). Proteomic analysis of human spermatozoa proteins with oxidative
4718 stress. *Reproductive Biology and Endocrinology*, 11(1), 48. [https://doi.org/10.1186/1477-7827-11-48](https://doi.org/10.1186/1477-
4719 7827-11-48)

4720 Shevchenko, A., Tomas, H., Havli, J., Olsen, J. V., & Mann, M. (2006). In-gel digestion for mass
4721 spectrometric characterization of proteins and proteomes. *Nature Protocols*, 1(6), 2856–
4722 2860. <https://doi.org/10.1038/nprot.2006.468>

4723 Sigdel, A., Liu, L., Abdollahi-Arpanahi, R., Aguilar, I., & Peñagaricano, F. (2020). Genetic dissection
4724 of reproductive performance of dairy cows under heat stress. *Animal Genetics*, 51(4),
4725 511–520. <https://doi.org/10.1111/AGE.12943>

4726 Skakkebæk, N. E., Lindahl-Jacobsen, R., Levine, H., Andersson, A.-M., Jørgensen, N., Main, K. M.,
4727 Lidegaard, Ø., Priskorn, L., Holmboe, S. A., Bräuner, E. V., Almstrup, K., Franca, L. R.,
4728 Znaor, A., Kortenkamp, A., Hart, R. J., & Juul, A. (2022). Environmental factors in declining
4729 human fertility. *Nature Reviews. Endocrinology*, 18(3), 139–157.
4730 <https://doi.org/10.1038/s41574-021-00598-8>

4731 Skerrett-Byrne, D. A., Anderson, A. L., Hulse, L., Wass, C., Dun, M. D., Bromfield, E. G., De Iuliis, G.
4732 N., Pyne, M., Nicolson, V., Johnston, S. D., & Nixon, B. (2021). Proteomic analysis of koala
4733 (*phascolarctos cinereus*) spermatozoa and prostatic bodies. *Proteomics*, 21, 2100067–
4734 2100067. <https://doi.org/10.1002/pmic.202100067>

4735 Smedley, D., Haider, S., Durinck, S., Pandini, L., Provero, P., Allen, J., Arnaiz, O., Awedh, M. H.,
4736 Baldock, R., Barbiera, G., Bardou, P., Beck, T., Blake, A., Bonierbale, M., Brookes, A. J.,
4737 Bucci, G., Buetti, I., Burge, S., Cabau, C., ... Kasprzyk, A. (2015). The BioMart community

4738 portal: An innovative alternative to large, centralized data repositories. *Nucleic Acids*
4739 *Research*, 43(Web Server issue), W589–W598. <https://doi.org/10.1093/nar/gkv350>

4740 Solanki, S., Kumar, V., Kashyap, P., Kumar, R., De, S., & Datta, T. K. (2023). Beta-defensins as
4741 marker for male fertility: A comprehensive review†. *Biology of Reproduction*, 108(1), 52–
4742 71. <https://doi.org/10.1093/biolre/ioac197>

4743 Steptoe, P. C., & Edwards, R. G. (1978). BIRTH AFTER THE REIMPLANTATION OF A HUMAN
4744 EMBRYO. *The Lancet*, 312(8085), 366. [https://doi.org/10.1016/S0140-6736\(78\)92957-4](https://doi.org/10.1016/S0140-6736(78)92957-4)

4745 Stival, C., Puga Molina, L. del C., Paudel, B., Buffone, M. G., Visconti, P. E., & Krapf, D. (2016).
4746 Sperm Capacitation and Acrosome Reaction in Mammalian Sperm. In M. G. Buffone (Ed.),
4747 *Sperm Acrosome Biogenesis and Function During Fertilization* (pp. 93–106). Springer
4748 International Publishing. https://doi.org/10.1007/978-3-319-30567-7_5

4749 Stouffer, R. L., & Woodruff, T. K. (2017a). Nonhuman Primates: A Vital Model for Basic and
4750 Applied Research on Female Reproduction, Prenatal Development, and Women's Health.
4751 *ILAR Journal*, 58(2), 281–294. <https://doi.org/10.1093/ilar/ilx027>

4752 Strasburger, E. (1905). Die Samenanlage von Drimys Winteri und die Endospermembildung bei
4753 Angiospermen. *Flora Oder Allgemeine Botanische Zeitung*, 95, 215–231.
4754 [https://doi.org/10.1016/S0367-1615\(17\)31496-9](https://doi.org/10.1016/S0367-1615(17)31496-9)

4755 Suarez, S. S., & Pacey, A. A. (2006a). Sperm transport in the female reproductive tract. *Human*
4756 *Reproduction Update*, 12(1), 23–37. <https://doi.org/10.1093/humupd/dmi047>

4757 Sutter, A., & Immler, S. (2020). Within-ejaculate sperm competition. *Philosophical Transactions of*
4758 *the Royal Society of London. Series B, Biological Sciences*, 375(1813), 20200066–
4759 20200066. <https://doi.org/10.1098/rstb.2020.0066>

4760 Szamatowicz, M., & Szamatowicz, J. (2023). Implantation of embryos. The way for the
4761 improvement of the cumulative live birth rate (CLBR) in the assisted reproductive
4762 technology (ART). *Ginekologia Polska*, 94(4), 326–329.
4763 <https://doi.org/10.5603/GP.a2022.0054>

4764 Szklarczyk, D., Kirsch, R., Koutrouli, M., Nastou, K., Mehryary, F., Hachilif, R., Gable, A. L., Fang, T.,

4765 Doncheva, N. T., Pyysalo, S., Bork, P., Jensen, L. J., & Von Mering, C. (2023). The STRING

4766 database in 2023: Protein-protein association networks and functional enrichment

4767 analyses for any sequenced genome of interest. *Nucleic Acids Research*, 51(D1), D638–

4768 D646. <https://doi.org/10.1093/NAR/GKAC1000>

4769 The UniProt Consortium. (2021). UniProt: The universal protein knowledgebase in 2021. *Nucleic*

4770 *Acids Research*, 49(D1), D480–D489. <https://doi.org/10.1093/nar/gkaa1100>

4771 Tollner, T. L., Venners, S. A., Hollox, E. J., Yudin, A. I., Liu, X., Tang, G., Xing, H., Kays, R. J., Lau, T.,

4772 Overstreet, J. W., Xu, X., Bevins, C. L., & Cherr, G. N. (2011). A Common Mutation in the

4773 Defensin DEFB126 Causes Impaired Sperm Function and Subfertility. *Science Translational*

4774 *Medicine*, 3(92), 92ra65-92ra65. <https://doi.org/10.1126/scitranslmed.3002289>

4775 Torabi, F., Bogle, O. A., Estanyol, J. M., Oliva, R., & Miller, D. (2017). Zona pellucida-binding

4776 protein 2 (ZPBP2) and several proteins containing BX7B motifs in human sperm may have

4777 hyaluronic acid binding or recognition properties. *Molecular Human Reproduction*, 23(12),

4778 803–816. <https://doi.org/10.1093/molehr/gax053>

4779 Toufexis, D., Rivarola, M. A., Lara, H., & Viau, V. (2014). Stress and the Reproductive Axis. *Journal*

4780 *of Neuroendocrinology*, 26(9), 573–586. <https://doi.org/10.1111/jne.12179>

4781 Valcarce, D. G., Riesco, M. F., Cuesta-Martín, L., Esteve-Codina, A., Martínez-Vázquez, J. M., &

4782 Robles, V. (2023). Stress decreases spermatozoa quality and induces molecular alterations

4783 in zebrafish progeny. *BMC Biology*, 21(1), 70. <https://doi.org/10.1186/s12915-023-01570-w>

4785 Van Gassen, S., Gaudilliere, B., Angst, M. S., Saeys, Y., & Aghaeepour, N. (2020). CytoNorm: A

4786 Normalization Algorithm for Cytometry Data. *Cytometry*, 97(3), 268–278.

4787 <https://doi.org/10.1002/cyto.a.23904>

4788 van Oosterhout, C., Marcu, D., & Immler, S. (2022). Accounting for the genetic load in assisted
4789 reproductive technology. *Clinical and Translational Medicine*, 12(5), e864.
4790 <https://doi.org/10.1002/ctm2.864>

4791 Vandenberghe-Dürr, S., Gilliet, M., & Domizio, J. D. (2024). OLFM4 regulates the antimicrobial and
4792 DNA binding activity of neutrophil cationic proteins. *Cell Reports*, 43(10).
4793 <https://doi.org/10.1016/j.celrep.2024.114863>

4794 Vicens, A., Borziak, K., Karr, T. L., Roldan, E. R. S., & Dorus, S. (2017). Comparative Sperm
4795 Proteomics in Mouse Species with Divergent Mating Systems. *Molecular Biology and*
4796 *Evolution*, 34(6), 1403–1416. <https://doi.org/10.1093/MOLBEV/MSX084>

4797 Vieira, L. R., Hissa, D. C., de Souza, T. M., Chayenne A., S., Evaristo, J. A. M., Nogueira, F. C. S.,
4798 Carvalho, A. F. U., & Farias, D. F. (2020). Proteomics analysis of zebrafish larvae exposed
4799 to 3,4-dichloroaniline using the fish embryo acute toxicity test. *Environmental Toxicology*,
4800 35(8), 849–860. <https://doi.org/10.1002/TOX.22921>

4801 Villani, M. T., Morini, D., Spaggiari, G., Falbo, A. I., Melli, B., La Sala, G. B., Romeo, M., Simoni, M.,
4802 Aguzzoli, L., & Santi, D. (2022). Are sperm parameters able to predict the success of
4803 assisted reproductive technology? A retrospective analysis of over 22,000 assisted
4804 reproductive technology cycles. *Andrology*, 10(2), 310–321.
4805 <https://doi.org/10.1111/andr.13123>

4806 Wang, S. H., Cheng, C. Y., Chen, C. J., Chen, H. H., Tang, P. C., Chen, C. F., Lee, Y. P., & Huang, S. Y.
4807 (2014). Changes in protein expression in testes of L2 strain Taiwan country chickens in
4808 response to acute heat stress. *Theriogenology*, 82(1), 80–94.
4809 <https://doi.org/10.1016/J.THERIOGENOLOGY.2014.03.010>

4810 Weber, J. E., & Russell, L. D. (1987). A study of intercellular bridges during spermatogenesis in the
4811 rat. *American Journal of Anatomy*, 180(1), 1–24. <https://doi.org/10.1002/aja.1001800102>

4812 Wei, H., Li, W., Zeng, L., Ding, N., Li, K., Yu, H., Jiang, F., Yin, H., Xia, Y., Deng, C., Cai, N., Chen, X.,

4813 Gu, L., Chen, H., Zhang, F., He, Y., Li, J., & Zhang, C. (2024). OLFM4 promotes the

4814 progression of intestinal metaplasia through activation of the MYH9/GSK3 β /β-catenin
4815 pathway. *Molecular Cancer*, 23(1), 124. <https://doi.org/10.1186/s12943-024-02016-9>

4816 Westerveld, G. H., Gianotten, J., Leschot, N. J., van derVeen, F., Repping, S., & Lombardi, M. P.
4817 (2004). Heterogeneous nuclear ribonucleoprotein G-T (HNRNP G-T) mutations in men
4818 with impaired spermatogenesis. *Molecular Human Reproduction*, 10(4), 265–269.
4819 <https://doi.org/10.1093/molehr/gah042>

4820 J. A. Ramos-Vara, M. A. Miller, 2014. (2014). When Tissue Antigens and Antibodies Get Along.
4821 <https://journals.sagepub.com/doi/full/10.1177/0300985813505879>

4822 Widlak, W., & Vydra, N. (2017). The Role of Heat Shock Factors in Mammalian Spermatogenesis.
4823 In D. J. MacPhee (Ed.), *The Role of Heat Shock Proteins in Reproductive System
4824 Development and Function* (pp. 45–65). Springer International Publishing.
4825 https://doi.org/10.1007/978-3-319-51409-3_3

4826 Wigby, S., & Chapman, T. (2004). Sperm competition. *Current Biology*, 14(3), R100–R103.
4827 <https://doi.org/10.1016/j.cub.2004.01.013>

4828 Wilson-Leedy, J. G., Kanuga, M. K., & Ingermann, R. L. (2009). Influence of osmolality and ions on
4829 the activation and characteristics of zebrafish sperm motility. *Theriogenology*, 71(7),
4830 1054–1062. <https://doi.org/10.1016/j.theriogenology.2008.11.006>

4831 Wootton, R. J. (1985). Energetics of Reproduction. In P. Tytler & P. Calow (Eds), *Fish Energetics:
4832 New Perspectives* (pp. 231–254). Springer Netherlands. [https://doi.org/10.1007/978-94-011-7918-8_9](https://doi.org/10.1007/978-94-
4833 011-7918-8_9)

4834 Wright, L. I., Tregenza, T., & Hosken, D. J. (2008). Inbreeding, inbreeding depression and
4835 extinction. *Conservation Genetics*, 9(4), 833–843. [https://doi.org/10.1007/s10592-007-9405-0](https://doi.org/10.1007/s10592-007-
4836 9405-0)

4837 Xie, C., Shen, H., Zhang, H., Yan, J., Liu, Y., Yao, F., Wang, X., Cheng, Z., Tang, T.-S., & Guo, C.
4838 (2018). Quantitative proteomics analysis reveals alterations of lysine acetylation in mouse
4839 testis in response to heat shock and X-ray exposure. *Biochimica et Biophysica Acta (BBA) -*

4840 *Proteins and Proteomics*, 1866(3), 464–472.
4841 <https://doi.org/10.1016/j.bbapap.2017.11.011>

4842 Xie, H., Li, W., Guo, Y., Su, X., Chen, K., Wen, L., & Tang, F. (2023). Long-read-based single sperm
4843 genome sequencing for chromosome-wide haplotype phasing of both SNPs and SVs.
4844 *Nucleic Acids Research*, 51(15), 8020–8034. <https://doi.org/10.1093/nar/gkad532>

4845 Yamaguchi, Y., Nagase, T., Makita, R., Fukuhara, S., Tomita, T., Tominaga, T., Kurihara, H., & Ouchi,
4846 Y. (2002). Identification of multiple novel epididymis-specific beta-defensin isoforms in
4847 humans and mice. *Journal of Immunology (Baltimore, Md.: 1950)*, 169(5), 2516–2523.
4848 <https://doi.org/10.4049/jimmunol.169.5.2516>

4849 Zhang, L., & Elias, J. E. (2017). Relative Protein Quantification Using Tandem Mass Tag Mass
4850 Spectrometry. In L. Comai, J. E. Katz, & P. Mallick (Eds), *Proteomics: Methods and*
4851 *Protocols* (pp. 185–198). Springer. https://doi.org/10.1007/978-1-4939-6747-6_14

4852 Zheng, Y., Deng, X., & Martin-DeLeon, P. A. (2001). Lack of Sharing of Spm1 (Ph-20) among
4853 Mouse Spermatids and Transmission Ratio Distortion1. *Biology of Reproduction*, 64(6),
4854 1730–1738. <https://doi.org/10.1095/biolreprod64.6.1730>

4855 Zhu, Q., Emanuele, N. V., & Van Thiel, D. H. (2004). Calponin is expressed by Sertoli cells within rat
4856 testes and is associated with actin-enriched cytoskeleton. *Cell and Tissue Research*,
4857 316(2), 243–253. <https://doi.org/10.1007/s00441-004-0864-z>

4858 Zhu, Y.-F., Cui, Y.-G., Guo, X.-J., Wang, L., Bi, Y., Hu, Y.-Q., Zhao, X., Liu, Q., Huo, R., Lin, M., Zhou,
4859 Z.-M., & Sha, J.-H. (2006). Proteomic Analysis of Effect of Hyperthermia on
4860 Spermatogenesis in Adult Male Mice. *Journal of Proteome Research*, 5(9), 2217–2225.
4861 <https://doi.org/10.1021/pr0600733>

4862 Zigo, M., Kerns, K., & Sutovsky, P. (2023). The Ubiquitin-Proteasome System Participates in Sperm
4863 Surface Subproteome Remodeling during Boar Sperm Capacitation. *Biomolecules*, 13(6),
4864 996–996. <https://doi.org/10.3390/BIOM13060996/S1>

4865 Zmudzinska, A., Bromke, M. A., Strzezek, R., Zielinska, M., Olejnik, B., & Mogielnicka-Brzozowska,
4866 M. (2022). Proteomic Analysis of Intracellular and Membrane-Associated Fractions of
4867 Canine (*Canis lupus familiaris*) Epididymal Spermatozoa and Sperm Structure Separation.
4868 *Animals : An Open Access Journal from MDPI*, 12(6), 772.
4869 <https://doi.org/10.3390/ani12060772>
4870